

SLOPE ANALYSIS FOR RESERVOIR ENGINEERING

Prediction of the response of existing landslides and intact slopes to changes in stability, particularly in relation to reservoir filling, including seismic effects, optimising the design of remedial measures and surveillance.

ABSTRACT

In the last decade, laboratory testing, theoretical developments, and improved access to computing facilities have enhanced the level of geotechnical input that can be put into slope stability assessment. This thesis brings together the results of geotechnical investigations on a number of projects where the stability of slopes affected civil engineering works. It includes research into laboratory behaviour of soils and development of general principles that have been required to meet specific demands. The techniques, which encompass a number of aspects of geomechanics, have been demonstrated by applications to case history data.

Laboratory testing of landslide materials at residual strength has been carried out to examine recently reported findings on the residual strength characteristics of soils subject to rapid shearing. The laboratory testing has then been used as a basis for quantitative estimation of the rates of movement expected in activated landslides and for designing remedial measures.

Field assessment of strength parameters for both stable slopes and landslides has been carried out using Casagrande's resistance envelope procedure. The principles have been extended to allow application to specific conditions of engineering interest, and the value of the procedure in practice has been demonstrated with case histories.

The prediction of the effects of changes in groundwater on slope stability has been examined at length. The principle application is in reservoir engineering where design predictions are required to determine whether piezometric rises will be likely to exceed values which would affect slope stability. Unsteady state modelling of groundwater response to reservoir filling or drawdown has been carried out. The groundwater modelling has been linked to stability analyses so that predictions may be made for the time dependent changes in safety factor of a slope containing multiple confined or unconfined aquifers.

The seismic stability of slopes has been discussed, principally with regard to the effect of strong earthquake shaking on existing landslides, including those subjected to remedial works and submerged by reservoir filling.

Case histories have been given where landslide disasters could have been mitigated, had there been recognised procedures to follow, from the time at which incipient slope movements were first observed. Recommendations for appropriate procedures for slope assessment, surveillance and alarm criteria have been proposed.

CONTENTS

ABSTRACT

CHAPTER 1. INTRODUCTION

- 1 Introduction
 - 1.1 Background
 - 1.2 Lay-out of the thesis

CHAPTER 2. LITERATURE REVIEW OF LABORATORY STRENGTH TESTING

- 2.1 Introduction
- 2.2 The effect of rate of shearing on residual strength
 - 2.2.1 Review of laboratory findings: theses and papers.
 - 2.2.2 Discussion of the Literature Review
 - 2.2.2.1 Measurement of rate effects
 - 2.2.2.2 Loss of soil during testing
 - 2.2.2.3 Mechanism of strength loss during rapid shearing
 - 2.2.2.3 Pore pressures expected during residual shear
 - 2.2.2.4 Summary of alternative explanations
 - 2.2.2.5 Contrary arguments
- 2.3 Concluding remarks

CHAPTER 3. LABORATORY TESTING

- 3.1 Introduction
- 3.2 Effect of saturation on shear strength
 - 3.2.1 General
 - 3.2.2 Basic concepts of effective stress in unsaturated soils
 - 3.2.3 Parametric study
 - 3.2.4 Laboratory ring shear tests
 - 3.2.5 Concluding remarks
- 3.3 High stress testing
 - 3.3.1 Introduction
 - 3.3.2 Adoption of linear residual strength for submergence
 - 3.3.3 Ring shear modification
 - 3.3.4 Concluding remarks

CHAPTER 4. FIELD ASSESSMENT OF DESIGN PARAMETERS

- 4.1 Introduction
- 4.2 Identification of a geotechnical model
- 4.3 Basis of the resistance envelope procedure
 - 4.3.1 General
 - 4.3.2 Modification of existing computer programs
- 4.4 Extensions to the resistance envelope procedure
 - 4.4.1 Determining the mohr envelope from tangent points
 - 4.4.2 Inclusion of tension cracking
 - 4.4.3 Partially saturated soils
 - 4.4.4 Saturation of partially saturated soils
- 4.5 Landslide strength parameters from the REP
 - 4.5.1 Basic approach
 - 4.5.2 Correction for side friction
 - 4.5.3 Comparison of field and laboratory strengths
- 4.6 Applications to slope design
 - 4.6.1 Cut slope design
- 4.7 Conclusions

CHAPTER 5. PREDICTION OF GROUNDWATER CHANGES ON RESERVOIR FILLING

- 5.1 Introduction
- 5.2 Basic principles of groundwater modelling
- 5.3 Sectional, steady state modelling cases
 - 5.3.1 Horizontal watertable
 - 5.3.2 Inclined unconfined watertable.
 - 5.3.3 Inclined watertable with no permeability barrier
 - 5.3.4 Artesian or sub-artesian pressures acting beneath an aquiclude
- 5.4 Regional, time-dependent groundwater flow modelling
 - 5.4.1 Introduction
 - 5.4.2 Program development
 - 5.4.2.1 Mathematical basis.
 - 5.4.2.2 Finite difference model
 - 5.4.2.3 Finite difference formulation.
 - 5.4.3 Program design
 - 5.4.3.1 Overall structure
 - 5.4.3.2 Aquifer model Geometry
 - 5.4.3.3 Input structure
 - 5.4.3.4 Program structure
 - 5.4.3.5 Derivation of 3-D safety factor algorithms
 - 5.4.3.6 Output structure
- 5.5 Groundwater modelling during landslide investigations
- 5.6 The role of groundwater modelling in reservoir safety assurance
 - 5.6.1 The piezometric lag problem
 - 5.6.2 Accuracy of time predictions
 - 5.6.3 Illustrative cases
 - 5.6.4 Application to reservoir filling
- 5.7 Concluding remarks

CHAPTER 6. MECHANISMS FOR RAPID LANDSLIDING

- 6.1 Introduction
- 6.2 Basic concepts of soil failure
 - 6.2.1 Peak and residual effective strengths
 - 6.2.2 Rate dependence of residual strength
- 6.3 Displacement-independent accelerating mechanisms
- 6.4 Displacement-dependent accelerating mechanisms
 - 6.4.1 Reduction of effective cohesion
 - 6.4.2 Reduction of effective friction
 - 6.4.2.1 Peak to residual strength
 - 6.4.2.2 Mechanical attrition
 - 6.4.3 Increase in pore fluid pressure
 - 6.4.3.1 Shear contraction.
 - 6.4.3.2 Monotonic loading
 - 6.4.3.3 Cyclic loading
 - 6.4.3.4 Frictional heating
 - 6.4.4 Coalescence of multiple slides
 - 6.4.5 Development of internal deformations
 - 6.4.6 Unstable failure surface geometry
 - 6.4.7 Secondary accelerating mechanisms
- 6.5 Concluding remarks

CHAPTER 7. PROCEDURES FOR ASSESSING LANDSLIDE MOBILITY AND REMEDIAL MEASURES

- 7.1 Introduction
- 7.2 Residual strength testing
 - 7.2.1 General
 - 7.2.2 Dependence of residual shear strength on rate of shearing
 - 7.2.3 Explanation for rate effects
- 7.3 Slope stability implications
 - 7.3.1 Susceptibility to rapid sliding
 - 7.3.2 Practical implications
- 7.4 Laboratory versus field behaviour
 - 7.4.1 Active shear band thickness
 - 7.4.2 Implications for predicting field behaviour
 - 7.4.3 Reservations
- 7.5 Interpretation of deformation monitoring
- 7.6 The extent of remedial measures
 - 7.6.1 Increase in safety factor
 - 7.6.2 Sensitivity of slide movement to safety factor changes
- 7.7 Further work
- 7.8 Conclusions

CHAPTER 8. SEISMIC STABILITY OF RESERVOIR SLOPES

- 8.1 Introduction
- 8.2 Literature review
 - 8.2.1 Earthquake case histories
 - 8.2.2 Laboratory testing
- 8.3 Geological precedent as a basis for stability assurance
 - 8.3.1 General
 - 8.3.2 Limitations of precedent arguments
- 8.4 Mechanisms for seismic displacement of slopes
 - 8.4.1 Introduction
 - 8.4.2 First time slides in previously unsheared material
 - 8.4.3 Slides on pre-existing surfaces
 - 8.4.3.1 General
 - 8.4.3.2 Specific mechanisms.
- 8.5 Calculation of seismic displacement of landslides
- 8.6 Stability of submerged slopes
- 8.7 Conclusions

CHAPTER 9. ALARM CRITERIA AND MONITORING FOR HAZARDOUS LANDSLIDES

- 9.1 Introduction
- 9.2 Factors related to alarm criteria
 - 9.2.1 Pre-set Alarm Criteria
 - 9.2.1.1 Empirical curve-fitting approaches
 - 9.2.1.2 Empirical threshold criterion approaches
 - 9.2.1.3 Geotechnical-empirical approach
 - 9.2.2 Monitoring Frequency.
 - 9.2.2.1 Background
 - 9.2.2.2 Specific recommendations for determining survey intervals.
 - 9.2.2.3 Prediction of accelerating slide movement.
- 9.3 Practical application of alarm criteria
 - 9.3.1 Steady Creep.
 - 9.3.2 Catastrophic failure records.
- 9.4 Concluding remarks

CHAPTER 10. CONCLUSIONS

REFERENCES

APPENDICES

APPENDIX 1. COMPUTER PROGRAM FOR DETERMINING FIELD STRENGTH PARAMETERS USING THE CASAGRANDE RESISTANCE ENVELOPE PROCEDURE

APPENDIX 2. COMPUTER PROGRAM FOR THE PREDICTION OF GROUNDWATER RESPONSE TO RESERVOIR FILLING, INCLUDING SAFETY FACTOR CHANGES

APPENDIX 3. SENSITIVITY ANALYSES FOR LANDSLIDE SUBMERGENCE

APPENDIX 4. CASE HISTORIES OF LANDSLIDE MOVEMENTS

APPENDIX 5. CASE HISTORIES OF SEISMICALLY REACTIVATED LANDSLIDES

APPENDIX 6. PORE PRESSURE EFFECTS IN RAPID LANDSLIDES

LIST OF FIGURES

- Photo 1. The Ruahihi canal failure
- Fig. 2-1 Simplified shear strength properties
Fig. 2-2 Ring shear sample
Fig. 2-3 Variation of residual strength of cohesive soils (from Tika, 1989 p 221)
Fig. 2-4 Residual strength rate effects (from Lemos, 1986 p 231)
Fig. 2-5 Residual strength rate effects (from Tika, 1989 p 388)
Fig. 2-6 Undrained pore pressure response
- Fig. 3-1 Saturation effects: parametric study of variable strength losses.
Fig. 3-2 Typical stress parameters for unsaturated soils
Fig. 3-3 Saturation effects: Parametric study for active slide (friction angle 25 degrees)
Fig. 3-4 Saturation effects: Parametric study for active slide (35 degree slope)
Fig. 3-5 Saturation effects: Parametric study for active slides at variable slopes.
Fig. 3-6 Sample E-43 Unsaturated - saturated shear tests
Fig. 3-7 Sample E-43 Unsaturated - wetted shear tests
Fig. 3-8 Strength loss on saturation at 50 kPa normal stress
Fig. 3-9 Strength loss on saturation at 116 kPa normal stress
Fig. 3-10 Strength loss on saturation at 446 kPa normal stress
Fig. 3-11 Strength loss on saturation (long term)
- Fig. 4-1 Resistance envelope principle (after Janbu, 1977)
Fig. 4-2 Resistance envelope for intact slopes
Fig. 4-3 Active slide example
Fig. 4-4 Resistance envelope for active slides
Fig. 4-5 Slope design and verification
- Fig. 5-1 Construction of piezometric lines for an unconfined aquifer
Fig. 5-2 Confined aquifer piezometric observations
Fig. 5-3 Construction of piezometric lines for a confined aquifer
Fig. 5-4 Numerical modelling of landslide aquifers affected by reservoir filling
Fig. 5-5 Program structure diagram for landslide groundwater modelling
Fig. 5-6 Derivation of safety factor sensitivity to pore pressure in limit equilibrium
Fig. 5-7 Piezometer responses, reservoir filling case
Fig. 5-8 Piezometer responses, controlled drawdown case
Fig. 5-9 Piezometer responses, drainage and filling case
- Fig. 6-1 Response of dense sand to unloading
- Fig. 7-1 Mobile range of slide gouge

- Fig. 7-2 Stick-slip behaviour of slide gouge
- Fig. 8-1 Effect of submergence of a translational slide subject to earthquake
- Fig. 9-1a Precursory velocities of slides
 Fig. 9-1b Precursory acceleration of slides
 Fig. 9-2 Rate dependence of residual strength
 Fig. 9-3 Residual strength dependence on shearing rate
- Fig. A1-1 Critical failure surfaces in the REP
 Fig. A1-2 REP stress coordinates
 Fig. A1-3 Design strength envelope from REP
 Fig. A1-4 Slope design for cuts
- Fig. A2-1 Drilling Fluid Record
 Fig. A2-2a Regional Model - Initial piezometric surface
 Fig. A2-2b Regional Model - Initial drainable head
 Fig. A2-3a Regional Model - Predicted piezometric surface, full pool
 Fig. A2-3b Regional Model - Predicted net drainable head, full pool
 Fig. A2-4 Section Model - Initial condition (1)
 Fig. A2-5 Section Model - Rising piezometric line (2)
 Fig. A2-6 Section Model - Rising piezometric line (3)
 Fig. A2-7 Section Model - Rising piezometric line (4)
 Fig. A2-8 Section Model - Steady state piezometric line (5)
 Fig. A2-9 Section Model - Sensitivity analysis
 Fig. A2-10 Piezometer responses, drainage and filling case
 Fig. A2-11 Slide drawdown effects
 Fig. A2-12 Slide piezometric responses, proposed drainage
 Fig. A2-13 Slide piezometric responses, drainage and delayed filling
- Fig. A3-1 Sensitivity to decrease in friction angle
 Fig. A3-2 Sensitivity to decrease in cohesion
 Fig. A3-3 Sensitivity to increase in piezometric level
 Fig. A3-4 Sensitivity to reservoir rise
 Fig. A3-5a Average Stress conditions on failure surface
 Fig. A3-5b Stress vectors for changed piezometric conditions
 Fig. A3-5c Examples for determining safety factor changes
 Fig. A3-5d Examples for determining absolute safety factors
 Fig. A3-6 Sensitivity of displacement to changes in safety factor
 Fig. A3-7 Sensitivity to failure surface waviness

Fig. A4-1a Gepatsch Slide Area- Displacement analysis model
Fig. A4-1b Gepatsch Slide Movements (from Lauffer et al, 1967)
Fig. A4-2a Dirillo Reservoir Slide - Displacement analysis model
Fig. A4-2b Dirillo Slide Movements (from Jappelli & Musso, 1981)
Fig. A4-3 Slide activated by toe excavation
Fig. A4-4 Comparison of field and laboratory rate effects

Fig. A6-0 Electrical heating effects in the ring shear
Fig. A6-1 Abbotsford Landslide
Fig. A6-2 Abbotsford movement, final month
Fig. A6-3 Abbotsford movement, final day
Fig. A6-4 Earthquake displacement model, OBE
Fig. A6-5 Earthquake displacement model, MCE
Fig. A6-6 Earthquake displacement model, Oweka Slide



Photo 1. The Ruahihi canal failure

CHAPTER 1

INTRODUCTION

1.1 BACKGROUND

Several landslide disasters, including some in recent years, have brought attention to the apparent unpredictability of landslide mobility. Because many slopes exhibit some form of creep movement, the distinction between acceptable and unacceptable modes of landslide movement has, on occasions, not been correctly interpreted, with catastrophic consequences.

Assessment of a newly observed landslide in an emergency situation, often takes place on an ad hoc basis. Time may preclude any recourse to information from laboratory testing, or an understanding of mechanisms which may precipitate rapid mobility. The lack of any code of practice or acknowledged procedures for assessment of the rapid landsliding is a limitation to the present state-of-the-art.

This thesis collates work undertaken on a number of projects over the last 15 years, where the stability of slopes, particularly those affected by reservoirs with adjacent highways, has been a principal factor. Developmental work was carried out to address immediate geotechnical problems. However, most of the procedures have general application therefore the emphasis has been on principles as well as specific cases. The thesis is intended to provide a substantiated geotechnical approach where engineering works require appreciation of the strength and deformation properties which govern the static and seismic stability of slopes.

1.2 Lay-out of the Thesis

The thesis contains 10 chapters and 6 appendices.

Chapter 2 briefly reviews previous laboratory work on the measurement of the residual strength of soils, with emphasis on recent research using fast rates of shear in fine grained soils.

Chapter 3 describes the type of laboratory testing carried out for a number of civil engineering projects, to characterise soils - both in active landslides and in apparently stable slopes that were to be de-stabilised by proposed works. Both saturated and unsaturated soils were studied.

Chapter 4 addresses the determination of design parameters using field rather than laboratory methods. The resistance envelope method was first proposed by Casagrande but has seldom been reported in case histories. The theory has been extended to include unsaturated soils that will be submerged by reservoir filling. A listing of the appropriate

computer source code and examples are contained in Appendix 1.

Chapter 5 documents procedures developed during studies for a series of 5 proposed hydro-electric power projects where numerous very large, active landslides were to be submerged by reservoir filling. Design procedures to determine the degree to which the stability of landslides would be affected by groundwater changes are detailed. Computer source code for determining changes in piezometric levels and safety factors is given in Appendix 2. Sensitivity analyses are provided in Appendix 3.

Chapter 6 explores the variety of mechanisms which need to be considered when assessing the potential for rapid landsliding, with emphasis on first-time slides.

Chapter 7 discusses landslide mobility with emphasis on pre-existing active slides. Methods are developed for estimating the displacement and also rate of movement expected from a given decrease in safety factor, and the increase in safety factor required to arrest a creeping slide. Case histories are given in Appendix 4.

Chapter 8 examines the factors affecting the seismic stability of stable slopes, dormant landslides and actively creeping slides. Criteria for assuring the resistance of a newly submerged landslide to earthquake shaking are identified. A supporting literature search summary is contained in Appendix 5 and detailed evaluation of pore pressure effects is given in Appendix 6.

Chapter 9 brings together aspects from all the above chapters to establish alarm criteria for hazardous landslides, to ensure appropriate reaction of personnel when any form of landslide movement begins.

Chapter 10 summarises the principal conclusions for practical application.

CHAPTER 2

LITERATURE REVIEW OF LABORATORY STRENGTH TESTING

2.1 INTRODUCTION

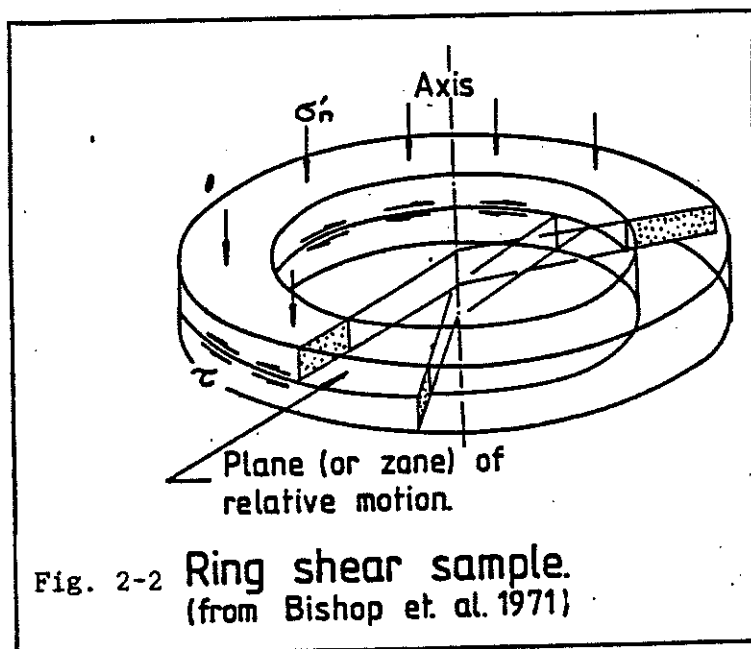
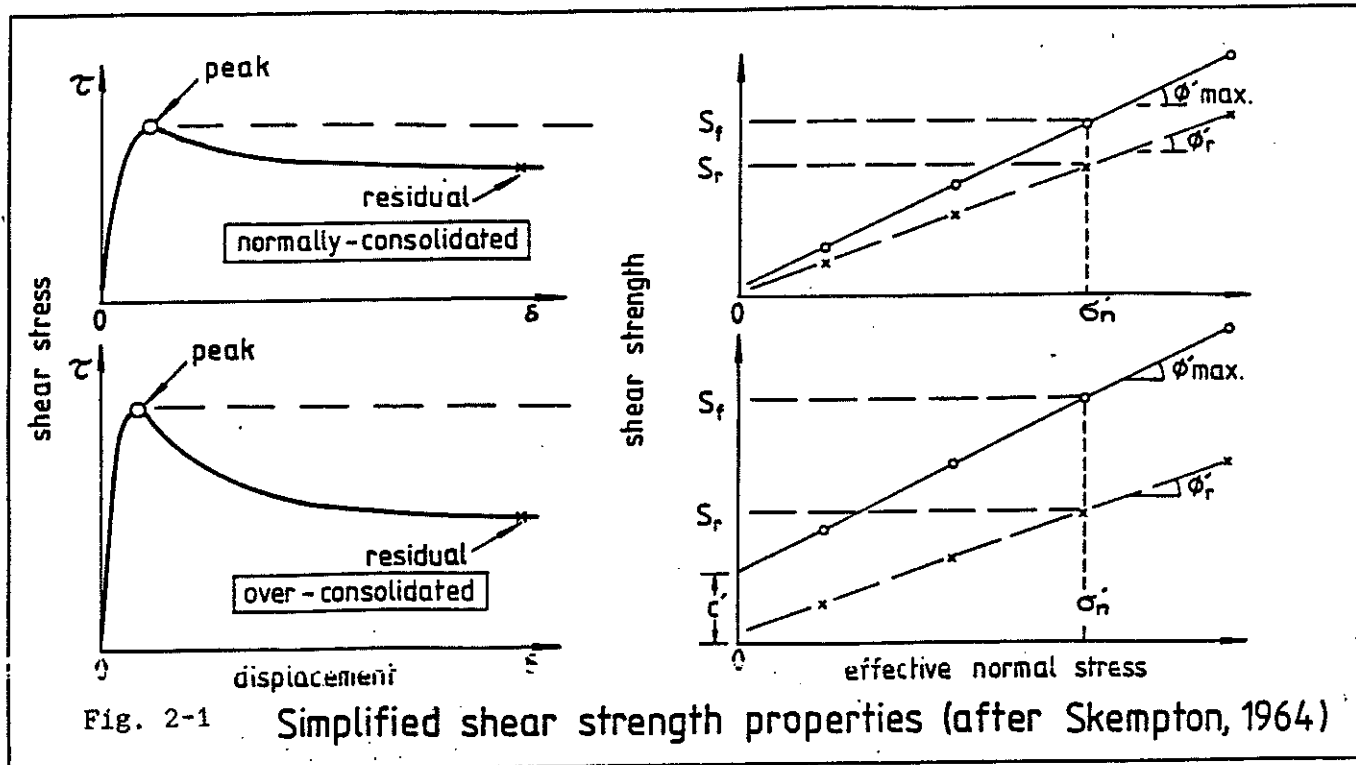
In the last decade, a number of papers have been published on the effects of shearing at both slow and fast rates of shear, in the ring shear apparatus.

The purpose of ring shearing is to identify the strength of soils when subjected to indefinitely large displacements. Fig. 2-1 (after Skempton, 1964) illustrates the commonly accepted concepts of peak and residual strength. Skempton (1977) reports that shear displacements of about 1 or 2 metres may be required to achieve residual values. Determinations for fine grained soils are most successfully made in a ring shear apparatus (Bishop, 1971; Bromhead, 1979) with which an annulus of soil (Fig. 2-2) can be sheared to give displacements as great as desired. Other methods for obtaining residual strength parameters include multiple reversal direct shear and cut plane triaxial testing but results may be somewhat unconservative, particularly in highly plastic soils at low normal stresses.

Ring shear testing has formerly been expensive, but the development of 'smear' devices such as that described by Bromhead (1979) has reduced the costs of apparatus construction. The Bromhead apparatus uses an annular soil sample 5 mm thick with inner and outer diameters of 70 and 100 mm respectively, confined radially between concentric rings. It is compressed vertically between porous loading platens which are roughened to prevent slip at the soil/platen interface.

The apparatus developed by the writer has a shear annulus with the same dimensions as the Bromhead apparatus. However the platens are much more porous to allow more rapid drainage, and the upper platen is slightly concave (40 mm radius) to facilitate formation of a more planar failure surface. Also the side walls are chamfered (5 degrees) away from the confining rings to minimise edge effects and the separation gap is much smaller (20 microns) to minimise loss of soil during shearing. In addition, testing may be either stress controlled or "strain" controlled, ie shear and normal stresses may be held constant and displacement rate measured, or displacement and normal stress held constant and shear stress measured. Friction losses (in all bearings) have been accounted for in calculations, and assurance of the machine calibration has been obtained by comparative testing with 4 other machines (both direct and ring shear) with a range of soil types, showing quite satisfactory agreement (mostly less than 3%, but less than 5% for all cases).

The study of the effects of shearing at different displacement rates has been used to determine the response of soils at residual strength. Rate dependent properties from gouges sampled from failure surfaces in slopes can then be used to assess the acceleration of landslides under creeping (non-seismic) conditions and under earthquake loading.



2.2 THE EFFECT OF RATE OF SHEARING ON RESIDUAL STRENGTH

2.2.1 Review of laboratory findings: theses and papers.

(i) Lupini, Skinner & Vaughan (1981). The drained residual strength of cohesive soils.

Three modes of residual shear behaviour were described in this paper: a turbulent mode, a transitional mode and a sliding mode, the mode depending on dominant particle shape and on the coefficient of inter-particle friction.

The turbulent mode occurs when behaviour is dominated by rotund particles, or, possibly in soils dominated by platy particles, when the coefficient of inter-particle friction is high. Residual strength is high, no preferred particle orientation occurs and brittleness is due to dilatant behaviour only. Photomicrographs of failure surfaces formed in the laboratory show no preferred orientation of particles.

The sliding mode occurs when behaviour is dominated by platy, low friction particles. A low strength shear surface of strongly oriented platy particles then develops, with the active shear band thickness ranging typically from about 0.002 to 0.020 mm.

The transitional mode occurs when there is no dominant particle shape, and involves turbulent and sliding behaviour in different parts of a shear zone. Shear zones showed a multiplicity of well-formed but discontinuous surfaces (terminating at groups of sand grains), rather than a single poorly-oriented surface or zone. The zones containing the discontinuous surfaces were quite wide (about 2 mm) but the surfaces or sub-zones themselves were apparently thin (about 0.02 mm).

(ii) Skempton (1985): Residual strength of clays in landslides, folded strata and in the laboratory.

This paper discusses the residual strength behaviour of a soil in relation to its clay content. At less than about 25% clay, behaviour is similar to that of silts and sands, with relatively high residual strengths. Above about 50% clay content, residual strength is entirely controlled by sliding of platy particles. When the clay fraction lies between 25 and 50% there is a transitional type of behaviour, residual strength being dependent on the percentage of clay particles as well as on their nature. Residual strength is little affected by variation in the slow rates of displacement encountered in reactivated landslides and in the usual laboratory tests, but at rates faster than about 100 mm/min qualitative changes take place in the pattern of behaviour. A substantial gain in strength is followed, with increasing displacement, by a fall to a minimum value. In clays and low clay fraction silts this minimum is not less than the slow or static residual, but in clayey silts (with clay fractions around 15-25%) the minimum can be as low as one half the static value.

Reference is made to the thickness of shear zones identified in the field (0.02 mm).

One sample from Kalabagh Dam with CF 47%, was prepared at about its plastic limit, pre-consolidated to 900 kPa and sheared under 205 kPa normal stress. At rates of 400 mm/min the strength was nearly double that at slow shear but reduced slightly with displacement. It was suggested that some qualitative change in behaviour occurs at rates exceeding about 100 mm/min, ie disturbance of the originally ordered structure to give 'turbulent' shear, in contrast with sliding shear when the particles are oriented parallel to the plane of displacement. It was also suggested that negative pore pressures may be generated and, as displacement continued, these were dissipated within the body of the sample thus leading to a decrease in strength. Turbulent shear was inferred because on reimposing the slow rate, a peak was observed with the strength falling to the residual only after considerable further displacement.

A second sample from the same site but with only 3% clay showed similar behaviour except that much less displacement was required to reach residual after fast shearing. (Note also that other variables were changed also. The normal stress was increased to 490 kPa, ie halving the OCR value adopted for the first specimen.)

A third sample with 21% CF showed more anomalous behaviour. This was preconsolidated to 900 kPa, then tested at both 200 and 495 kPa normal stress. All tests showed that a fast strength maximum was obtained, significantly higher than the slow residual, but in this type of soil, the fast minimum strength was about half the slow residual. Although not highlighted by Skempton, the data show that the maximum fast strength increased with increasing OCR. This supports the writer's hypothesis (discussed in detail below) that negative pore pressures may have developed during the initial phases of fast shear because the pore pressure parameter A (for the soil away from the immediate shear zone) should become more negative with increasing OCR.

Skempton concludes that while explanations are not clear, the 'significance in relation to earthquake engineering design is obviously considerable'.

(iii) Lemos, Skempton & Vaughan (1985): Earthquake loading of shear surfaces in slopes.

Rate effects are discussed in this paper for a range of soil types. At 'slow' rates of shear (less than about 100 - 1000 mm/day) where drained conditions apply, the term 'conventional rate effects' was used where the soil shows continuously increasing strength with increasing shear stress. For the opposite case, the term 'reversed rate effect' was used, ie where at slow rates of shear, a decrease in strength was found with increasing shear stress. Soils which show sliding shear show conventional rate effects. Soils which show turbulent shear, were reported to typically show a reversed rate effect.

The paper summarises the alternative types of behaviour exhibited when a shear surface is formed at residual strength by slow drained shearing, and then subjected to more rapid displacement rates -

- (a) There is an initial threshold strength on the shear surface, mobilised without further displacement, which is a function of the rate of fast loading, and which is considerably in excess of the 'slow' residual strength.
- (b) There is often a further increase of strength with fast displacement on the shear surface. This is termed the fast maximum strength.
- (c) The strength is then likely to drop with further fast displacement. This is termed the minimum fast strength. The minimum fast strength is usually higher than the slow residual strength, but in silty soils, it may be lower.
- (d) If after fast displacement of a soil in which sliding or transitional shear occurs, the shear surface is tested slowly, then an initial peak strength greater than the slow residual strength is measured, indicating that fast shear has caused disordering of the shear surface.

Lemos et al conclude that for a soil which shows a drop in residual strength with fast shearing 'if this strength loss were induced during an earthquake, it could lead to large, fast and potentially catastrophic movements which would continue post-earthquake.'

(iv) Vaughan, Lemos & Tika (1985): Strength loss on shear surfaces due to rapid loading.

The claim in this paper is that 'the influence of fast rates of displacement on the strength of shear surfaces in cohesive soils must be considered in the study of seismic slope stability'.

Some soils studied in laboratory ring shear tests showed a maximum fast strength greater than the slow residual strength (positive rate effect) and some the opposite (negative rate effect).

In the latter case then 'any failure, whether induced by earthquake loading or not, may accelerate to catastrophic velocities. This type of behaviour is the principal subject' of the paper.

Negative rate effects appeared to correlate with clay fraction, namely with those soils containing between about 10 and 40% clay.

Vaughan et al, conclude that for silty soils (with negative rate effects), 'if earthquake shaking produces a critical combination of displacement and velocity in an existing slide initially at its residual strength, its reactivation will involve large and fast movements which will continue after shaking ceases'.

(v) Lemos (1986): The effect of rate of shear on residual strength of soil.

Details of the papers by Skempton (1985), Lemos et al (1985) and Vaughan et al (1985) are contained in an lengthy Ph.D thesis on ring shear tests by Lemos.

The data are clearly presented, although more than one variable was often changed between tests, making unequivocal interpretation difficult. (Alternative explanations for Lemos's findings are made below.)

Photomicrographs show that the shear surfaces formed in the laboratory are commonly about 0.02 mm, ie similar in thickness to the field observations quoted above.

Lemos concludes that 'a knowledge of the strength of (pre-existing shear) surfaces under rapid loading is necessary if stability during and after an earthquake is to be examined'. In a low plasticity clay 'a runaway failure may take place. The drastic drop in shear resistance with displacement may be the cause of some of the catastrophic failures observed in the field.' (No specific cases are established.)

(vi) Tika (1989): The effect of fast shearing on the residual strength of soils.

Tika continued Lemos's line of investigation of rate effects and identified five types of rate effects:

Type I showing a constant residual strength irrespective of the rate of displacement. These are soils that exhibit turbulent shear mode, eg sands and sandy silts with PI less than 9, sand content greater than 20% and clay content less than 10%.

Type II showing either a negligible to moderate increase or a slight decrease of residual strength with an increasing rate of displacement, followed by a significant drop of strength to less than the slow residual value at higher rates of displacement. These usually show turbulent or transitional shear, have PI between 9 and 21, and variable grading but often silty.

Type III showing a decrease of residual strength with an increasing rate of displacement, followed by an increase and then a significant drop of strength to less than the slow residual value at higher rates of displacement. These show a transitional or sliding shear mode and PI between 24 and 26.

Type IV showing a decrease of residual strength with an increasing rate of displacement, followed by an increase above the slow residual value at higher rates of displacement. These are low plasticity clays and silty clays.

Type V showing an increase of residual strength with an increasing rate of displacement. These are clays with a sliding shear mode, PI between 36 and 51, and clay content exceeding 48%.

Explanations for the changes in strength with fast shearing were:

- * Viscous effects.
- * Structural changes taking place in the shear zone for soils showing transitional or sliding shear mode.
- * Pore pressure inhomogeneities with the microfabric of the soils.
- * Changes in the porosity of the shear zone, but without significant excess pore pressures.

A summary of the variation in residual strength of cohesive soils with rate of displacement given by Tika (221) is reproduced in Fig. 2-3. This shows that the fast residual strength is commonly about 50% of the slow residual strength and may be as low as 10%.

Tika concluded that 'the negative rate effect is an intrinsic soil property and that it does not depend on heat or pore water pressure generation'.

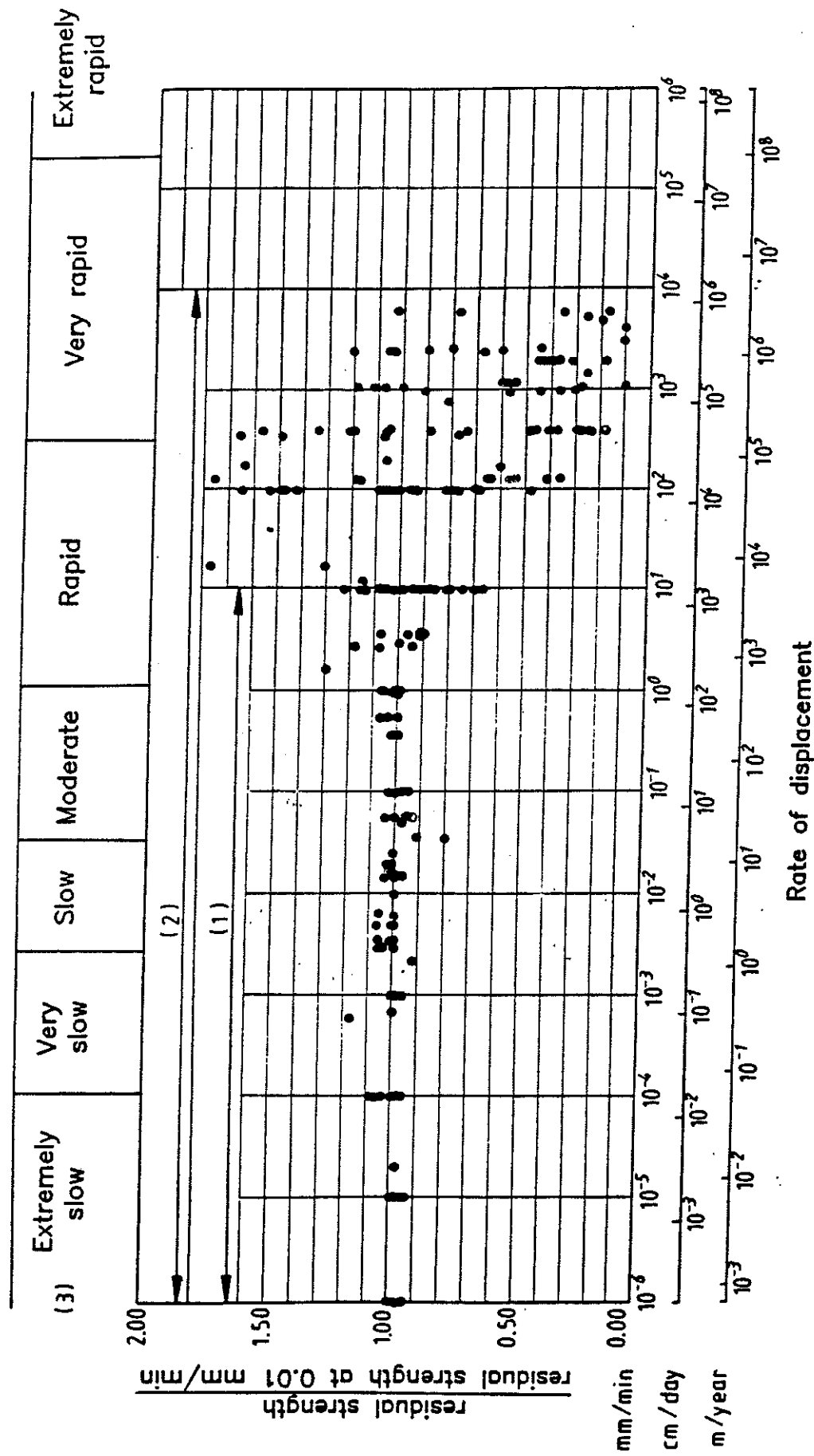
2.2.2 Discussion of the Literature Review

2.2.2.1 Measurement of rate effects

Determining the rate effect characteristics over the 'slow' range is a particularly time consuming task, because natural variations in the ring shear strength are large compared with the differences which are being measured. The only way to determine rate effects reliably is to alternate the displacement rate between a standard value and the rate of interest, until a consistently repeatable change in shear strength is obtained.

Materials from projects in many parts of New Zealand have been tested by the writer, using a ring shear apparatus. Both stress controlled and strain controlled methods were used. In no case has a 'reversed' rate effect (decreasing strength with increasing displacement rate over 'slow' ranges) been detected. If such a material property exists, it might suggest that for these cases, a creeping landslide would be stabilised by decreasing its safety factor (eg loading the head or removal of its toe). Intuitively, field behaviour suggests that there might be a misconception somewhere along the path to such a conclusion. Laboratory testing techniques and/or apparatus effects need to be closely assessed, before suggesting that this laboratory observation can be presented as a field phenomenon.

It is not possible to directly compare stress controlled and strain controlled tests, because the steady state condition cannot be sustained for a long period in a stress controlled test on laboratory sized samples. (Natural variations in strength as a function of platen rotation in the ring shear apparatus, invariably lead to unsteady displacement rates, as discussed in Chapter 7.) However, a creeping landslide is effectively a stress controlled



- (1) Range between the field lowest and field highest rate of movement for reactivated landslides and mud-flows (Skempton, 1985).
- (2) Range of rates of displacement used in this research work.
- (3) Range of movement scale (Varnes, 1978).

Fig 2-3 Variation of residual strength of cohesive soils with rate of displacement
(From Tika, 1989)

'test' where the large scale will suppress the proportionate fluctuations in resultant strength. Under these conditions, a steady state phenomenon should be independent of whether stress control or strain control is applied. For this reason, the type of control is not considered to be a likely explanation for the apparent lack of field observation of the reverse rate effect.

Lemos et al (1985) report two soils (Cowden Till and Happisburgh Till) which show reversed rate effects. On further discussion Skempton (pers comm) checked Lemos's test results and indicated that the scatter in the Cowden Till data, is such that the (extremely strong), reversed rate effects reported originally, could not be substantiated unequivocally. Skempton did suggest that the Happisburgh Till data appeared more reliable, but the reversed rate effect is much weaker in this case. Samples of neither material were available for confirmatory testing by the writer.

2.2.2.2 Loss of soil during testing

A common feature of ring shear testing is the loss of material from the sides of the confining rings. Lemos did not consider this significant. It is clear from examination of his data, that all three of the examples reported by Skempton (1985) reduced in thickness by about 0.02 mm in 50 mm of shearing displacement. In other words, if it could be assumed that at least some of an original shear zone (0.02 mm thick from the evidence above) **must have been displaced/replaced** or at least disturbed in some manner, in 50 mm of fast shearing, then the **applicability of the fast laboratory tests to the field situation must be highly questionable**. All the above tests were carried out to about 200 mm displacement, ie the opportunity was present for the **shear zone to be totally replaced 4 times** during each individual stage of fast shearing. It appears highly significant to the writer, that for those tests which show marked loss of strength, losses become pronounced by the stage at which displacement reaches about 50 mm.

An example of the way in which Lemos (p 213-217) tested at varying rates of shear is appended (Figs. 2-4a to 4e). This case has been selected because it includes testing with the confining ring gap closed. Stage 4 was fast sheared at 400 mm/min, with the gap open and minimum strength decreased to about half the slow residual value. Only the last stage was fast sheared with the gap closed. For this stage (following Stage 16) it was reported:

"A last stage of 400 mm/min was carried out with the gap closed, in order to assess the influence of the soil squeezed through the gap on the decrease in strength during the fast stage. Although the amount of soil squeezed was small and some friction was developed in the gap, there was quite a sharp drop in the shear resistance. The soil resistance can only be assessed qualitatively because of the friction in the gap."

Kalabagh Dam sample 910
Test No 3

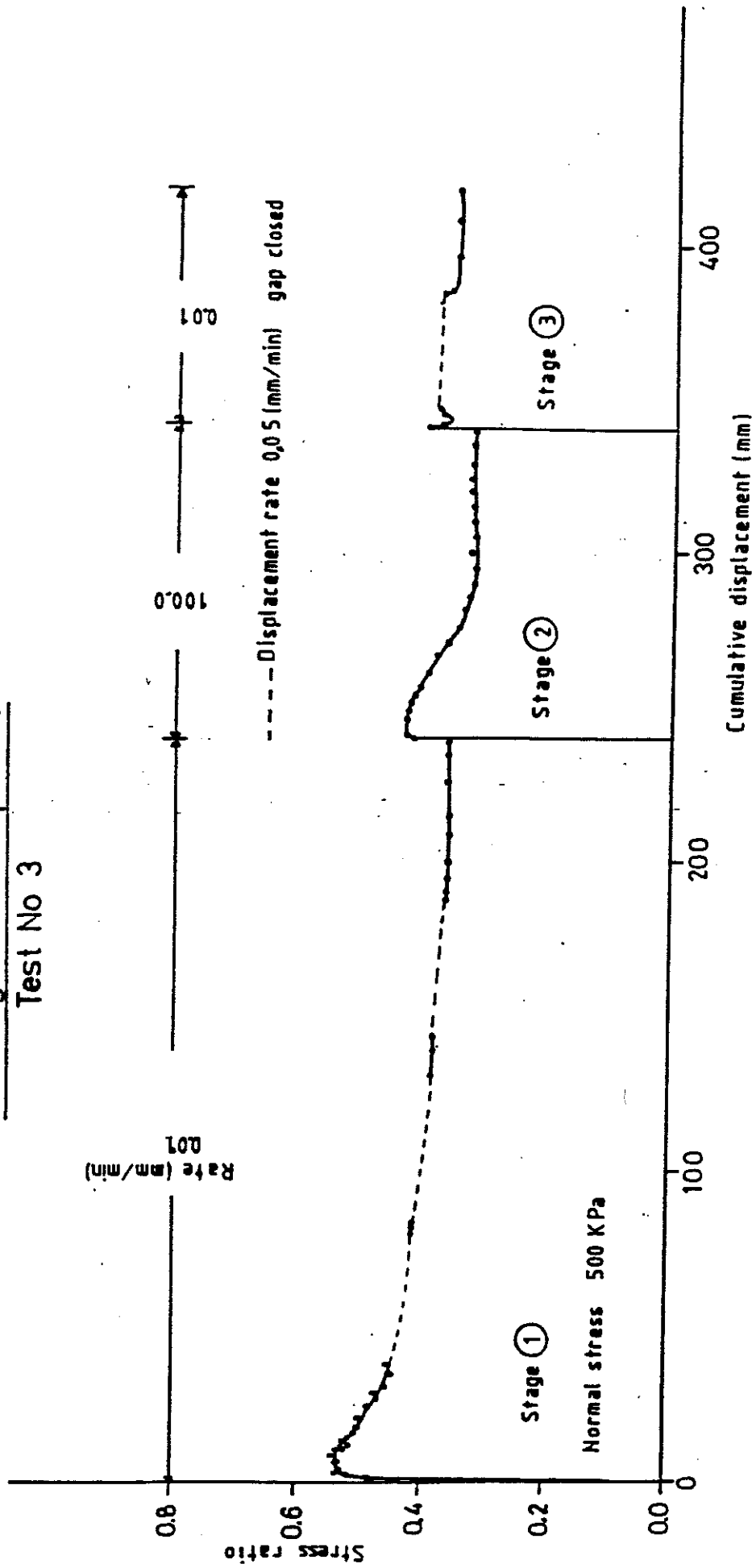


Fig. 2-4a Residual strength rate effects
(from Lemos, 1986 p 231)

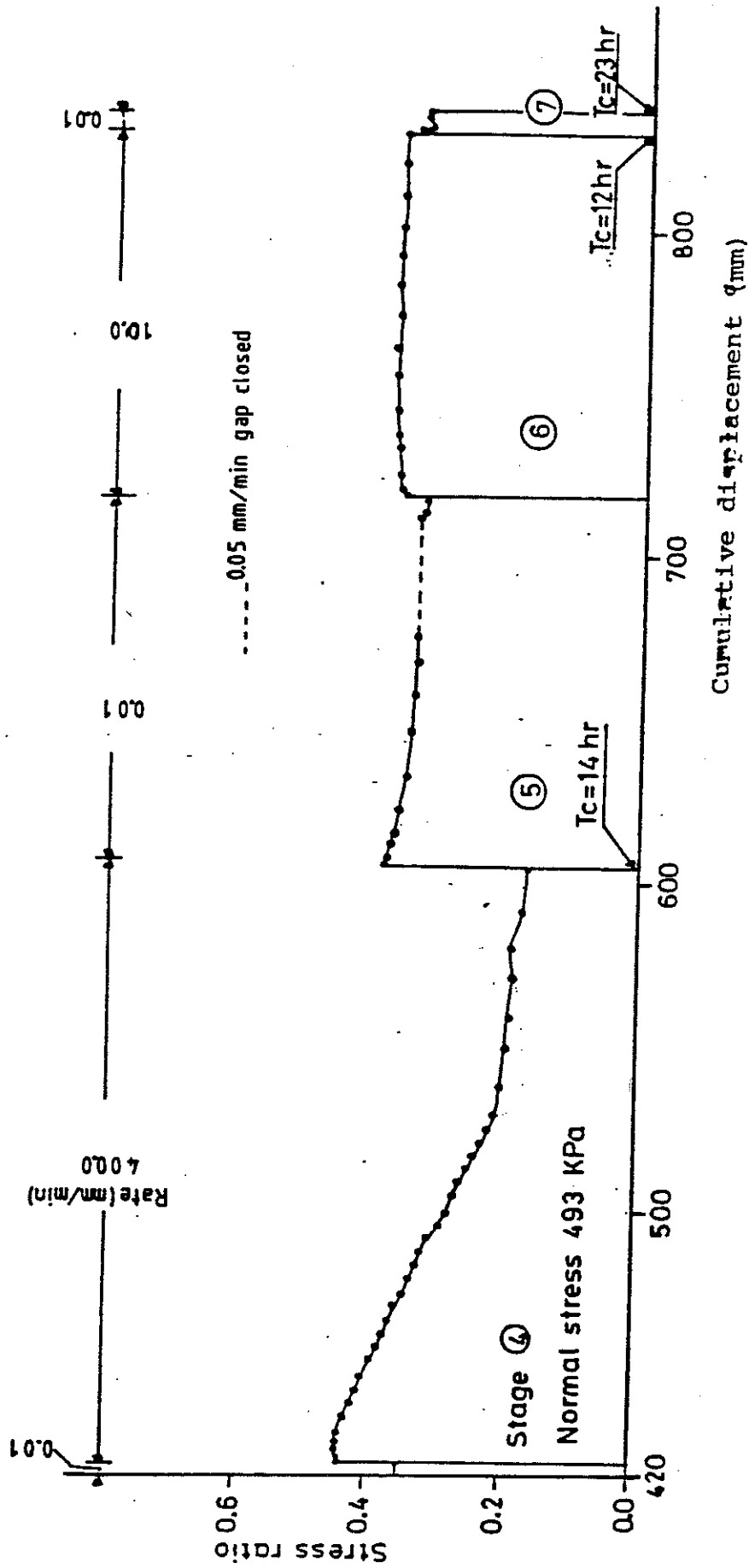


Fig. 2-4b Residual strength rate effects
 (from Lemos, 1986 p 232)

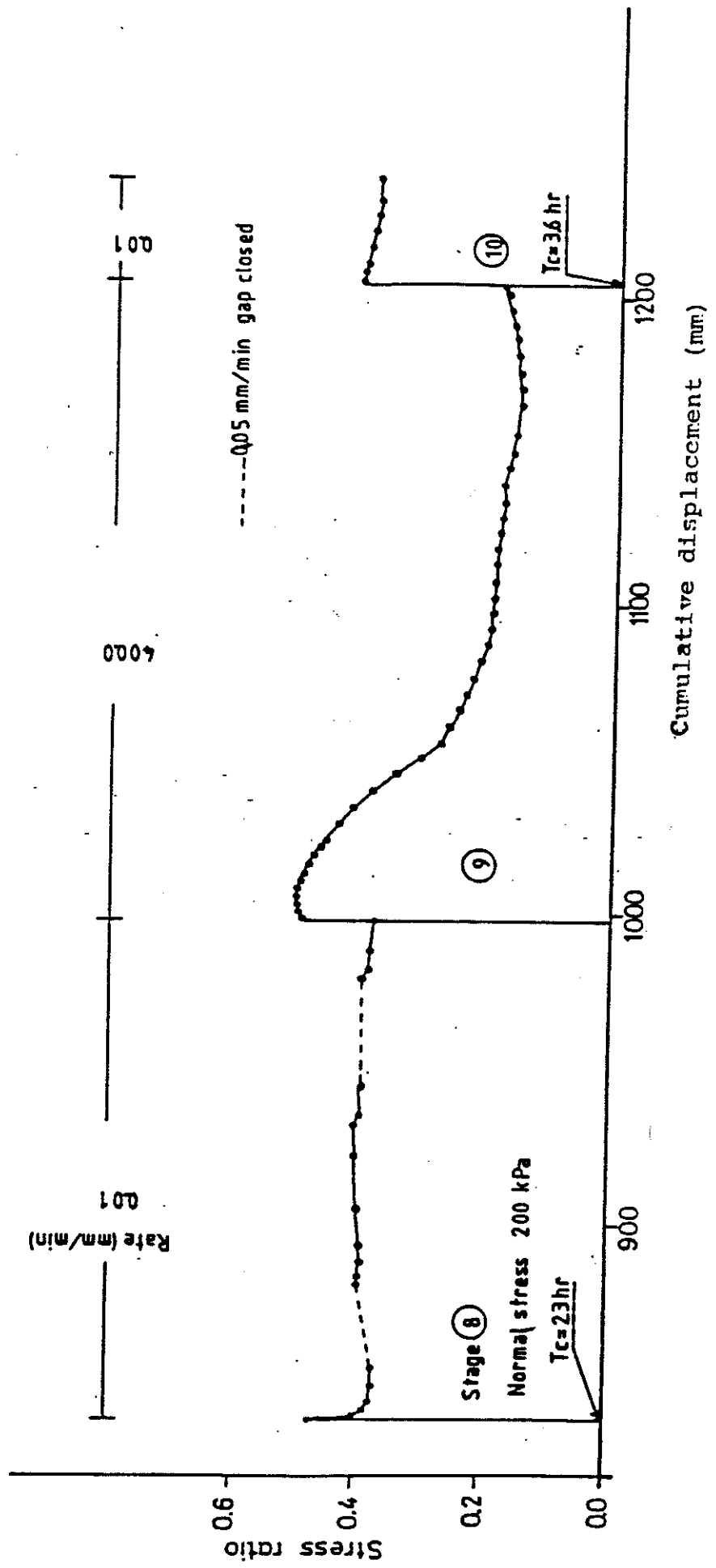


Fig. 2-4c Residual strength rate effects
 (from Lemos, 1986 p 233)

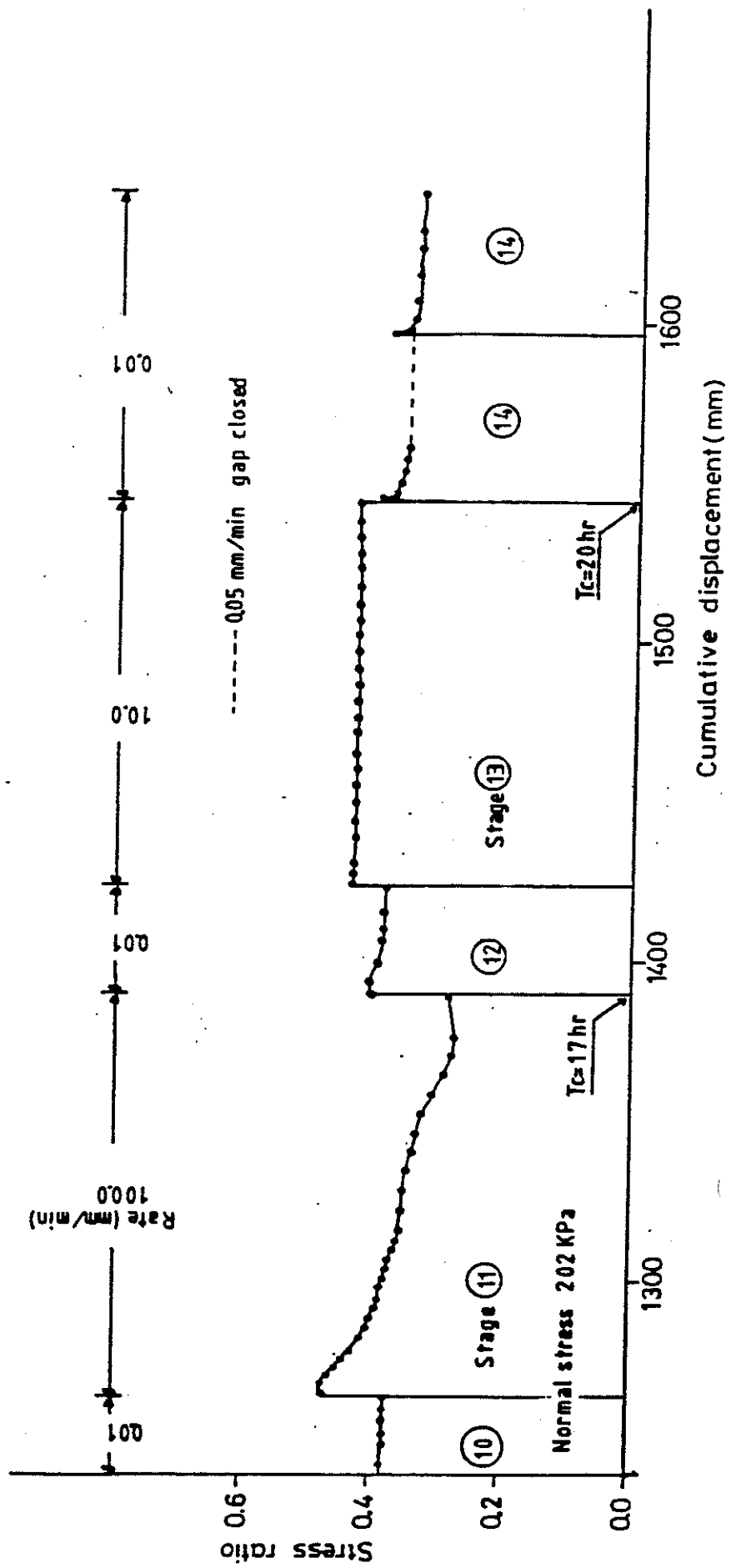


Fig. 2-4d Residual strength rate effects
 (from Lemos, 1986 p 234)

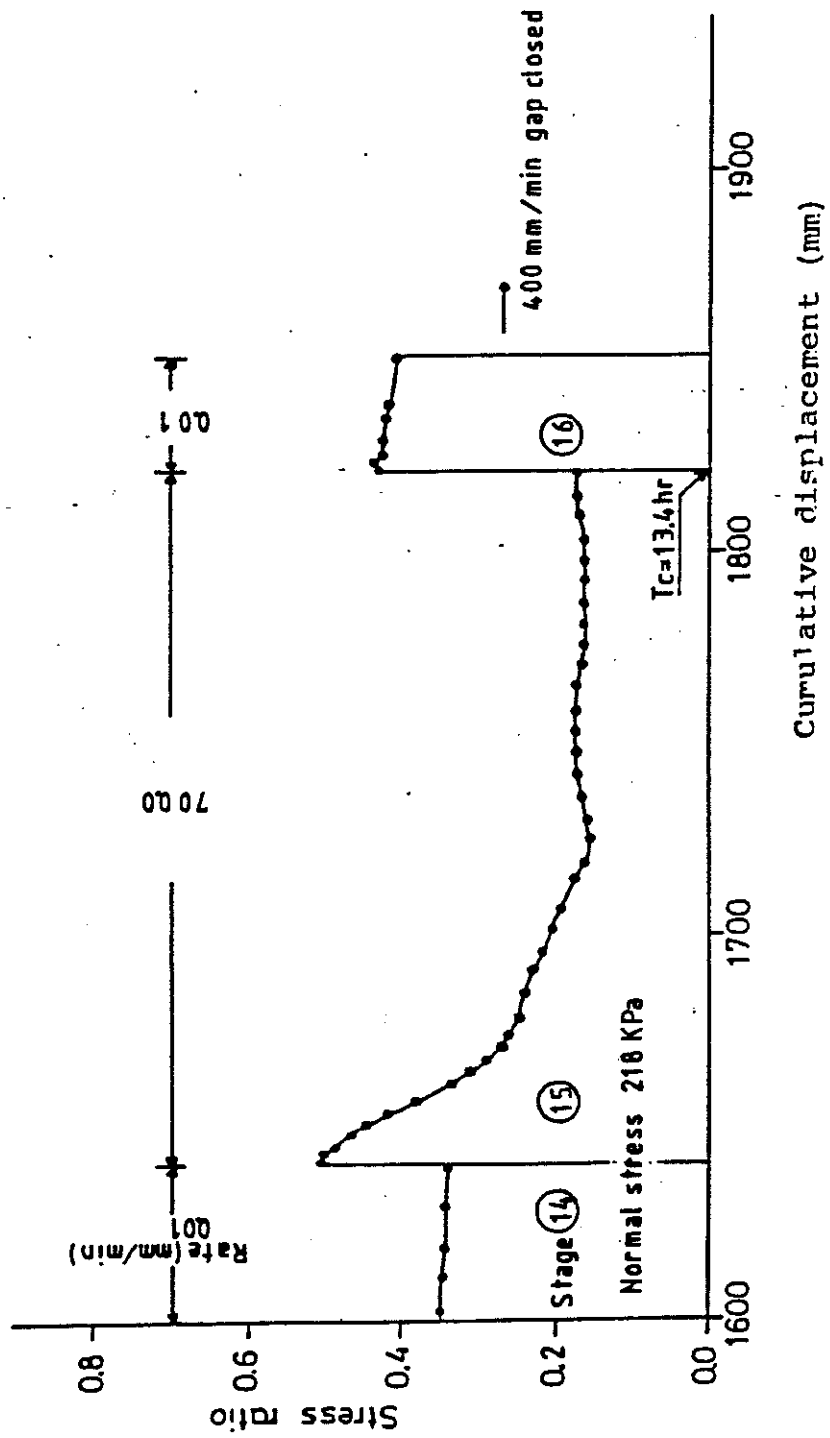


Fig. 2-4e Residual strength rate effects

(from Lemos, 1986 p 235)

Lemos concluded that the drop in strength "does not seem to have been due to the soil loss" however there must be reservations because:

(i) The test was qualitative, not quantitative, and it is unclear how the assessment was made.

(ii) Some soil was in fact still lost.

2.2.2.3 Mechanism of strength loss during rapid shearing

Tika (1989) undertook a number of tests to investigate mechanism for the loss of strength at fast rates of displacement. One argument put forward (p 183) was that in cases where fast shearing was continued for a time which was comparable to the consolidation time, then strengths should have reverted to the slow strength (under the excess pore pressure hypothesis) because excess pore pressures created by fast shearing would have had time to dissipate. The writer suggests that Tika may not have accounted for the changes which are on-going as a result of loss of soil. Excess pore pressures would be continually maintained by the new soil entering the shear zone, and the low strength persisting during prolonged fast shear (Tika, Fig. A2.55) meets (rather than refutes) that expectation.

Tika attempted to measure pore pressures directly with a transducer placed at the base of the sample. The measures taken to de-air the base are well described, (p. 168) but de-airing of the sample is not. The response of the system to an increase in normal stress on the sample is given as 25 minutes and 55 minutes for sample thicknesses of 9.8 and 12.5 mm. Tika's initial tests with pore pressure monitoring provided results which reportedly "cannot be considered conclusive with regard to the role of pore pressure during fast shearing".

The writer has also attempted installation of a transducer in the base platen of a ring shear apparatus. De-airing was readily accomplished in the base, but it proved impractical to de-air the sample itself. Less than 5% of the expected pore pressure (from instantaneous loading of a "saturated" sample) was recorded in the transducer. The only means envisaged to obtain meaningful results would be sedimentation in de-aired water or air replacement (eg the carbon dioxide method sometimes used for saturation of triaxial specimens) and then shearing within a waterbath of de-aired water. This has not been pursued in view of the time required for sample preparation, and apparatus redesign.

Tika (1989) has addressed the problem of loss of soil from the confining ring gap. It was reported that in two tests 'the gap was completely closed. Hence the loss of soil was slight.' The 'slight' loss was not quantified. The first test was Stage 17 of Test 3. The data table for Stage 17 states "No recording was performed". The second was Test 17 (Tika's p 388-391), appended here as Figs. 2-5a to 2-5d. In this test the confining ring gap was closed and the minimum stress ratio during fast shear was 0.14. By stages 15, 16 and 17,

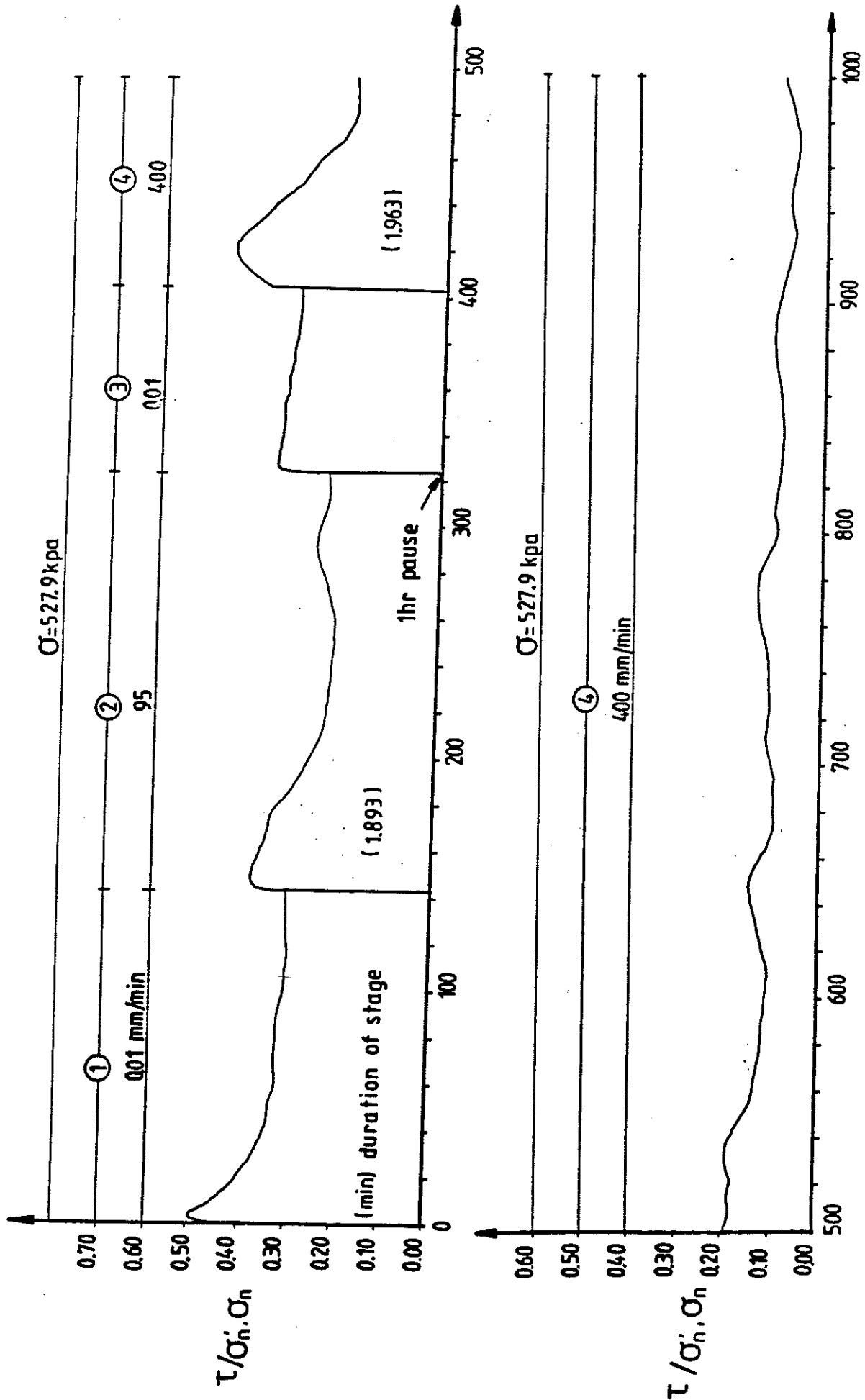


Fig. 2-5a
 (From Tika, 1989) - Ring shear test 17 on clayey siltstone D

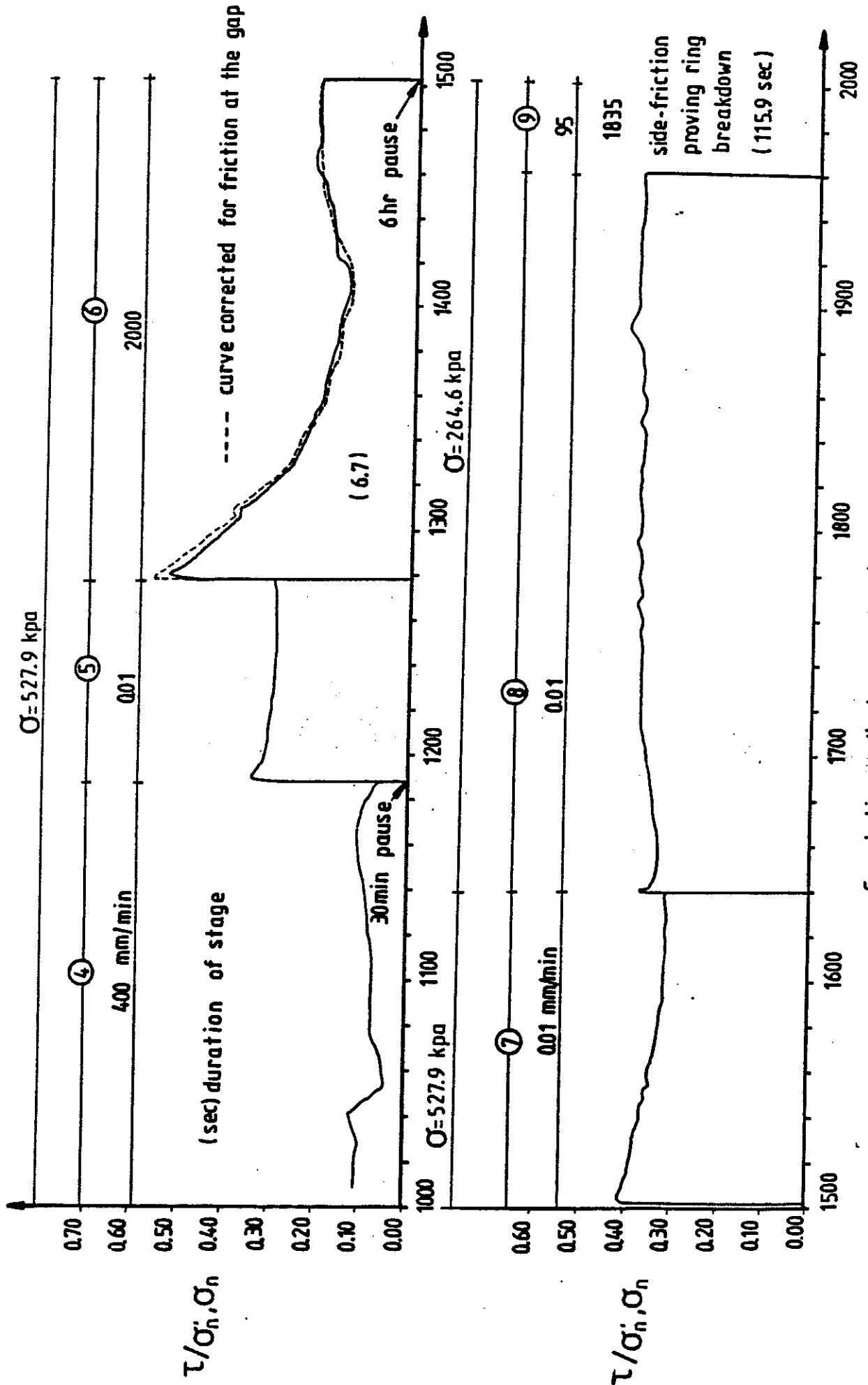


Fig 2-5b

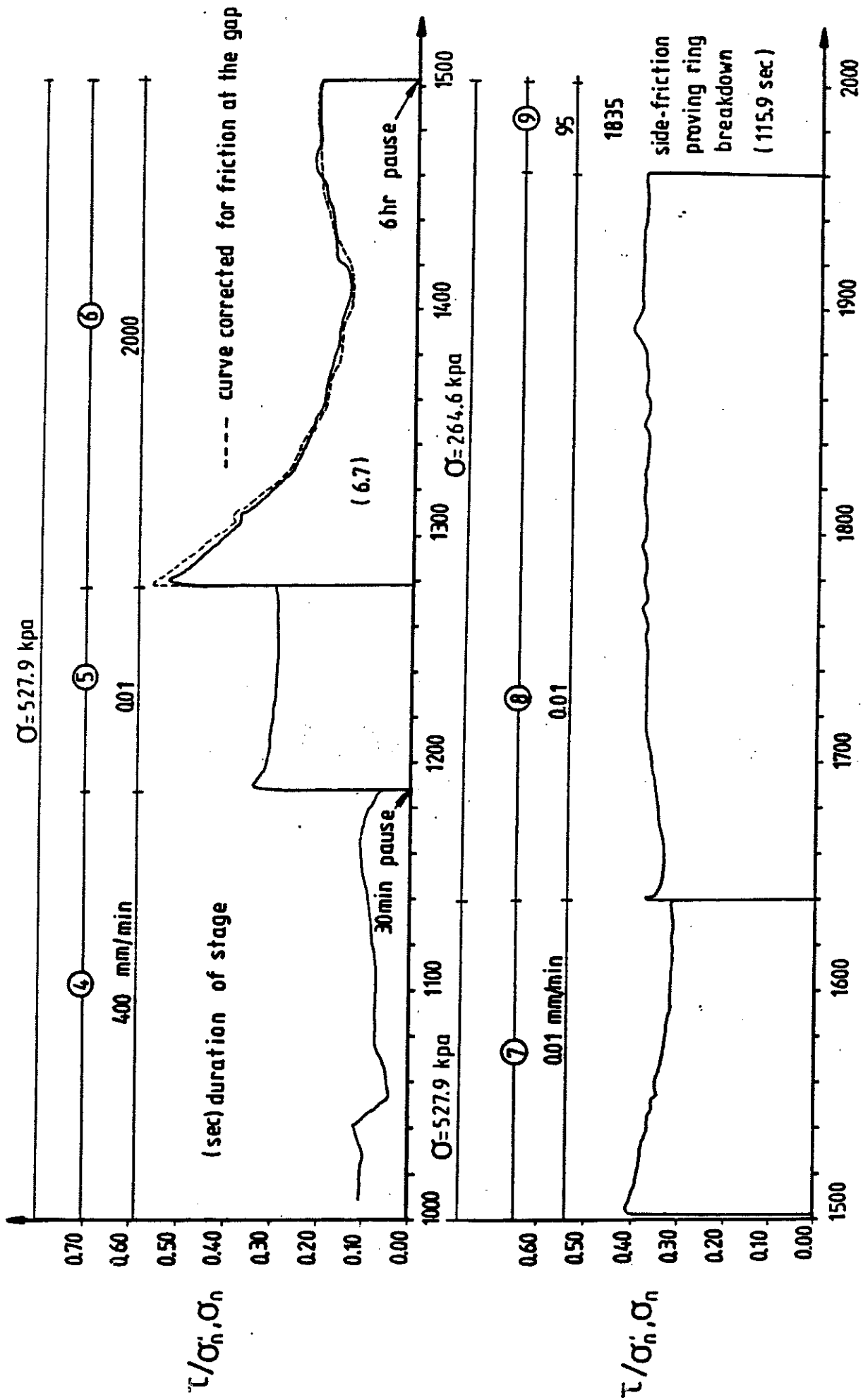


Fig 2-5b
Ring shear test 17 on clayey siltstone D

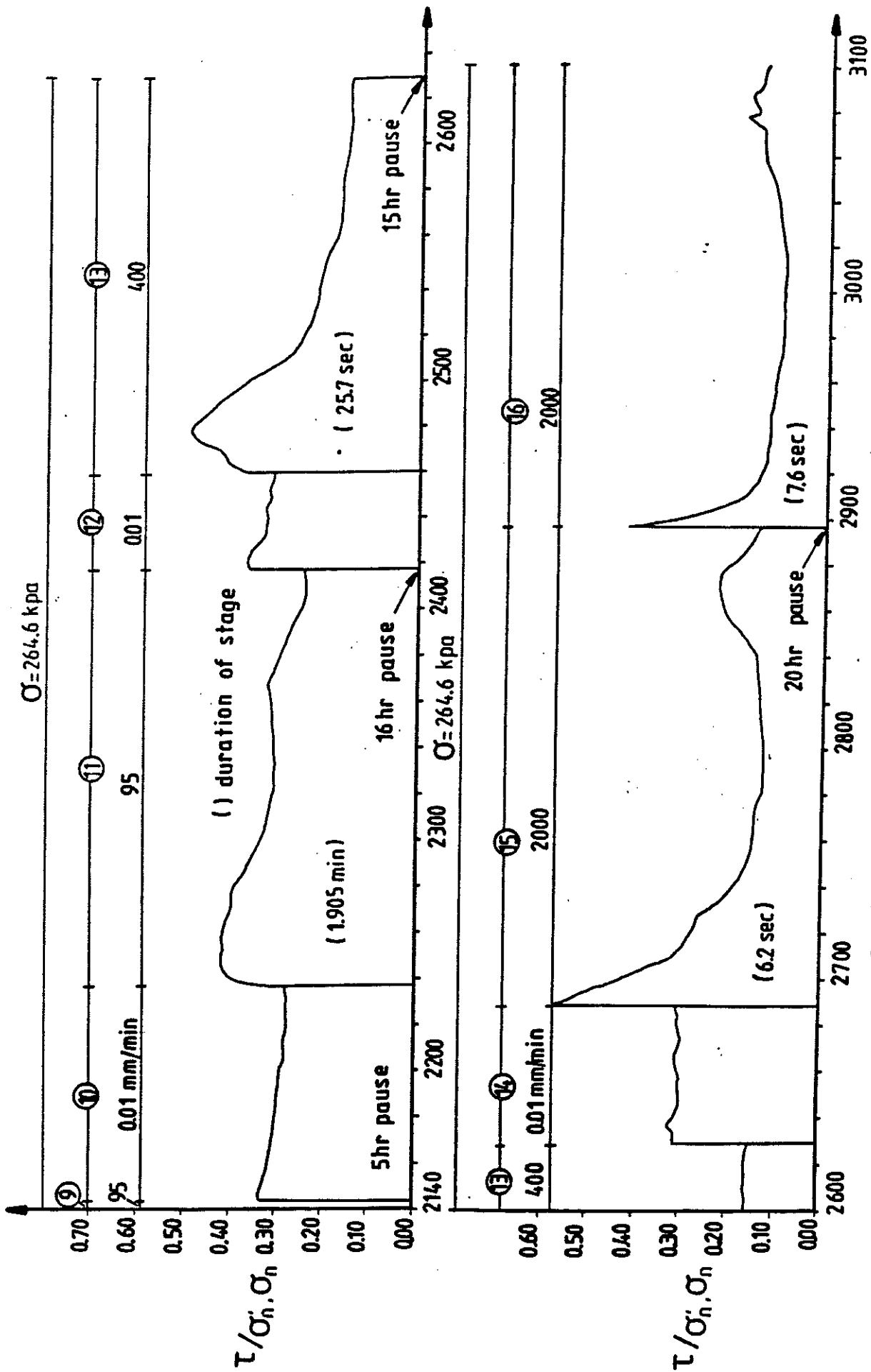


Fig. 2-5c
 Ring shear test 17 on clayey siltstone D
 (From T1ka, 1989)

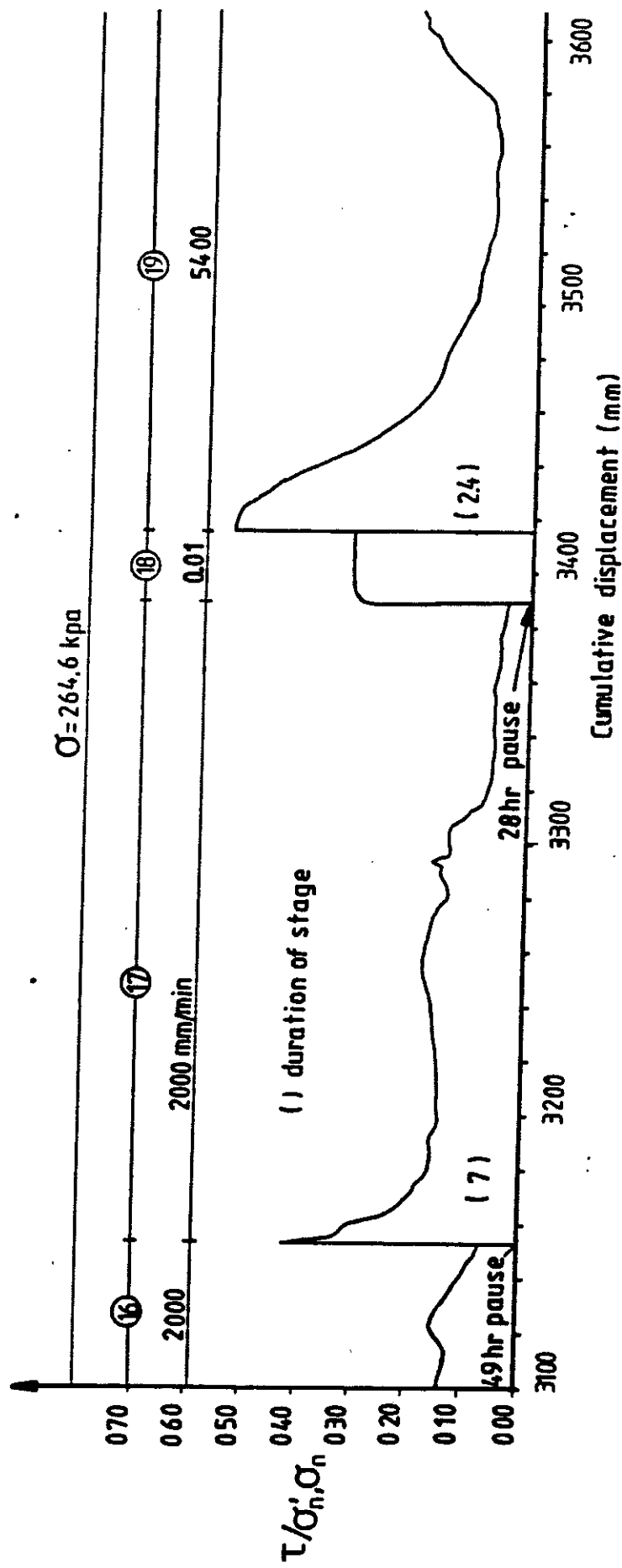


Fig. 2-5d
 Ring shear test 17 on clayey siltstone D
 (From Tika, 1989)

another variable had been changed, ie the normal stress had been halved, thus no rigorous comparison can be made. However the minimum stress ratios for these stages were 0.126, 0.098 and 0.99, ie even if only the highest of the last 3 values is taken, there appears to be a **distinct reduction in strength** caused by opening the confining ring gap. Tika states that at lower normal stresses, soil losses are reduced. Therefore the change of more than 1 parameter between tests does not detract from the alternative argument that excess pore pressures may well be the most logical explanation for the observed phenomenon.

Tika (p. 185) found that 'faster rates of displacement had to be applied for the loss of strength to occur' when comparing interface tests with soil-soil tests. A simple explanation for this phenomenon is, in the writer's view, that replacement of soil in the failure may be substantially reduced in an interface test, therefore any strength changes from soil replacement would be reduced accordingly.

2.2.2.3 Pore pressures expected during residual shear

To consider pore pressure effects in the ring shear test, it is appropriate to refer to the commonly observed pore pressure response found from the standard triaxial test. It has often been demonstrated in triaxial testing of soils using undrained tests with pore pressure measurement of back-pressure saturated, isotropically consolidated samples, that for a moderately overconsolidated silty or clayey soil, the excess pore pressure will initially become positive. (See Fig. 2-6, Stage I). However it soon reduces, becoming negative at relatively small strains, (Stage II). For obvious practical limitations, most triaxial testing must be stopped at about this condition, but the state of the soil would be far from residual in a uniformly strained sample. It appears reasonable to suggest that if the pore pressure response could be monitored through to residual conditions, improved packing through alignment of platy particles would cause a reduction of the negative excess pore pressure (Fig. 2-6 Stage III) or even positive pressures. Ultimately, the rate of change of pore pressure with strain must tend asymptotically to zero, by definition of the steady state condition (Stage IV, steady state). If consolidation is allowed at any time, then the excess pore pressures will become zero and the subsequent rate of change of pore pressure with displacement will be slightly different as a result of the change in void ratio that takes place during the consolidation phase. However, pore pressure changes with displacement are **most unlikely to be zero** for any soil which is changing from the a state of small strain to the highly strained residual strength condition in an active shear band.

In the ring shear apparatus a fully drained, anisotropically consolidated condition is developed (both within the body of the sample and at the shear zone) by the end of each slow shearing stage. This has a marked effect on the pore pressure response during further straining. If anisotropic consolidation has been completed at the Stage I condition, (ie drainage has allowed some water to leave the sample) then on further straining, pore pressures will decrease. If anisotropic consolidation has been completed at the Stage II or III conditions, (water would have entered the sample) then on further straining, pore pressures will increase.

Undrained pore pressure response
Shearing of overconsolidated soil
to large strains

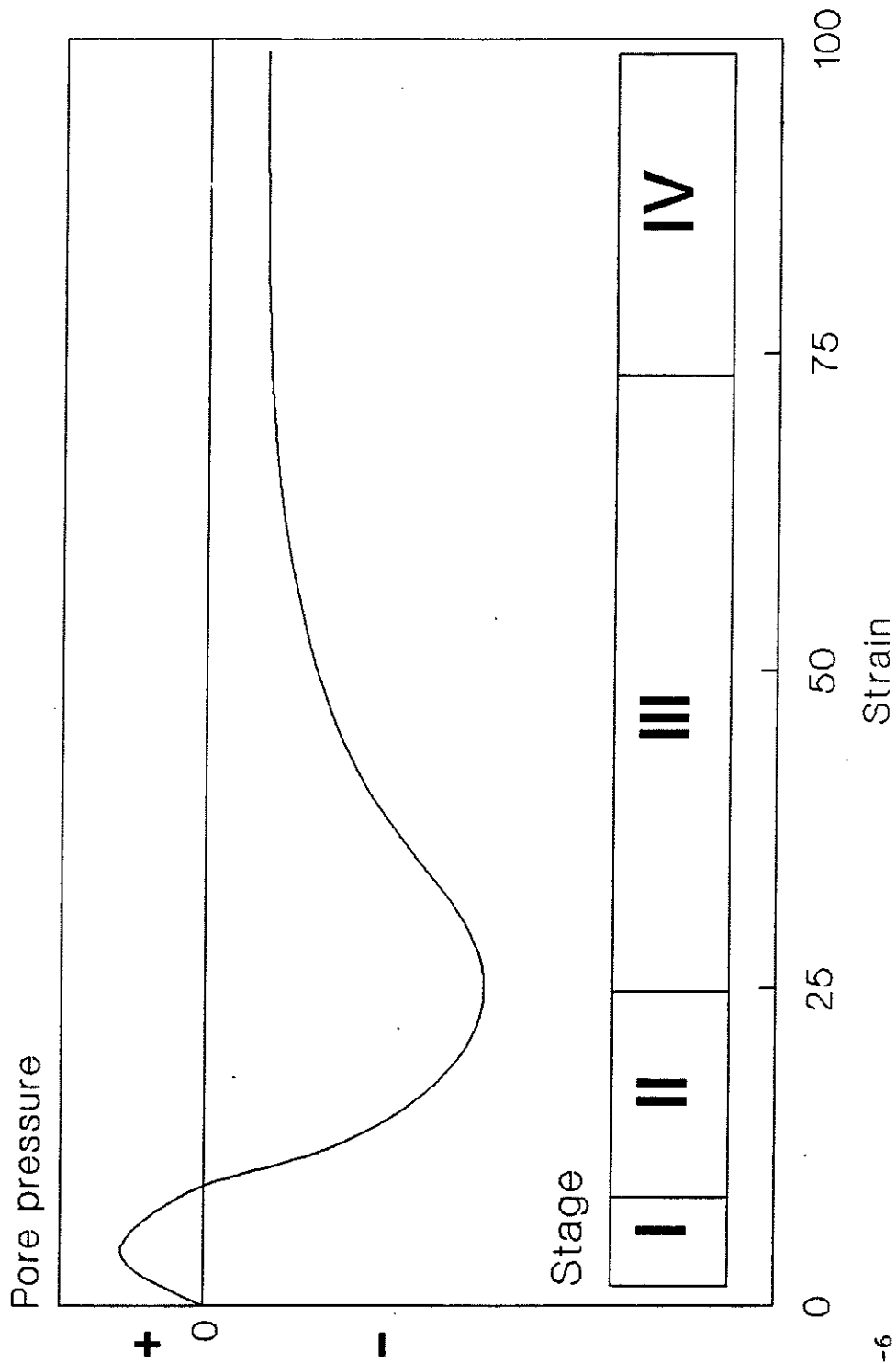


FIG 2-6

In the Bishop type ring shear, the presence of vanes would suggest that after slow shearing, the state of the soil would grade towards the shear surface, through all four stages (I to IV). The point being made is that **pore pressures may either increase or decrease** as a result of extended straining. Only soils which have been fully strained to the residual condition can be expected to have no pore pressure response to strain.

Therefore, in ring shear testing, where fast shearing causes extrusion of soil from the apparatus, the pore pressure response of the replacement soil cannot be dismissed. The replacement soil is clearly both anisotropically consolidated and its particles are not aligned in the residual state condition. Excess pore pressures (either positive or negative) must be expected whenever soil is extruded from the ring shear apparatus.

This alternative explanation for the interpretation of rate effects in soils subjected to rapid shear in the laboratory, leads to the possible conclusion that an **apparatus effect, of no relevance to field conditions**, may have been observed. Much of the soil which was initially at slow residual strength in the thin shearing zone of the ring shear would have been extruded from the gap in the confining rings, and predominantly new soil (without the structure or void ratio appropriate to the residual strength state) has been tested.

2.2.2.4 Summary of alternative explanations

The following possible explanations should be considered before adopting strength parameters from fast ring shear tests.

- (i) The maximum fast strength is produced partly by steady state rate dependence (where general drainage and no soil replacement occurs) but the effect may be either enhanced or diminished because the effective normal stress would be altered by excess pore pressures transmitted to the failure surface after being induced within the body of the sample, by soils in either the Stage I II, or III condition.
- (ii) The minimum fast strength is produced by a combination of opposing effects:
 - (a) rate dependence with steady state drainage
 - (b) excess pore pressure transmitted from the body of the sample
 - (c) replacement soil with effective strength greater than residual
 - (d) excess pore pressure developed from replacement soil
 - (e) partial equalisation and drainage of excess pore pressures

The process is compounded as soon as the fast shear strength decreases below the slow residual value, because then pore pressures transmitted from the body of the sample will change in sign.

(iii) The reason that the minimum fast strength appears lower in the laboratory for silty soils rather than with sands or clays, is simply because there are multiple effects involved, some predominating as particle size decreases and vice versa. Their combination produces greatest strength decreases in silty soils.

Firstly, the steady state rate dependence of residual strength is more marked in more finely graded soils, as shown in Chapter 9, Fig. 9-3. Secondly, both the permeability (and hence rate of transmission of excess pore pressures) and magnitude of excess pore pressures, should increase with increasing particle size, initially promoting the effects described in (ii) above. However, if the grading of the soil is sufficiently coarse to allow complete dissipation of pore pressure throughout the sample, strength will be unaffected by excess pore pressures. Thirdly, the thickness of the active shear zone and hence the rate of extrusion of soil at the confining ring gap would be expected to increase with increasing particle size.

The 'reversed' rate effect at slow displacement rates has not been confirmed from testing of any soil testing in the ring shear apparatus designed by the writer.

The 'conventional' rate effect (increasing residual strength with displacement rate) is probably explained by a combination of particle rheology and pore pressure dissipation. The former may be a strength dependence caused by the observed phenomenon of greater resistance to breakage and bending under fast loading (ie as seen in the standard concrete compression test) and could be confirmed by testing dry soils. The pore pressure effect is, however, likely to be more significant. Although overall 'steady state' conditions can be achieved in a ring shear test, the discontinuous nature of any particulate medium will require both positive and negative pore pressures to develop momentarily as individual grains collide or are pulled apart on an active shear surface. The relevant consideration is that the local drainage is likely to be at a slower rate for negative pore pressure changes than for positive changes. The reasoning is that soil with positive pore pressure would be slightly below its critical void ratio (more dense) and hence of slightly lower permeability. The converse would apply to zones of positive pore pressures. Therefore equalisation would take a longer time for negative pore pressures than for positive, resulting in a net decrease. According to the effective stress principle, the net decrease in pore pressure necessitates an increase in average effective stress. The increase in average effective stress will increase when less drainage is able to occur, ie as the rate of shearing increases. The expected result would be a net increase in strength with increasing displacement rate.

(iv) The initial peak strength observed when reshearing at slow rates after fast displacement is due simply to the presence of new material, introduced into the failure zone during fast shearing. Continued displacements are required to allow this soil to attain the structure and void ratio applicable to the residual state condition.

2.2.2.5 Contrary arguments

Tika concluded that 'the pore water pressures, measured during fast shearing cannot account for the loss of strength'. In view of the difficulty of measuring pore pressures in this situation, it is hard to reconcile these conclusions with Tika's measurements which show that once fast shearing ceases (ie no new soil is being introduced into the active failure zone) pore pressures do account for a very large proportion of the effect. Furthermore, if the concept of ongoing introduction of new soil into the failure zone is accepted, it is clear that pore pressure adjustment will be least at the centre of the annulus (because by symmetry, the soil in this point will be subject to minimal lateral force and hence minimal replacement). Logically, zero excess pore pressures must be present immediately adjacent to the confining rings, maximum excess pore pressure would be expected at about the quarter points in the annulus, reducing to much smaller values at the annulus centreline. After cessation of shearing, excess pore pressures would initially be expected to equalise, ie increase at the centre of the sample and decrease at the quarter points.

Tika (p 188 equation 6.2) investigated the influence of frictional heating on pore pressure generation. It is stated (p 194) that the coefficient of volume compressibility of the soil was 'estimated from the consolidation stage of the ring shear tests'. For the case used it is the swelling (rather than consolidation) modulus that should have been adopted. Unless the swelling modulus is used the pore pressures would be grossly underestimated. Nevertheless, the writer suggests that loss of soil from the confining rings and the degree of saturation achieved in the soil would be much more dominant effects.

2.3 CONCLUDING REMARKS

(i) There are practical objections to the laboratory findings of a drop in fast minimum strength to below the slow residual:

(a) No field examples have been cited by the originators, for which fast movements can be reasonably explained by the laboratory phenomena. To the contrary, Tika (p 49) states 'the results ... are unrelated to field observations of earthquake induced landslides or other fast movements'. Tika tested soil from the large Ontake landslide triggered by the Naganoken-Seibu earthquake of 1984. The results 'indicating a negligible rate effect, did not corroborate the anticipated loss of strength at increasing rates of displacement required to interpret the high mobility of the landslide'.

(b) Terzaghi (1950) refers to the forgiving nature of fine grained soils (at residual strength): " if a violent earthquake shock strikes a slope on plastic clay with low sensitivity, it will hardly have any effect beyond the formation of tension cracks along the upper edge ... because the viscosity of the clay interferes with more extensive displacements under impact"

(c) The extensive review of case histories in Appendix 5, has found no examples of seismically induced landslides which require such a mechanism to be invoked in any example involving silty soils, ahead of widely acknowledged explanations such as liquefaction, first-time sliding, etc.

(ii) The effect of earthquake loading of shear surfaces in slopes may best be judged from field evidence (geological precedent in similar materials), at least until laboratory procedures for fast shearing of soils at residual strength can be demonstrated to be applicable to field conditions.

CHAPTER 3

LABORATORY TESTING

3.1 INTRODUCTION

In the course of work carried out for various slope stability projects, considerable evaluation of appropriate strength parameters to use in analysis and design has been carried out. This chapter has been limited to only those aspects which are considered to be new approaches or which show how a technique has been applied in practice. The topics covered are the changes in effective strength caused by saturation of partially saturated soils at residual strength and high stress testing. These address strength parameters determined from laboratory testing while a complementary approach which is primarily based on field assessment of strength parameters is contained in Chapter 4.

3.2 EFFECT OF SATURATION ON SHEAR STRENGTH

3.2.1 General

A search of the available literature has revealed very little information, either qualitative or quantitative, that addresses the effect of saturation on strength parameters.

Kenney (1986) reports that in

"natural environments the surfaces of clay minerals are covered by water molecules, and therefore they are wet even in so-called 'dry' natural conditions. In the case of minerals such as quartz and calcite, water acts as an antilubricant (ie. water causes $\tan \phi$ to increase). Therefore, it should not be assumed that wetting caused by raising a reservoir, will cause the reduction of $\tan \phi$ of either rock or soil.

The property $\tan \phi$ is also affected by the magnitude of normal stress, decreasing slightly as normal stress is increased. Submergence by a reservoir will usually cause decreases of normal stress and therefore will usually cause small increases in $\tan \phi$.

Taking account of these two influences, it is concluded that an acceptable assumption regarding the static friction coefficient of rock or soil is that it is unaffected by reservoir level.

Soils that are in an unsaturated state possess pore water tensions that elevate the shear strength of the soil. Submergence reduces the pore water tensions and reduces shear strength."

The last two paragraphs appear to be in reversed order, for Kenney's meaning to be clear. The article does not attempt any quantitative justification of the problem.

In view of the limited information available, a parametric study and a laboratory programme was undertaken to examine the validity of assuming no significant change in strength with saturation.

3.2.2 Basic Concepts of Effective Stress in Unsaturated Soils

The effect of soil suction on slope stability has been addressed in the literature with respect to superficial potential failure surfaces (maximum depth of only a few metres). However, the studies found, relate only to peak strength parameters and do not address the effect of total saturation expected by reservoir formation. No case history of suction loss on saturation for a deep seated slide has been located. Furthermore, no case history has yet been located which addresses the residual strength of partially saturated soils, either in the field or the laboratory.

The peak strength characteristics of partially saturated soils have been addressed by Bishop & Blight (1963), whose formulation is summarised below. More recent work has been carried out by others (including Fredlund), suggesting alternative constitutive relationships.

For unsaturated soils, the extended effective stress equation (Bishop & Blight 1963) is:

$$\sigma' = \sigma - u_a + \chi(u_a - u_w) \dots\dots\dots(1)$$

where,

- σ' is the effective normal stress
- σ is the total normal stress
- u_a Is the pore air pressure
- u_w is the pore water pressure, and
- χ is an experimentally determinable coefficient

The coefficient chi takes into account the proportions of pore space over which u_a and u_w act and the effects of the surface energy forces at the air-water interfaces in the soil. If it is assumed that over a limited range of normal stress the material may be characterised by a linear strength envelope, the shear strength is given by in the usual manner by:

$$\tau = c' + \sigma' \tan \phi' \dots\dots\dots (2)$$

where c' and ϕ' are the effective cohesion and friction.

Combining (1) and (2) gives:

$$\tau = c' + (\sigma - u_a)\tan\phi' + \chi(u_a - u_w)\tan\phi' \quad \dots\dots\dots (3)$$

In terms of apparent cohesion (c), it is evident that by collecting the terms that are independent of σ from (3)

$$\tau = c + (\sigma - u_a)\tan\phi' \quad \dots\dots\dots (4)$$

where

$$c = c' + \chi(u_a - u_w)\tan\phi' \quad \dots\dots\dots (5)$$

For the steady state condition of a partially saturated soil (in the field for a long term situation) u_a will be zero. Therefore:

$$\tau = c' + \sigma \tan\phi' - \chi u_w \tan\phi' \quad \dots\dots\dots (6)$$

For the case where residual conditions pertain and c' is zero, it might be expected that:

$$\tau = \sigma \tan\phi_r' - \chi u_w \tan\phi_r' \quad \dots\dots\dots (7)$$

where the subscript r refers to residual strength. However more detailed study of this case is made in a subsequent section.

3.2.3 Parametric Study

To examine the likely effects of loss of suction on shear strength of typical slides a parametric study was attempted, as detailed below, to provide some insight regarding the accuracy to which properties would need to be determined.

Initially, equation (3) was input to the equation for limiting equilibrium (with $F = 1.0$) of a translational slide (Skempton & Hutchinson, 1969). Various values were considered for the strength loss, ie. $c' + \chi(u_a - u_w)\tan\phi'$, assuming full loss of this amount on saturation. Additionally, it was assumed that one third of the area of the slide toe would become saturated because the critical pool level (the depth of submergence that provides the greatest decrease in safety factor) for a gently arcuate slide frequently approaches

that proportion. For these conditions, the relationship between decrease in safety factor and slide depth is given in Fig. 3 - 1

The decrease in safety factor clearly diminishes with increasing depth of slide, but in order to evaluate the significance of the problem, likely values of the strength loss component $\chi(u_a - u_w)\tan\phi'$ need to be determined for the specific situation.

This may be conservatively estimated from a combined field/laboratory method. The suction ($u_a - u_w$) may be determined in the field, or from a very large in situ sample brought back to the laboratory, with a tensiometer. The residual friction angle can be determined in the laboratory with a saturated remoulded sample, and a probable upper bound for (χ) adopted from Bishop & Blight (op cit).

Again, the results are likely to be conservative for reasons discussed below. In particular, suction will be enhanced by excavation unloading of the tested sample. This can be minimised by deep penetration of the tensiometer into the excavation wall, or by using a reconsolidation technique in the laboratory.

Results from in situ tensiometer tests for one case of a clayey silt gouge, were field matrix suctions of 20 - 60 kPa, with no tendency for reduced suctions on deep seated crushed zones. Field tests carried out to determine whether suction decreased with further penetration away from the excavated face showed no significant trends. There are practical difficulties in installing a tensiometer more than about 1 m from any excavated face, so some (perhaps most) of the suction values recorded would be expected to have been caused by excavations. However, assuming conservatively that the above values are representative, the shear strength component for this case may be estimated approximately by substituting average measured values in conjunction with expected values from Bishop & Blight:

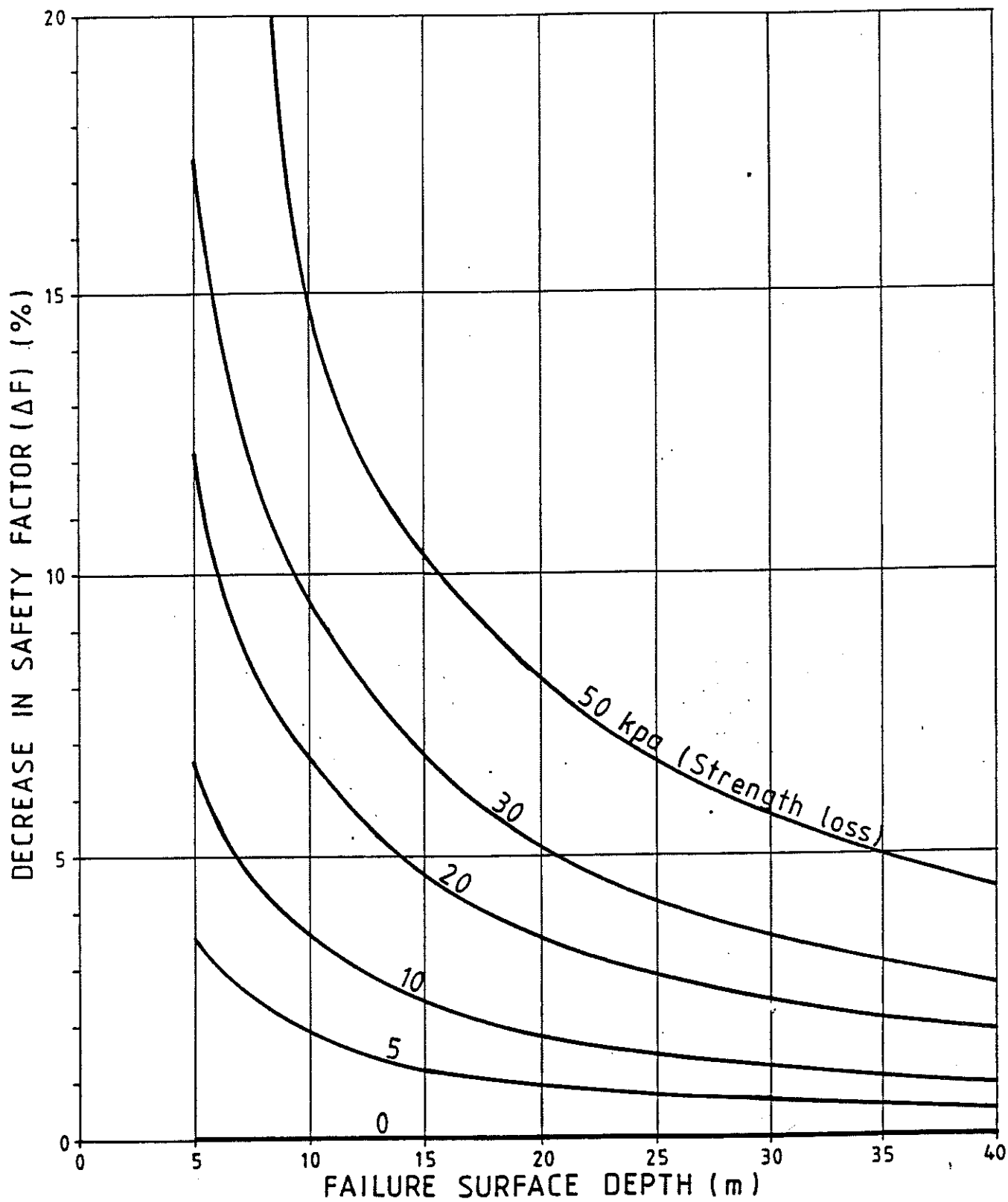
$$c = \chi (u_a - u_w) \tan\phi' = 0.9(40) \tan(23) = 15 \text{ kPa}$$

Taking this value, the initial conclusion from Fig. 3-1 was that the safety factor reduction on saturation could be quite significant for failure surfaces less than 10 m deep, about 3% for failure surfaces 15-20 m deep and less than 2% for failure surfaces deeper than 30 m.

To refine these estimates, typical values for suction parameters were sought from a literature search. No case history or information relating to partially saturated soils at residual strength could be located.

The difference in suction parameters between soils at low strains and those at high strains has not been reported, but it appeared reasonable to suggest that decreases in matrix suctions on saturation should be no worse for the residual strength case.

Accordingly, typical values from Bishop & Blight (1963) were adopted for a preliminary parametric study. The inferred relationships for suction parameters are shown in Figs



SATURATION EFFECTS : Parametric study of variable strength losses

3-2a and 3-2b. These represent oversimplifications, but appeared adequate for preliminary assessment.

By using these with the equilibrium equations for a translational slide with safety factor of 1.0 when unsaturated, the change in safety factor due to loss of strength on saturation may be estimated. (Note that any additional decrease in stability due to positive pore pressures would still need to be calculated separately, in the usual way). Four additional criteria need to be defined in order to substitute for unknowns:

- (i) the proportion of the failure surface area that will be submerged. A value of one third was adopted, but the effect of alternatives may be determined linearly.
- (ii) the effective residual cohesion of the failure surface material, taken as zero.
- (iii) the effective residual friction angle.
- (iv) the average topographic slope.

As both of the latter quantities will vary significantly from case to case, two parametric studies were carried out.

In Fig. 3-3 an effective residual friction angle of 25 degrees was assumed and sensitivity to topographic slope considered. In Fig. 3-4, a topographic slope of 35 degrees was assumed and effective friction angle taken as a variable. A combined parametric study is given in Fig. 3-5. To facilitate use of this figure, the following example has been shown:

Known conditions: 35 degree slope, 16 m deep failure surface, zero effective cohesion, one third of slide to become saturated.

Implies: 6% decrease in safety factor, soil effective friction angle of 29.5 degrees, strength due to suction of 32 kPa.

The implications of this preliminary study are that strength loss on saturation is relatively insensitive to topographic slope and friction angle within the ranges commonly encountered, but the depth to the failure surface is highly significant as it appears that:

- (i) failure surfaces less than 10 m deep appear to be highly affected by saturation, with safety factor decreases of over 10%.
- (ii) failure surfaces 15-20 m deep might still be significantly affected by saturation with safety factor decreases of about 5%.
- (iii) failure surfaces deeper than 30 m would be affected minimally (less than 1%).

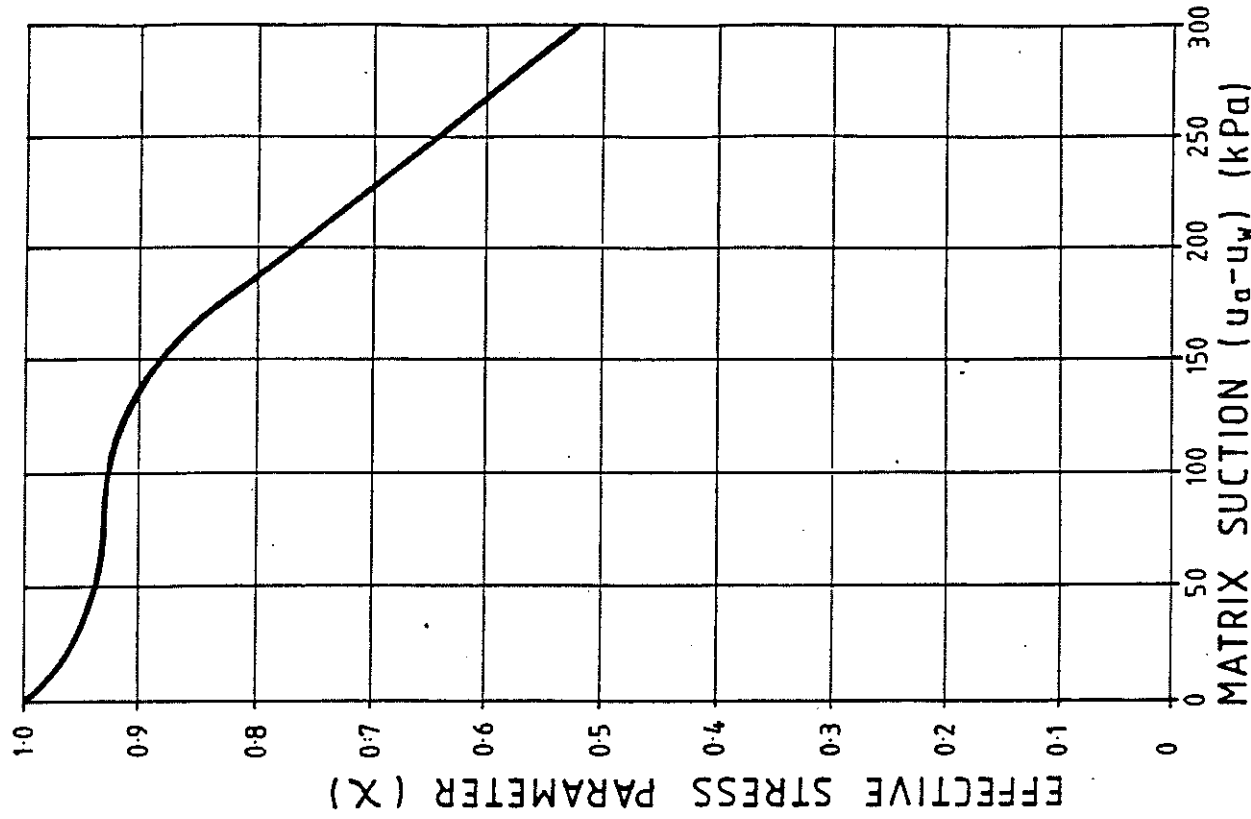
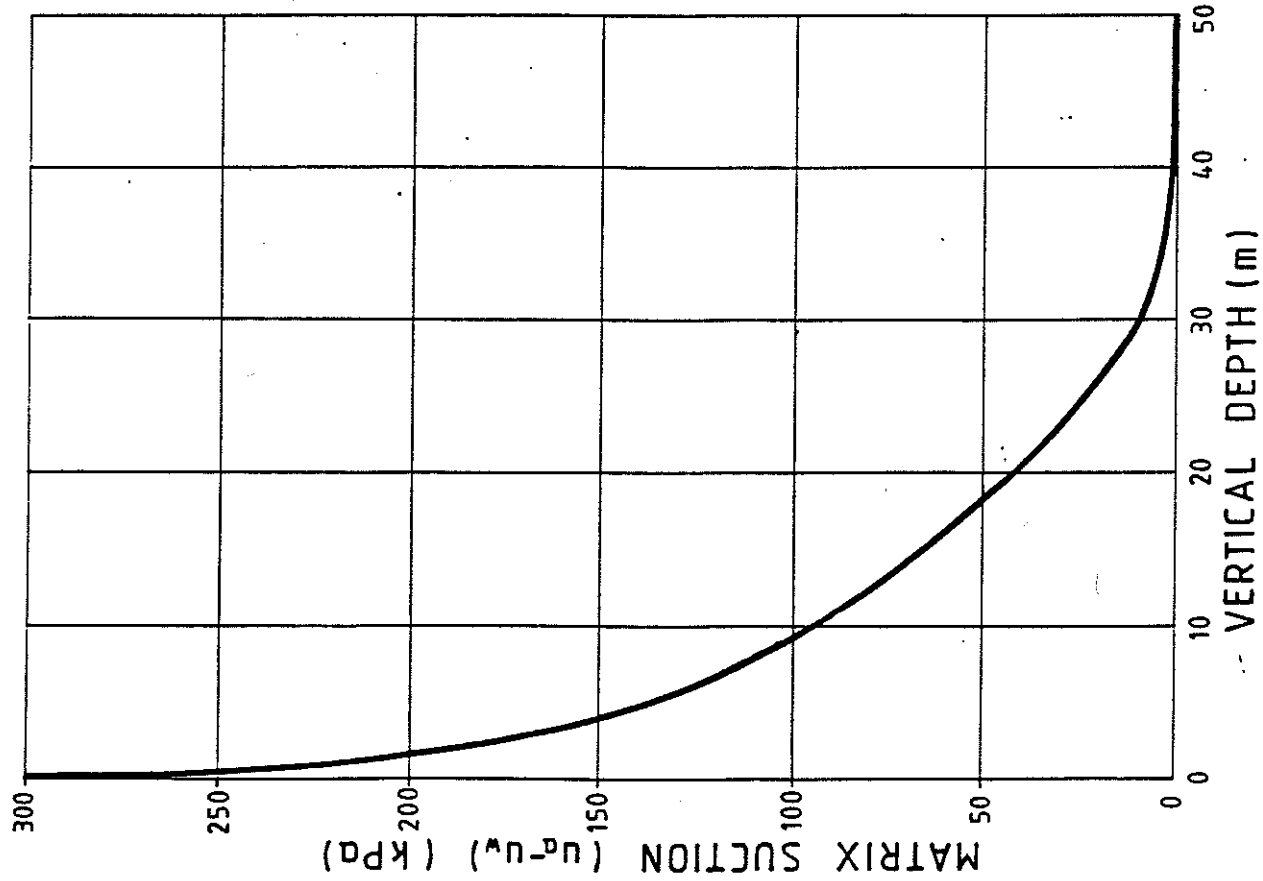


Fig. 3-2

TYPICAL STRESS PARAMETERS FOR UNSATURATED SOILS

b

a

3.2.4 Laboratory Ring Shear Tests

As described in detail below, one sample (E-43, a clayey silt) from the active failure surface of a slide subject to no groundwater influence was extensively tested to examine the effects of saturation. Particles larger than 1.18 mm were removed from a bulk sample which was then thoroughly mixed to allow re-testing of identical sub-samples.

The residual strength of saturated samples was determined in the ring shear in the usual manner, indicating a friction angle of about 23 degrees and pseudo-cohesion of 4 kPa.

Samples were remoulded at field moisture content (8.2%) and tested in the ring shear apparatus, pre-shearing for 1 metre before determining the residual strength of the partially saturated samples. After steady state conditions were achieved, water was added to both sides of the sample and a small hydraulic gradient imposed. This allowed comparison for three states referred to as: (a) saturated, (b) unsaturated (in situ moisture) and (c) wetted (Figs. 3-6 and 3-7). Results are shown in terms of the usual Mohr envelopes.

A range of normal stresses from 50 to 500 kPa was investigated. Testing indicated that at 50 kPa normal stress, sample edge effects and equipment resolution affected repeatability (Fig. 3-8). The initial objective was to test at as low a normal stress as practical in order to focus on definition of suction effects which might be expected to be proportionately less significant at high normal stresses. An optimum normal stress level appeared to be at about the in situ overburden pressure of the sample (116 kPa). Repeated testing was therefore carried out at this level (Fig. 3-9), showing reasonable repeatability. The result was a significant decrease in strength with wetting.

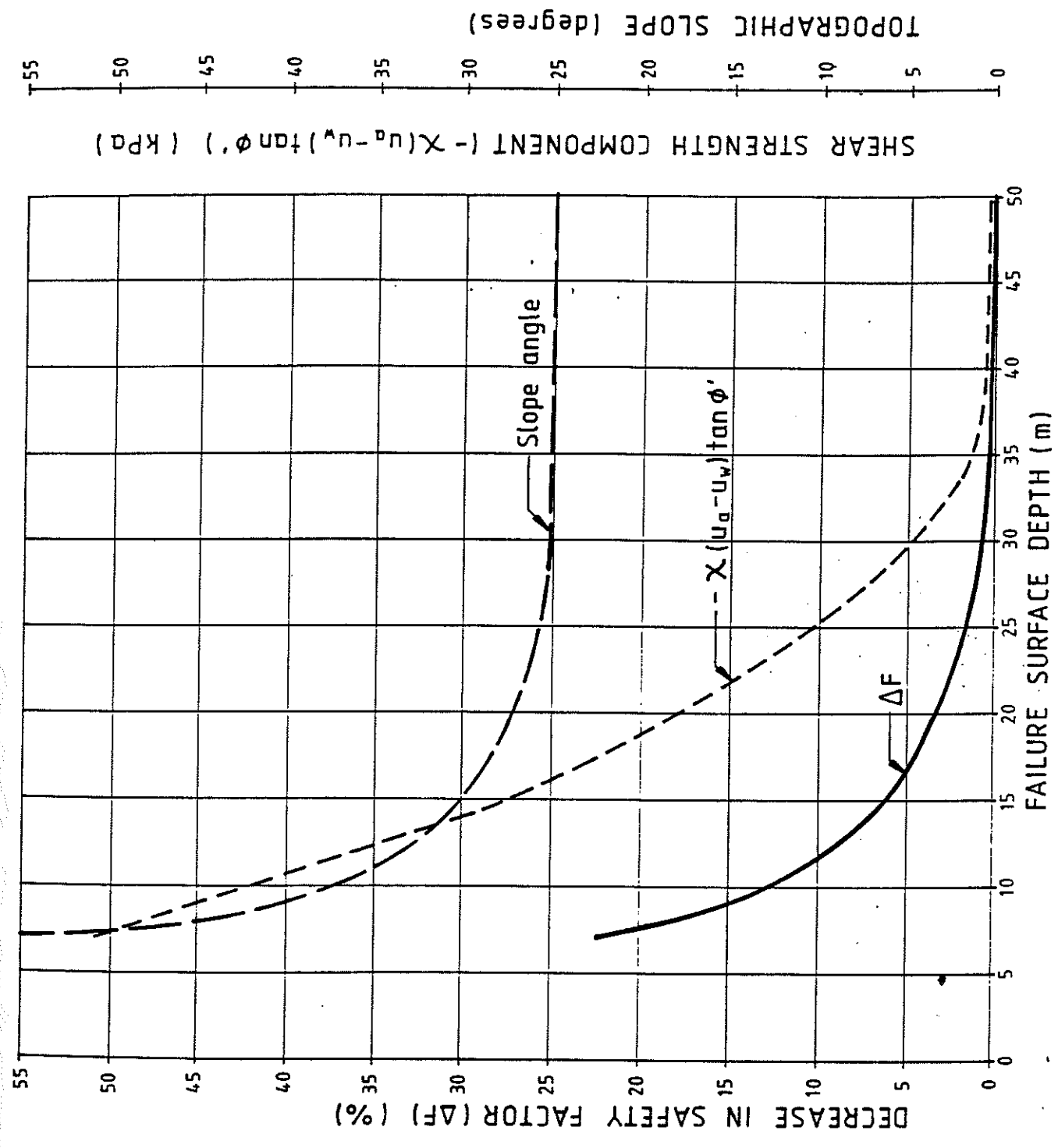
Testing at a normal effective stress of 446 kPa (Fig. 3-10) indicated strength losses on wetting in a similar manner. This was contrary to the initial expectation of much reduced strength loss at increased normal stresses. Repeatability testing was carried out, and this demonstrated consistent results, even when testing was continued for many days confirming that no excess pore pressures were causing anomalies.

It became clear that wetting induced a **dramatic reduction in strength** from that at the in situ moisture content to a value **much less than the saturated residual strength**. Testing was therefore extended to 5 days, (Fig. 3-11) and the picture became clearer. Strengths gradually increased to the saturated residual. Further trials demonstrated that although both time and displacement dependence existed, the latter was the principal factor: pore pressure equalisation took several hours but displacements of many metres were required before strengths increased asymptotically to the true (saturated) residual strength.

An attempt was made to reconcile the test results in terms of the partially saturated effective stress parameters. However, it is clear from the work of Bishop and Blight, that the term $\chi(u_a - u_w)\tan\phi'$ cannot increase with increasing normal stress. From equation (3) and Fig. 3-8 it follows that the residual effective friction angle for the partially saturated state (ϕ'_{pr}) must take on a greater value when sheared in a dry

SATURATION EFFECTS: Parametric study for active slide (soil friction angle 25°)

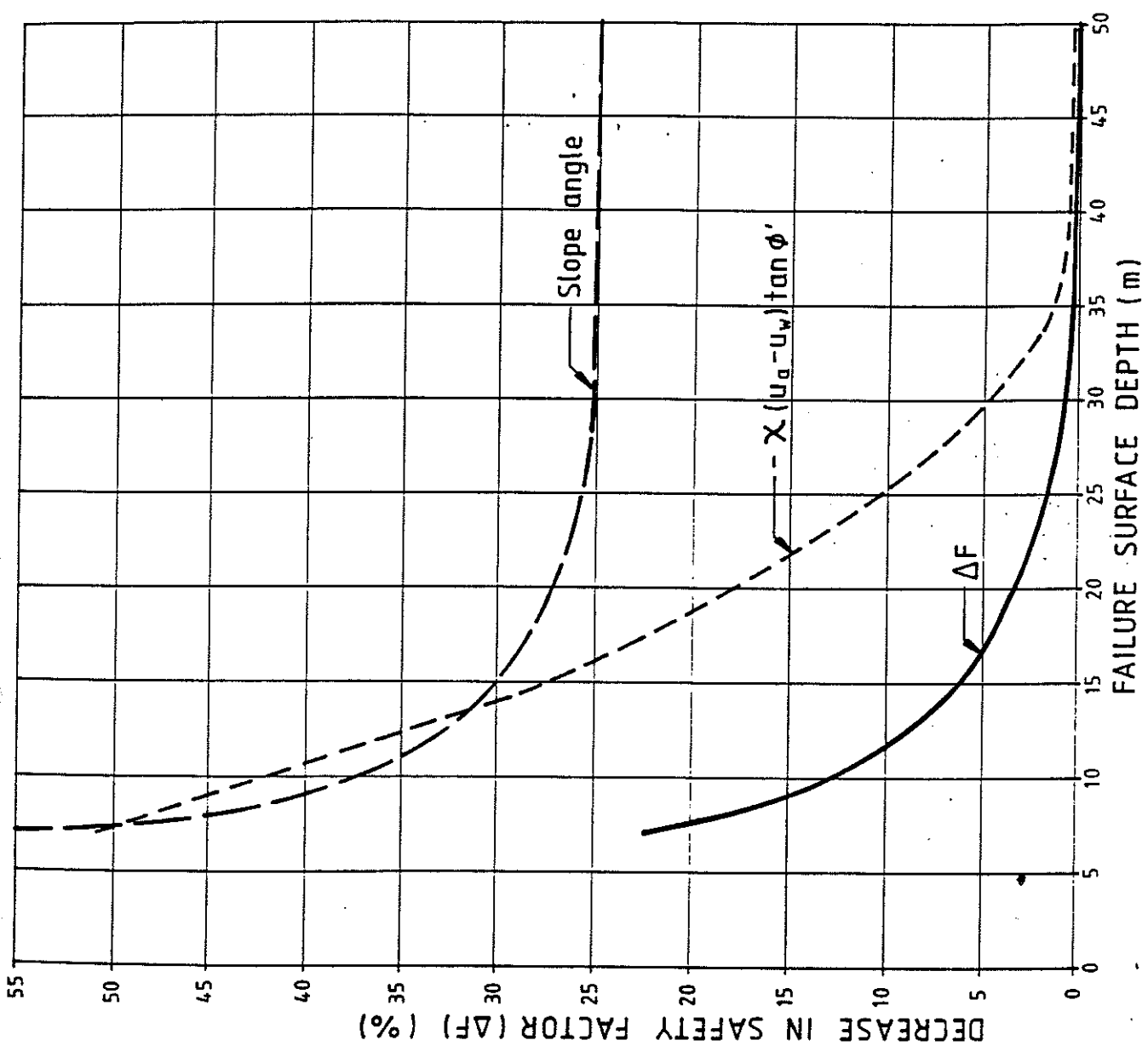
FIG. 3-3

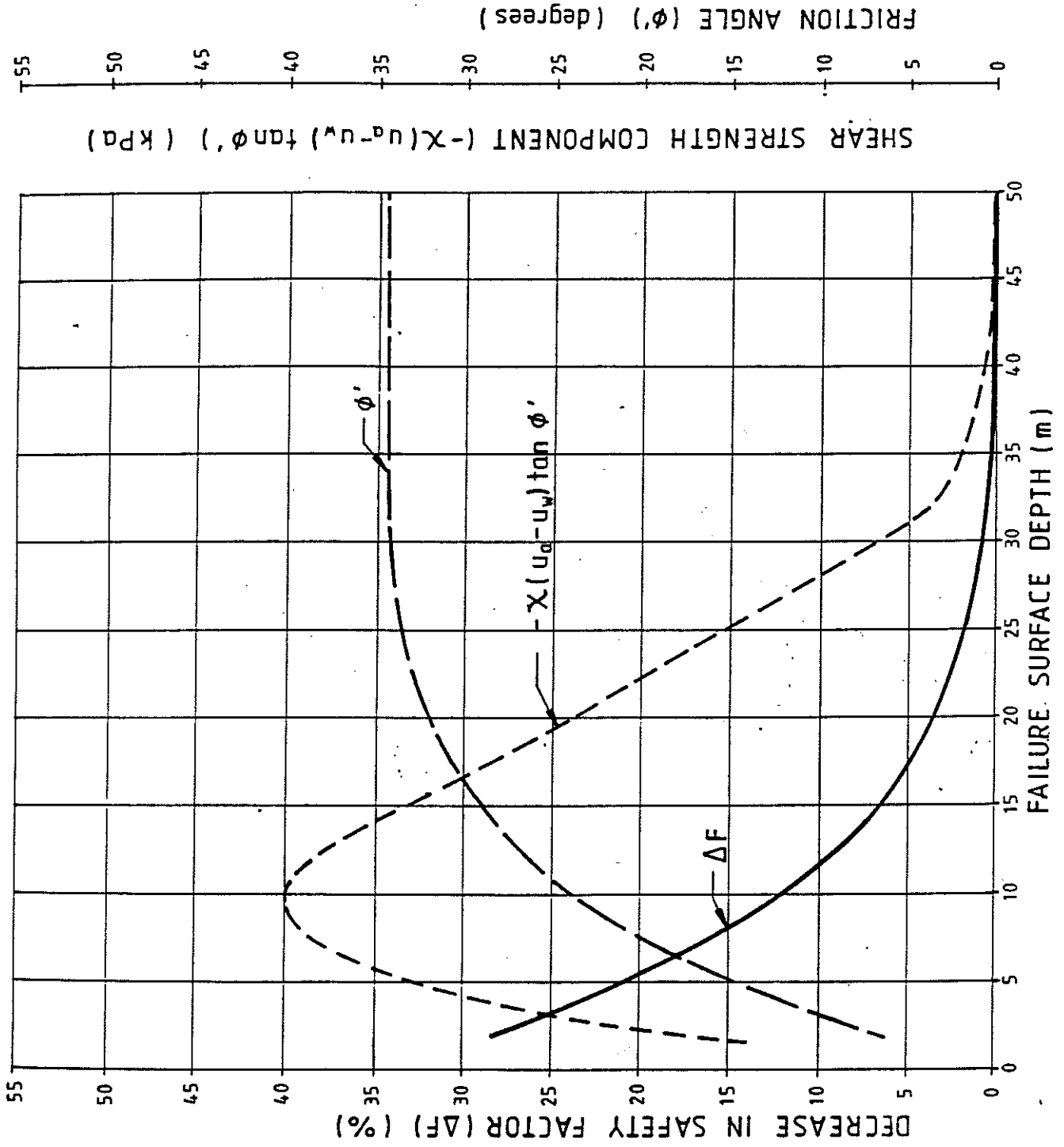


DECREASE IN SAFETY FACTOR (ΔF) (%)

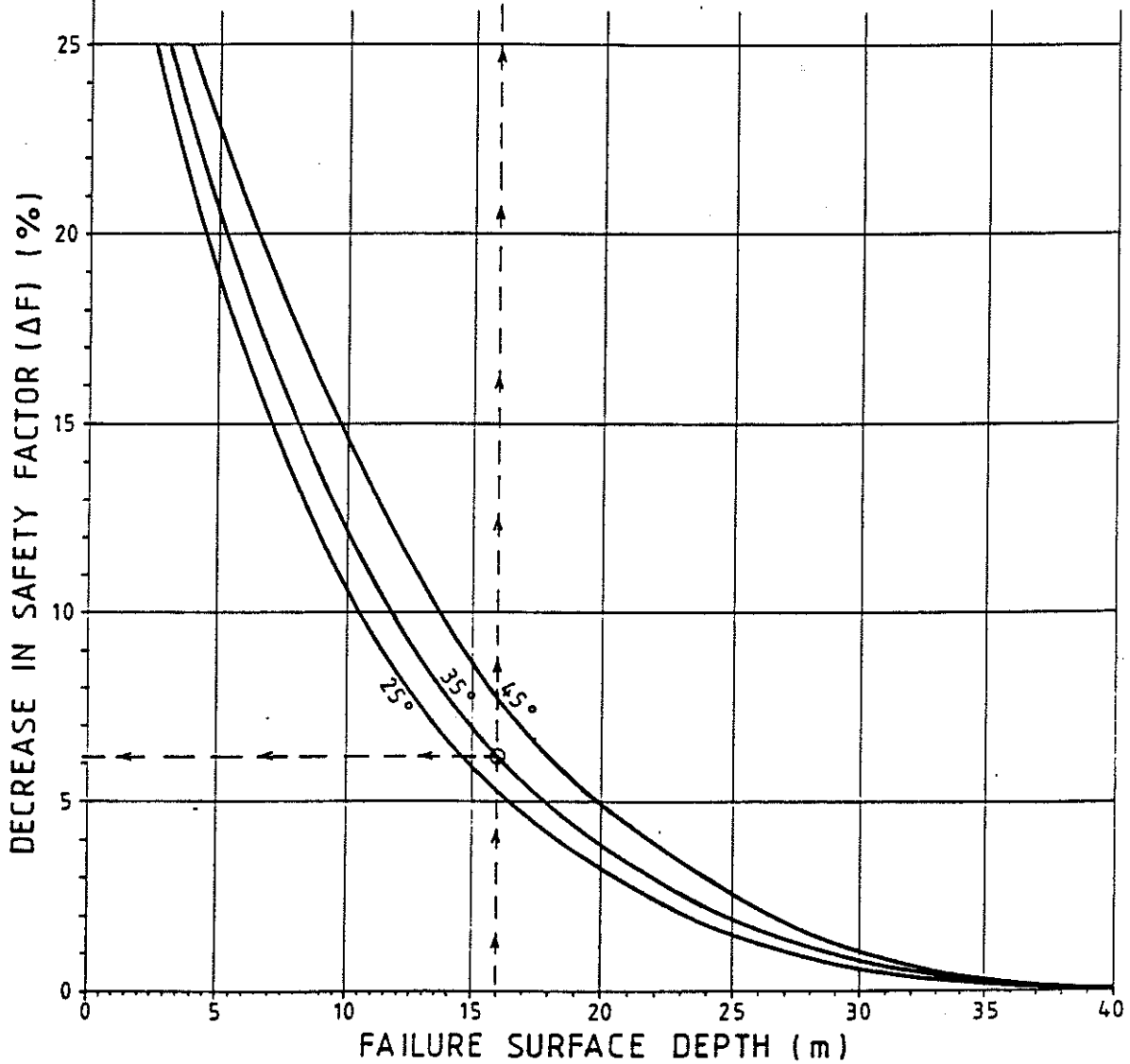
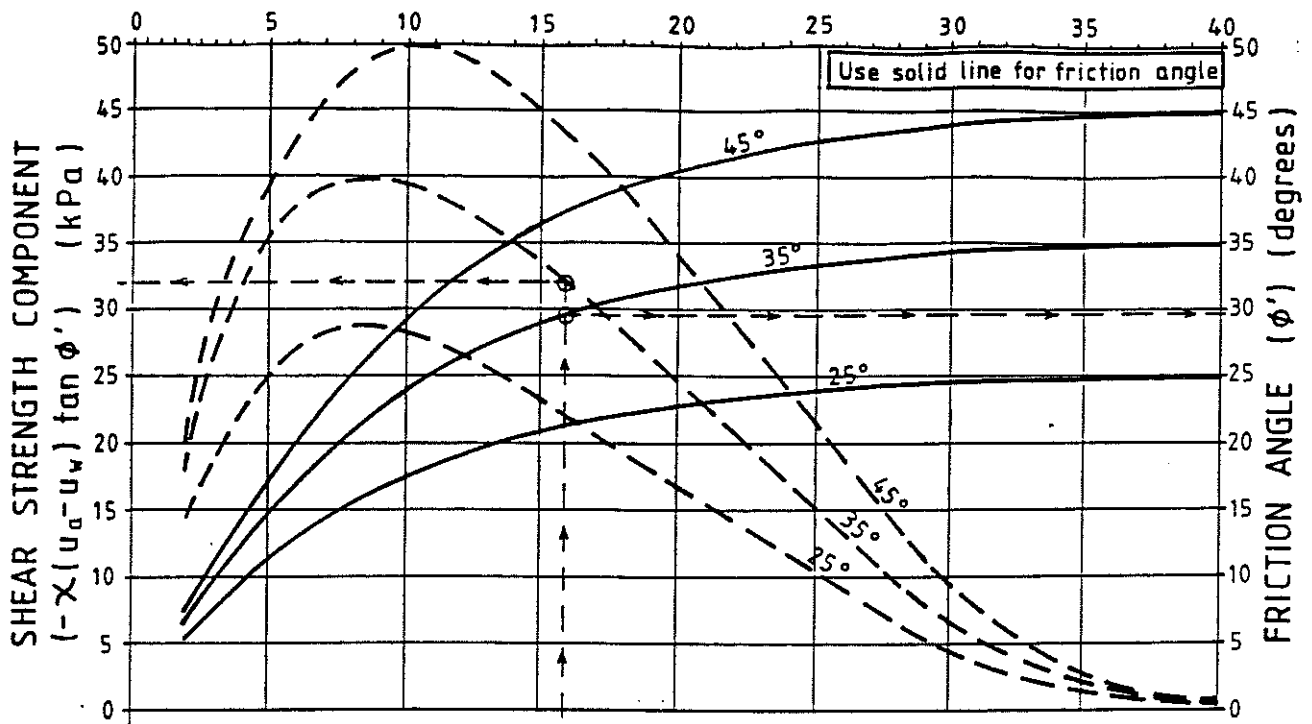
TOPOGRAPHIC SLOPE (degrees)

SHEAR STRENGTH COMPONENT ($-\chi(u_a - u_v) \tan \phi'$) (kPa)





SATURATION EFFECTS : Parametric study for active slide (35° slope)



SATURATION EFFECTS : Parametric study for active slides at variable slopes.

RESIDUAL SHEAR STRENGTH TEST

E43 saturation test

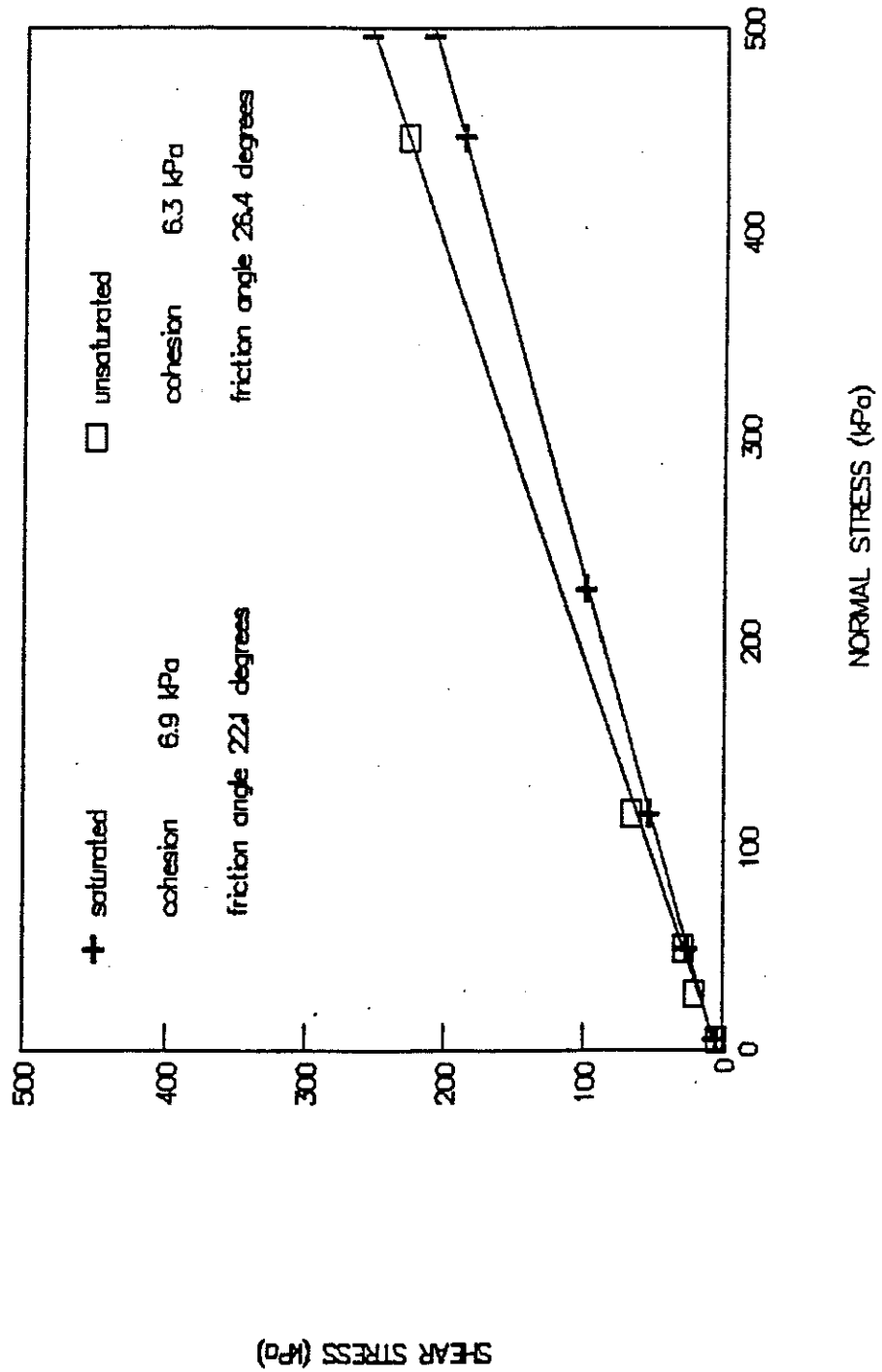


Fig. 3-6

RESIDUAL SHEAR STRENGTH TEST

E43 saturation test

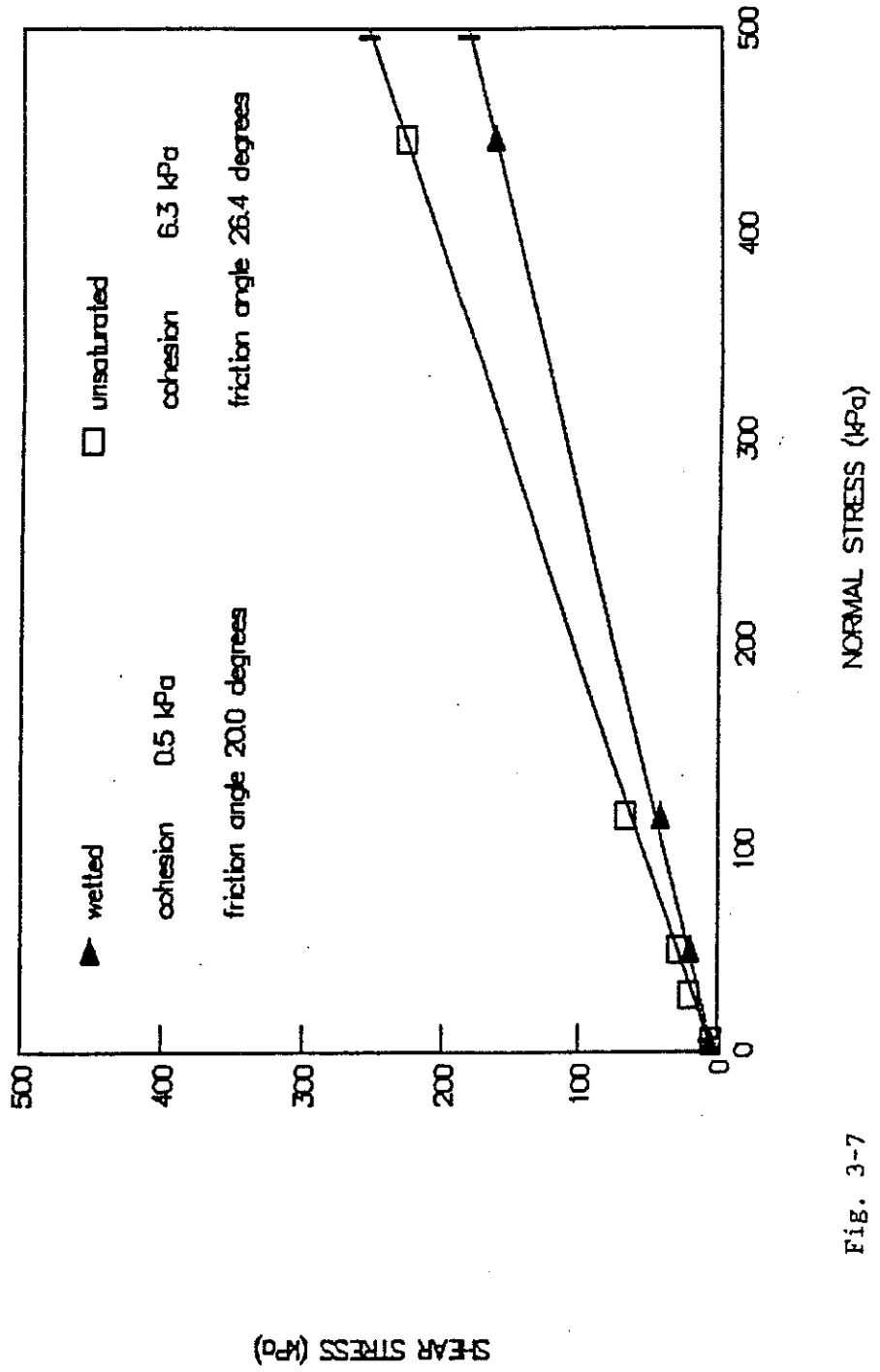
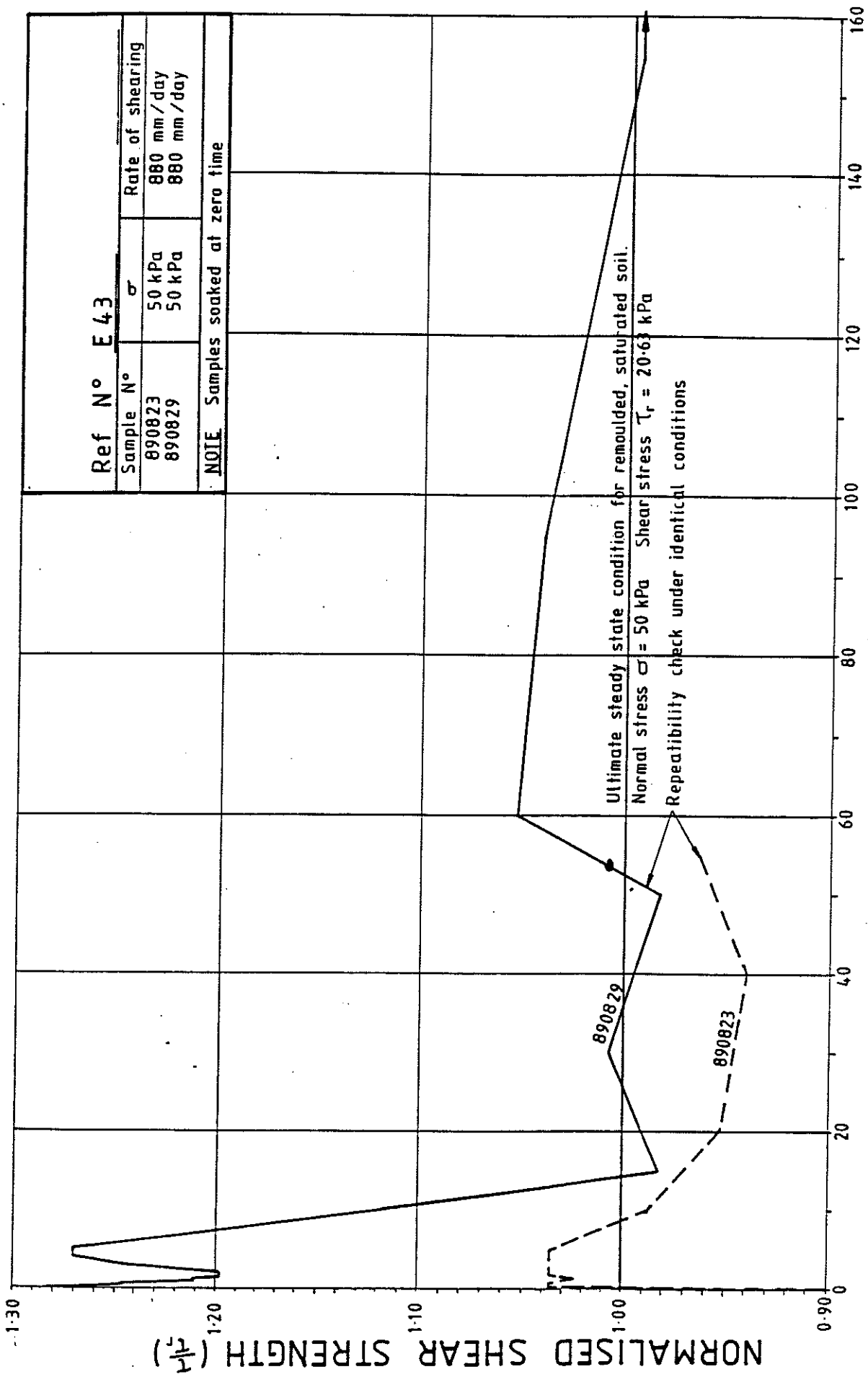


Fig. 3-7



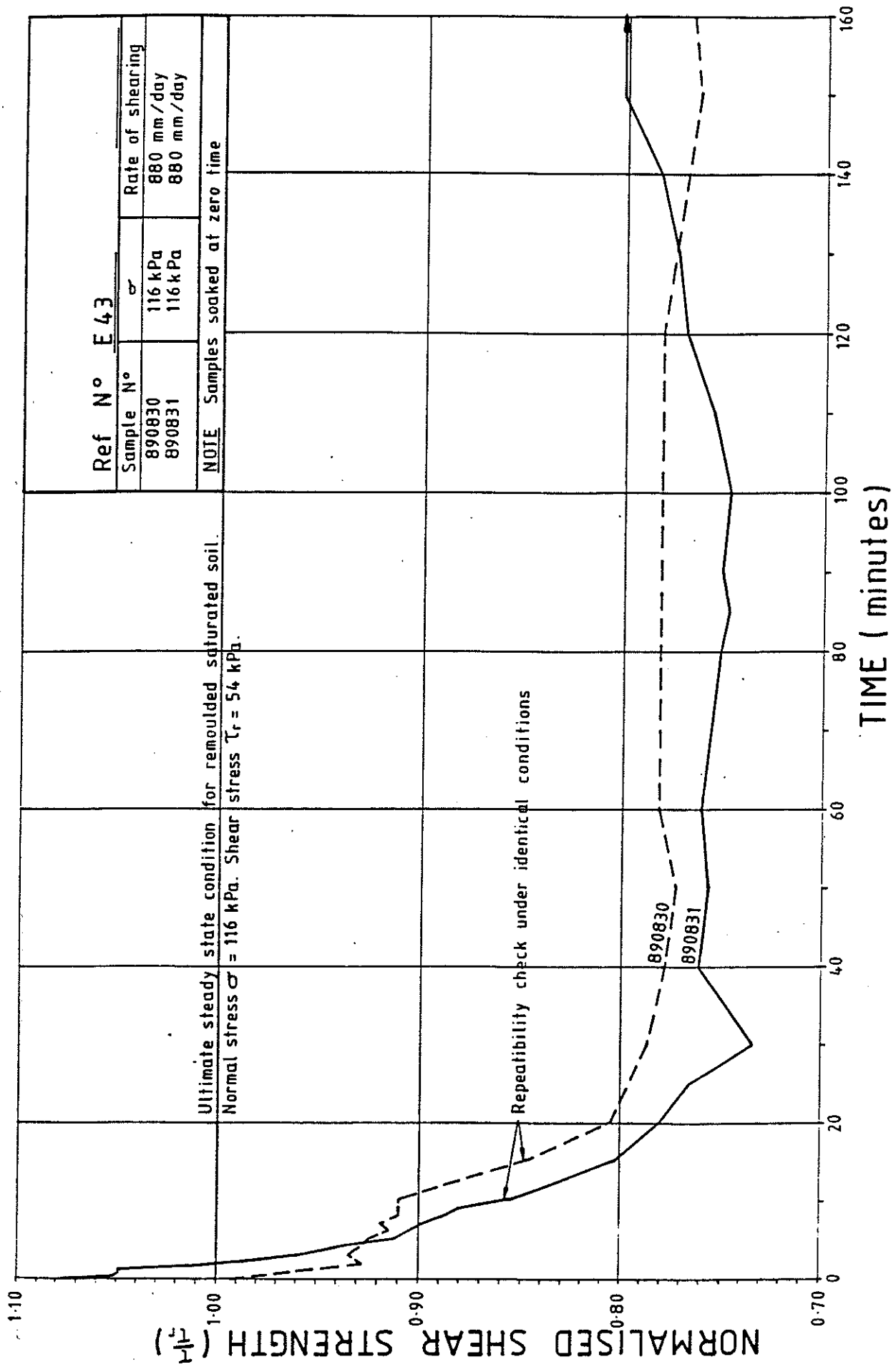
Ref N° E 43

Sample N°	σ	Rate of shearing
890823	50 kPa	880 mm/day
890829	50 kPa	880 mm/day

NOTE Samples soaked at zero time

Ultimate steady state condition for remoulded, saturated soil.
 Normal stress $\sigma = 50$ kPa Shear stress $\tau_r = 20.63$ kPa
 Repeatability check under identical conditions

STRENGTH LOSS ON SATURATION



Ref N° E 43		
Sample N°	σ	Rate of shearing
890830	116 kPa	880 mm/day
890831	116 kPa	880 mm/day

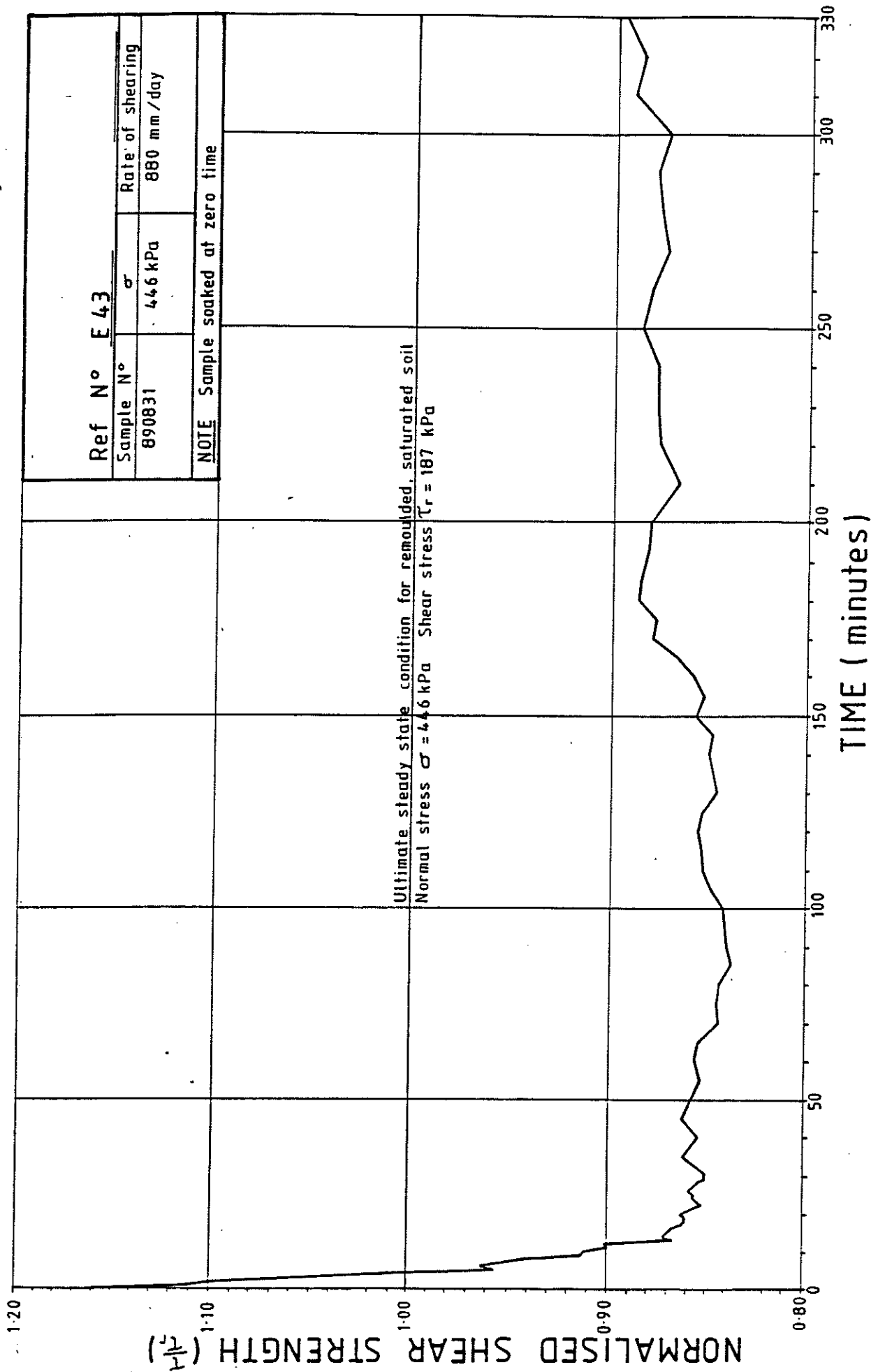
NOTE: Samples soaked at zero time

Ultimate steady state condition for remoulded saturated soil.
Normal stress $\sigma = 116$ kPa. Shear stress $\tau_r = 54$ kPa.

Repeatability check under identical conditions

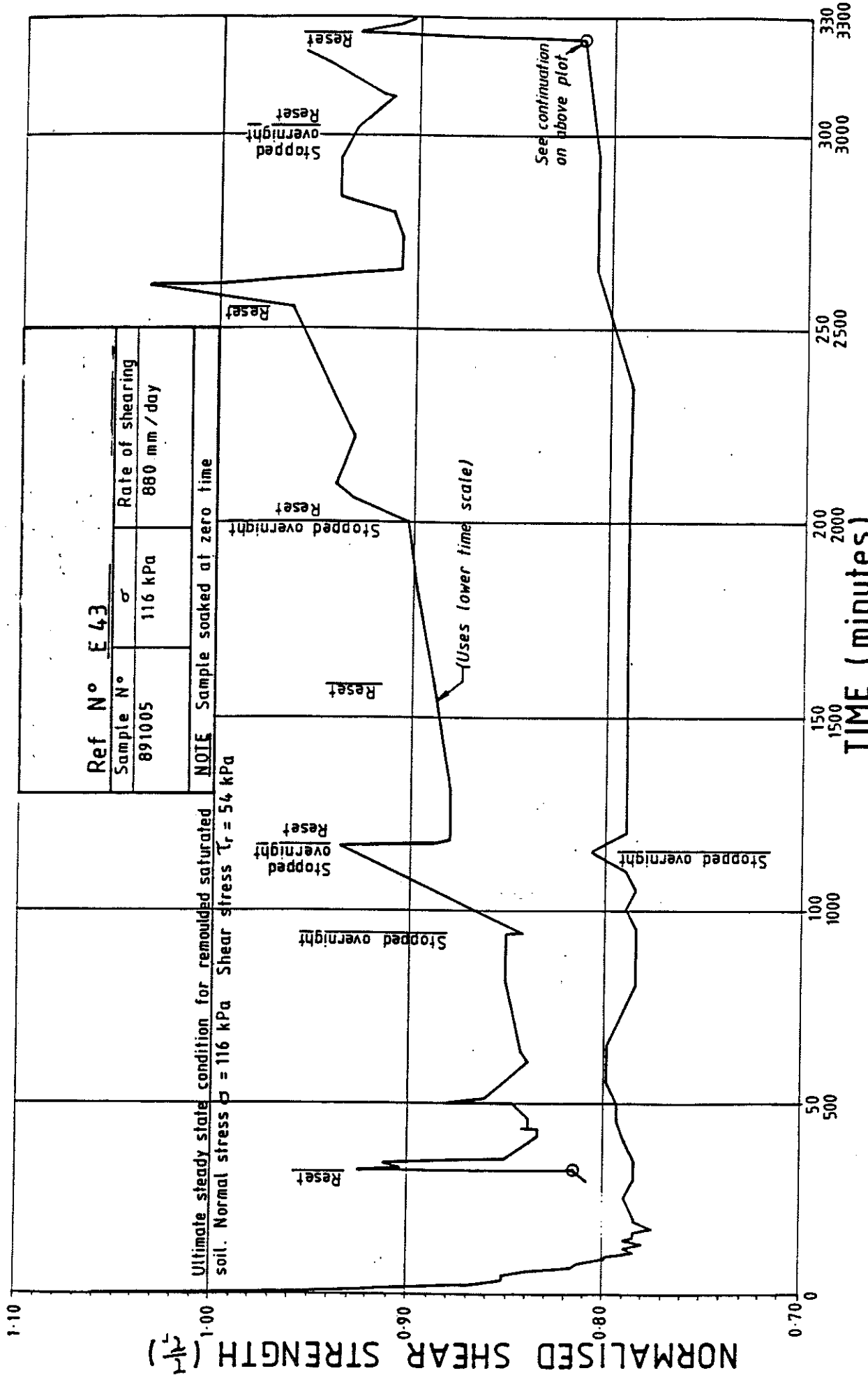
STRENGTH LOSS ON SATURATION

Fig. 3-9



STRENGTH LOSS ON SATURATION

Fig. 3-10



Ref N° E 43	
Sample N°	σ
891005	116 kPa
Rate of shearing	
880 mm / day	

NOTE: Sample soaked at zero time
 Ultimate steady state condition for remoulded saturated soil. Normal stress $\sigma = 116$ kPa Shear stress $\tau_r = 54$ kPa

STRENGTH LOSS ON SATURATION

Fig. 3-11

condition compared to a saturated sample. The shear strength equation (for this soil) therefore needs to be generalised to:

$$\tau_{pr} = c'_{pr} + (\sigma - u_a) + \tan\phi'_{pr} + \chi(u_a - u_w)\tan\phi'_{pr}$$

where the subscript pr refers to the partially saturated residual state.

This implies that if the pre-sheared partially saturated sample were to be fully saturated and not subjected to further shear displacement (so that re-ordering of clayey particles did not affect results, then an effective friction angle higher than the saturated residual would be expected. In other words it appears that this phenomenon is not a function of soil suction. This does not appear unreasonable, as in the softened condition of a saturated soil, elongate particles would be more readily aligned with their long axes parallel to the direction of shearing, than in the case of partially saturated soil.

The points of interest are:

- (i) The residual effective friction angle of a partially saturated fine grained soil may be significantly higher than the saturated residual friction angle in spite of many metres of shear displacement under moderately high normal stresses.
- (ii) The initial decrease in strength that takes place on first wetting a fine grained partially saturated soil, is likely to be to a value significantly less than the saturated residual strength.

The strength loss on saturation is given by:

$$\tau_{pr} - \tau_r = c'_{pr} - c'_r + (\sigma - u_a)(\tan\phi'_{pr} - \tan\phi'_r) + \chi(u_a - u_w)\tan\phi'_{pr}$$

For the sample tested, extrapolating to $(\sigma - u_a) = 0$ allows an estimate of the strength loss on saturation under zero normal stress, ie:

$$\tau_{pr} - \tau_r = c'_{pr} - c'_r + \chi(u_a - u_w)\tan\phi'_{pr}$$

Results obtained for sample E-43 were:

Unsaturated	$\tau_{pr} = 6.3 \text{ kPa}; \phi'_{pr} = 26.4 \text{ degrees}$
Wetted	$\tau_w = 0.5 \text{ kPa}; \phi'_w = 20.0 \text{ degrees}$
Saturated	$\tau_r = 6.9 \text{ kPa}; \phi'_r = 22.1 \text{ degrees}$

Substituting gives:

$$(c'_p - c'_r) + \chi(u_a - u_w)\tan(26.4) = 6.3 - 6.9 = -0.5 \text{ kPa}$$

Because $c'_p - c'_r$ is unlikely to be negative, and $(u_a - u_w)$ would be large (over 80 kPa) for this sample, it appears that χ will be very small for the residual state in a sample with low saturation. Regardless, for this sample, the term $\chi(u_a - u_w)\tan\phi'_{pr}$ is clearly of little significance for slides more than a few metres deep.

The response of unsaturated soils at residual conditions is therefore in marked contrast to the response of unsaturated soils in peak strength conditions.

Considering long term stability ($u_a = 0$) it appears that the strength loss on saturation is given by:

$$\tau_{pr} - \tau_r = \sigma(\tan\phi'_{pr} - \tan\phi'_r) - 0.5 \text{ kPa}$$

Because the strength loss is, for practical purposes, almost independent of the failure surface depth, then for the sample tested (E-43) and assuming one third of the slide becomes saturated, the decrease in safety factor would be:

$$\delta F = 0.33 (1 - \tan\phi'_r / \tan\phi'_{pr}) \times 100\% = 6\%$$

A decrease of this magnitude would be very significant.

Of principal concern was the finding that the apparent strength of an unsaturated fine grained soil immediately after wetting is lower than the saturated residual strength. The result was most surprising, and many checks were made to confirm no source of error existed. The phenomenon may be partly due to positive pore pressures set up by collapse of the unsaturated soil as displacement causes remoulding. Thus the effect is dependent both on time and displacement, rather than time alone. Another conjectural possibility is that when fine grained soils of low moisture content are sheared, segregation may take place with fines collecting at the failure surface with shearing in the turbulent shear (Chapter 2). However with increasing moisture content, sliding shear may predominate on first wetting, followed by remixing and reverting to transitional or turbulent shear.

Another possibility is that loss of soil from the ring shear apparatus is much less for unsaturated samples, therefore greater particle attrition takes place, changing the character of the failure zone soil. On wetting faster loss of soil would lead to increasing residual strength. In other words this phenomenon also, may be an apparatus effect of no relevance to field conditions. Photo-micrographs of samples would be most

informative, and should allow the mechanism to be correctly interpreted.

Unfortunately, other priorities precluded further investigation of this phenomenon which has apparently not been reported in any literature.

In the meantime, for conservatism it is necessary to accept that the laboratory data may be valid. Therefore using the same assumptions made above, the immediate decrease in safety factor is given approximately by:

$$\delta F = 0.33 (1 - \tan\phi'_w / \tan\phi'_{pr}) \times 100\% = 9\%$$

A decrease of this magnitude is in excess of the rate dependence of residual strength for this soil type (see Chapter 7), and large slide displacements would be expected if wetting took place slowly. If wetting took place suddenly, or if creep displacement did not take place until a sizeable proportion of the failure surface was wetted, then the slide may be predisposed to rapid sliding.

However, the principal assumption made for both of the previous estimates is that the moisture content of the test sample is equal to the highest that has ever been sustained by the slide during active movement. Because sample E-43 was recovered from within 5 m of the surface after a prolonged dry period, the result will be conservative. The extent of conservatism is unknown, but is believed to be considerable in view of the low moisture content of this sample. In practice, slide movement would most likely be associated with the passage of wetting fronts after prolonged rainfall. In this case, truly residual conditions may be operative in the slide concerned. These uncertainties cannot be resolved with remoulded samples (required for all ring shear testing). The results are conservative, but probably excessively so.

The benefit of this test programme is the finding that, for residual strength conditions in unsaturated soils, suction appears to have little significance. The potential for strength loss arises from the property that unsaturated clayey soils appear not to develop their lowest effective friction values unless saturated. Further (frictional) strength loss can then develop if movement takes place after saturation.

Matrix suction is strongly affected by moisture. However, it appears likely that frictional characteristics will relate to the highest moisture condition experienced during shear displacement and are unlikely to be greatly affected by moderate transient decreases in moisture conditions. (This aspect could be readily proven in the laboratory.) If correct, this inference offers a simple means to determine the strength loss on saturation of any accessible failure surface, simply by testing undisturbed samples to determine loss in frictional residual strength from the in situ moisture to the saturated state. The loss of any 'cohesive' component should be small and could be largely attributed to the present day (moisture dependent) suction effects.

3.2.5 Concluding Remarks

This testing has been confined to one specific sample (a moderately plastic clayey silt gouge), however the following generalisations are suggested for any soils whose strength characteristics are affected by platy minerals (silts and clays), ie as commonly found in landslide gouges:

- (i) the effect of saturation on fine grained soils containing pre-sheared failure surfaces appears to be markedly different from the effect of saturation on peak strength.
- (ii) if a (pre-sheared) slide gouge is found to be unsaturated then the effect of saturation will be dependent on the slide history -
 - (a) if the gouge has ever been subjected to effective wetting (eg by a descending wetting front) and has experienced concurrent movement, then the effect of saturation on shear strength will be small.
 - (b) if pre-shearing has taken place only under unsaturated moisture conditions, saturation is likely to induce a substantial decrease in safety factor on failure surfaces regardless of their depth, dip angle, or other factors.
- (iii) Preliminary evaluation of the effect of saturation on slide gouges may be carried out using disturbed samples (to give conservative results simply). However the results are likely to be too conservative for practical purposes where safety factors are marginal.
- (iv) The only realistic method of quantifying the effect of saturation on the residual strength of pre-sheared surfaces is in the direct shear apparatus using undisturbed, oriented samples at in situ moisture, followed by wetting and then full saturation. The reduction in frictional rather than cohesive component requires determination (ie. varying normal stresses should be used).

3.3 HIGH STRESS TESTING

3.3.1 Introduction

When estimating the decrease in safety factor caused by submergence of a slide where residual strength conditions pertain, the use of a linear strength envelope (with zero residual cohesion) is preferred, in order to ensure that unconservative assessments do not occur. Any non-linearity of the strength envelope (concave downward curvature) used in analysis can produce very optimistic outcomes, particularly if a relatively high value (eg 100 kPa pseudo-cohesion¹) is adopted. Conventional test equipment can test up to about 1000 kPa, but high stress testing is necessary to define failure envelope curvature for landslides which are deeper than 50 m.

3.3.2 Adoption of Linear Residual Strength for Submergence

The rationale for not adopting curved strength envelopes without convincing evidence to the contrary is as follows:

- (i) Significant pseudo-cohesion cannot be proven to be present in the field -
 - (a) Laboratory tests may indicate curvature, but the laboratory apparatus has limitations, particularly in relation to edge effects which tend to be a function of normal stress.
 - (b) If a curved envelope is produced in the laboratory, testing achieves equilibrium in a matter of days. The long term presence of pseudo-cohesion (how much is present after several weeks, let alone years) cannot be stated with sufficient confidence to substantiate its use in design
 - (c) The use of the Casagrande REP (Chapter 4) will often show that for residual strength slides, there will be little or no indication of curvature of the multiple slope resistance envelope, hence a linear envelope may be adopted with little or no conservatism. Furthermore, from case histories referenced in Chapter 4, curvature of the strength envelope is less for the field mobilised apparent stresses than for the ring shear tests. Work on first-time slides by Skempton (1977) indicates (for a relatively low range of normal stresses) effective cohesion of only 1 kPa in clays and recommends that zero cohesion be adopted for design. The same recommendation is made by Hoek & Bray (1977).

¹ the terms pseudo-cohesion and pseudo-friction angle are used here to indicate the instantaneous residual strength parameters in terms of effective stresses, ie. the intercept and slope of the tangent to a non-linear strength envelope at a given normal stress.

- (d) The laboratory sample uses a nominal sample thickness (eg 5 mm the ring shear apparatus) sheared at a discrete zone. A different thickness of active shear band in the field, may give rise to a different degree of curvature of the strength envelope.

(ii) The property providing pseudo-cohesion is not clearly quantifiable. On reduction of normal effective stresses (with submergence) there is no reason to suppose a significant increase in roughness of the failure surface will result for the type of feature observed in the field. An increase in the coefficient of friction (the ratio of shear to normal effective stress, without differentiating between friction and cohesion) with reducing normal stress might be attributable to swelling characteristics of clay minerals.

(iii) There are other phenomena, not readily quantifiable, which, if neglected, tend to cause unconservative results (ie. predicted decreases in safety factor which are less than actual values). The neglect of envelope curvature may at least offset some of these effects. Those phenomena providing unconservative results are:

- (a) loss of suction on saturation
- (b) reduction in frictional strength on saturation

(iv) From testing carried out by the writer, and published data both from case histories and laboratory residual strength tests, the highest residual pseudo-cohesion that might be adopted in design would be 10 kPa. In the case of large deep seated landslides, this is of little significance (Appendix 3).

One feature is that all available published laboratory seen, deal with average normal stresses of less than about 1000 kPa (ie about 50 m of overburden). At larger normal stress levels, failure envelope curvature (as measured in the laboratory) would be expected to be more significant. However the problem remains that there is no assurance from case histories. High levels of pseudo-cohesion cannot therefore be convincingly demonstrated to be valid field properties appropriate for adoption in design.

3.3.3 Ring Shear Modification

In spite of the reservations given above, work to determine envelope curvature at high normal stresses was attempted in order to estimate how much conservatism might be involved with the analysis of deep slides or those failure surfaces where waviness causes strong redistribution and concentration of stresses. The standard ring shear apparatus (100 mm diameter cell) was modified from the former 10:1 leverage for loading to 50:1, allowing normal stresses of over 10,000 kPa to be readily applied. Many problems were encountered, eg compression of the sample resulted in the need to ensure that all coarse sizes had been removed to prevent bridging, slow rates of consolidation required long testing times, sample extrusion was significant etc. Preliminary results for gouges of moderate plasticity from one landslide, showed no apparent decrease in frictional strength with normal stresses up to 10,000 kPa. On the contrary, in some instances a very slight increase was recorded. In similarly well graded soils, this phenomenon has

formerly been attributed to the improved interlock obtained between coarser particles when the volume of a low strength matrix is decreased by consolidation of the finer grained matrix. A highly plastic clay was also tested, as most case histories report that failure envelope curvature is more marked in such soils. Preliminary results gave strength parameters (as normal stresses were increased to 3200 kPa) of 9 kPa pseudo-cohesion and 8 degrees friction.

3.3.4 Concluding Remarks

In view of the minimal levels of pseudo-cohesion found, the apparatus problems experienced and the lack of confidence in ever applying the results in design (even if significant envelope curvature could be demonstrated in the laboratory) the test programme was deferred in view of other priorities.

It was concluded that for a residual strength landslide subject to a decrease in normal effective stress (as with reservoir filling) the use of a curved strength envelope (or invoking of 'pseudo-cohesion') may be appropriate for providing explanations for observed anomalies in field response of an active slide subjected to a change in safety factor, but is not appropriate for conservative performance prediction or reliable design.

CHAPTER 4

FIELD ASSESSMENT OF STRENGTH PARAMETERS

4.1 INTRODUCTION

Slope stability analyses and design commonly rely on shear strength parameters determined from laboratory testing. Frequently, however, laboratory strengths may differ from field values or typical particle sizes may be too large to enable representative samples to be used in shear test equipment. The resistance envelope procedure (REP) allows realistic determination of strength parameters applicable in the field. When Casagrande originally proposed the method in 1950, the lack of general access to computing facilities was a major limitation. However, recent advances have transformed the method to one which can be applied rapidly, provided an appropriate program is available. A simple technique can be used to determine the change in peak strength parameters that may be expected on saturation of a partially saturated soil. Because the REP is seldom used, the application of the method is described in detail, together with a computer program and examples of case histories where slopes have been affected by a number of projects, some completed and others in progress.

4.2 IDENTIFICATION OF A GEOTECHNICAL MODEL

In order to carry out geotechnical design, a soil model needs to be identified and appropriate parameters determined. This requires categorising of site materials into discrete units with common properties. In practice this involves firstly, identification of general geological formations and then further subdivision into geotechnical units.

Published geological maps provide the starting point, however these may show the basement rock type when the overburden materials are more likely to be of engineering interest. Site specific engineering geological mapping is then required to identify geotechnical units.

For slope stability purposes, each geotechnical unit is required to have the same strength properties and density, (geomorphology and groundwater conditions may vary). Identification of units, therefore requires familiarity with engineering geological field description and some judgment. Where uncertainty exists about the persistence of one unit, a new unit can be assigned. (At a later stage of investigation, units can readily be re-combined provided common properties are established.)

The purpose of identifying distinct geotechnical units for field assessment of strength parameters is that interpretations can be made on slope profiles that are outside the specific site of interest. Also, later stage investigations can maximise the use of interpolation and extrapolation from sampling and testing.

Within each geological formation, new units may be identified on the basis of:

- (i) mineralogy and/or grain size variation (either laterally or vertically) in the original material
- (ii) faulting or landsliding (formation of locally sheared or crushed zones)
- (iii) weathering (vertical change in grain size and mineralogy)

Judgment is required where changes are gradational rather than abrupt.

4.3 BASIS OF THE RESISTANCE ENVELOPE PROCEDURE

4.3.1 General

Figure 4-1 (after Janbu, 1977) illustrates an existing slope profile within which a number of trial shear surfaces may be drawn. Each surface is assumed to pass through a single soil type with a conventional linear shear strength envelope.

Using standard limit equilibrium methods, (Bishop, 1955; Janbu, 1973; Sarma, 1973) the average mobilised shear stress required for stability and the corresponding average normal stress may be plotted for each trial shear surface. (The average stress is found from the weighted average along each shear surface.) For a number of shear surfaces in a single soil type in this slope, a corresponding number of points may be plotted. The upper boundary curve enveloping these points is termed the resistance envelope for the single slope. Similarly, trial surfaces may be grouped for a common soil type comprising a number of slope profiles to form a multiple slope resistance envelope.

The procedure is effectively a series of analyses in which consideration is given to all possible combinations of soil cohesion and friction although no specific soil strength is assumed. Either total or effective stress principles may be used as appropriate. Field conditions must include moderately steep slopes of the relevant material type somewhere (not necessarily in the immediate vicinity of the site) to avoid overconservative results. The resistance envelope, by definition, provides a lower bound to the Mohr Envelope for the material. As such it can be used as a conservative strength envelope for design. In many situations where other factors govern design, no further definition of strength parameters is required. However techniques discussed in Section 4.3.2, can be adopted to define the Mohr envelope more accurately, from the resistance envelope.

For final design, slopes with marginal stability can benefit from a complementary approach using both the REP and selective laboratory testing. However, an early appreciation of material strengths can be quickly gained for preliminary assessment using the REP alone.

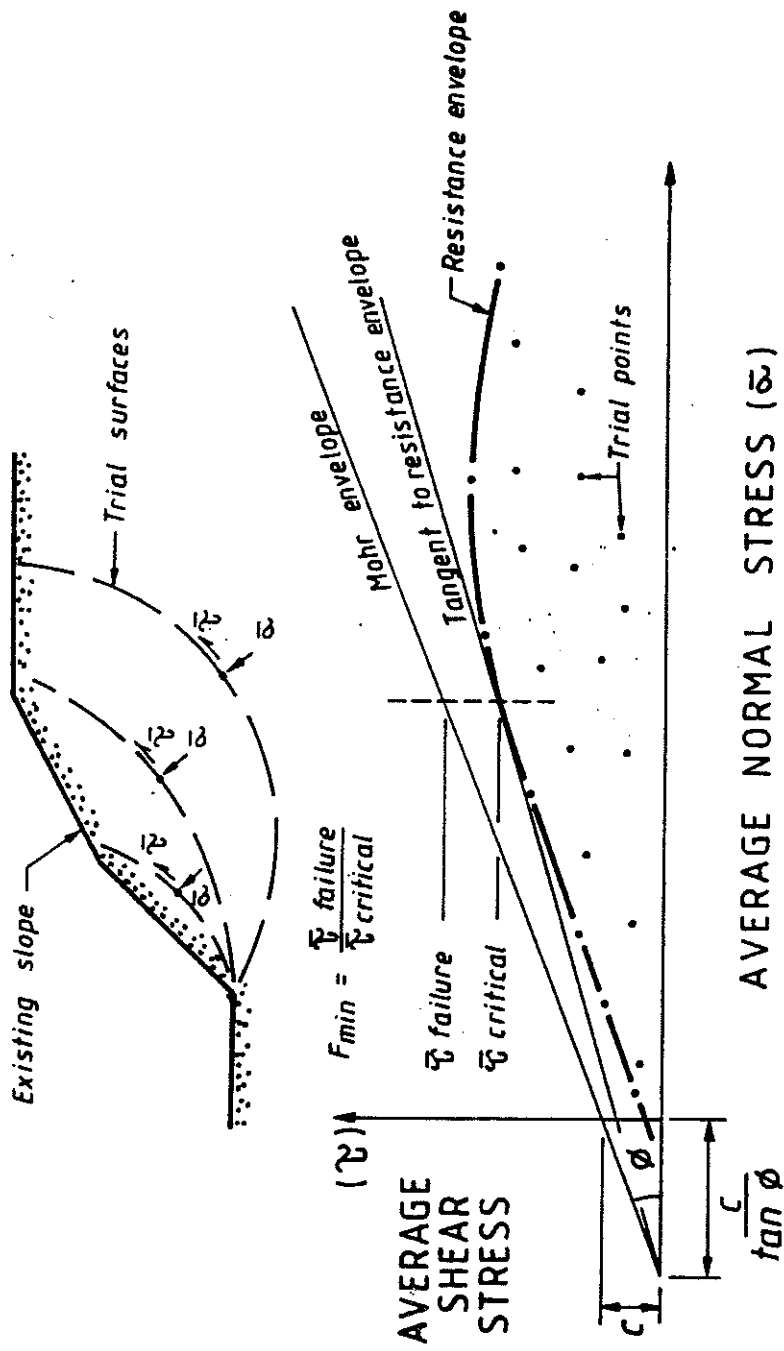


FIG. 4-1

If the shear strength of the soil is known, the Mohr Envelope may be constructed on the resistance envelope diagram and the conventional factor of safety for the slope may be determined simply by the minimum value of the ratio of available to mobilised shear stresses.

Because no specific soil strengths are assumed, the method is more powerful than the standard "back-analysis" in which only one surface (usually of a landslide) is analysed under a limited range of strengths. The technique for parameter variation and inclusion of a search routine for critical shear stresses over a wide range of normal stresses, maximises the quantitative information that can be gained from field observations.

The method (originally suggested by Casagrande in 1950), has been applied more recently by Hutchinson et al (1973) and Chandler (1976, 1977). Appendix 1 provides details of the steps needed for practical application of the REP and includes comparative examples.

4.3.2 Modification of existing computer programs

Of the limit equilibrium slope analysis programs generally available, none could readily be applied to generation of resistance envelopes. However, all methods of slices would generate internally the required parameters. Accordingly, modifications to source codes are quite straightforward to allow appropriate output of the average shear and normal stresses. The only caution required is to confirm that the variables used for effective or total stresses are correctly interpreted.

Appendix 1 provides a FORTRAN listing of a simple modification to a slope analysis program. The latter has been well proven from its widespread use with geotechnical consultants.

To avoid the need for tedious checking and manual processing of output data, straightforward file processing programs have been written. These are also detailed in Appendix 1. A program is included for graphical viewing of the slope topography, onto which is superimposed the locations of critical circles found during an automatic search routine. Another provides a file for graphical viewing of the resulting Casagrande resistance envelope, for either a single slope or for multiple slopes. In the latter case, the individual slopes are distinguished by the use of different data point symbols.

4.4 EXTENSIONS TO THE RESISTANCE ENVELOPE PROCEDURE

4.4.1 Determining the Mohr Envelope from Tangent Points

In many field situations, river undercutting or other works of nature or man, provide steep slopes which provide the critical points on a resistance envelope. (A critical point

is where the average shear stress on a potential failure surface has its maximum value for a given average normal stress.) The resistance envelope for most slopes will be somewhat curved, while the Mohr Envelope is generally linear. Therefore there will be only a limited range of normal stresses over which the resistance envelope will approach the Mohr Envelope. Where an incipient crack or development of a discrete slide can be observed in the field, the REP provides a method to estimate field strengths with much improved reliability. The procedure is as follows.

(i) Determine (or reasonably estimate) the geometry of the slide (including failure surface) at the time of incipient failure

(ii) Analyse the incipient failure condition to determine the corresponding average shear and normal effective stresses on that critical failure surface. These coordinates should lie on the resistance envelope for the slope.

(iii) Draw the tangent to the resistance envelope, at the coordinates corresponding to the critical failure surface.

This line provides the best estimate for the Mohr Envelope, (provided a non-linear failure criterion does not apply).

The procedure is an improvement on the "back-analysis" technique in that it acknowledges not only that a critical failure surface with safety factor of unity has been found, but uses the location of that surface to refine the appropriate values of cohesion and friction. Also, the information that failure did not occur on potential failure surfaces elsewhere in the slope is used, as well as the actual failure. (The resistance envelope must curve below the Mohr envelope at these less critical points.)

To some degree, a similar procedure can be followed where neither failure nor incipient cracking is present. If a series of slopes in one material type are surveyed for use in a multiple slope resistance envelope, a subjective judgment based on field experience, can be made to select which slope profile is likely to be the most critical, and whether failure is likely to be deep seated or shallow. When the respective resistance envelopes are plotted together, the Mohr Envelope should approach the multiple slope resistance envelope most closely in the vicinity of the points from the slope profile judged most critical. Where experience is limited, such assessments normally require independent verification with some form of laboratory testing.

4.4.2 Inclusion of Tension Cracking.

Ideally, the potential depth of tension cracking should be allowed for in the REP. In practice this requires an initial guess for tension crack depth, and an iterative procedure to refine the initial estimate. Where slopes are relatively high and the cohesion is small, tension cracking can be ignored because its significance in design can be minimised by the consistent omission of cracking in both the observational and predictive models.

4.4.3 Partially Saturated Soils

Analysis of partially saturated (or unsaturated) soils follows the same general principles. However, the effects of negative porewater pressures (from soil suction) are implicit, that is, a total stress analysis is made. An additional assumption inherent in this approach is that the soil suction is independent of depth. While unlikely to be strictly true, the use of the same assumption in analysis and design will largely result in cancellation of these errors.

Suction is clearly seasonally dependent. In practice, wetting fronts will descend through the soil profile, but under sustained rainfall events (which will be the most critical to consider) the only practical assumption that can be made is that suction is uniformly low throughout the region above the watertable. A major advantage of the resistance envelope procedure is that full scale models have been invoked, which have demonstrated their strength capability over time and therefore provide parameters which are based on the worst climatic conditions experienced since the formation of that slope profile. Other techniques for interpreting the long term reliability of soil suction (eg instrumentation with tensiometers) suffer from the inevitable disturbance of the environment which is being measured and likelihood of missing the worst long term events because of practical limitations to the frequency and duration of data acquisition.

It may be noted that the use of total stress parameters which are not derived from undrained tests do not involve the uncertainties and theoretical objections to which total stress analyses are usually subject, (Janbu 1977).

An example of a resistance envelope in an partially saturated soil is shown in Figure 4-2. This was derived from slopes in which the absence of groundwater on trial surfaces was either known or reasonably assumed. (A non-critical trial point is generated if the assumption is false.)

The points plotted in Figure 4-2 relate predominantly to the more critical trial circles analysed. Initially, the only available computer program required manual input for individual trial surfaces and all of these results are plotted. Subsequently, the program developments described above enabled systematic searching for critical surfaces with automatic rejection of many hundreds of trial points which provided no additional information, ie, all points falling below the existing boundary envelope.

Figure 4-2 shows the usual shape of a multiple slope resistance envelope which is a result of the fact that long slopes often fail by superficial erosion rather than deep seated sliding, therefore it is not common to find critical points at high normal stresses. Critical slopes from river erosion or road cutting, frequently allow good definition of the resistance envelope at low normal stresses. The Mohr Envelope for the soil concerned is probably close to linear with total stress parameters of 12 kPa cohesion and 36 degrees friction. However, a curved non-linear (or bi-linear) envelope is a possibility. Curved envelopes have been well documented for intact and fractured rock, coarse rockfill, dense sands and highly plastic clays. In granular materials the phenomenon has been

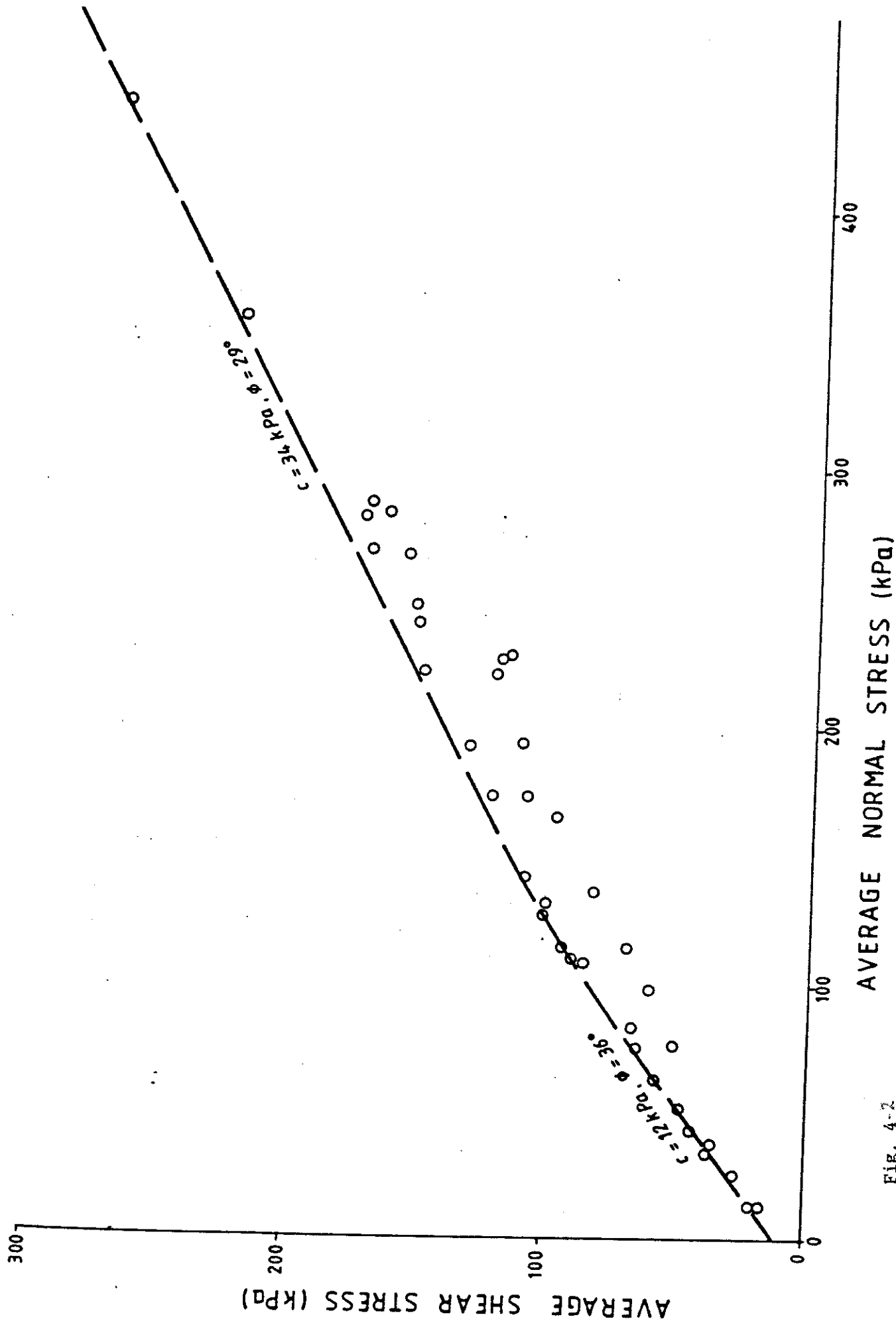


FIG. 4-2

explained by changes in the dilatational component of strength because the rate of volume increase at failure diminishes and eventually becomes negative with increasing confining stress. In clay rich soils, curvature of the Mohr envelope may be attributable to more marked alignment of platy particles with their long axes parallel to the plane of shearing at high normal stresses.

In this example, the conservative approximation to a bi-linear envelope could be used for design purposes, with the change at about 160 kPa normal stress, ie:

	Normal stress range	
	0-160 kPa	160-600 kPa
Apparent cohesion	12 kPa	16 kPa
Apparent friction angle	36 degrees	29 degrees

4.4.4 Saturation of Partially Saturated Soils

The total stress parameters found to characterise unsaturated soils are clearly not directly attributable to the same material below the watertable. The strength characterisation of partially saturated soils has been addressed by Bishop & Blight (1963). More recent work has been carried out by others (notably Fredlund), suggesting slightly different constitutive relationships, but the original formulation by Bishop and Blight is conceptually simpler and just as adequate.

For unsaturated soils, the extended effective stress equation (Bishop & Blight 1963) is:

$$\sigma' = \sigma - u_a + \chi(u_a - u_w) \dots\dots\dots(1)$$

where,

- σ' is the effective normal stress
- σ is the total normal stress
- u_a is the pore air pressure
- u_w is the pore water pressure, and
- χ is an experimentally determinable coefficient

The coefficient χ takes into account the proportions of pore space over which u_a and u_w act and the effects of the surface energy forces at the air-water interfaces in the soil. If it is assumed that over a limited range of normal stress the material may be characterised by a linear strength envelope, the shear strength is given in the usual manner by:

$$\tau = c' + \sigma' \tan \phi' \dots\dots\dots (2)$$

where c' and ϕ' are the effective cohesion and friction.

Combining (1) and (2) gives:

$$\tau = c' + (\sigma - u_a)\tan\phi' + \chi(u_a - u_w)\tan\phi' \quad \dots\dots\dots 3)$$

In terms of apparent cohesion (c), it is evident that by collecting the terms that are independent of σ from (3)

$$\tau = c + (\sigma - u_a)\tan\phi' \quad \dots\dots\dots (4)$$

where,

$$c = c' + \chi(u_a - u_w)\tan\phi' \quad \dots\dots\dots (5)$$

For the steady state condition of a partially saturated soil (for a long term situation) u_a will be zero. Therefore:

$$\tau = c' + \sigma \tan\phi' - \chi u_w \tan\phi' \quad \dots\dots\dots (6)$$

The pore water pressure in an unsaturated soil (u_w) is negative (suction), hence the term $-\chi u_w \tan\phi'$ represents a positive contribution to shear strength. Also, for low compressibility materials this term is practically independent of normal stress and hence differentiating Equations (2) and (6) above gives:

$$\delta\tau/\delta\sigma = \delta\tau/\delta\sigma' = \tan\phi'$$

That is, although a total stress analysis has been used, the slope ($\tan\phi$) of the strength envelope is the same as for effective stress, which indicates that the apparent and effective friction angles are equal. This applies to both a linear or bi-linear strength envelope, although an allowance must be made for the relevant normal stress ranges, as discussed below.

On saturation, effective cohesion will be less than the apparent cohesion owing to loss of soil suction together with loss of strength of any soluble cementing minerals. If the conservative assumption is made that most of the peak strength change is due to loss of soil suction, and the material is truly frictional when saturated, then putting $c' = 0$ and $u_a = 0$ for long term stability and combining Equations (2) and (4) gives:

$$\sigma' = \sigma + c/\tan\phi$$

This means that the effective normal stress can be found by translating the Mohr Envelope for total stresses, along the normal stress axis (rather than by decreasing the shear stress ordinates as might be intuitively assumed). The significance of the change in normal stress rather than shear stress becomes relevant when a markedly non-linear strength envelope is considered. However the effect can be seen slightly when substituting the values for the case in Fig. 4-2, giving:

	Normal stress range	
	0 - 176 kPa	176-600 kPa
Effective cohesion	0 kPa	25 kPa
Effective friction angle	36 degrees	29 degrees

Using these principles, strength parameters found from the REP, may used to readily determine parameters for the same soils where they are below the watertable.

4.5 LANDSLIDE STRENGTH PARAMETERS FROM THE REP

4.5.1 Basic Approach

The REP has particular application where engineering works are affected by a number of active landslides in a single material type. In this case detailed subsurface investigations may be limited to a small percentage of the slides, for which the REP may be used to determine strength parameters (for use in assessment or design of remedial works). This approach allows inferences to be soundly based for the remainder of the slides, using minimal subsurface investigations. In cases where both active and inactive slides are involved, the resistance envelope for the active slides will necessarily define the Mohr Envelope for the failure surface material, therefore the safety factors of the in-active slides may be reasonably estimated.

The example shown in Figure 4-3 is a multiple slope resistance envelope derived from 6 large active landslides (most with volumes between 1 and 5 million cubic metres). All these slides had moved some tens of metres, and hence were expected to have developed substantial gouges along their failure surfaces. Cored drillholes with multiple piezometers installed allowed identification of gouge zones, bedrock and watertables (frequently perched). Good seismic velocity contrasts usually enabled interpolation of the drillhole information from refraction surveys. One typical section (Slide A) is shown in Figure 4-4. Creep movements of typically 3 to 20 mm per year were established from surface deformation monitoring and this activity suggested that relatively small rises in slide mobilising forces would induce further activation. The Mohr Envelope was therefore taken as equivalent to the resistance envelope (zero cohesion and effective friction angle of 28 degrees) with negligible conservatism.

4.5.2 Correction for Side Friction

From the published case histories (op. cit.) it appears that the most reasonable means of assessing the three dimensional nature of deep seated slides is by the use of an earth pressure coefficient for the inclusion of side friction. Commonly for slides where the maximum depth to length ratio and the maximum depth to width ratio are small (less

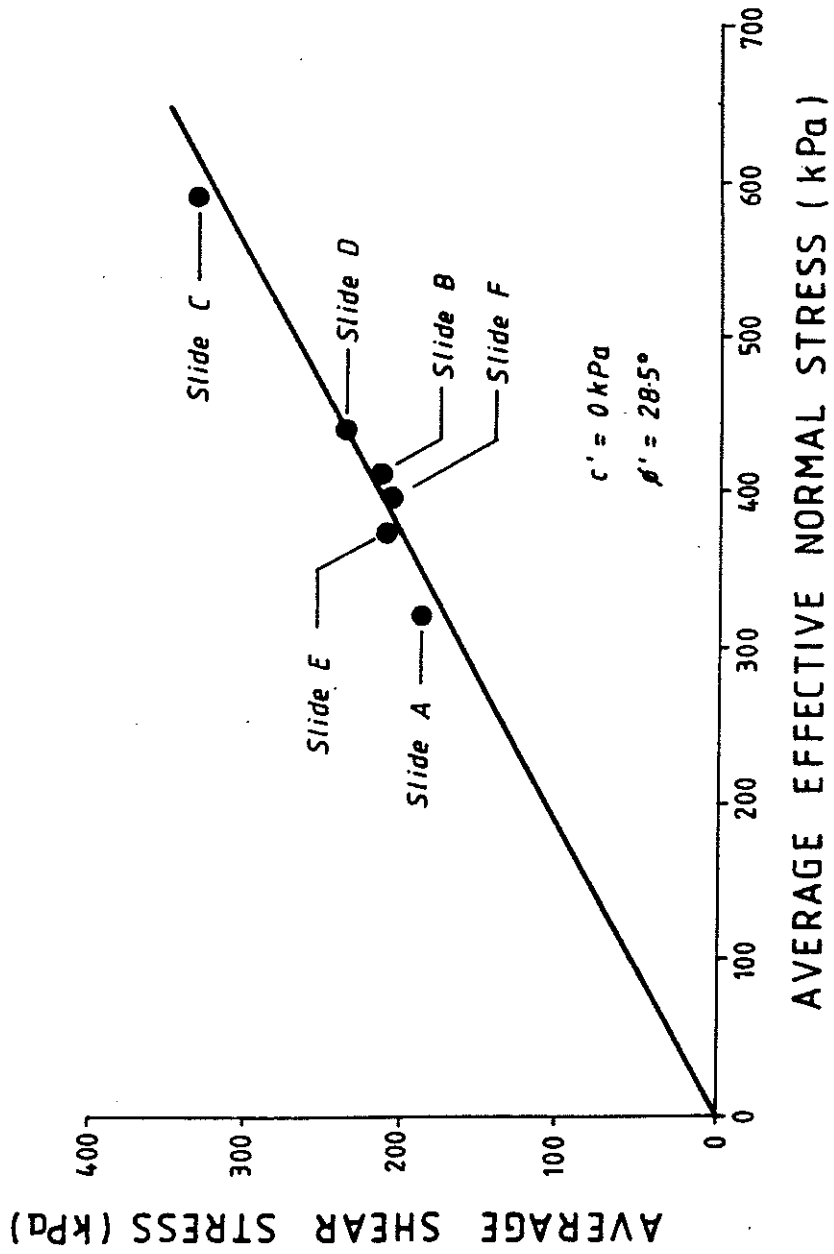


FIG. 4-3

than about 0.15 and 0.3 respectively) side friction contribution will be less than 5% of the overall shear surface resistance. For slides in Figure 4-3, a 3% contribution was typical. Although small, this effect was included in these examples, assuming active earth pressure. The alternative concept of at rest earth pressure is not considered to be a likely state for slides which have experienced substantial displacement and the active earth pressure model was supported in these cases by field evidence of inward sloping lateral scarps which diverged downslope.

4.5.3 Comparison of field and laboratory strengths

A significant difference between the reported laboratory residual strengths and field mobilised values was established in the above case. When laboratory strength parameters were used for analyses of active slides, calculated factors of safety much less than 1.0 (between 0.6 and 0.9) resulted. This finding clearly points to the value in determining field mobilised strengths (rather than relying on laboratory testing), particularly where coarse particle sizes are involved. The following factors may contribute to the difference between laboratory and field strengths.

- (i) Laboratory samples often require sieving of the coarse fraction to permit compatibility between maximum particle size and apparatus dimensions.
- (ii) Only a small proportion of a failure surface can reasonably be tested in the laboratory, and landslide materials will often show a large range in properties. The thickness of slide gouges will also vary and may locally be pinched out.
- (iii) Waviness of slide gouge seams is common. Such failure surface irregularity has been previously reported to produce field strengths greater than laboratory residual values.
- (iv) Slides which have neither circular arcuate, nor planar translational failure surfaces require conjugate shear planes or internal deformations to occur within the sliding mass in order to produce kinematic failure mechanisms. Depending on the degree to which this is acknowledged by the different analysis methods, the result may be an apparent mobilised strength along the failure surface which is marginally greater than the laboratory strength.
- (v) In dormant slide areas, some healing of gouge may take place. This would result in an increase in the effective cohesion of a soil through electro-chemical changes at mineral-water interfaces or cementation by minerals precipitated from percolating water. Calcite or ferruginous cementing agents may contribute to strength increases.

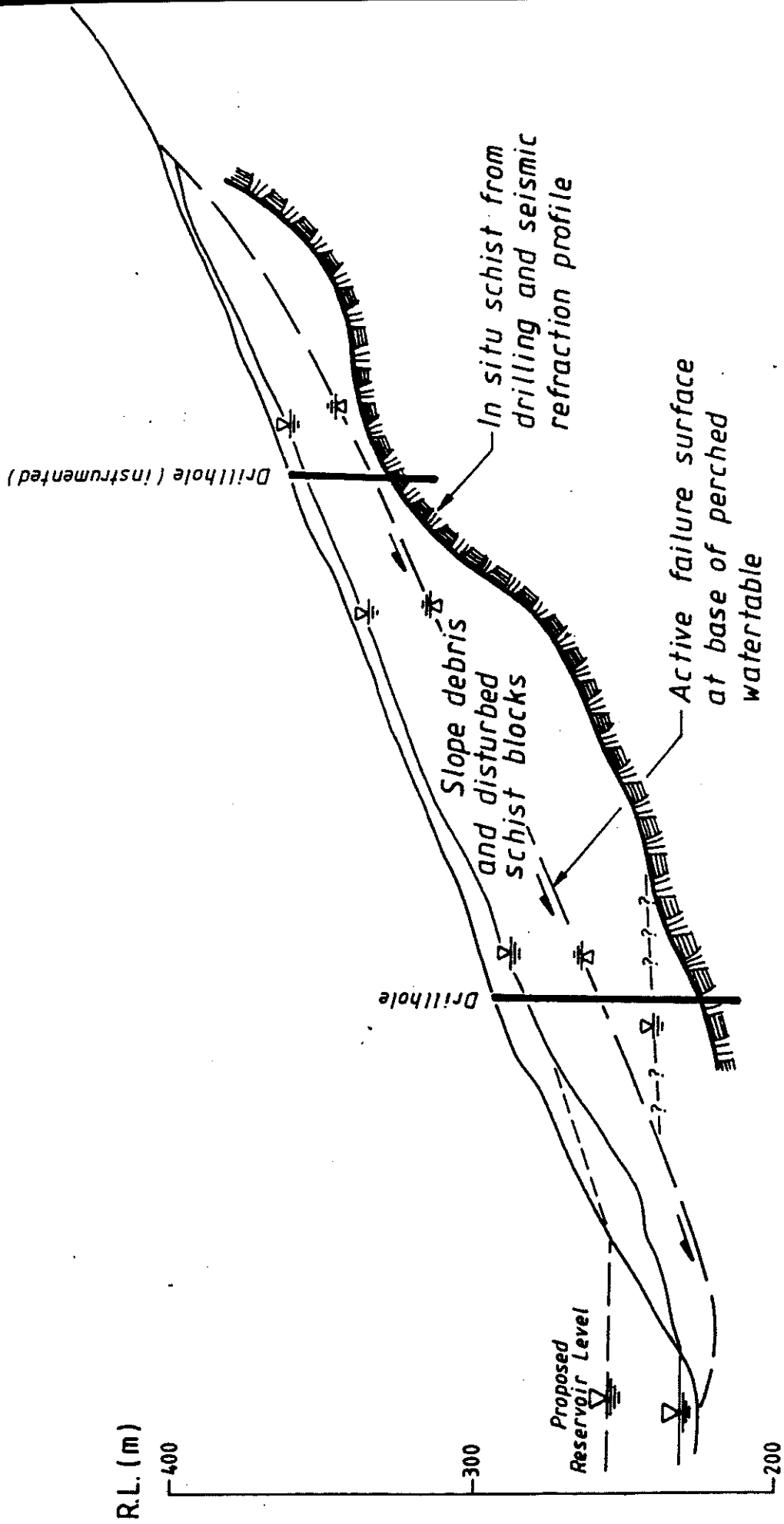


FIG. 4-4

4.6 APPLICATIONS TO SLOPE DESIGN

4.6.1 Cut Slope Design

The resistance envelope determined from field observations may readily be used for the design of cut slopes using standard limit equilibrium analysis. Figure 4-5 shows the general slope design carried out using the strength parameters determined from Figure 4-2. An additional safety factor would normally be incorporated, depending on hazard and risk rating.

Verification of the usefulness of design based on the REP was obtained subsequent to the reporting of Figure 4-5. In this case, a large transition batter was cut in the same material. Laterally, both the cut height and batter angle had been increased and a failure involving 60,000 cubic metres of material occurred as the works were nearing completion. The pre-failure slope heights and batter angles at various stations are shown superimposed in Figure 4-5, as are the corresponding values for a section surveyed through the centroid of the slide after failure. All sections for which failure should have been expected did fail and the slide centroid came to rest after several metres of displacement, with its deflated geometry giving a safety factor close to 1.0.

This has the advantage of being a prediction made before the event and the agreement with expectation was more than adequate for practical purposes.

4.7 CONCLUSIONS

(i) The resistance envelope procedure is a technique which appears under utilised. When the method was originally proposed in 1950, the lack of access to computing facilities would have been a major limitation. However, recent advances have transformed the method to one which can be applied rapidly.

(ii) The programs listed in Appendix 1 allow field assessment of strength parameters for many situations to be carried out at considerably lesser cost than would be entailed in recovery of undisturbed samples and laboratory testing.

(iii) The principal advantages of the REP are that full scale models which have withstood time and representative climate, can be invoked. Conventional limit equilibrium methods are used to maximise the information available from observation and investigation of either stable or failing slopes.

(iv) Both field and laboratory data can be utilised in a complementary fashion to minimise cost while increasing the reliability of design. The method overcomes limitations imposed by material types which are not amenable to laboratory testing.

(vii) Extensions to the REP may be used to refine strength estimates from field observations, and to determine strength parameters for saturated soils on the basis of a resistance envelope generated from unsaturated soils.

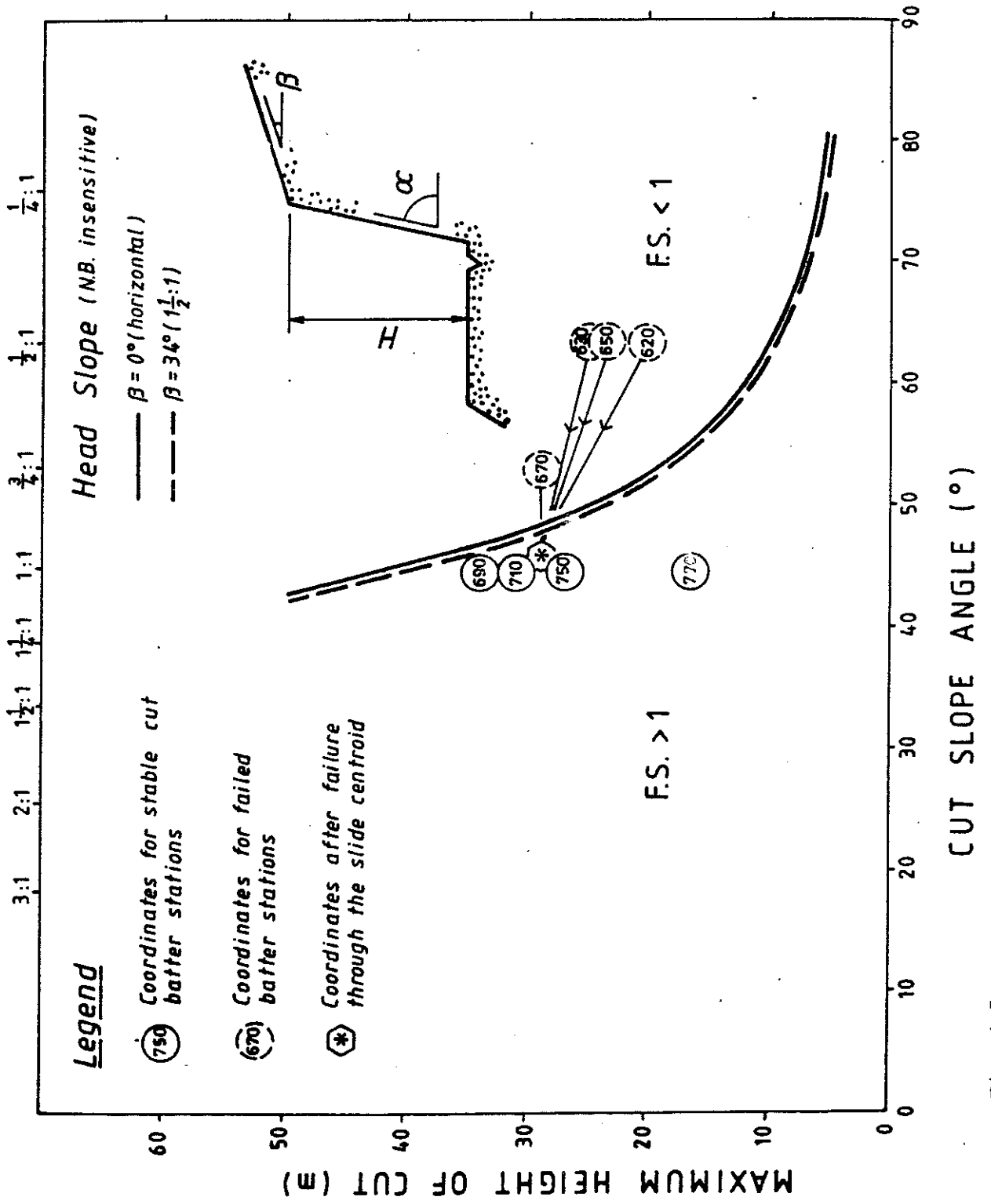


Fig. 4-5

CHAPTER 5

PREDICTION OF GROUNDWATER CHANGES ON RESERVOIR FILLING

Construction of piezometric profiles in slopes from limited field data, prediction of piezometric changes induced by reservoir filling and the accompanying time dependent changes in stability.

5.1 INTRODUCTION

When investigating the stability of natural slopes, piezometric information is generally limited to that obtainable from a small number of drillholes with multiple piezometers installed. In some instances a seismic profile will define the watertable profile where it exhibits an adequate wave speed contrast with the unsaturated zone. However there is a general need to establish standard methods for establishing realistic piezometric profiles required for limit equilibrium analysis, in the following situations:

- (i) Where sparse piezometric data points recorded in the field require extrapolation and/or interpolation over the full extent of the slope being considered.
- (ii) Where it is necessary to predict the response of an existing watertable or aquifer in slopes subjected to submergence (by reservoir filling, drawdown or continuous cycling during operation).
- (iii) Where an excavation extends below the original watertable, the final re-adjusted position of the phreatic surface is often of significance.

Slope analyses used to predict changes in stability are highly sensitive to the assumed changes in piezometric conditions. Small variations to the position of the future piezometric surface location will readily reverse the implications of analyses for a given slope: for example, from submergence providing an increase in safety factor to providing a significant decrease. Where the groundwater table extends horizontally into the slope, it is reasonable to assume any rise in river or reservoir level will maintain this condition for most situations. However, where there is any gradient to the piezometric surface extending away from the original river or reservoir level, the effects of increased submergence are less readily predicted.

A literature search has been carried out to obtain references which provide either case histories of the response of inclined watertables to reservoir filling, or a theoretical treatment. Applicable information or case histories are extremely rare. Subjective qualitative interpretation (on where to draw a future piezometric line) is likely to be the overriding factor in any subsequent stability analyses. In many cases, groundwater modelling may be doubtful in view of the range of unknowns, but it does provide the basis for a parametric study prior to reservoir filling. The main value of modelling is in refinement which can be carried out to predict ultimate conditions once the piezometric monitoring data from the initial stage of filling become available.

The application in this chapter is principally to intact slopes or landslides affected by reservoirs but the same procedures may be adopted for foundation excavations or mining (both underground and open cast) where the prediction of re-adjusted watertable locations are paramount to meaningful calculations of inflows and/or stability analyses of both cut and dump slopes.

The first sections of this chapter present the basic application of groundwater response prediction to the assessment of landslides submerged by reservoirs, with case histories which have been interpreted simplistically, assuming only steady state conditions of downslope flow along cross sections of a landslide, and with minimal mathematical treatment.

The subsequent sections discuss the development of a computer program which integrates geohydrological and geotechnical concepts for more generalised assessment of a landslide mass or layered slope, including the effects of lateral flows, remedial measures (drainage drives and drillholes), and changing reservoir levels for both steady and unsteady state conditions.

5.2 BASIC PRINCIPLES OF GROUNDWATER MODELLING

Two appropriate texts which set out all terminology and standard groundwater modelling concepts used in this report, are Rushton & Redshaw (1979) and Hunt (1983). Various alternative techniques are available for the study of groundwater flow. The four principal categories are analytical, graphical, physical and numerical. With generally improved access to computing facilities, the last approach has recently been favoured in view of its advantages of flexibility, speed of solution and minimal cost.

5.3 SECTIONAL, STEADY STATE MODELLING CASES

The following situations are commonly encountered in reservoir engineering:

- * The watertable extends almost horizontally into the slope.
- * The watertable is inclined, unconfined and has an impermeable base.
- * The watertable is inclined but no permeability barriers are present.
- * Artesian or sub-artesian pressures act beneath an aquiclude.
- * Multiple or leaky aquifers are present.

Simple interpretations for each of these cases are outlined below.

5.3.1 Horizontal Watertable.

This is the simplest case, and is found only where highly permeable formations are present (eg alluvium) or catchments do not extend far from the river. Provided permeability does not decrease in the materials affected by reservoir filling, the horizontal watertable should reform at the new lake level. If less permeable materials are present at the higher levels, in most cases the end result will be the same. Continuity suggests that pressures are unlikely to exceed lake level anywhere, although siltation may generate a more adverse stability condition in the long term.

5.3.2 Inclined Unconfined Watertable.

This is one of the more common situations encountered, particularly where an active landslide is present and gouge generated in the failure surface has caused a perched watertable to develop as an unconfined aquifer. Fig. 5-1 shows a case of a slide which is creeping slowly (ie safety factor of unity) at present. Reservoir filling will cause toe submergence and corresponding readjustment of the original inclined watertable (P1). To consider likely upper and lower bounds of response it may be assumed (a) that the future piezometric line (P2) will run horizontally until it reaches the former inclined line (P1), this is clearly optimistic, (b) the new line (P3) is found by translating the initial piezometric line uniformly upwards over the full length of the slide by the height which the reservoir is raised above the slide toe, an unduly pessimistic approach. Taking this model as drawn, typical material properties have been input for stability analysis. A buttress fill (assumed as free-draining or constructed against the slide with an intermediate drainage layer) is shown. Without submergence, the buttress would increase the existing safety factor (using standard limit equilibrium methods) by about 15% with little sensitivity to the inferred present watertable position. However, the effect of toe submergence to the level shown would be a subsequent decrease in stability by either 5 or 16% depending on whether P2 or P3 piezometric lines are input. The overall net effect from the initial (pre-buttress and pre-lake) condition will therefore be +10% or -1% for the optimistic and pessimistic assumptions respectively.

Note that the initial condition shows a relatively low watertable in the toe zone therefore the trend is for submergence to decrease the safety factor. In a perched watertable example with toe pore pressures which are high initially, lake-filling will sometimes increase the safety factor (a phenomenon best envisaged as submergence counteracting the former seepage forces).

Reality will lie somewhere between the optimistic and pessimistic extremes, with the former being a good approximation for very steep piezometric gradients and the latter close for low gradients. In practice most active slides contain moderate inclinations, therefore some form of logical reasoning is required to establish a likely solution. Inclined watertables become established in order to provide the hydraulic gradient that is necessary to effect the lateral transmission of the long term average inflow of water to the aquifer (presumably originating from rainwater infiltration, seepage from creeks, etc). When a reservoir is formed the perched aquifer thickness at the toe will rise correspondingly. Therefore to satisfy continuity, a lesser hydraulic gradient will pass the

- - - - - FAILURE SURFACE 1,
- - - - - SUBMERGENCE LINE 1,
- - - - - PIEZOMETRIC LINE 1, 2, 3,
- SOIL BOUNDARY LINES

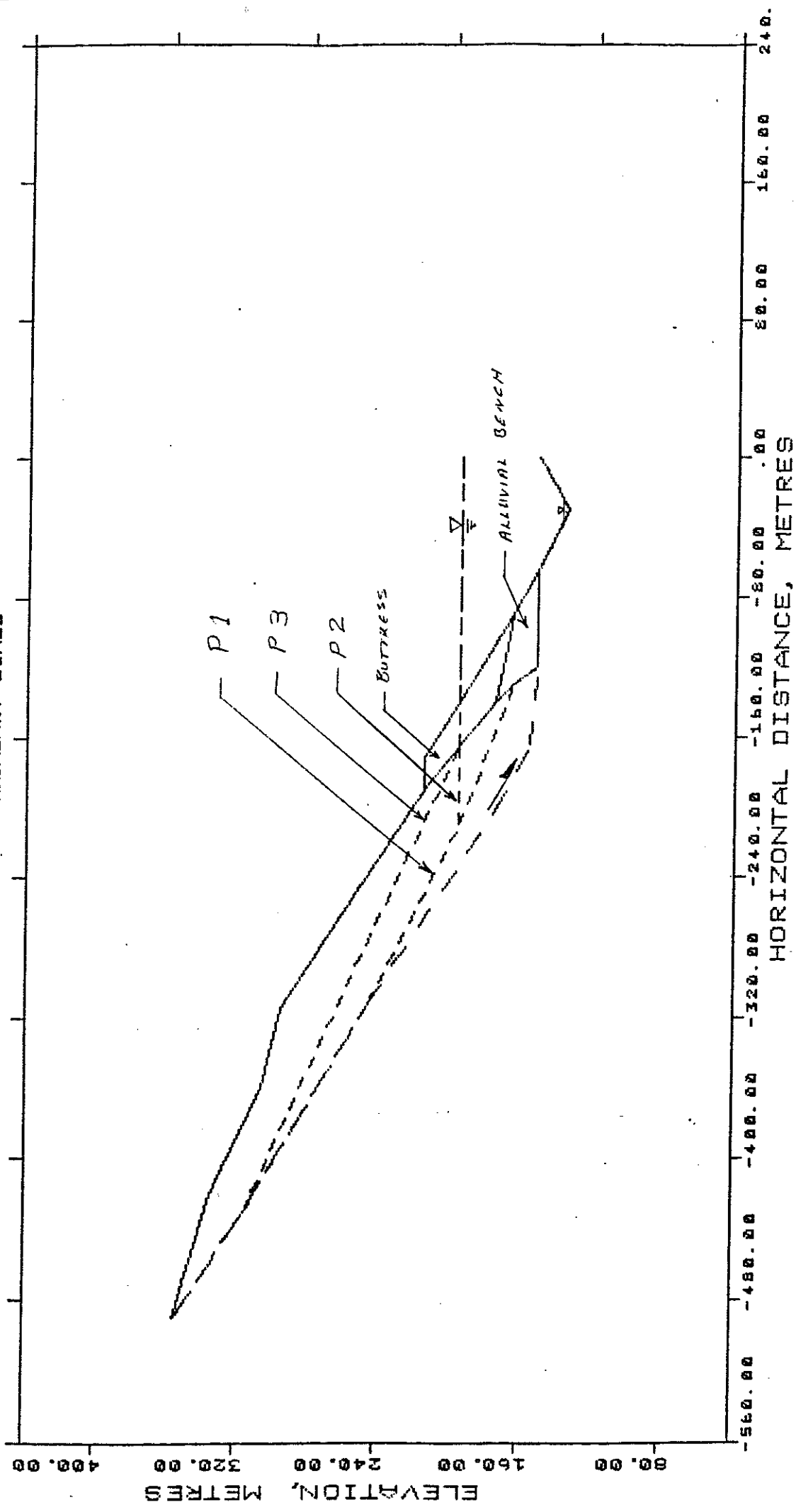


Fig. 5-1 Construction of piezometric lines for an unconfined aquifer

same groundwater flow through the increased cross sectional area of the saturated portion of the slope. There are thus two equations to satisfy: continuity and Darcy's Law.

The first step is to set up a model for the existing situation, using piezometric and permeability information from at least 1 drillhole (with multiple piezometers installed). Two or more drillholes along the length of the aquifer are preferable. Boundary conditions must also be determined or a range of possible situations examined. Recharge sources must then be considered and a logical steady state model derived for the pre-existing conditions. This is essentially a 'calibration' process. The next step is to introduce the new boundary conditions (raised reservoir) and determine the new steady state flow net from standard procedures that acknowledge the relevant constitutive relationships. This may be done using the traditional graphical method (flow net construction) or using numerical methods.

The flow net, has practical limitations in that only sectional flow can be considered, and unsteady flow situations (namely reservoir filling or drawdown) cannot be addressed. For the steady state case for section flow, infiltration may be incorporated by noting that in this case, the phreatic surface is not a streamline, and recharge will cause the streamlines to diverge from the phreatic line by an angle A, given by:

$$A = 90 - \arctan(\tan(B)/(p/k))$$

(Rouse, 1949) where:

B is in the inclination of the phreatic surface,
p is the recharge from infiltration
k is the permeability in the flow direction

It is of interest to note that the dimensionless ratio p/k is the governing factor, ie explicit knowledge of infiltration and permeability individually is not required for the steady state case.

In view of the practical limitations to the graphical procedure, numerical treatment only has been addressed for reservoir engineering.

Three possible approaches for numerical analysis are discussed below.

(A) Analytical solution

Using the Dupuit assumption, the relevant equations have been formulated for the sectional flow case for an unconfined aquifer case by Dr. Bruce Hunt, pers comm. (The Dupuit assumption, ie equipotential lines are taken as vertical, or piezometric head is independent of depth reduces the 2-dimensional model for flow in a section to a 1-dimensional problem. As this terminology can be confusing, the terms section model for

downslope flow, or regional flow for cases where lateral flow is incorporated, will be used in this chapter.)

The main limitations to the analytical method is its assumption of constant slope for each aquifer. The slope may be divided into segments, but the solution is time consuming.

(B) Finite element method.

Groundwater programs that accommodate infiltration are available. One version tried was SEEP, a section modelling program written for the IBM PC. The data for a number of field examples were entered, but for these cases which were long in relation to their height, the problem would not execute. At the time of commencing this study, no other finite element groundwater programs were available to the writer. A microcomputer version for the Golder's package (Golder Associates, 1979) is now available, as is the program MODFLOW (McDonald et al 1988). Both are versatile in their application, but neither are structured for stability analysis or input of progressively changing reservoir levels.

(C) Finite difference method.

A third alternative numerical approach to predicting watertable response in the unconfined aquifer case is the use of a finite difference model. The sectional model required can be produced readily by simplifying the regional model (documented in Section 5.4) to one with invariant conditions laterally.

5.3.3 Inclined Watertable With No Permeability Barrier

In this case, the Dupuit approximation is not valid, but a flow net may be constructed. The solution would usually be close to that of a parallel rise in the watertable. In practice, this situation would seldom arise as lower permeability strata are likely to be found at depth, the Dupuit approximation may then be adopted and calculation carried out as for (C) above.

5.3.4 Artesian or Sub-Artesian Pressures Acting Beneath an Aquiclude

There are two sub-categories to be considered here, although both may be treated in the same manner:

- (i) Fully confined aquifer (for the extent of the potential failure surface being considered), and
- (ii) Semi-unconfined aquifer (ie with a transition from confined conditions at the toe to unconfined conditions upslope).

In turn, two situations can apply to each of the aquifer types, ie the potential failure surface being considered may be either the overlying (confining) aquiclude itself, or a surface within (or more likely at the base of) the confined aquifer. In both sub-categories, 'calibration' of the existing model is required as above except that the source of recharge is assumed to be an inflow (q) with an upslope source, rather than areal infiltration from above.

The assumptions necessary for evaluation, are that continuity and Darcy's Law apply to the region beneath the confining horizon. The result is that a rise in toe water level will require an equal rise in piezometric levels everywhere in the pressurised section of the aquifer. At some distance into the slope, the confined aquifer will adjoin an unconfined system with an associated source of recharge. Above this point (the confined/unconfined junction) the problem is simplified if the lower aquifer has constant transmissivity, ie the phreatic surface will be raised by an amount equal to the rise in toe water level and the length of the confined section will increase accordingly. If the lower aquifer has variable transmissivity, a flow net or numerical model may be constructed after 'calibration' to determine the necessary q/k ratio and variation in transmissivity for the existing condition.

There are 3 points to note with a confined or semi-unconfined system:

(i) An upper aquifer with and unconfined groundwater system is likely to be present also or will develop on reservoir filling. Before carrying out any analyses of failure surfaces which pass at least in part above the upper aquiclude, it will be necessary to calculate the piezometric line for the upper aquifer using (II) above. Similarly, pressures should be evaluated on both sides of the aquiclude below a confined aquifer. When considering failure surfaces passing along any aquiclude (eg along a gouge surface) stability analyses should be calculated using the higher of the piezometric levels across the boundary. (The available shear strength will be dictated by the side of the aquiclude which exhibits the lower effective stress.)

(ii) The piezometric line will not emerge from the reservoir shoreline, but will intercept the submergence line at some distance out into the reservoir (directly above the point where the aquiclude terminates on the slope).

(Both the above points apply to the unconfined inclined aquifer case but usually to a lesser extent.)

(iii) A simple model for confined sectional flow is appropriate only when the slide width is large in relation to its length. Gross over-estimation of piezometric rises on reservoir filling will occur otherwise, and analysis of lateral flows (a regional model) is essential for realistic interpretation.

Example

Fig. 5-2 shows the field data obtained for a confined aquifer case. The piezometric pressures acting at the failure surface (proven to be sub-artesian from the drillhole water level record) are shown. In addition to the two piezometers, it may also be inferred that the pressure at the toe of the slide is given by the pressure head at river level. If sufficient data were available regarding the confined aquifer, a flow net could be constructed. However, for the purpose of this example linear interpolation and extrapolation between and beyond the known pressures has been adopted. The model for determination of the absolute safety factor for initial conditions is then established (P1 on Fig. 5-3).

For toe submergence, the entire piezometric surface is raised equally by an amount equal to the height of reservoir rise (P2 on Fig. 5-3). Note that both P1 and P2 meet the river and lake levels (respectively) at points vertically above the extremity of the slide toe, rather than at the shoreline. Line P2 is likely to be very conservative because lateral flows have not been considered - see note (iii) above. However, for the sectional model, high artesian pressures are predicted over part of the slide, therefore the limit equilibrium stability analysis would need to be checked to ensure that the algorithm used does not allow effective stresses to reduce below zero.) This slide also contains a perched watertable above the slide base, therefore the procedure as outlined for an unconfined aquifer would next be followed to ensure that the greater of the piezometric pressures on either side of the failure surface is adopted for analysis.

5.3.5 Multiple or Leaky Aquifers

Where the permeability of an aquitard is not several orders less than the adjacent strata, seepage through it may become significant. This would require more extensive field instrumentation and definition of permeability characteristics of the relevant strata. For preliminary investigation, a range of assumptions for the hydro-geological model might be investigated in a sensitivity analysis. However, for the relevant situations above, a reservoir rise will usually raise pressures on both sides of the aquiclude. The differential head and consequent leakage are therefore likely to be relatively insensitive to reservoir position. Therefore for preliminary interpretation, the aquitards may be taken as aquicludes allowing sectional modelling as above. The results may be overly conservative. More realistic modelling may be warranted, as described in the next section.

5.4 REGIONAL, TIME-DEPENDENT GROUNDWATER FLOW MODELLING

5.4.1 Introduction

This section expands on the basic concepts discussed so far, and documents the computer program LSFLOW which has been developed for determining the time dependent changes in the safety factor of a landslide (or other slope) where piezometric levels on existing or potential failure surfaces will be affected by reservoir filling. Other

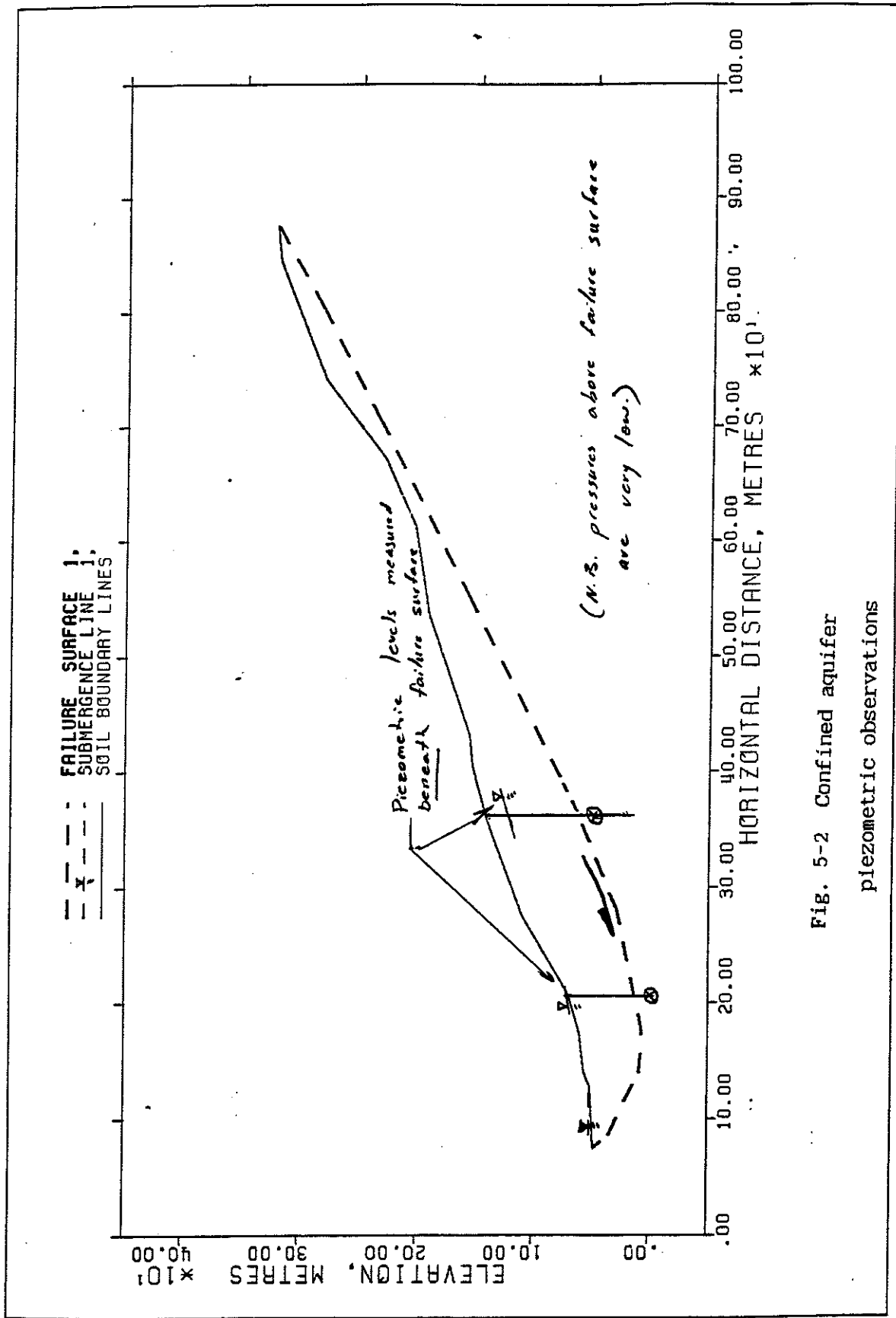


Fig. 5-2 Confined aquifer
piezometric observations

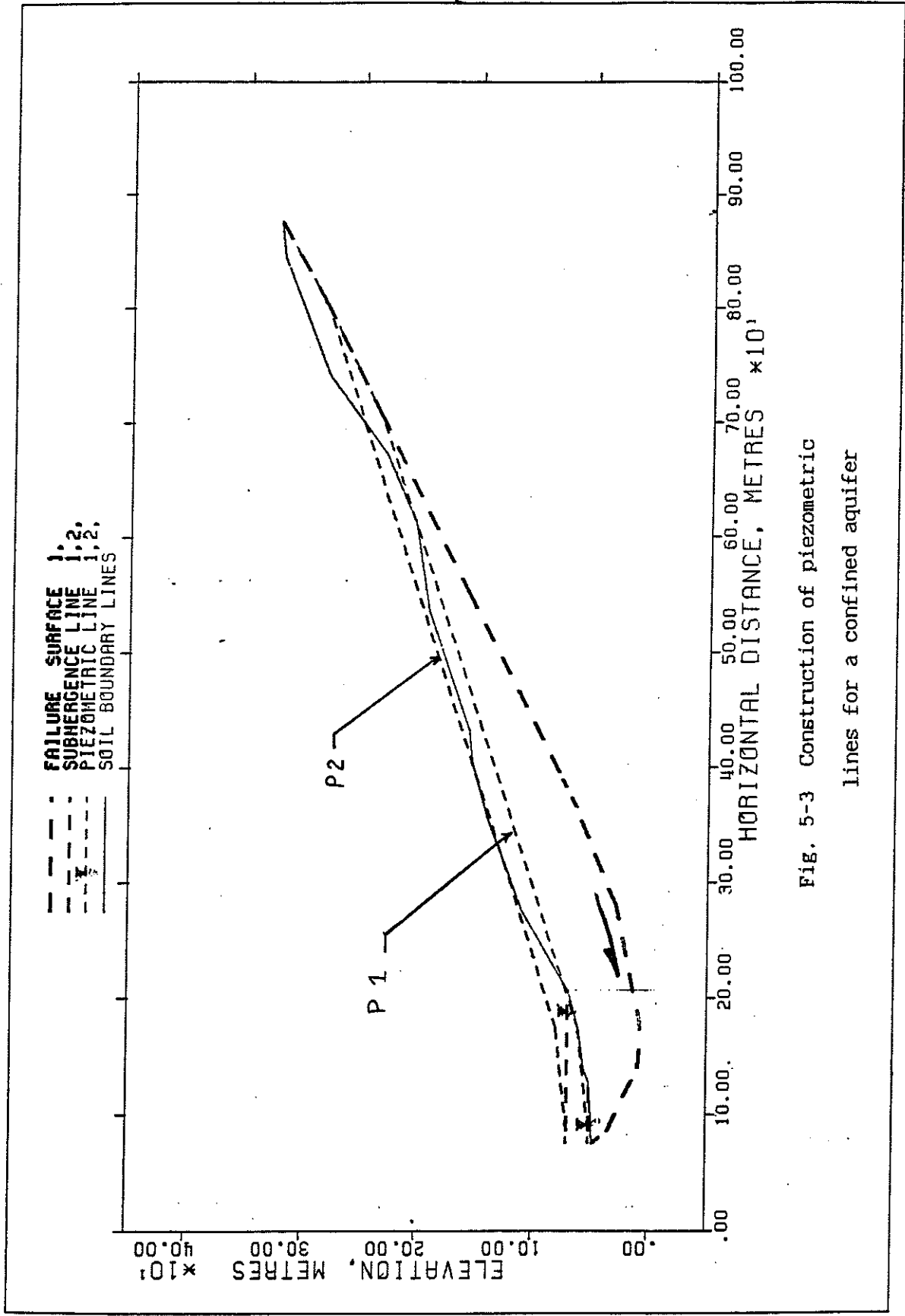


Fig. 5-3 Construction of piezometric lines for a confined aquifer

aspects which can also be modelled with the program are rapid or slow drawdowns, water level cycling during daily and annual operation, remedial drainage from drives or drillholes, and the effects of varying rainfall infiltration (from removal of vegetation, seasonal or long term climatic changes etc).

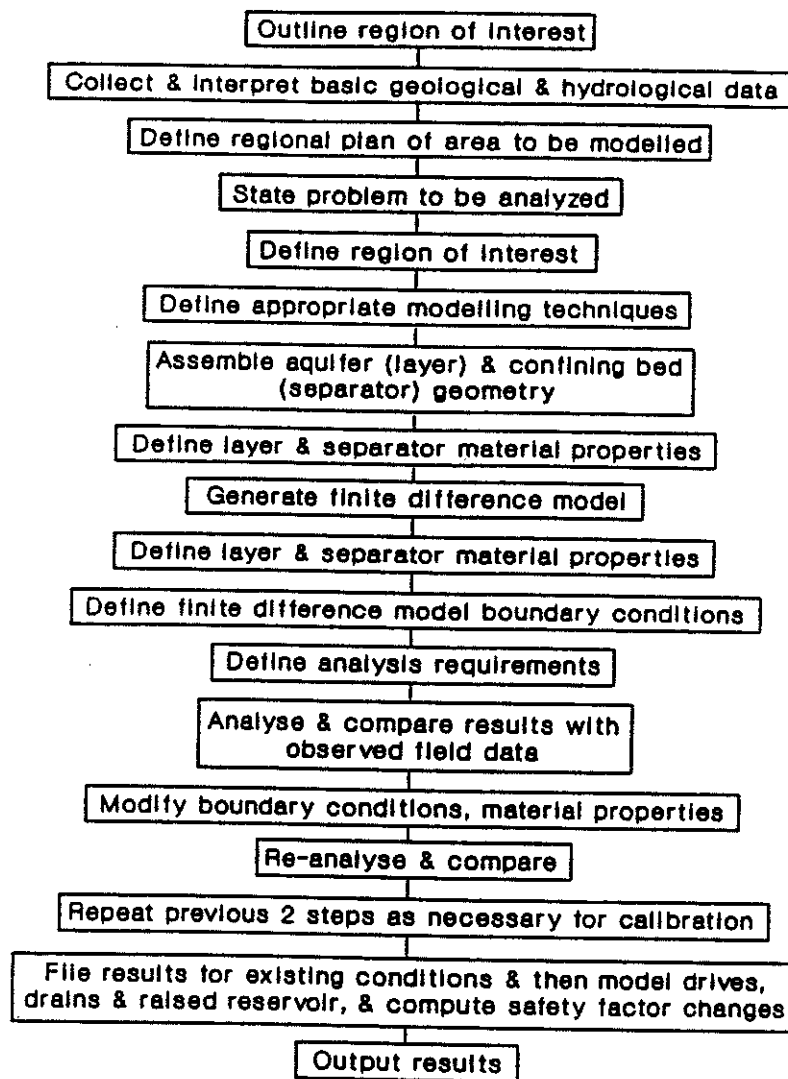
LSFLOW was written to allow rapid preliminary assessment of the effects of reservoir filling in a situation where there are a large number of landslides or slopes where stability is suspect. The effect of reservoir filling on stability and alternative options for remedial measures may be readily appraised with this program. Adaption to non-standard conditions can be carried out readily by modification of the relevant subroutines. This facilitates very rapid production of results, although reasonable familiarity with the relevant groundwater theory and algorithms is required. For this reason, the documentation given here is at programmer's level and assumes the user has a good working knowledge of basic geohydrology modelling principles. In practice it has been found that this is an efficient way of modelling the wide variety of aquifer cases found in landslides. (Initial work was aimed at producing a program which would be user friendly for all cases, but each new case studied has required minor program modification to suit specific conditions.) The Dupuit approximation (assuming equipotentials are vertical within each aquifer) is used, however vertical flow components are acknowledged indirectly. For final analysis or design, a modelling procedure that has improved capability for accounting for vertical flow components and allows mutual interaction between multiple aquifers, may be preferable.

The program itself, is only one item in the necessary sequence of steps required to reach an overall appreciation and understanding of the groundwater processes in a landslide aquifer. The most time consuming and vital steps, are assembly of the basic geological and hydrological data in the first place, and development of a conceptual model. The full process is illustrated in Fig. 5-4, and the way in which the program LSFLOW contributes is shown Fig. 5-5.

5.4.2 Program Development

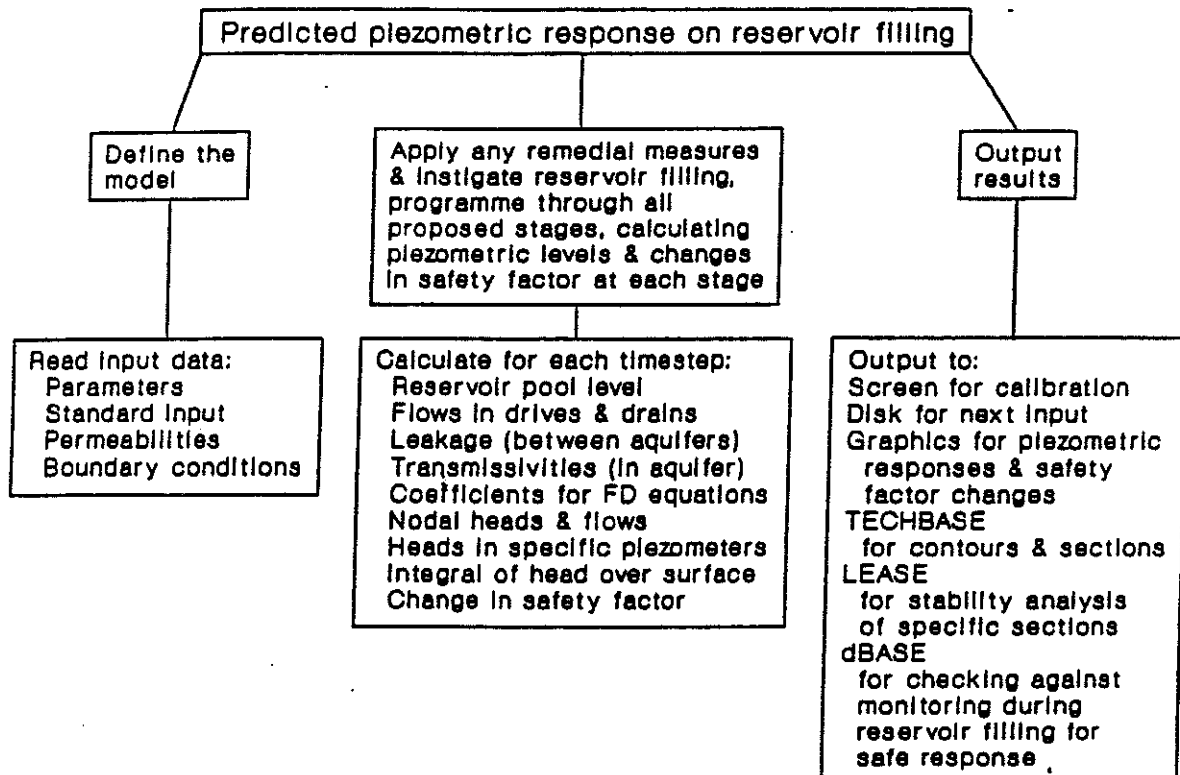
5.4.2.1 Mathematical basis.

The flow of groundwater within an aquifer can be adequately described using two equations, Continuity and Darcy's Law. The continuity equation (or Law of Conservation of Mass) accounts mathematically for the requirement that the increase in volume of water within any element of the aquifer is equal to the difference between the inflow and the outflow during any given time interval. The flow between any two adjacent elements is given by Darcy's Law to be proportional to the negative hydraulic gradient between those elements, with the constant of proportionality being the aquifer transmissivity.



Numerical modelling of landslide aquifers affected by reservoir filling.

Fig. 5-4



Programme structure diagram for landslide groundwater modelling.

Fig. 5-5

Combination of these 2 fundamental relationships, integrating and applying the divergence theorem, leads to the partial differential equation:

$$\nabla \cdot (T \nabla h) - (K'/B')(h-h') - Q/A + R = S (\partial h / \partial t) \dots \dots (1)$$

Where:

T is transmissivity in the plane of the aquifer

K'/B' is the leakance (ratio of vertical permeability to vertical thickness) of separator (aquitard) between the head in the aquifer and the external head (h')

h is the piezometric head

h' is the head external to the aquifer

Q/A is the outflow from wells per unit area

R is the areal recharge from infiltration

S is the storage coefficient

t is time

A complete derivation of equation (1) is given by most texts on groundwater modelling (eg Hunt, 1983; Rushton and Redshaw, 1979).

Note that this is a general unsteady state relationship. Steady state solutions can be determined simply by setting a large output time, or using a very small value for storage coefficient.

For the type of field problem encountered, analytical solutions are usually impractical or impossible. Accordingly, either physical or numerical models must be adopted. The former have limitations of cost, time and difficulty of modelling other than steady state conditions. Numerical solution using finite difference approximations has been adopted, as a straightforward method which can be readily modified to specific situations.

5.4.2.2 Finite difference model

Numerical modelling of the groundwater flow equation can be carried out using one of three common techniques: finite element, finite difference or the boundary integral equation. In each of these methods, approximations are introduced by describing the continuous functions of flow and piezometric head in terms of some discrete grid. Time is similarly divided into discrete timesteps. Accuracy can be made appropriate to the field data by adopting a suitably fine model.

The finite difference discretisation used in this program is based on the system described by Hunt (1983). Some variations have been required to allow automatic mesh generation, greater generalisation and adaption to the variety of situations found in landslides.

The aquifer is modelled as a rectangular system of nodes with equi-dimensional spacing, ie a grid with rows and columns. The conventions established are that the first row is the most upslope line of nodes, while the last row is defined as a series of fixed heads, ie to coincide with the river or reservoir level. For this reason the grid must be aligned as closely as possible so that the last row parallels the river with each node in that row located within the river or on the opposite bank. Irregular boundaries may be readily simulated by inputting appropriate values for permeability of any node outside the area of interest (zero values for inactive nodes adjacent to a no-flow boundary and very large values for nodes adjacent to fixed head boundaries). Node numbering begins at the lower left node and continues sequentially in an anti-clockwise direction until all exterior nodes are numbered. No flow is assumed between adjacent nodes forming the exterior no-flow boundary. Internal nodes are sequentially numbered down each column working from left to right.

5.4.2.3 Finite difference formulation.

A number of assumptions are made:

Darcy's Law is valid.

The density of water remains constant (independent of pressure).

Storage in an unconfined aquifer is dependent on the effective porosity but not the local pressure.

Storage in a confined aquifer is derived from linear elastic deformation of the aquifer.

The head distribution is independent of salinity, temperature, barometric pressure etc.

The Dupuit approximation is realistic.

Hunt (1983) provides a straightforward derivation of alternative finite difference approximations to equation (1). The sequence he adopts is:

(i) Approximate the piezometric head at each node with a finite degree polynomial whose coefficients are written in terms of the piezometric head at each adjacent node.

(ii) Specify an approximation for the boundary condition at each exterior node.

(iii) With the same number of equations as there are nodes, the unknown heads may be solved for simultaneously.

The equations could be solved directly, however to minimise execution time and computer storage requirements, an iterative method of solution was adopted. Gauss - Seidel was used initially but this proved unacceptably slow, therefore the standard method of successive over-relaxation (SOR) was added with the optimum SOR factor calculated before each iteration. This provided more than tenfold increase in the rate of convergence.

The original formulation by Hunt, provided for cases of constant transmissivity only, a condition which assures stable convergence. Because substantial change in transmissivity is almost invariably associated with reservoir filling, the facility for change was added. Accompanying numerical instability resulted, but this was effectively overcome by the addition of an additional constant transmissivity loop within each timestep. Assurance of uniqueness of a convergent solution is always available because when numerical stability develops, it occurs in the early iterations and shows extreme oscillatory growth in amplitude.

5.4.3 Program Design

5.4.3.1 Overall structure

The program consists of a main program, which calls in turn, a number of subroutines. The primary subroutines perform specific independent functions of data input, processing and output. A number of secondary and tertiary subroutines are called by one or more of the primary subroutines. Fig. 5-5 shows the fundamental elements of the program structure.

The regional groundwater flow algorithms have been adapted from Hunt's FORTRAN source code. The adaptations include subroutines which allow more generalised formulation for varying transmissivity, varying boundary conditions, confined and unconfined flow, and approximate simulation of vertical flows. A range of aquifer conditions, may be accommodated such as inclined aquicludes, drainage drives, horizontal drains, and time variant reservoir levels including controlled or rapid drawdown. Further subroutines calculate relevant output fields for subsequent post-processing to produce contour drawings of predicted steady state piezometric surfaces (either with or without remedial measures and lakefilling). Also generated are plot files giving the time dependent response of each piezometer which the model predicts from the specified sequence of drainage and/or lakefilling, and the accompanying changes in safety factor of the slide.

The program is designed to simulate non-steady flow, with steady state conditions produced indirectly by continuing execution to a large output time. The period of simulation is divided into a series of "constant boundary condition stages" within which the conditions such as recharge, drainage and fixed heads (river or reservoir level) are taken as invariant. Each constant boundary condition stage is divided into a series of timesteps which are further divided into a series of "constant transmissivity" stages, to avoid numerical instability. The system of finite difference equations written for each

node is solved to determine either the head at variable head nodes, or flows at fixed head nodes at the end of each timestep. One of two alternative iterative solution methods is used to solve for the unknown heads or flows at each timestep. The solution sequence uses 4 nested loops: a constant boundary condition loop, within which there is a timestep loop, within which there is a constant transmissivity loop, which in turn contains an iteration loop.

5.4.3.2 Aquifer Model Geometry

The regional flow model requires the definition of a rectangular grid of equally spaced nodes, as described above. The Dupuit approximation is made, which requires that flows be predominantly horizontal rather than vertical. Variation of permeability with depth can be accommodated, provided the Dupuit approximation remains appropriate. Variation of aquifer permeability laterally, relies primarily on the geological interpretation (particularly with regard to location of faults identified from surface lineaments, outcrops and subsurface intersections) and secondarily on observed piezometric gradients between piezometers and the river, while also giving due regard to other constraints such as topographic depressions (side creeks) seepages and springs.

5.4.3.3 Input Structure

The input structure of the program is optional in as much as a fully ordered input can be used (by persons unfamiliar with the program), or through use of defaults and systematic abbreviated input.

Fully ordered input requires specification of all input data in a sequential listing for each node. A pre-processing program is necessary for efficient assembly of input data. The alternative which has proved most practicable, is to generate only the required inter-nodal relationships in pre-processing, and input or generate all other data from subroutines of the main program. The main input file that requires continual modification during the calibration process is that for lateral distribution of permeability. Adoption of a basic predominant permeability for the model, with redefinition at only those nodes where permeability contrasts are required has proved the most rapid means of matching the model with the observed piezometric levels. There are thus 2 data files that must be input: one showing the relationship between nodes on the finite difference mesh and the other containing the nodal permeabilities and aquifer boundaries.

5.4.3.4 Program Structure

The program (listed in Appendix 2) is written in TURBO-BASIC, providing an easily modified structure which is similar to that of PASCAL. Conversion to the latter or FORTRAN would be straightforward. Problems with 500 to 700 nodes require a maths co-processor for reasonable execution times (about 2 minutes for each adjustment during calibration using an 80386 processor).

The main program is short, and calls a large number of subroutines. The function of each subroutine is explained in Appendix 2.

5.4.3.5 Derivation of 3-D Safety Factor Algorithms

Where natural slopes or landslides are affected by reservoir filling, it is the change in safety factor caused by groundwater changes that is of principal interest rather than inferred absolute values of safety factor. This allows direct determination of whether the resultant effect of reservoir filling and remedial measures results in a state of net enhancement or otherwise.

The type of situation usually encountered, requires stability analysis to be carried out on more than one section to adequately represent the effect of small changes in groundwater conditions. This is especially so in common cases where the arcuate shape (both in long section and cross section) of potential failure surfaces is combined with local depressions of piezometric surfaces in the vicinity of discrete drainage drillholes or drives.

The approach to stability analysis in conjunction with the groundwater modelling, has therefore been to assess the ongoing piezometric changes at each node in the model, so that the overall effects can be computed in a very straightforward fashion, yet with reasonable accuracy.

The steps involved are:

S1. Using an appropriately accurate limit equilibrium method:

S1.1 Compute the initial safety factor and mobilised friction angle on as many sections as required for adequate definition of conditions prior to reservoir filling or remedial measures. (At each step, use an average value weighted according to section areas, if more than one section is involved.)

S1.2 Compute the change in safety factor from the initial condition to the ideal gravity drainage condition (including any buttressing or other slope modifications) before reservoir filling, (dF_i).

S1.3 Compute the change in safety factor from the ideal gravity drainage condition before reservoir filling to the ideal drainage condition at full reservoir level, (dF_f).

S2. Input the relevant slide parameters to LSFLOW. The program will then automatically carry out:

S2.1 Calculation of the sensitivity of the safety factor of the slide to a change in pore pressure of 1 kPa acting over 1 square metre of the slide. (Further explanation is given below).

S2.2 Calculations pertaining to the piezometric situation at each timestep and the corresponding reservoir level programmed for that time, these are:

S2.2.1 The change in safety factor from the ideal drainage condition before filling to the ideal drainage condition for the particular partial pool level at that time, (dFp). (Usually determined from linear interpolation of dFf.)

S2.2.2 The areal integral of the change in piezometric head insofar as it relates to pore pressures which affect the failure surface. This is carried out at each timestep and includes any effects from the progressive construction of drives and raising of the reservoir. All changes in head are calculated relative to the ideal gravity drainage condition corresponding to the level of the reservoir at that timestep. The product of the head integral and the safety factor sensitivity, then gives the change in safety factor from ideal drainage condition (with the reservoir at the level planned for that timestep) to the current model condition (dFh).

S2.2.3 The total change in safety factor (dF) from the initial condition to the current condition, ie simply from:

$$dF = dFi + dFp + dFh$$

S2.3 Output to disk, in a form suitable for plotting of the timestep, reservoir level and safety factor. (See example below.)

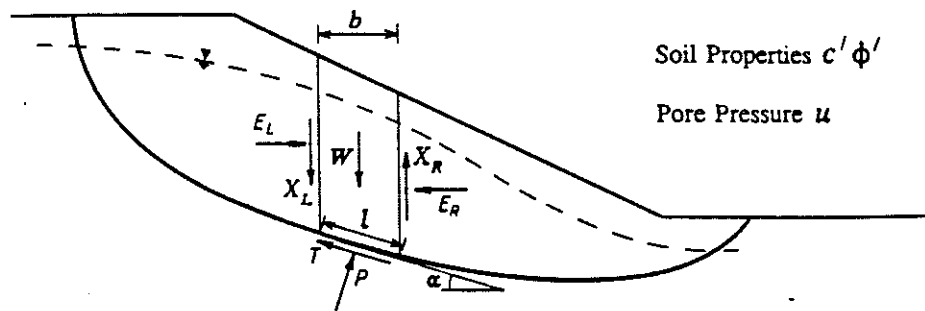
The procedure involves a number of steps, but these are quite straightforward in practice, and allow the advantages of using a rigorous limit equilibrium analyses as the basis for the safety factor computations with fine tuning using quicker (non-iterative), simply verifiable methods.

Calculation of the safety factor sensitivity.

The change in safety factor corresponding to a change in pore pressure may be readily derived from any of the various limit equilibrium methods of slices. Fig. 5-6 shows the geometry of a typical slice and the results of differentiating the safety factor (F) with respect to pore pressure (u). Note that the Ordinary Method provides an explicit solution because this is the only method in which the safety factor appears only on one side of the equation. All other methods require solution by iteration. To simplify the solutions for other methods, it has been assumed that the total normal stress on the base of each slice is changed by external loads (change in reservoir level) but unaffected by change in internal pore pressure. This is not strictly true because there will be small adjustments to the total normal stress on the base of each slice with a change in internal pore pressure, as a result of

- (i) the change in density associated with saturation (discussed further below) and,
- (ii) the re-distribution of inter-slice stresses.

Forces for Slice i



'Ordinary' Method.

$$F = \frac{\Sigma (c' + (W \cos \alpha - ul) \tan \phi')}{\Sigma W \sin \alpha}$$

$$\therefore \frac{\partial F}{\partial u_i} = \frac{-l_i \tan \phi'}{\Sigma W \sin \alpha}$$

$$\text{but } l_i = \frac{b_i}{\cos \alpha_i}$$

$$\therefore \frac{\partial F}{\partial u_i} = \frac{-b_i \tan \phi'}{\cos \alpha_i \Sigma W \sin \alpha}$$

Bishop's Simplified (as for 'Ordinary' Method)

$$\frac{\partial F}{\partial u_i} = \frac{-b_i \tan \phi'}{\cos \alpha_i \Sigma W \sin \alpha}$$

Janbu Simplified

$$\frac{\partial F}{\partial u_i} = \frac{-f_o b_i \tan \phi'}{\cos^2 \alpha_i \Sigma W \tan \alpha}$$

Janbu's rigorous and Spencer

$$\frac{\partial F}{\partial u_i} = \frac{-b_i \tan \phi'}{\cos^2 \alpha_i \Sigma (W - (X_R - X_L)) \tan \alpha}$$

Sarma (After many approximations)

$$\frac{\partial F}{\partial u_i} = \frac{-3.33 b_i \sin \phi'}{\cos \alpha_i W}$$

Fig. 5-6

Derivation of Safety Factor Sensitivity to Pore Pressure in Limit Equilibrium Methods

It is intuitively apparent that the effect of the latter will be very small. This can be readily confirmed for any specific slide by inputting appropriate changes to a rigorous limit equilibrium model. All cases so far considered, have shown the effect to be negligible. The circumstance which would tend to provide limited accuracy occurs when the change in pore pressure is the result of changes in bulk density associated with saturation of an unconfined aquifer above the failure surface and the effective porosity is high (say 0.1 or more). In this case changes in safety factor will be over-estimated, eg the simplistically calculated change in stability of -10%, may be only -9%. It may be appropriate to consider more accurate computation when the effective porosity exceeds about 0.15.

Further explanation of safety factor sensitivity is discussed in Appendix 3.

5.4.3.6 Output Structure

Four output files are generated from normal execution of LSFLOW.

The main output file name is prompted for on completion. This displays all output data in the form of a table corresponding to the layout of nodes. Typical output (adjustable from the respective subroutine) includes nodal values for:

- Piezometric levels at the end of the simulation
- Piezometric levels at the start of lakefilling
- Increase in piezometric levels during lakefilling
- Increase in piezometric heads affecting the failure surface only.
- Net drainable head affecting the failure surface.
- Flows from springs
- Flows from drives, horizontal drains or pumped wells.

Much of the input data is output also for checking in tabular form, eg:

- Lateral permeability distribution
- Infiltration (net after evapotranspiration)
- Concentrated recharge or wells
- Node number
- Aquifer boundaries
- Leakance
- Confinement condition

The second output file prompted for, is an intermediate file for storing all data held in memory at the end of the simulation. This file is written in the standard format for normal input. A specific set of conditions can therefore be filed and recovered for ongoing execution at a later stage.

The third output file is generated throughout the simulation and filed automatically without prompting by the user. The file "PZRISE.OUT" is produced whenever the option for a rising reservoir is called, and contains the time varying responses of piezometric

levels for all piezometers which have ports within the aquifer. The file contains a series of columns in a format suitable for importing to a plotting program such as Harvard Graphics. Column 1 is the elapsed time in months, from the start of reservoir filling. Column 2 is the water level at the toe of the slide at that time. One column then follows for each specified piezometer location installed in the aquifer and the predicted piezometric level at the given time is listed. The last column gives the change in safety factor (from the initial condition before reservoir filling) calculated over the entire slide at the given time. The latter allows appreciation of the likely effects of excessively rapid filling or rapid drawdown as well as producing the expected result for the steady state condition at full pool.

The fourth file is also generated automatically, and isolates all piezometric heads at the end of the simulation into the file "PZLEVEL.OUT" which is formatted for direct input to contouring programs such as SURFER (Golden Software Inc.) or any similar plan contouring program.

The outputs from case histories are shown graphically and on contour drawings in Appendix 2. The end product - the time dependent change in safety factor as the reservoir is filled or drawn down is also shown in Fig. 5-7 for discussion in the following section.

5.5 GROUNDWATER MODELLING DURING LANDSLIDE INVESTIGATIONS.

Where landslides have moved many tens or hundreds of metres downslope, the geological model is unlikely to be simple. Determining the location of persistent failure surfaces is usually compounded by core losses that are most likely to occur in these zones of interest. However, in many cases, it has been found that aquifers are controlled by the principal failure surfaces, because the latter usually provide marked permeability contrasts. Determination of groundwater pressures with multi-port piezometer installations can therefore be used to delineate stacked aquifer systems and confirm a geological model through groundwater modelling.

Piezometric gradients of the cases studied have been highly variable. Even in apparently similar materials, gradients can vary from about 0.05 to 0.5 from the valley floor. The sources of groundwater information are surface seepages, seismic velocity contrasts, drilling fluid records, geologging, packer tests or rising/falling head tests for permeability, temporary piezometers installed during drilling and permanently installed piezometers.

The modelling methods require some over simplification but this is made commensurate with the nature and extent of field information. Once the mesh for the initial model has been set up, subsequent updating can be carried out rapidly. Preliminary models will necessarily be subject to change but it has been found that modelling at an early stage provides the following benefits.

- (i) An overall appreciation of the magnitude of the effect of reservoir filling on slope stability can be obtained at the outset, both by the geologist and designer.

(ii) Drillholes and instrumentation may be optimised (in number and position) by determining locations in key areas where maximum drainable head (Appendix 2) is predicted to develop after lakefilling, or where greatest sensitivity can be demonstrated from variation within the expected range of geological models.

(iii) The modelling frequently throws light on the geological model, either supporting or pointing to alternative conceptual models and suggesting a course for verification. A common example is the location of permeability barriers - both steeply dipping and at low angles (faults and failure surfaces).

(iv) Remedial measures can be optimised. Interaction and refinement can provide substantial cost savings on large scale remedial drainage.

Consistency of any postulated piezometric profile with a limit equilibrium stability model allows confirmation that the slide mechanism has been correctly identified. Where active creep deformations are taking place, safety factors close to 1.0 are required for rational geotechnical models. Otherwise, a reassessment of piezometric assumptions, strengths and geometry is necessary. Unconservative predictions for safety factor changes can result if the pre-existing piezometric levels are incorrectly modelled. Therefore where groundwater information is sparse, conservative levels are assessed for pre-existing watertables. (Conservative predictions are usually generated by low levels in unconfined aquifers and high levels in confined aquifers.)

5.6 THE ROLE OF GROUNDWATER MODELLING IN RESERVOIR SAFETY ASSURANCE

5.6.1 The Piezometric Lag Problem

On first filling of a reservoir, the existing groundwater levels within the toe areas of slopes would rise relatively quickly to the new external water level, because a large source of recharge would be present. However, in slopes of moderate or low permeability (less than about 1×10^{-6} m/s, the watertable is likely to have a significant upslope gradient (as a result of rainfall infiltration). Above the full pool level, the groundwater would take considerable time to reach an 'ultimate' condition which would thereafter fluctuate only slightly depending on season and precipitation. (Examples are given in Appendix 2). This delay in achieving steady state flow is a result of the limited recharge quantities to fill the effective porosity of material above lake level. Recharge rates are limited. Piezometric pressures can therefore be expected to increase more slowly once they reach lake level, approaching ultimate (steady state) values asymptotically with time.

The time for piezometric pressures to rise to their ultimate values can be a **major factor in relation to safety assurance** in moderate or low permeability materials. During reservoir filling, all slopes (including landslides) would be stabilised to some extent. Safety factors are likely to rise, because externally acting water forces (acting against the

(ii) Drillholes and instrumentation may be optimised (in number and position) by determining locations in key areas where maximum drainable head (Appendix 2) is predicted to develop after lakefilling, or where greatest sensitivity can be demonstrated from variation within the expected range of geological models.

(iii) The modelling frequently throws light on the geological model, either supporting or pointing to alternative conceptual models and suggesting a course for verification. A common example is the location of permeability barriers - both steeply dipping and at low angles (faults and failure surfaces).

(iv) Remedial measures can be optimised. Interaction and refinement can provide substantial cost savings on large scale remedial drainage.

Consistency of any postulated piezometric profile with a limit equilibrium stability model allows confirmation that the slide mechanism has been correctly identified. Where active creep deformations are taking place, safety factors close to 1.0 are required for rational geotechnical models. Otherwise, a reassessment of piezometric assumptions, strengths and geometry is necessary. Unconservative predictions for safety factor changes can result if the pre-existing piezometric levels are incorrectly modelled. Therefore where groundwater information is sparse, conservative levels are assessed for pre-existing watertables. (Conservative predictions are usually generated by low levels in unconfined aquifers and high levels in confined aquifers.)

5.6 THE ROLE OF GROUNDWATER MODELLING IN RESERVOIR SAFETY ASSURANCE

5.6.1 The Piezometric Lag Problem

On first filling of a reservoir, the existing groundwater levels within the toe areas of slopes would rise relatively quickly to the new external water level, because a large source of recharge would be present. However, in slopes of moderate or low permeability (less than about 1×10^{-6} m/s, the watertable is likely to have a significant upslope gradient (as a result of rainfall infiltration). Above the full pool level, the groundwater would take considerable time to reach an 'ultimate' condition which would thereafter fluctuate only slightly depending on season and precipitation. (Examples are given in Appendix 2). This delay in achieving steady state flow is a result of the limited recharge quantities to fill the effective porosity of material above lake level. Recharge rates are limited. Piezometric pressures can therefore be expected to increase more slowly once they reach lake level, approaching ultimate (steady state) values asymptotically with time.

The time for piezometric pressures to rise to their ultimate values can be a **major factor in relation to safety assurance** in moderate or low permeability materials. During reservoir filling, all slopes (including landslides) would be stabilised to some extent. Safety factors are likely to rise, because externally acting water forces (acting against the

direction of slide motion) would have greater influence than internal pore pressures. Creeping slides are therefore likely to slow down or effectively come to rest during the filling period if this takes place in a short interval. Renewed or accelerated movements of creeping slides would be expected only after some time when piezometric levels within the slope approach ultimate values. This 'lag' in landslide response is highly significant in relation to hazards presented. Precautionary measures in the event of any accelerating slide movements will be limited because:

(i) cessation of filling (or slow drawdown) could no longer be used as an option to arrest slide movements because the safety factor would continue to decrease regardless, and,

(ii) as piezometric pressures rise within the slopes, rapid drawdown could not be attempted because even more dramatic decreases in safety factors would result.

The latter aspect is well appreciated by dam designers and also borne out in practice as evidenced by the widespread reservoir slope failures that occurred during rapid drawdown following the Teton Dam failure. However the former has not been publicised to the writer's knowledge, and when pointed out to the designers on one project, led to major reconsideration of policy in relation to remedial measures.

5.6.2 Accuracy of Time Predictions

Prior to the commencement of reservoir filling, the prediction of times for piezometric levels within the slopes to become adjusted to the changing boundary conditions (during and after filling) will have limited accuracy. Time dependent modelling requires not only the aquifer geometry but also the separate determination of the permeability, infiltration and storativity. In view of the difficulties in measuring any of these three parameters with accuracy, time predictions would be only to about an order of accuracy prior to filling or a large scale field test. Sensitivity analyses are required. However, piezometric monitoring during any remedial drainage and reservoir filling allows continuous refinement (calibration of models) for both the response time and the ultimate piezometric levels. Calibration of models is achieved by determining recharge and permeability values needed to meet all known piezometric levels. Where unsteady flow has been induced by drainage drives, pump testing or fluctuating river levels, the storativity may be estimated also and transmissivities refined.

The advantage of modelling is that before a reservoir is about one third filled, reasonable calibration should have been achieved for prediction of near-ultimate piezometric levels (and safety factors) for the more critical later stages of filling. In particular, where the hazard/risk is significant a rate of filling can be determined such that piezometric lag will be negligible. Alternatively, if slow creep is detected at any stage after filling has begun, the future displacements and movement rates can be more realistically determined, using the concepts given in Chapter 7 and Appendix 4. Re-appraisal of the hazard/risk assessment and the need for, urgency, and quantitative extent of remedial measures can then be judged on an informed basis.

5.6.3 Illustrative Cases

Appendix 2 provides some results from cases studied. As the principal development in this chapter, is the concept of understanding the way in which the safety factor of a slope will change with time, key figures from the appendix are included below.

The time dependent (transient) piezometric responses determined from LSFLOW are illustrated in Figures 5-7, 5-8 and 5-9. The case concerned was a preliminary model of a large but apparently dormant slide.

Figure 5-7 shows a nominal lake filling programme and the predicted response of a line of observation piezometers positioned progressively further upslope (from PZ-1 to PZ-4). Also shown is the change in safety factor accompanying this specific filling programme. As expected, the piezometers at lower levels (closer to the reservoir) respond more quickly and show greater changes in piezometric levels than those further upslope.

Figure 5-8 shows the same situation, except that the effect of a controlled drawdown of the reservoir has been investigated (as might be required in the event of unexpected movement of this or any other slide in the reservoir). The influence of any proposed rate of drawdown can be readily investigated in this manner to determine the effect on the safety factor of the slide. In this case, it has been assumed that the reservoir has just been filled to full pool level when drawdown is necessitated. A controlled drawdown of 10 m over a 2 month period has been modelled. Comparison of the safety factor changes in Figures 5-7 and 5-8, shows that for the model parameters used, the slide will become temporarily more unstable than if no drawdown had been carried out, (although in the longer term drawdown will, as expected, be less unfavourable). The conclusion from this model is that the proposed drawdown rate of 10 m in 2 months is too rapid, and a slower drawdown would be considered for the next model.

Figure 5-9 models an assumed drainage drive in the central third of the slide. The drainage was assumed to begin at the same time as reservoir filling to illustrate the offsetting effects of the two processes. This illustrates the way in which drainage affects the various piezometers, and how design can be optimised by looking at the resultant effect on the safety factor, which in this case does not reach a minimum value at the long term (steady state) case, but at an intermediate value.

There are a number of other aspects which come from examination of these comparative figures, and similar models which examine sensitivity to the less well defined parameters used. The role of groundwater modelling is therefore a primary tool in understanding potential problems through awareness of safety factor implications. It also provides insight to design proposals for remedial measures (optimising the positions of drainage drives) and allows informed planning for control of filling or drawdown rates.

LSFLOW EXAMPLE PROBLEM RESERVOIR FILLING CASE

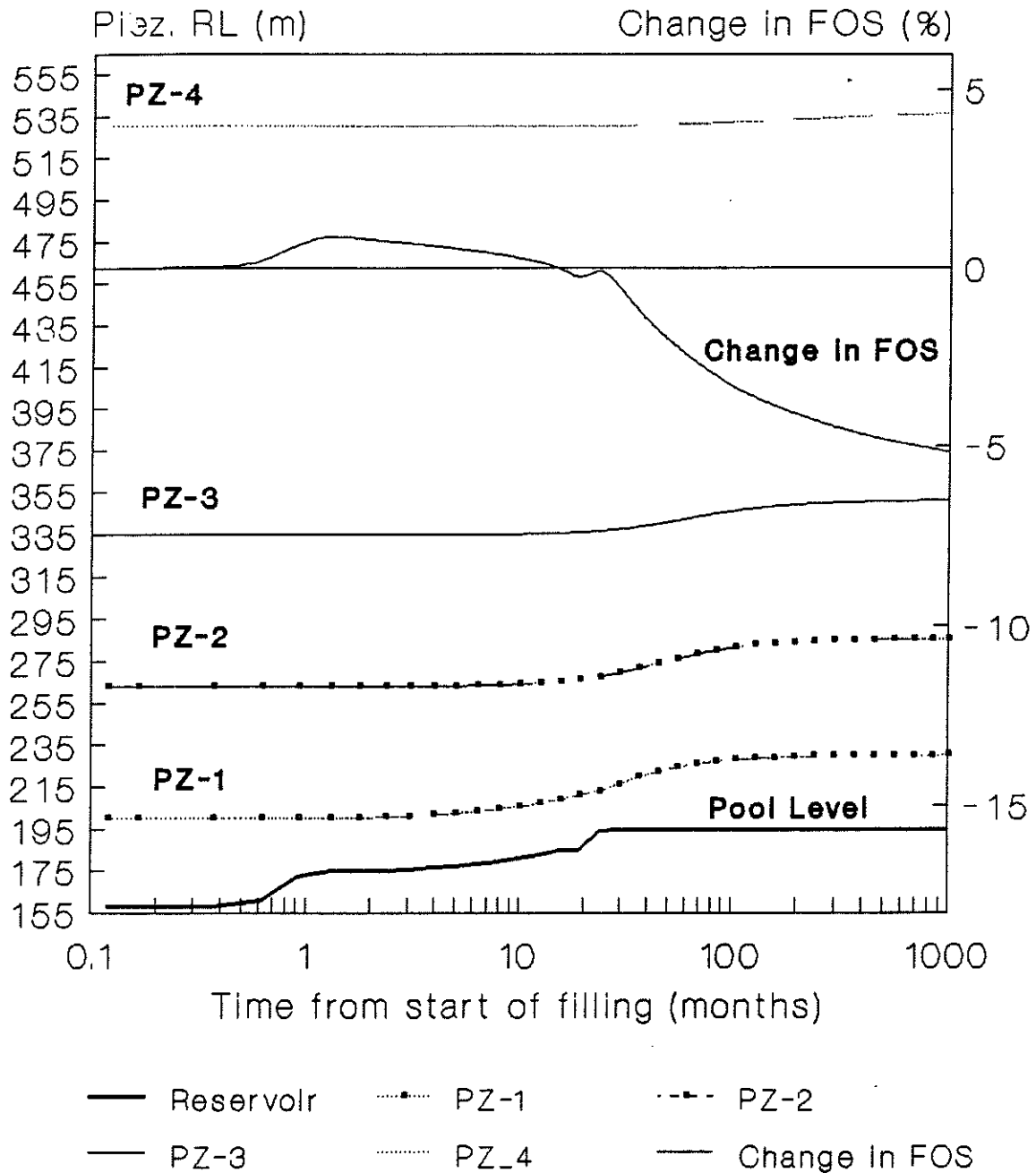


Fig. 5-7 Piezometer Responses

LSFLOW EXAMPLE PROBLEM CONTROLLED DRAWDOWN CASE

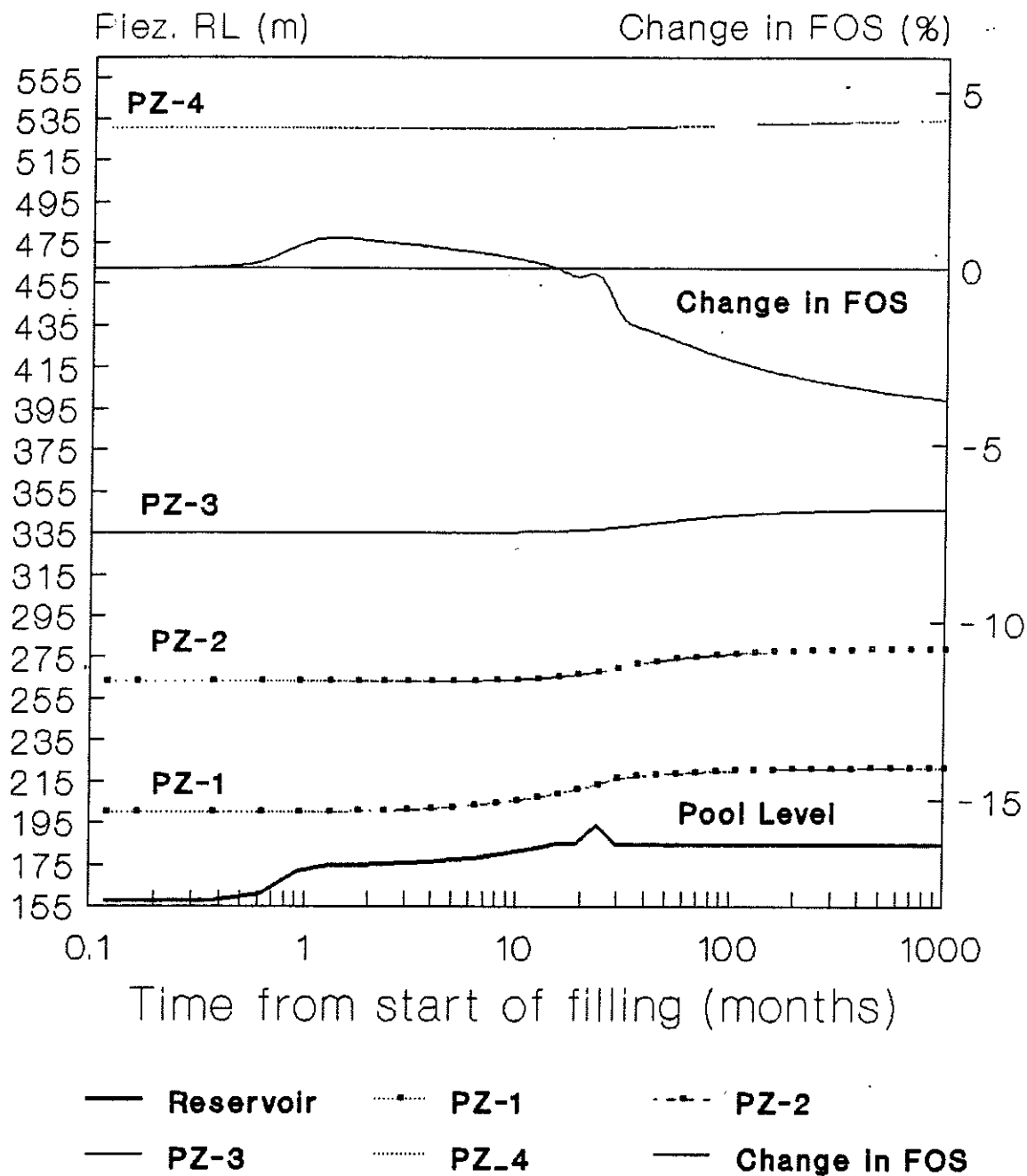


Fig. 5-8 Piezometer Responses

LSFLOW EXAMPLE PROBLEM DRAINAGE AND FILLING CASE

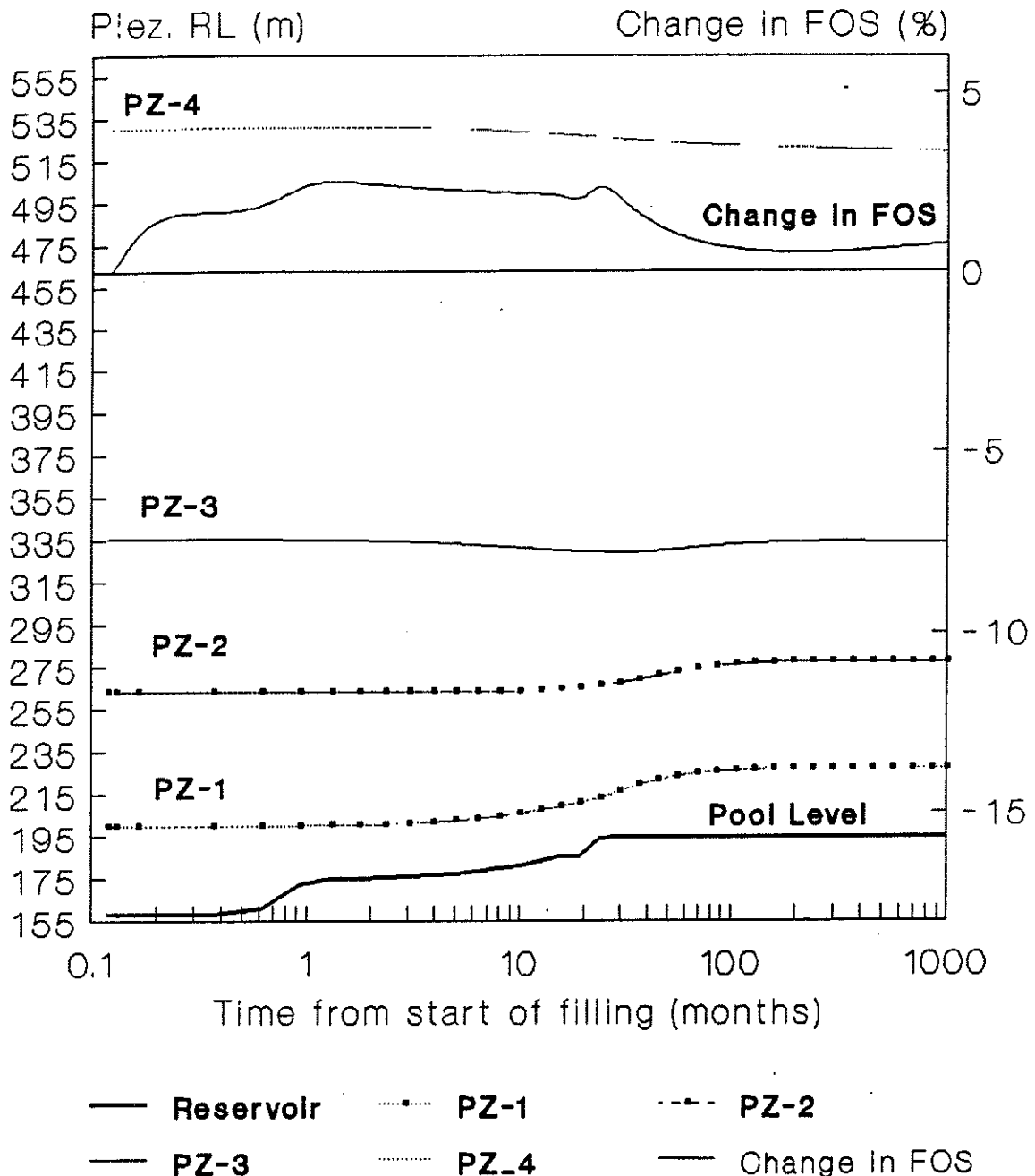


Fig. 5-9 Piezometer Responses

5.6.4 Application to Reservoir Filling

In reservoir engineering, the principal functions of groundwater modelling are to quantify the need for remedial measures and to provide safety assurance during filling, operation and drawdown. Piezometric levels may be predicted at intermediate stages of filling and for the ultimate steady state condition. At any stage therefore, appropriate monitoring of critical piezometers can confirm the accuracy of models and provide forewarning of pore pressures trending towards values that will induce unacceptable decreases in safety factors. Modelling is therefore a key element in the application of the observational method, and the relevant steps applied to reservoir filling are:

- (a) Carry out investigations sufficient to establish at least the general nature, pattern and parameters of the groundwater system.
- (b) Assess the most probable aquifer conditions and the most unfavourable conceivable deviations from these conditions.
- (c) Carry out design, based on what is judged to be the most reasonable (preferred) aquifer model. This forms the working hypothesis of behaviour anticipated under the most probable conditions.
- (d) Select appropriate piezometric and deformation monitoring parameters to be observed as lakefilling proceeds and calculate the anticipated values on the basis of the preferred model.
- (e) Calculate values of the same parameters under the most unfavourable conditions compatible with the available data for the aquifer.
- (f) Select in advance, a course of action for every foreseeable significant deviation of the observational findings from those predicted on the basis of the preferred model. At this stage some assessment of consequences and probability of all models is required, in order to reach decisions on whether action (remedial measures) should be instigated before reservoir filling. Some models will have an appropriately low probability of realisation.
- (g) Measure the pre-selected piezometric and deformation monitoring parameters during filling.
- (h) Modify designs or carry out remedial measures to suit actual conditions.

5.7 CONCLUDING REMARKS

A technically based approach to prediction of piezometric conditions for slope analysis has been put forward, principally because changes in safety factors (induced by submergence) are markedly more sensitive to initial and final pore pressures than other factors such as density or shear strength (within the limits established from both field and laboratory testing) or the precise geometry of the failure surface.

The accord of the model with reality will be only as good as the hydrological/geological model provided by the field investigator. Because of the usual limitations to accurate definition of field parameters, it is essential that due regard be given to the simplifying assumptions required in modelling. However, in many cases sensitivity analyses will provide significant appreciation of the complexities of the physical situation, allowing timely action to be taken to significantly reduce the risk of catastrophic slope failure.

CHAPTER 6

MECHANISMS FOR RAPID LANDSLIDING

6.1 INTRODUCTION

In many landslide situations, one aspect of particular concern is not only whether movements will occur but what rates of movement are to be expected, in order to ascertain if the degree of slide mobility could present a hazard. This chapter attempts to collate known and conjectured mechanisms for rapid failure of slopes, principally where "first-time" slides are involved, to provide a rational basis for assessment of active or potentially active landslides.

6.2 BASIC CONCEPTS OF SOIL FAILURE

6.2.1 Peak and Residual Effective Strengths

The concepts of peak and residual strengths of soil have been discussed in Chapter 2. Depending on the initial structure of the material, there will exist a greater or lesser separation of the peak and residual strength envelopes. Any displacement of a "first-time" slide will result in a transition from the peak, towards the residual strength, leaving a net accelerating force acting on the slide mass.

Skempton (1977) suggests that movements totalling about 1 or 2 metres may be required to achieve residual strength in fine grained soils. Accordingly, the most convenient means of simulating this condition has been in the ring shear apparatus (Bishop, 1971; Bromhead, 1978) in which an annulus of soil may be subjected to indefinitely large displacements.

6.2.2 Rate Dependence of Residual Strength

Skempton and Hutchinson (1969) note that the strength of soils is dependent on shearing rate even when these rates are slow enough to permit full drainage. A value of about 1% increase in strength per tenfold increase in strain rate was obtained in strain controlled ring shear tests. Further discussion is contained in Chapter 7.

6.3 DISPLACEMENT-INDEPENDENT ACCELERATING MECHANISMS

Many external factors acting independently of slide displacement can affect the resultant force acting on a slide mass (Terzaghi, 1950). Apart from earthquake loading, these factors (eg change in submergence or groundwater, redistribution of mass etc) usually occur slowly or by deliberate design, and are hence more predictable than displacement-dependent accelerating mechanisms. The latter appear to have a key role in hazard assessment and will therefore be examined in detail.

6.4 DISPLACEMENT-DEPENDENT ACCELERATING MECHANISMS

Those factors which decrease the available resistance of a soil along a slide failure surface while displacement progresses, provide the potential for rapid movement when accelerating forces are left unbalanced. If strength decreases with displacement (or velocity) then the safety factor of a creeping slide will decrease in a compounding manner thus providing the potential for extreme rates of movement. For this reason those soil characteristics which can provide displacement dependent accelerating mechanisms have been singled out for deliberate consideration, in any instance where the risk of rapid movement needs to be assessed.

6.4.1 Reduction of Effective Cohesion

Reduction or elimination of effective cohesion is the most obvious source of significant loss in strength. Failure may be very brittle with little warning, when a large proportion of available resistance is cohesive. An example where this was apparently a significant contributory factor in a catastrophic slide, is the Madison Canyon Rockslide. (Hadley, 1978).

Cohesion may be present in soils previously at residual strength (with zero cohesion) through healing by cementing agents or desiccation. The latter has been demonstrated to create effective as well as apparent cohesion, (Allah and Sridharan, 1981).

6.4.2 Reduction of Effective Friction

6.4.2.1 Peak to residual strength

In dense granular materials or overconsolidated fine grained, the density component of strength (Cornforth, 1973) can equal more than 30% of the available peak strength, allowing rapid failure after peak strength has been mobilised and continued shearing then increases the void ratio to its critical value. Normally consolidated clays will still exhibit substantial differences between their peak and residual strengths as platy minerals become aligned parallel to the direction of shearing.

6.4.2.2 Mechanical attrition

Granular materials composed of weak rock and subjected to moderate or high normal stresses will suffer particle breakdown in shear until a sufficient matrix of fines is created to "cushion" any further degradation. Formation of such gouge invariably results in a decrease of available frictional resistance.

6.4.3 Increase in Pore Fluid Pressure

6.4.3.1 Shear contraction.

Excess pore pressure, resulting from densification of a soil that is above its critical void

ratio, has been the mechanism involved for many catastrophic slides in both granular and cohesive 'quick' soils, eg the Aberfan disaster (Bishop, 1969).

6.4.3.2 Monotonic loading

Landsliding is generally a slope reducing process which transfers load from the head of a slope to the toe. This process of slope adjustment causes a general reduction in shear stress within the soil and particularly to the soil located beneath the failure zone. If this soil is a dense granular material which was previously subjected to at least a moderate degree of shear mobilisation, the pore pressure parameter A (Skempton, 1954) would be negative, regardless of the amount of shear stress reduction (as opposed to the more common case of a reversal of the sign of A under increasing deviatoric stress). This concept was investigated in the laboratory (R Davis, pers comm). Figure 6-1 shows the stress path for a dense sand which was sheared in a drained triaxial test until a high degree of shear was mobilised and the sample was dilating rapidly. The deviatoric stress was then removed in an undrained test (to simulate rapid unloading). The resulting pore pressures were small, but clearly positive.

Skempton's B parameter also provides an explanation for pore pressure rises within a failure zone. For a typical slide, the geometry of the failing mass involves a thickening from the toe to the central regions. In the vicinity of the toe of such a slide, an element of soil close beneath the failure surface will be subjected to an increase in total confining pressure as displacements take place. Since B is always positive, then saturated or near saturated soil elements beneath the failure surface, will incur significant excess pore pressures which can then be transmitted to the overlying failure surface.

Pore pressure responses of this nature would be most marked where failure is taking place in a low permeability soil (which inhibits drainage to the materials above the failure surface) underlain by fully saturated materials.

A feature of slides which have been subjected to excess pore pressures induced during sliding is that they can only be arrested naturally by a change in slide geometry (mainly self-buttressing at the toe) which is significantly more effective than the geometry required to counter sliding in the absence of excess pore pressures. It follows that on coming to rest the long term factor of safety of such a slide (after pore pressure dissipation) may be substantially greater than unity. The East Abbotsford Landslide (Salt et al 1979) was suggested as an example where the undrained response of dense saturated soils beneath the failure surface, contributed to unexpected acceleration.

6.4.3.3 Cyclic loading

Pore pressure increases in both granular and cohesive soils have often been demonstrated during cyclic loading. The usual form of cyclic loading is from a displacement-independent source, ie seismic shaking. However a displacement-dependent origin is possible where the failure surface is undulating. Movement would cause a cyclic normal stress, and consequent cyclic shear stress affecting the materials within and on

Response of dense sand to unloading
Stress path

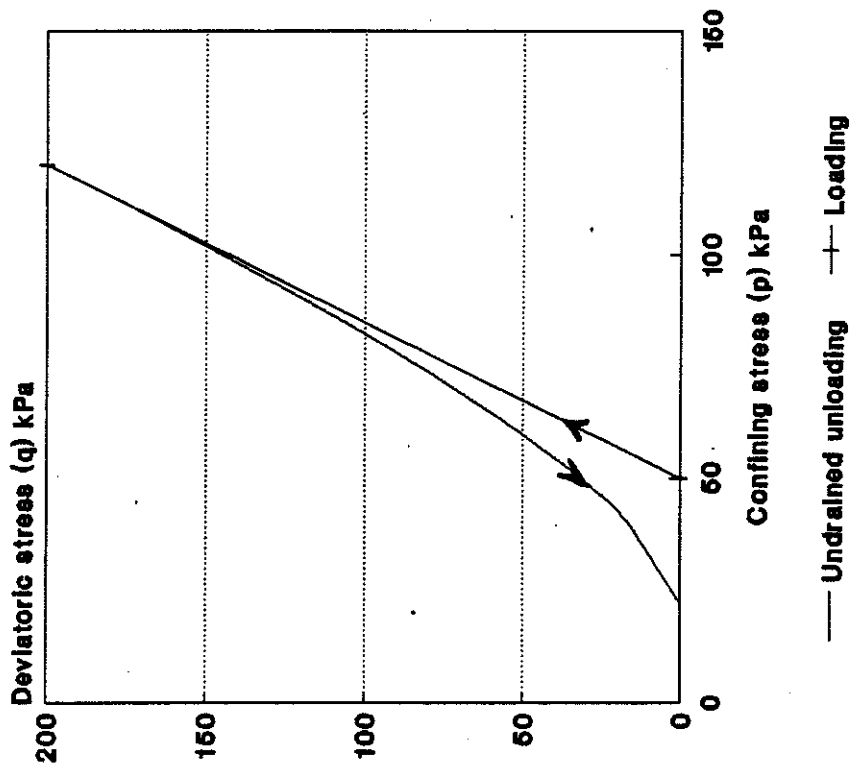


Fig. 6-1a

Response of dense sand to unloading
Increase in pore pressure

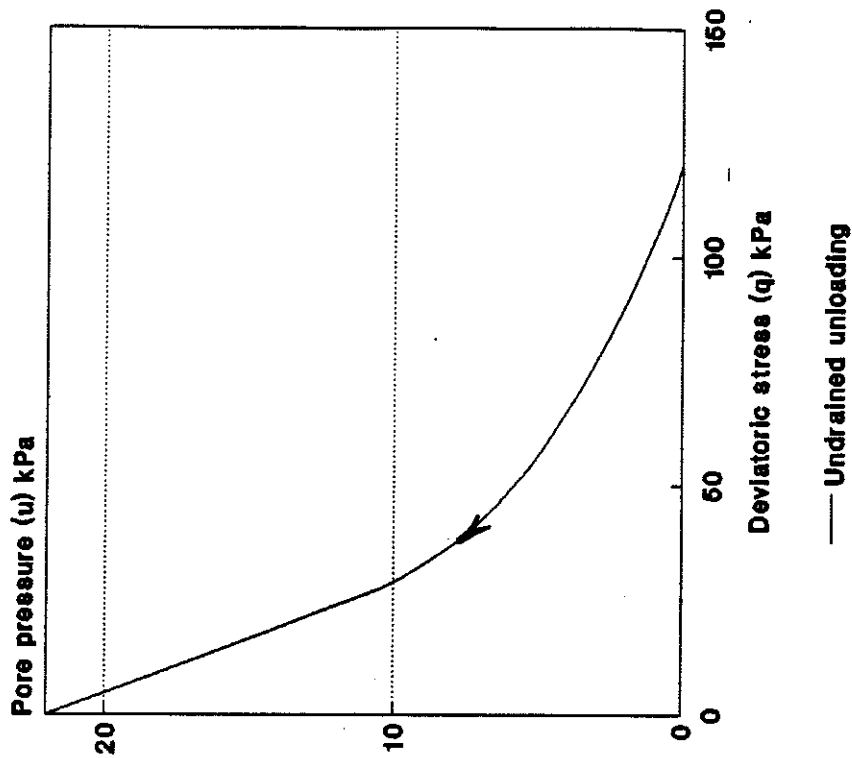


Fig. 6-1b

either side of a wavy failure surface. In the latter case the piezometric pressure at the failure surface could still be readily affected by pore pressures transmitted from the adjacent materials.

6.4.3.4 Frictional heating

Pore pressure increase through frictional heating appears to be the currently most favoured mechanism to account for the extreme rapidity of the Vaiont Slide (Patton & Hendron, 1985). Appendix 6 discusses this more fully, demonstrating that for the phenomenon to be significant, specific soil properties are required.

Also the rate of introducing energy must be short with respect to the soil permeability and boundary drainage conditions. If the velocity of a slide is made to increase gradually, a new temperature differential from the failure zone to the surrounding soil will become established so that at no time do significant excess pore pressures develop. Excess pore pressure is dependent on a sufficiently rapid energy increment.

As well as at Vaiont, the pore fluid heating explanation may have contributed to the accelerations of other extraordinarily rapid slides, eg the Goldau Slide (Terzaghi, 1950).

6.4.4 Coalescence of Multiple Slides

When a group of individual slides merge to form common boundaries, lateral shear restraint reduces, giving a means for sudden increase in the resultant accelerating force. An example is given by the Lower Baker Slide (Peck, 1967).

6.4.5 Development of Internal Deformations

The concept of internal deformations required for movement of non-circular slides has been discussed by Karal (1979). This can lead to rapid movement if the deforming slide mass is brittle or contains saturated soil exhibiting a positive value for the pore parameter A (Skempton, 1954). A lurching response ("stick-slip") is likely to result if the slide mass (above the failure surface) is composed of low permeability saturated soil with negative A value, because newly formed internal shear surfaces would provide temporarily increased effective strength until the negative pore pressures dissipated.

6.4.6 Unstable Failure Surface Geometry

A slide containing material with some degree of tensile strength and having a general failure surface profile which is upwardly convex, can present an unstable situation where the factor of safety decreases with displacement because the average inclination of the slope increases towards the toe. More commonly (in materials without significant tensile strength) a tension crack would form and the steeper toe portion would break away. However, slides with unstable failure surface geometry have been observed where suction is present in colluvial mantles overlying a smoothly rounded bedrock surface.

6.4.7 Secondary accelerating mechanisms

Various mechanisms have been postulated to explain the very rapid movement of slides eg hydrodynamic wave pressures (Corbyn, 1982); aqua-planing (Trollope, 1980); fluid vaporisation (Habib, 1975) and fusion (Erismann, 1979).

In most cases, velocities must be substantial before the above mechanisms can operate. Primary accelerating mechanisms are therefore regarded as being sufficient to create a hazardous situation, regardless of aggravation by secondary accelerating mechanisms.

6.5 CONCLUDING REMARKS

In order to evaluate the potential for rapid movement of a marginally stable slope, an attempt has been made to collate known and conjectured mechanisms which could contribute to the displacement-dependent acceleration of landslides. While it is unlikely that this list of mechanisms is exhaustive, all rapid slides reviewed during the course of this work, can be explained by conditions favouring one or more of these mechanisms.

The presence in a creeping slope of any conditions which could lead to displacement-dependent acceleration needs to be evaluated when addressing the alarm criteria given in Chapter 9.

An ideal slide which provides no attributes likely to lead to rapid failure must be subject to only small increases in external forces (see Chapter 7) and exhibit all of the following:

- (i) a thick, moderately permeable shear zone which is non-wavy and is at residual strength,
- (ii) unchanged history (since the previous movement) with respect to effective stresses on the failure zone,
- (iii) stable failure surface geometry (concave upward) with no capacity for coalescing with adjacent slides
- (iv) no capacity for development of unfavourable internal deformations

In most landslide cases encountered, one or more of the unfavourable factors will be present. The reason that most landslides do not reach catastrophic rates of movement is that displacement-dependent accelerating mechanisms are countered by positive rate-dependence of shear strength which is examined at length in the next chapter.

CHAPTER 7

PROCEDURES FOR ASSESSING LANDSLIDE MOBILITY AND REMEDIAL MEASURES

7.1 INTRODUCTION

Large landslides, sometimes dormant but usually creeping at rates of several tens of millimetres per year on deep seated failure surfaces are common in mountainous terrain, where foliated rocks are present. Where roading, submergence or other works are planned to affect landslides, assessment of their future behaviour is required. Commonly, reactivation or slight increases in historic creep rates will occur when only small decreases in stability are induced, and the potential for rapid landsliding then becomes a prime concern. This chapter relates to case studies involving unstable slopes in schist - a rock type which is usually subject to extensive landsliding on dip slopes in any area of high relief. However the general principles are described are intended for application to slopes containing other materials.

Assessment of active landslides involves:

- (i) The use of precedent, using field indications of the past and present behaviour of large active and dormant slides in the immediate locality.
- (ii) Interpretation of surface and sub-surface deformation surveys of movement rates, taking measured hydrological factors into account.
- (iii) Examination of documented case histories of slides in similar materials.
- (iv) Laboratory testing using conditions corresponding to those existing in the field, together with conventional limit equilibrium methods to assess the influence of proposed works.

Combination of the above four courses is required for a full appraisal of slope stability. While all factors may indicate that any slide movement occurring should be steady, performance is usually monitored to confirm expectations. However, limits on acceptable magnitudes of velocity and acceleration should be established for each slide before any development takes place. Previously identified criteria indicative of unsteady behaviour are essential, as omissions of these appear to be principal reasons for misjudgments leading to notable landslide disasters. There are many cases where monitoring information has been diligently recorded, but the implications of the readings (interpreted with due regard to established geotechnical characteristics) have not been considered. The opportunities to be forewarned have therefore been missed.

Information on how to assess the potential for rapid mobility (unsteady yielding) of landslides is rare in geotechnical literature. Hutchinson (1977) has pointed out "the difficulties of assessing the degree of stability of existing slopes or landslides and of

deciding what is an appropriate degree of improvement" and emphasised the need for further work in this field.

In order to derive relevant properties for the analysis of landslides in the cases studied, a simple ring shear apparatus (Chapter 3) has been used to test soils sampled from the relevant gouge zones. The specimen may be sheared, by many rotations, to produce a sample which has effectively suffered a displacement of several metres. Testing may then be carried out to determine residual strength characteristics in terms of effective stresses. The modified apparatus has the facilities to impose rates of shear displacement from less than 0.01 mm/day (3 mm/year) to as high as desired. This encompasses the main rates of movement that often require field monitoring (3 to 100 mm/year) and also those higher speeds likely to present a more immediate hazard. In addition to the normal strain controlled testing, the apparatus may alternatively be used in a stress controlled mode, as only the latter is directly applicable to the field situation.

This article details the inferences that may be drawn from recent laboratory testing and field observations of active slides. Quantitative answers to the following questions are suggested.

- (i) If an existing landslide is suspected to be marginally stable and its factor of safety is to be reduced (eg by mass re-distribution, toe submergence etc), can the nature of any movement be predicted (particularly acceleration, velocity and total displacement likely to occur before coming to rest).
- (ii) If a landslide is actively moving, is rapid acceleration likely?
- (iii) If a landslide is reactivated as result of de-stabilising factors such as toe submergence (or removal of material from the toe), can reservoir filling (or cutting from the toe) be continued or must further reductions in safety factor necessarily be delayed until movement stops or reduces to a former value?
- (iv) If landslide stabilisation is proposed, what increase in factor of safety is necessary?

Case histories found in the available literature demonstrate that where landslides present hazards, there is a marked variance in the level of caution exercised by different organisations. This is probably attributable to observations that pre-existing slides usually move only slowly and steadily, yet occasional examples of unsteady, rapid mobility exist. (For example the slide into the Vaiont Reservoir which in terms of lives lost, is one of the most notable accidental disasters in engineering history.)

Suggestions are made for the evaluation of surface and subsurface monitoring records and determination of criteria which indicate the need for any remedial action on mobile landslides. The specific test data are relevant only to the cases studied, but it is suggested that the approaches which have been developed, may be applied elsewhere.

7.2 RESIDUAL STRENGTH TESTING

7.2.1 General

Skempton and Hutchinson, (1969), discuss the most readily applied method of active landslide evaluation, namely limit equilibrium analysis using effective stresses, ie residual strengths in conjunction with appropriate pore pressures. This allows confirmation of the mechanics of a slide and enables the effects of any proposed changes to be quantified in terms of a conventional factor of safety.

7.2.2 Dependence of Residual Shear Strength on Rate of Shearing

Residual strength has been shown to be slightly dependent on rate of shearing; Skempton and Hutchinson reported approximately one per cent increase in effective strength per tenfold increase in displacement rate. Results of comprehensive multi-stage tests on moderately plastic clayey silt gouge from a landslide in schist derived material are shown in Fig. 7-1. The quite significant changes in shearing stress are demonstrated to be functions of effective normal stress and displacement rate. For ease of presentation, all shear strengths have been normalised with respect to the shear stress developed at an arbitrary standard shearing rate of 10 mm per day. Note that the conventional limit equilibrium factor of safety is given by the reciprocal of the normalised shear stress ratio which is plotted as the abscissa (independent variable) because in the field situation, displacement rate is the dependent factor. Strain rates cannot be accurately determined in the ring shear apparatus, but a very thin specimen (4 mm) has been used. Test data for the very slow displacement rates are limited at this stage because of the extremely long times required to obtain individual results in this region. However, from testing of various soils, the downward curvature (at low and moderate normal stresses) shown in Fig. 7-1, tends to become asymptotic to a lower bound which for a given normal stress, gives the minimum dynamic strength. Similarly at fast displacement rates, shear stress ratios become asymptotic to the maximum strength ratio. Laboratory results show considerable variation at rates higher than about 50 mm/day in saturated low permeability soils. Frictional heating effects on pore pressures of certain very low permeability soils have been demonstrated to be quite significant in this respect (Appendix 6). Some variations are also noticeable at low normal stresses and these may be attributable to peripheral effects which have a proportionately greater influence in the shear apparatus at low stresses. Repeatability of the results therefore decreases at lower stress levels.

The adoption of a shearing rate of 10 mm/day as corresponding to a safety factor of exactly 1.00 has been done for practical purposes. Conventionally, the point of incipient movement should be adopted, but in practice, this value is not unique (as will be explained further) and testing at very slow rates of shear is particularly time consuming. With reference to the error margin in determining the absolute safety factor of a slide, the difference between the safety factor definitions is inconsequential. For comparison of relative safety factors however, the definition used in this discussion is appropriate as a practical reference base.

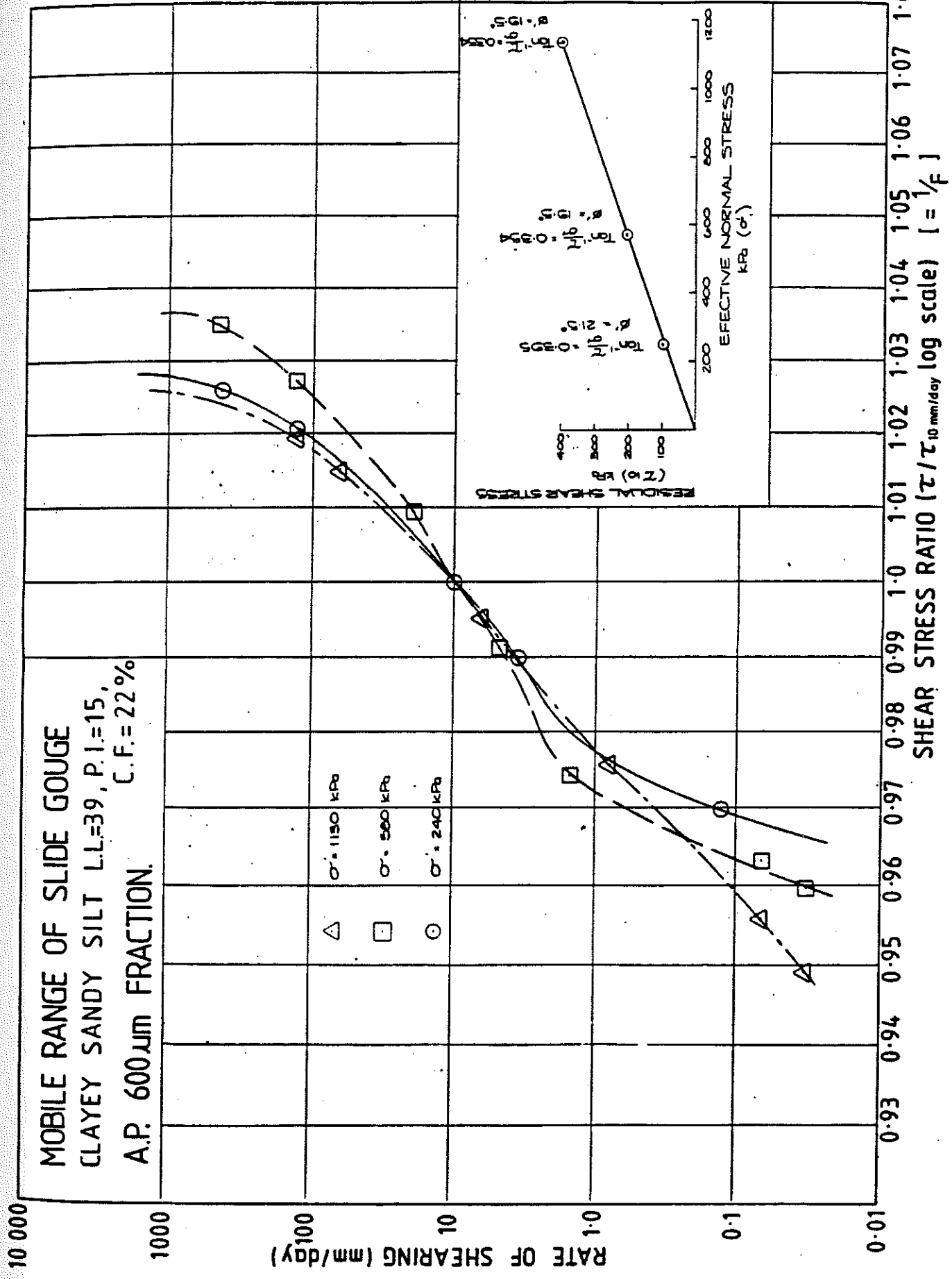


Fig. 7-1

7.2.3 Explanation for Rate Effects

A possible explanation for the observation that residual strength increases with displacement rate) was given in Chapter 2, ie it may be a combination of particle rheology and dissipation of excess pore pressures. The former may be a strength dependence caused by the observed phenomenon of greater resistance to breakage and bending of individual particles fast loading (ie as clearly evidenced by concrete compression tests carried out at other than the standard rate). The pore pressure effect is, however, likely to be more significant.

Although overall 'steady state' conditions can be achieved in a ring shear test, the discontinuous nature of any particulate medium will require both positive and negative pore pressures to develop momentarily as individual grains collide or are pulled apart on an active shear surface. The relevant consideration is that the local drainage is likely to be at a slower rate for negative pore pressure changes than for positive changes. The reasoning is that soil with positive pore pressure would be slightly below its critical void ratio (more dense) and hence of slightly lower permeability. The converse would apply to zones of positive pore pressures. Therefore equalisation would take a longer time for negative pore pressures than for positive, resulting in a net decrease. According to the effective stress principle, the net decrease in pore pressure necessitates an increase in average effective stress. The increase in average effective stress will increase when less drainage is able to occur, ie as the rate of shearing increases. The result must be a net increase in strength with increasing displacement rate.

7.3 SLOPE STABILITY IMPLICATIONS

7.3.1 Susceptibility to Rapid Sliding

The average normal effective stress on the failure surface of a landslide may be estimated from standard limit equilibrium methods (Janbu, 1973). The highest normal stress used in the laboratory tests shown in Fig. 7-1 was 1130 kPa. Where the watertable is low, this corresponds to an average depth of slide of about 50 metres. With this normal stress it is evident from Fig. 7-1 that the shear stress at minimum dynamic strength may be increased by about 8% before the graph ultimately begins to steepen as it approaches the maximum strength. The significance of the steep gradient is that a very small increase in shear (ie very small decrease in safety factor) will induce a disproportionately large increase in slide velocity. A slide in this state will yield in an unsteady manner with rapid acceleration imminent.

Conversely, if a correspondingly deep seated slide is initially stationary, its factor of safety may be decreased by at least say 6% without likelihood of rapid failure, providing other factors do not intervene, (Chapter 6). The difference in shear stress ratio which can be developed over the available range in displacement rates, will here be termed the mobile range. Upper or lower bounds to the mobile range may be adopted to give

appropriate conservatism, depending on the use to which this characteristic is being applied.

Fig. 7-1 explains previous contradictory results (Hungry, 1981) on whether drained shear strengths are rate dependent: tests carried out with a limited range of variables have led to the apparently conflicting conclusions. The reason is that there is very little rate dependence at either very slow or fast shearing rates, at very low normal stresses or in permeable soils with low proportions of silt and clay.

It is suggested that for a range of materials (silty sands, silts and clays), the dependence of residual shear strength on shearing rate is a fundamental rheological property, with significant engineering applications.

7.3.2 Practical Implications

(i) Determination of the mobile range of a soil representative of material from a failure surface, allows quantification of the percentage decrease in factor of safety that can safely be imposed on a pre-existing slide, before rapid mobility (unsteady failure) is likely. Provided changes are imposed slowly, mass redistribution or toe submergence of an active slide may be carried out and continued steady yielding should result. This inference is consistent with observed performance in the field. (Note this applies only to pre-existing slides. "First-time" slides cannot be analysed this simply.) If the approximate geometry of a slide failure surface is known, then the rate at which mobilised shear stresses decrease as the slope angle deflates with displacement may be computed (Appendix 4), to estimate the distance the slide will move before returning to a stationary condition (or to the steady rate of movement prevailing before imposition of the reduced safety factor).

(ii) If a landslide is known to move intermittently, as is commonly encountered in earthflows moving only rarely after extreme rainfall events, then the mobile range at the appropriate level of normal stress is numerically equal to the increase in factor of safety required to prevent further movement. For example, from Fig. 7-1, slides failing in the test material, and having average depths of 10 or 50 metres, would require respective increases in safety factors of about 6 and 10% to just prevent further movement in equivalent environmental conditions. This assumes conservatively that most of the mobile range was formerly utilised. However, if a record of the former displacement rates has been kept, then the appropriate lesser increase in safety factor needed to just arrest movement may be read from the mobile range curve. Any additional factor of safety deemed necessary to allow for uncertainty should be related to the risk present and recommendations on this aspect are made below.

(ii) The nominal rate of shearing at 10 mm/day cannot reasonably be used to define a meaningful factor of safety of 1.0, as apart from very shallow slides, the 'point of movement' of a slide (invoking the full static strength) will require a distinctly higher safety factor. From Fig. 7-1, a slide in this material with average normal effective stress

of say 1100 kPa would require a safety factor of $1.0/0.94$, ie about 1.06. (This assumes strength parameters had been derived from a ring shear test at 10 mm/day.) This error would be of little consequence where an absolute factor of safety is being estimated, but would usually be quite significant where a relative change in stability is being considered, as with a slide to be influenced by reservoir filling. The above neglects, for the moment, the difference between static strength and minimum dynamic strength, but this will be discussed later in Section 7.7.

7.4 LABORATORY VERSUS FIELD BEHAVIOUR

7.4.1 Active Shear Band Thickness

The relative thicknesses of active shear bands forming failure surfaces may cause differences between laboratory and field behaviour. The 4 mm thick sample used in the laboratory is constrained by the nature of the apparatus to fail in as thin a band as possible. Preliminary measurements with intermittently dyed samples suggested that the active shear band developed during ring shear of this soil was apparently about 0.5 mm in thickness. However, more recently reported work discussed in Chapter 2 (Tika, 1989) documents more accurate measurement of shear band thicknesses found in the ring shear apparatus. Depending on soil type, very thin shear bands (20 microns) may develop.

A significant difference between the field and laboratory samples is that in the field, multiple shear surfaces and/or thick shear bands may be present. This should not affect the mobile range or its shape, provided results are plotted on a logarithmic scale, ie it is suggested that the laboratory test produces a characteristic curve for the soil. However, assuming the displacement rate across an active shear band is a direct function of shear strain rate and active shear band thickness, the displacement rate in the field will exceed that obtained in the ring shear apparatus by the ratio of the shear band thicknesses (field to laboratory). That is, if failure does occur in a shear band rather than along a discrete failure surface, then it is strain rate rather than displacement rate that is fundamentally related to shear stress. For example, if under a given shear stress the active shear band could be increased ten times in thickness, the displacement rate would also increase tenfold. In Fig. 7-1, the characteristic curve would retain the same size and shape but its position would be translated to the new velocity ordinates.

If a landslide (with unknown shear band thickness) reactivates as a result of changes in safety factor and displacement rates are recorded, the match point solution (discussed in most texts on groundwater hydraulics, eg Todd, 1950 for Theis's method) will apply to the interpretation and prediction of movement. The limit equilibrium changes in factor of safety of a slide may be computed for changed field conditions, and plotted logarithmically against slide displacement rate, but the number of shear bands and their active thicknesses will not usually be known. The normalised shear stress ratios may be computed, but these cannot be directly related to the same ratios for the laboratory test

data. However, translating the field data to the known characteristic curve (or 'type curve') allows quantitative estimates of:

- (i) the critical field velocity (at which unsteady yielding is imminent)
- (ii) the additional decrease in factor of safety that may be imposed before the critical field velocity is reached
- (iii) the approximate thickness of the active shear band.

7.4.2 Implications for Predicting Field Behaviour

(i) In situations where a pre-existing slide is being reactivated, namely where progressive toe submergence from a rising reservoir is causing increases in slide velocity, a decision may be made on whether reservoir filling may continue, or cease until a greater margin against unsteady yielding is obtained by displacement self-stabilisation (where geometry allows), or specific remedial measures. Due considerations of risk and hazard potential, and assessment of independent alarm criteria detailed in Chapter 9, are still required.

(ii) The shear band thickness may be roughly estimated, allowing qualitative appraisal of the potential for rapid mobility under conditions of sudden stress change (namely rapid drawdown or earthquake).

(iii) If the approximate thickness of the active shear band can be determined in the field, the analysis described above may be applied in reverse to fix the translated position of the characteristic curve. Likely increases in displacement rate with submergence may then be estimated directly. This has the advantage that the behaviour of a slide can be estimated before any reservoir filling takes place, as opposed to the approach when shear band thickness is unknown, where filling must be commenced to provide monitoring data. Variations in present movement rates of active slides taken in conjunction with piezometer readings and river level observations, may allow full or partial characterisation before reservoir filling.

7.4.3 Reservations

(i) Fig. 7-1 relates to the fine fraction (all passing 0.6 mm) of schist derived gouge. The effects of larger particles and soils of differing USC groups require further investigation. Additional results are reported in Chapter 9, but initial indications are that rate dependence of residual strength is a fundamental property of fine grained soils.

(ii) The shape of the mobile range curve has not been well defined at low displacement rates. Further data points could be obtained using very slow rates of testing, but many days (perhaps over a week) would be required for each data point. At displacement rates of over about 50 to 500 mm/day, the determination of strength - rate dependence is likely to be complicated by undrained behaviour caused by the extrusion of soil, which occurs in laboratory shear tests (Chapter 2). However, at these rates, most landslides would be presenting a very high potential for accelerated failure (Chapter 9).

(iii) A complication when considering the mobile range characteristics is that stick-slip movement (episodic creep) is commonly observed in periodically dormant landslides. Present indications are that the percentage increase in shear stress required to reactivate a stationary slide is small in relation to the mobile range for all except possibly very shallow slides. Further discussion is made below.

(iv) Even though residual strength conditions may pertain in a creeping landslide a continuing decrease in safety factor may cause a greater thickness of the shear band to become activated, or additional discrete shear surfaces may form.

In this case movement rates would be faster than expected from the laboratory characteristic curve (the field curve would be translated in proportion to the increase in active shear band thickness). However in this case, the mobile range would not be altered, and there should be no change in the percentage change in safety factor that could still be sustained before rapid failure.

Conversely, under conditions of increasing safety factor, the rate of displacement of an active slide may decrease more rapidly than expected as remedial measures are applied.

(v) The effects of frictional heating on pore pressures developed in overconsolidated low permeability soils during more rapid movements should be considered, as discussed in Appendix 6.

Until these aspects are investigated further, the acceptance of critical field velocity predictions made using the match point method should be regarded with caution. However, the laboratory characteristic curve (Fig. 7-1) obtained is a good qualitative guide, ie if the factor of safety of a slide is decreased and yet the logarithmic plot against velocity yields a concave downward curve, then it may be inferred that a significant margin exists before unsteady failure. Conversely, a concave upward curvature suggests that a critical situation is imminent. Until more data are available, predicted critical field velocities should be reduced by at least order of magnitude (depending on assessed risk and hazard) for conservative assessments of landslides reactivated during reservoir filling. Where no previous monitoring is available, critical field velocities may be assessed

conservatively from the laboratory curve. For example from Fig. 7-1 for a slide with average thickness about of 25 metres, a displacement rate of about 200 - 300 mm/day might be regarded as the upper range of steady yielding, therefore a limit of somewhere between 50 and 100 mm/day might be set as the maximum acceptable displacement rate for a slide which is closely monitored in a relatively low risk/hazard situation. Well before maximum rates are approached, interpretation of surface and sub-surface monitoring (Chapter 9) would be required to assess the potential for unsteady behaviour.

7.5 INTERPRETATION OF DEFORMATION MONITORING

Monitoring of surface displacements has been the traditional means of predicting future activity of an incipient slide. Apart from earthquake induced slides and some failures in steep rock slopes, warning movements typically occur. Terzaghi (1950) reports; "If a landslide comes as a surprise to eye witnesses, it would be more accurate to say that the observers failed to detect the phenomena which preceded the slide". However, Terzaghi offers no suggestions of techniques for interpretation of factors relevant to rapid failure prediction.

Slide displacement, velocity and acceleration, all provide information which aids prediction of future mobility.

(i) Displacement - Examination of resultant downslope displacement vectors relative to the topographic slope and position on the slide readily provides information on:

- (a) how deep-seated a slide is (to estimate average effective normal stresses and hence allow selection of the corresponding strength rate dependence properties),
- (b) whether a significant non-circular motion is occurring and
- (c) whether retrogressive segments are developing or distortion is taking place within the sliding mass.

The implications of (b) and (c) above are discussed in Chapter 6.

(ii) Velocity and acceleration - in an active landslide, these parameters are of particular relevance to alarm criteria and their interpretation in relation to strength rate effects is discussed further in Chapter 9.

7.6 THE EXTENT OF REMEDIAL MEASURES

7.6.1 Increase in Safety Factor

Design of stabilisation measures for an existing slide, which has established a form of equilibrium with its environment (ie where only creep movements are being recorded) presents a more simple problem than the determination of an appropriate geometry for a newly constructed slope. The latter requires the provision of an absolute safety factor which reflects the uncertainty in available strength and future peak pore pressures. However, the precedent conditions established for an active slide which has existed for many years, allow stabilisation measures to be assessed in terms of a percentage increase in safety factor, rather than as an absolute value. Appropriate safety factor increases will be determined primarily by:

- (i) whether complete arrest of all movements is required,
- (ii) hazard and risk assessment.
- (iii) allowance for the accuracy of the analysis where both adverse and favourable changes have been inflicted

In the first case, the appropriate mobile range curve may be used to determine the increase in factor of safety required to reduce displacement rates. An additional increase in safety factor may be required depending on hazard and risk assessment (according to a standard code, eg G.C.O, 1984 see Appendix 1). An example of the second case is where a slide is to be adversely affected by submergence and this is to be countered by buttressing. To allow for inaccuracies in this instance, a reasonable approach might be firstly to ensure that the restraint just restores the original factor of safety and then apply further buttressing equivalent to say 50% of the adverse component. This amounts to a partial safety factor of 1.5 on the unfavourable effect, although the total safety factor would be only slightly greater than 1.0. Attempts to provide total safety factors similar to those used for first time slides as in the design of retaining walls or earth dam slopes (1.5 or even 1.2) are impractical and unnecessary for large existing slides where relative rather than absolute safety factors are appropriate.

7.6.2 Sensitivity of Slide Movement to Safety Factor Changes

For small changes in safety factor of an active slide, the mobile range curve may be approximated by a straight line on the log/log plot. However, because of the expanded scale used for the abscissa, the likely change in creep rate caused by a quantifiable change in safety factor can be predicted with the simple approximation:

$$v_t = v_i \times R^p \quad \dots\dots\dots (1)$$

Where v_i is the initial downslope velocity, v_f is the predicted future downslope velocity after an increase in safety factor of $p\%$, and R is the mobile range coefficient for the failure surface material when tested appropriately (with due regard to the velocity range, normal effective stress and shear band thickness). From Fig. 7-1, R has a value of about 4 for this soil taking a large range of shear stress ratios. This indicates that an increase in safety factor of 1% would be expected to reduce sliding rates by about one quarter. Alternatively, a 1 percent decrease in stability will cause about a fourfold increase in movement rate. Note that the expression is **exponential**, ie a 5% decrease in safety factor gives a velocity increase of over 1000 times (4 raised to the 5th power). From the earlier discussion it is evident that caution is required when extrapolating to very low or high velocities as wide-range coefficients can yield quite **unconservative** velocity predictions. Looking at narrower ranges, in the central portion, R is as low as 2, while at the very low creep rates R is an order or more larger (about 50 at low to moderate normal stresses), ie in certain conditions a decrease in safety factor of 1% would increase creep rates by about 50 times in this soil type.

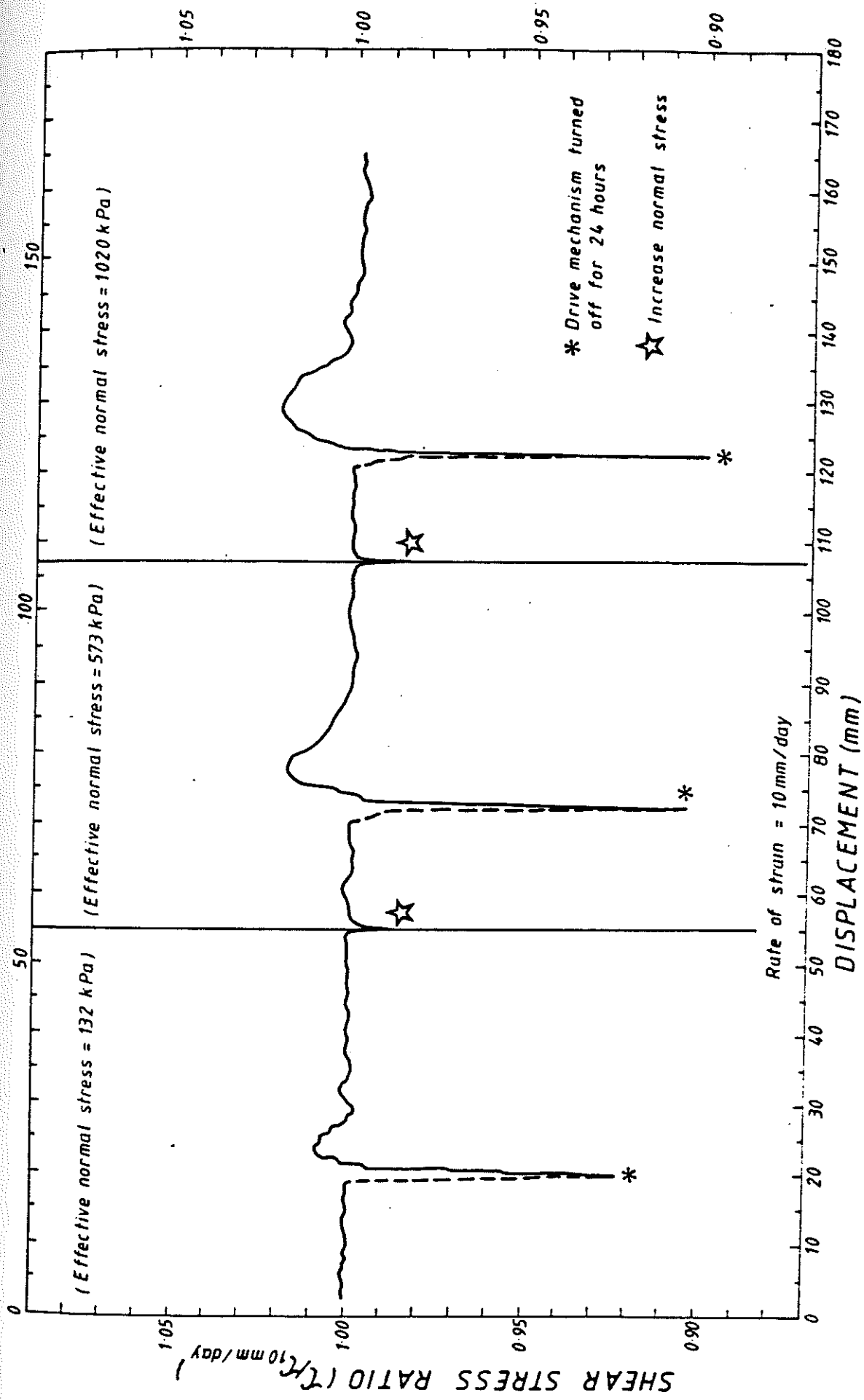
The applicability of the mobile range coefficient in practice has been documented by analysing the movement history for a number of case histories. However in each case, the decrease in safety factor by submergence was countered to some degree by geometric changes resulting from displacement so an approach was developed to quantify the effect with reasonable accuracy. Details and case histories are contained in Appendix 4.

7.7 FURTHER WORK

Stick-slip behaviour (episodic creep) has been investigated by a number of researchers investigating the nature of faulting. This type of movement appears to be a characteristic of many creeping slides for which detailed monitoring records are kept. The explanation is now evident from testing of materials sheared to residual strength. If the shear stress is reduced, the mobile range curve is followed directly as given by Fig. 7-1 until movement ceases entirely at the minimum dynamic strength. However on increasing the shear stress again, no movement occurs until the shear stress exceeds the minimum dynamic strength by about 1 or 2% (Fig. 7-2). This difference between static and dynamic coefficients of friction has commonly been reported for various materials, and it appears soils are no exception. The strength difference is a function of time of stationary contact (Dieterich, 1978) and probably other factors such as soil type, normal effective stress and rate of change of shear to normal stress ratio. However, preliminary work indicates that this effect is small compared to the mobile range of large active slides. Large creeping slides in schist (with average depths of several hundred metres) do appear to move relatively more steadily than shallow slides, ie stick-slip is evidenced less in the field at high normal stresses. This is possibly explained by the absence of downward curvature at slow rates, noticed in the laboratory mobile range curve at the highest normal stress (Fig. 7-1).

Scott (1978) cites an example where the failure surface of an active rockslide was accurately monitored with a continuous recorder. Displacements of 0.25 mm were observed to be occurring regularly at 15 minutes intervals. Each movement event took place within 2 minutes, starting abruptly with a velocity of several hundred mm/day but reducing asymptotically to zero in about 2 minutes. A second recording station 15 m further upslope from the first, consistently showed the same behaviour except that it lagged by 1 minute, ie the slide 'shuffled' down the slope with a displacement wave speed of 15 m/min. It appears reasonable to conclude that stick-slip may be normal behaviour in most landslides where sufficiently accurate monitoring is available, and this is consistent with the laboratory observations of both strain and stress controlled tests. To support this point, other obvious examples of the same phenomenon may be cited, eg: crustal faulting, squeaking machinery and the violin string-bow interaction (Rice & Ruina, 1983).

The behaviour of soils sheared in a stress controlled rather than strain controlled manner also appears relevant. In the laboratory, strain (or rather displacement) rates are customarily imposed and the resulting shear stresses measured. Conversely, in the field, gravitational stresses act and displacement rate is therefore the observed parameter. To consider this effect, stress controlled tests were carried out on the same soil tested in Fig. 7-1. Shearing at a constant displacement rate was imposed until residual strength conditions pertained. Control was then reversed, applying constant shear and effective normal stresses, and observing the consequent rate of shearing. Unless initial rates were high, displacement rates always reduced slowly and finally ceased altogether. A possible explanation is that this behaviour may be attributable to secondary consolidation. The average measured shear stresses will normally show some variations in magnitude as different particles interlock, break or slide, although this effect is very small (Fig. 7-2). However, once stress control is imposed, then during a period of increasing interlock, displacement rates will reduce, allowing particles within the shear band more time to adjust to more favourable positions (in a similar manner to the usual process of secondary consolidation, ie settlement in the absence of excess pore pressure). This better packing would be expected to produce a marginal increase in shear strength, causing further slowing and so the process continues. In the field, the effect of larger scale is likely to minimise this type of behaviour but there is very little information available from case histories.



STICK-SLIP BEHAVIOUR OF SLIDE GOUGE

7.8 CONCLUSIONS

1. At present little information is available on procedures to adopt when pre-existing landslides are activated. This chapter outlines the principles that have been used to provide guidelines:

- (a) for assessment of the potential of landslides to move rapidly, and
- (b) on the need for and extent of remedial measures.

2. Testing of landslide gouge has established a clear relationship between residual strength, shearing rate, and effective normal stress. A family of characteristic curves which show the mobile range of a soil may be determined with a simple ring shear apparatus. Rate dependence of shear strength provides an explanation for the observation that landslides in which residual strength conditions pertain, usually move in a steady manner. Conservative limits to steady failure may be predicted.

3. Determination of the mobile range of gouge from an existing landslide where residual strength conditions are fully developed, allows straightforward quantitative assessments (using standard limit equilibrium analysis) of the following situations.

(a) If an existing landslide is suspected of being marginally stable and its factor of safety is to be gradually reduced (eg by mass redistribution, toe submergence etc), the nature of any movements can be predicted. (Namely acceleration, velocity and total displacement likely to occur before coming to rest). In particular the likelihood of rapid acceleration can be assessed.

(b) If a landslide (previously recognised or otherwise) is reactivated as result of works which involve de-stabilising factors such as toe submergence (or removal of material from the toe, head loading etc) a decision can be made on whether works should be continued, reversed, or deferred until the displacement rate of the slide reduces to an acceptable value.

(c) If landslide stabilisation is proposed, the appropriate minimum increase in factor of safety may be determined, depending on whether movements must be entirely arrested or if a specific creep rate is acceptable.

4. Assessment of landslide hazard and risk draws on all aspects of slope stability. Prediction of landslide behaviour based on study of rate effects in the laboratory, still requires independent verification from case histories (including specific local examples in the same material type). Ultimate confirmation, comes only from monitoring (discussed in Chapter 9.)

CHAPTER 8

SEISMIC STABILITY OF RESERVOIR SLOPES

8.1 INTRODUCTION

The likely effects of both near and far field earthquake ground motions on constructed fills, cuts and natural slopes, are addressed in this chapter, with particular emphasis on pre-existing landslides submerged by reservoir filling.

8.2 LITERATURE REVIEW

8.2.1 Earthquake Case Histories

A literature search has been carried out in an attempt to locate all available case history reports of the response of natural slopes to earthquakes. Each of these has been summarised in Appendix 5. The main conclusions reached on the basis of the literature search and the research herein are:

(i) First-time slides (usually not identified as potential slide areas beforehand) provide the greatest potential for rapid landsliding, particularly where the mobilised strength exceeds the residual strength by more than about 10% in non-plastic or highly overconsolidated plastic materials. (This figure may increase to about 20% for shallow failure surfaces in normally consolidated highly plastic clays.)

(ii) In an area where large scale rapid failures of natural slopes have occurred under non-seismic conditions it is highly likely that similar events will be generated during earthquake loading. However, the available documentation is inadequate to determine whether the converse applies. It is reported by Keefer et al (1979) that many earthquake induced landslides have occurred in areas with historic records of little or no slope instability under non-seismic conditions. In these cases it may be that minor rockfalls and liquefaction related events comprise the large majority of events.

(iii) Five specific mechanisms have been identified (see 8.5.2.2) whereby pre-existing landslides (creeping or dormant) may be activated significantly by earthquake. In the absence of conditions appropriate for the mechanisms identified, earthquakes appear to have very minor effect on large pre-existing slides. Because 'nil reports' receive little publicity, the seismic resilience of such slides is probably not always appreciated, but there are likely to be many instances similar to those reported by del Prete & Petley (1982), and Clague & Souther (1982) where the effects of at least moderate earthquakes on pre-existing slides are insignificant in relation to movements related to rainfall patterns.

8.2.2 Laboratory Testing

Chapter 2 reviews recent papers and theses which promote concepts based on laboratory ring shear testing, with significant implications for the earthquake stability of slopes.

Key points are repeated below:

Lemos et al (1985) conclude that for a soil which shows a drop in residual strength with fast shearing 'if this strength loss were induced during an earthquake, it could lead to large, fast and potentially catastrophic movements which would continue post-earthquake.'

Vaughan et al (1985) conclude that 'the influence of fast rates of displacement on the strength of shear surfaces in cohesive soils must be considered in the study of seismic slope stability', and, that for silty soils (with negative rate effects) 'if earthquake shaking produces a critical combination of displacement and velocity in an existing slide initially at its residual strength, its reactivation will involve large and fast movements which will continue after shaking ceases'.

Lemos (1986) concludes that 'a knowledge of the strength of (pre-existing shear) surfaces under rapid loading is necessary if stability during and after an earthquake is to be examined'. In a low plasticity clay 'a runaway failure may take place. The drastic drop in shear resistance with displacement may be the cause of some of the catastrophic failures observed in the field.'

A possible alternative explanation for the findings reviewed above are simply that an apparatus effect, of no relevance to field conditions, may have been observed. The soil which was initially at slow residual strength in the thin shearing zone of the ring shear is extruded from the gap in the confining rings, and predominantly new soil (without the structure or void ratio appropriate to the residual strength state) is tested.

The finding of a drop in fast minimum strength to below the slow residual in cohesive soils, is difficult to reconcile with field observations:

- (a) No field examples have been cited by the originators, for which fast movements can be reasonably explained by the laboratory phenomena.
- (b) Terzaghi (1950) advises of the forgiving nature of fine grained soils (at residual strength) subject to seismic loading.
- (c) The extensive review of case histories in Appendix 5 of this report, has found no examples of seismically induced landslides which require such a mechanism to be invoked, ahead of more likely explanations such as liquefaction, first time sliding, etc.

8.3 GEOLOGICAL PRECEDENT AS A BASIS FOR STABILITY ASSURANCE

8.3.1 General

The writer has studied a number of artificial reservoirs in seismically active zones where large existing landslides are actively creeping. Assessment of these has been on a precedent basis, where the field performance of nearby slopes in the same geologic terrain with similar slope geometry, geohydrology and materials has been used for risk assessment. The absence of substantial movements in historic time can be a guide for static stability. However a study of the geologic record is required to find evidence for seismic stability in the event of a major earthquake where return periods are usually from 500 to 5000 years. The numerous glacial advances from 10,000 to 500,000 years ago have frequently given rise to conditions which allow both landslides and fault traces to be reasonably well dated.

At least 2 cases exist where fault traces several metres high, transect active slides which have failure surfaces comprised of silty materials. The fact that these slides remained on moderately steep slopes and are still creeping, provide more instances of substantial seismic resistance where residual strength conditions pertain in silty gouge zones.

The quoted literature based on laboratory testing, indicates to the contrary. Hence, there has been considerable interest in whether the traditional field assessments should be supplemented with a study of laboratory effects, because thus far, the latter have been disregarded.

The remainder of this chapter assumes that loss of effective strength (in the absence of excess pore pressures) is not of significance in the field.

8.3.2 Limitations of Precedent Arguments

There are some reservations to the assumption that precedent can be invoked to give assurance of seismic stability.

(i) Climatic changes, or alteration of vegetative cover may affect the contribution of soil suction to stability, or affect the net infiltration and hence groundwater levels.

(ii) In the event of reservoir filling then effects on soil suction and groundwater levels would be more substantial. The state of effective stress would be significantly modified in the toe areas of a landslide. Residual strength characteristics are dependent on effective stress. The steady state void ratio of any failing gouge would tend to increase after reservoir filling, to conform with the unloaded condition. This effect would be small, but apparently favourable as it would increase seismic resistance in the short term.

(iii) The yield acceleration of any slide failing on frictional material would be substantially decreased by submergence. This effect, discussed further in Section 8.6, provides a significant limitation to the precedent argument because displacements under a given intensity and duration of seismic shaking would be markedly greater for a submerged slide than for the same slide in an unsubmerged state.

8.4 MECHANISMS FOR SEISMIC DISPLACEMENT OF SLOPES

8.4.1 Introduction

For the purpose of considering seismic susceptibility of slopes, the geotechnical classification of Hutchinson (1988) provides the most useful subdivision:

(a) First-time slides (in material not previously sheared by purely gravitational or seismic forces) and,

(b) Slides on pre-existing surfaces.

Additionally, it is necessary to consider,

(c) Composite slides, formed partly in unsheared material and partly on pre-existing shears.

Category (a) may also be used for slides which develop at least in part, for the first time, on defects caused by tectonism or stress relief.

8.4.2 First Time Slides in Previously Unsheared Material

First-time slides can present a significant problem in relation to failures in steep slopes of weakly or moderately cohesive materials.

The principal mechanism that provides the potential for rapid failure is the reduction in strength from peak to residual values. Rate dependence of shear strength (Chapters 2 and 7) can offset the effect of strength reduction from peak. First-time slides are not necessarily rapid. However, rapid failures can occur if significant strength degradation (even 5%) develops in a material with minimal or no rate dependence, ie granular materials.

It is concluded a first-time failure under seismic loading is the principal hazard to reservoir development.

8.4.3 Slides on Pre-existing Surfaces

8.4.3.1 General

Examination of geological evidence from field experience and the case histories reviewed, indicates that at least one of the following mechanisms must operate before a large pre-existing landslide (which has moved some tens of metres under gravitational forces) will be significantly affected by earthquake.

- I) Slide enlargement.
- II) Groundwater regime disruption.
- III) Erosional oversteepening
- IV) Tectonic deformation of the slide geometry.
- V) Seismic development of excess pore pressures.

The following section discusses each of the above in further detail, relating case history observations to laboratory testing and basic principles of soil mechanics.

8.4.3.2 Specific mechanisms.

(I) Slide enlargement.

This may be a retrogressive failure involving a sizeable mass of material from above the former headscarp, lateral widening, or inclusion of additional material below the former toe. In all cases part of the slide becomes a 'first-time' event with the accompanying characteristics for providing sudden acceleration, as discussed above. Case histories illustrating this process are (a) the slide near Whitecliffs - a retrogressive failure (Henderson, 1937), and (b) the very rapid Madison Canyon Rockslide (Hadley, 1978) which involved partly a first-time failure surface through an intact block at the slide toe.

(II) Adverse disruption of the groundwater regime.

There may be instances where incipient deformation from earthquake loading may affect the hydro-geology of a landslide directly. However the only case noted in the literature review was the catastrophic delayed activation of the Kaliman Slide, by the indirect mechanism of cracking leading to increased ingress of rainwater to the failure surface. This example highlights the need for immediate post-earthquake ground inspections and monitoring to provide forewarning of this process.

(III) Erosional oversteepening

Modification of the mass distribution of a pre-existing slide may occur (usually by erosion), reducing a marginal safety factor. Oversteepening will result where unloading of a shear surface previously in the residual state, provides partial restoration of peak strength, with reduction in normal effective stress. Stick-slip characteristics can also lead to mobilised strength being marginally greater than pre-existing residual values. Examples are erosion of a slide toe which is crossed by a river, or accumulation of colluvium on the head regions of a slide. Because any oversteepening effect is likely to be small in relation to the mobile range of the failure surface soil, movements rates would probably be slow. Likely cases are the 2 dormant slides reactivated by the Irpania earthquake. Both slides moved into watercourses: the slide toe of the first slide dammed a river and "small ponds developed in depressed parts of the slope and the gully beds were diverted". The second slide movements ended "when the river at the slope toe was dammed. ... After the movement .. the water levels dropped by a few metres." Reliable interpretation of these examples is not however possible because insufficient information is available on the slide histories and materials. It is possible that they may come in the 'slide enlargement' category with river down cutting causing the toe area of the failure surface to break through at a lower level than before, in previously unsheared material.

(IV) Tectonic deformation of the slide geometry.

An increase in the gradient of an active slide (as a result of tectonic tilt or vertical displacement of a fault trace trending across the slide), will cause increased rates of movement in accordance with the rate dependence of residual strength. If the mobile range is exceeded, then rapid failure is likely. For gouge with a moderate mobile range of about 7% and 25 degree friction angle, an active slide with low pore pressure ratio would probably require an increase of at least 2 degrees in the overall inclination of the slide to bring about rapid failure. However, if piezometric levels coincide with the ground surface, an overall increase of only about 1 degree could exceed the mobile range. An probable example of the initial stages of this mechanism is reviewed in Appendix 5 (Hebgen Lake earthquake): the Kirkwood Earthflow was subjected to tilting which may be inferred to correspond to about a 4% decrease in safety factor. No movement was observed immediately after the shock, or for 5 days, but thereafter rates of 1000 mm/day were recorded. The delay could be attributable to a negative value for the pore pressure parameter A, thus giving short term stability from negative pore pressures induced by the increase in shear stress after tilting.

(V) a. Excess pore pressure developed from cyclic shear densification.

For soils where fully residual conditions apply, ie where a soil has reached its critical void ratio after sustained shear strain, cyclic loading in the field situation is unlikely to induce excess pore pressures that are a significant proportion of the average effective confining stress. The difficulty in carrying out appropriate testing to prove this hypothesis is that residual state conditions are difficult to develop effectively in a suitably thick laboratory sample. Nevertheless, the widely accepted concept of critical void ratio (for a given effective confining stress)

suggests that even if excess pore pressures are generated in a gouge zone by earthquake loading, further displacement after the event would be expected to cause the reduced void ratio to soon revert to the critical value (or for some time, even slightly above, in materials subject to secondary consolidation). Some other mechanism would be required to give strength degradation in existing well developed gouges.

(V) b. Excess pore pressures developed by frictional heating.

A number of researchers have now suggested that rapid acceleration of landslides can be caused by conversion of potential energy of a moving slide mass into frictional heat energy on the failure surface. (A consensus of opinion now suggests that this is the only really plausible explanation for the extreme rapidity of the Vaiont Slide, viz. Romero, 1974; Anderson, 1985; Voight & Faust, 1982 and Hutchinson, 1988. Furthermore, Anderson has demonstrated the potential of this mechanism to cause rapid failure of landslides triggered by earthquakes.) The basic mechanism is that of strength loss due to excess pore pressures which result from frictional heating of pore fluid when the consolidation time for the shearing layer is large, compared with the time of movement.

In Appendix 6, the pore fluid heating phenomenon has been investigated further, both qualitatively (with laboratory data and field examples) and also quantitatively. Conventional soil mechanics principles (consolidation theory) and standard heat relationships (expansion, conduction and convection) have been combined to allow development of a numerical procedure for predicting excess pore pressures likely to develop in situ, from frictional heating.

8.5 CALCULATION OF SEISMIC DISPLACEMENT OF LANDSLIDES

The present state-of-the-art methods for calculating the seismic displacements of slopes, (eg Ambrayseys & Menu, 1988) use the Newmark approach to calculate displacement along a specified failure surface in a slope with safety factor greater than 1.0. The writer has used a more rigorous method (program DYNDISP from U.S. Bureau of Reclamation) which includes more extensive input data, including landslide parameters, vertical and horizontal acceleration components of the design earthquake etc. and found that the answers are for practical purposes, no different from the simple charts given by Ambrayseys & Menu.

Inherent in any conventional Newmark based method is the requirement that the predicted displacement of a landslide subjected to earthquake will tend infinitely large as the safety factor approaches 1.0. It would appear to follow therefore that any creeping landslide should experience very large displacements if subjected to earthquake shaking. Field evidence in fine grained soils is to the contrary (as discussed earlier in this Chapter, and in Appendix 5).

The rate dependence of residual strength provides a simple explanation and also a quantitative method for estimating the displacements of any creeping landslide subject to earthquake shaking. As discussed in Chapter 7, the safety factor of a slide is generally taken as 1.0 if it is creeping. However in fine grained soils, there will be a mobile range over which the safety factor of a moving slide can vary (eg about 8% for the soil in Fig. 7-1). For a slide undergoing very slow creep there would hence be an effective safety factor of 1.0 plus the mobile range (ie 1.08 for the soil concerned) against rapid displacement. Because any displacement experienced during an earthquake will occur in a short time frame, the safety of factor against rapid displacement may therefore be used to provide a meaningful estimate of displacement when adopting any Newmark based method.

The method was used to compute the earthquake displacement of the landslide from which the sample tested in Fig. 7-1 was taken. The slide has a gently arcuate failure surface, about 35 metres deep and contains about 8 million cubic metres of material. It is creeping intermittently at rates from 0 to 15 mm/year on a discrete failure surface.

Details are reported in the Appendix, but it was concluded that during the Operating Basis Earthquake (0.2 g peak ground acceleration), predicted displacements would be about 2 m, a result which is more in keeping with field observations in similar circumstances, than can be estimated from the Ambrayseys and Menu charts if the strength rate dependence is not accounted for.

There are additional complications

(i) Even though residual strength conditions pertain, the higher available shear strength will result in either increased or decreased strength under undrained loading depending on the sign of the pore pressure coefficient A (Skempton, 1954) of the failing soil. As yet there is no apparatus that can sensibly measure pore pressures for soils which have been fully conditioned to the residual state. It would also be necessary to define an equivalent direct shear pore pressure parameter for the conventional A parameter derived from the triaxial test. In soils at residual strength, the undrained change in pore pressure is likely to be small (less than say 10% of the change in shear stress), because the tendency for volume change would be small. This source of error in the proposed method of estimating slide displacements is therefore likely to be small compared with the main uncertainty, namely the selection of an appropriate design earthquake.

(ii) In highly overconsolidated low permeability saturated soils, larger displacements may result from significant excess pore pressures developed by frictional heating. This topic is examined in Appendix 6.

8.6 STABILITY OF SUBMERGED SLOPES

In the absence of excess pore pressures, the factor by which the yield acceleration of a potential sliding mass of frictional soil is reduced when going from the unsaturated unsubmerged state to the fully submerged condition is given by the ratio of the buoyant

to total densities of the soil, ie commonly about $1.4/2.3 = 0.6$. Slopes which would be able to just withstand shaking of say 0.3 g formerly, would therefore be expected to yield at just under 0.2 g after submergence. The phenomenon can be appreciated from the fact that shear resistance of frictional soil is given by its effective (buoyant) weight while earthquake forces will always act on the total weight of the mass (whether submerged or unsubmerged). In essentially frictional slopes, the majority of the seismic deformations would be below lake level, but upslope retrogression could also be expected.

Confirmation of the theoretical expectation that yield accelerations are lowered markedly with submergence, is provided by case histories in Appendix 5. During the Hebgen Lake earthquake, landslides occurred on relatively low angle slopes extending well below lake level. Steeper slopes away from the lake but closer to the epicentre were less affected. Similar observations were made at Matahina Reservoir following the Edgumbe earthquake. In this case sidling road fills bordering the reservoir were displaced many metres (in places half of the road width disappeared below lake level), while comparable fills closer to the epicentre experienced deformations of only a few hundred millimetres.

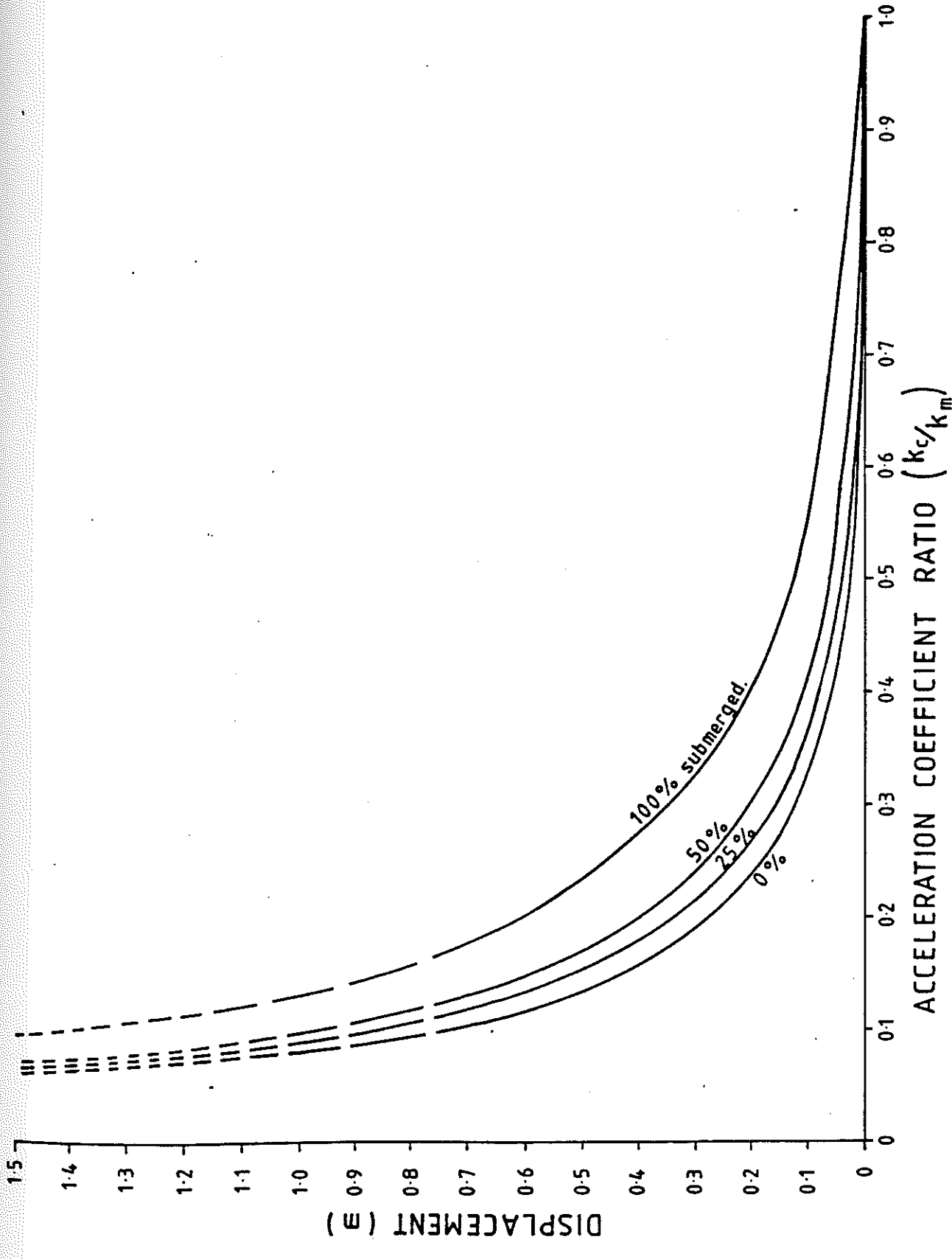
The relevance of a change in yield acceleration on submergence, is that displacement expected under a given intensity of seismic shaking will increase. Using the charts from Ambrayseys and Menu, (op. cit.) Fig. 8-1 has been produced to draw attention to the effect of submergence on a purely translational slope. Submergence of a purely translational slide at residual strength (with zero cohesion) will not reduce its safety factor, but will reduce its critical yield acceleration ($k_c g$). Displacements are a function of the intensity of shaking measured by the maximum acceleration of the ground motion time-history ($y_m g$). Depending on the value of the yield acceleration before submergence, displacements will increase by a factor of about 2 to 3 on submergence, provided the acceleration coefficient ratio (the yield acceleration divided by the maximum acceleration of the ground motion) is greater than about 0.15.

For an unsubmerged translational slide, the safety factor F can be related to yield acceleration from the approximation:

$$y_c = 0.4 (F-1)$$

(Obtained from a simple sliding block model.) If a slide is submerged and has a low gradient piezometric line, k_c will be reduced by the ratio of average effective stress to average total stress acting on the failure surface. For acceleration coefficient ratios less than 0.15 (safety factors less than about 1.1) prediction is difficult because large displacements would be anticipated. However, when considering the difference in earthquake displacements resulting from submergence, the factor of about 2 to 3 indicated above is likely to be an underestimate.

For an arcuate, rather than purely translational slide, similar effects will occur provided the failure surface soils are predominantly frictional. In general an arcuate slide will suffer a reduction in static safety factor on submergence. If buttressing is added to the toe, to just restore the original safety factor on submergence there will still be a net



Effect of submergence of a translational slide subject to an Earthquake

decrease in yield acceleration. A standard limit equilibrium analysis needs to be carried out for each case as there appears to be no simple approximation for estimating this effect. However, for cases of partially submerged slides which were studied, the reduction in yield acceleration was between 10 and 30%. This applied to slides which were buttressed just sufficiently to restore the precedent safety factor after submergence.

8.7 CONCLUSIONS

1. First-time slides (usually not identified as potential slide areas beforehand) provide the greatest potential for rapid landsliding, particularly where the mobilised strength significantly exceeds the residual strength on the failure surface.

2. Five specific mechanisms have been identified whereby pre-existing landslides (creeping or dormant) may be activated significantly by earthquake. In the absence of conditions appropriate for the mechanisms identified, earthquakes appear to have very minor effect on large pre-existing slides.

3. Other researchers have reported that earthquake loading of pre-existing landslides which contain silty materials, can have much more alarming consequences than has been concluded by the writer.

4. The rate dependence of shear strength must be included into Newmark methods for estimating the seismic displacement of slopes with safety factors close to unity.

5. In seismic areas, when assessing the stabilisation criterion for a hazardous slide submerged by reservoir filling, earthquake stability should be based on yield acceleration rather than the factor of safety. Precedent arguments will be otherwise invalid.

CHAPTER 9

ALARM CRITERIA AND MONITORING FOR HAZARDOUS LANDSLIDES

9.1 INTRODUCTION

Alarm criteria are required for two basic categories of landslide hazard:

- (i) Limited hazard, ie readily evacuated situations such as open pit mines or small slides where lives would not be threatened if alarm systems provide forewarning, an hour or so before rapid failure.
- (ii) High hazard, ie where a large population must be removed from the hazard area. One or more days may be required to evacuate dwellings. Examples are landslides threatening towns either directly or indirectly via effects on dams and reservoirs.

This article addresses principally the latter category, and discusses two large landslides which occurred in New Zealand, because they are considered particularly instructive with regard to the selection of alarm criteria.

These are the Abbotsford Slide, a natural slope failure; and the Ruahihi Slide, a fill slope failure. Both failures had been monitored for many weeks before catastrophic movements developed. In neither case, was sudden acceleration predicted.

9.2 FACTORS RELATED TO ALARM CRITERIA

The likelihood of rapid movements occurring without adequate forewarning can be minimised by considering:

- (i) The establishment of pre-set alarm criteria which are determined from geotechnical properties of the slide materials. In the event that specified thresholds are met, then it must be acknowledged that the slide is out of control and all measures necessary to mitigate damage from rapid movements should be taken immediately.
- (ii) Ensuring that monitoring intervals are appropriate to the rate of development of the slide. The possibility that a slide may accelerate unexpectedly between surveys must be addressed continuously, using standard geotechnical procedures.

9.2.1 Pre-set Alarm Criteria

9.2.1.1 Empirical curve-fitting approaches

Several investigators (Saito, 1969; Fukuzono, 1985; Varnes, 1982; Azimi et al, 1988) have addressed the prediction of time of failure.

Saito (1969), suggested an empirical creep law which implies that slide velocity will be inversely proportional to the remaining time to failure. This method has been applied to both first-time and residual strength slides, but has two limitations. Firstly, as Saito points out, creep laws should not be used where displacement independent accelerating factors apply. Secondly, several instances have been found where the time to failure would have been seriously overestimated. Creep laws appear better suited to predicting failure when the remaining time is only a few hours, rather than days.

Azimi et al (1988) propose an advancement on the Saito method, in that velocity may be inversely related to an exponential function of the remaining time to failure, and trial and error solutions are not involved. The proposed method to estimate remaining time to rapid failure is graphical. However from the proposed empirical relationships, it can be shown that the remaining time, $t(r)$ is estimated simply by:

$$t(r) = t(n).t(n)/(t(n-1)-t(n))$$

where $t(n-1)$ and $t(n)$ are successive time intervals corresponding to the two latest successive displacements of equal magnitude. In other words, the latest portion of the displacement versus time curve is divided into two equal intervals for displacement, to produce two successive time intervals. The data may be smoothed if appropriate and the distance interval selected should give due regard to survey accuracy and trends in the acceleration record.

Zavodni & Broadbent (1980) and Cruden & Masoumzadeh (1987) investigated empirical creep laws to provide a basis for predicting the timing of rapid movements. An inference from the former article is that rapid failure of a first-time slide can be expected if the acceleration increases linearly with respect to the velocity. (The constant of proportionality is likely to be in the range of 0.1 to 1.0/day.) Rapid failure is reportedly unlikely to occur within 24 hours if the velocity is less than 15 mm/day. Methods for extrapolation of displacement records, using monitoring criteria have been investigated by Voight & Kennedy (1979): an alarm criterion of 6 m displacement; and Vibert & Arnould (1987): a criterion of 90 mm/day velocity. One disadvantage of such predictions for timing of rapid failure is that wide ranges of possible failure times often result, depending on the curve fitting approximation used. Much of this work has been directed towards the more difficult fields of pit slope management and first-time slides (rather than those where residual strength conditions apply). However, little work has been done to derive creep laws based on effective strength characteristics determined from direct shear or ring shear tests using variable displacement rates.

9.2.1.2 Empirical threshold criterion approaches

Empirical alarm criteria are rarely reported in case histories. Johnson (1982) states that acceleration should be used as "the basis for predicting failures" but no specific threshold limits are recommended. Macrae (1982) gives examples where downslope velocities in the range of 30-35 mm/day were used for evacuation of open pit mines.

9.2.1.3 Geotechnical-empirical approach

This section will attempt to integrate the use of empirical alarm criteria (usually obtainable from deformation monitoring) with geotechnical characteristics of the relevant materials.

Velocity - Creep rates preceding catastrophic failures have been documented for many landslides. Downslope velocities of 50 to 100 mm/day were achieved by the Vaiont, Abbotsford and Ruahihi Slides (Fig. 9-1a) some days before their final rapid movements.

Acceleration - Where appropriately regular monitoring has been obtained, rational interpretation of landslide movement requires successive differentiations of the displacement-time record to obtain the acceleration history. This must be carried out in any instance where the displacement-time curve exhibits a concave upward shape. Examples are shown in Fig. 9-1b, where acceleration is shown to be increasing above 5 mm/day/day, either linearly or exponentially for 5 to 10 days prior to rapid failure.

Clearly, additional case histories of well monitored landslides would be desirable before confirming generalisations from the limited data examined. However, taken in conjunction with other case histories with less detailed movement records available, and including suggestions made by Johnson, Macrae, Zavodni & Broadbent (op cit), the following are suggested as critical limits for landslides where shearing (rather than toppling etc) is occurring.

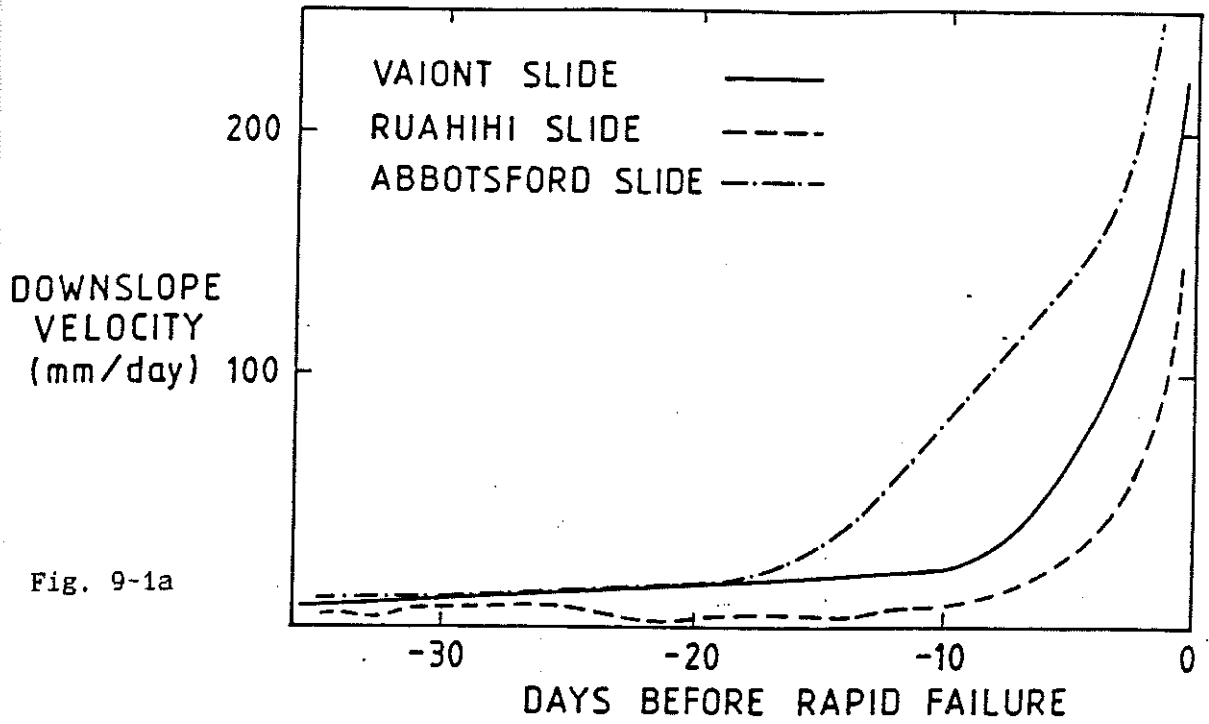
(i) Where residual strength conditions pertain, in a wide (but probably not exhaustive) range of materials:

Downslope velocity 50 mm/day
Downslope acceleration 5 mm/day/day

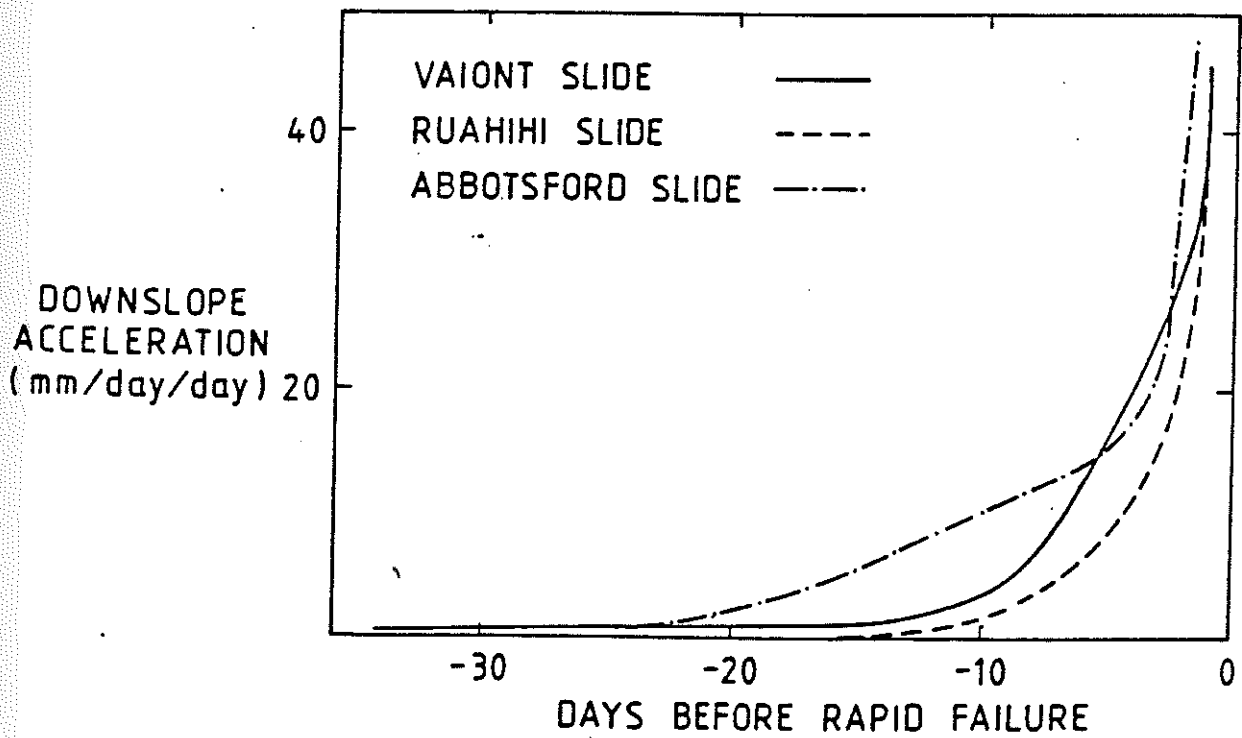
(ii) For first-time slides where displacements are small, a factor of ignorance (often about 5 but maybe up to 10) should be applied to the above values for residual strength slides, eg:

Downslope velocity 10 - 5 mm/day
Downslope acceleration 1 - 0.5 mm/day/day

PRECURSORY VELOCITIES OF SLIDES



PRECURSORY ACCELERATIONS OF SLIDES



Depending on the hazard being considered, remedial measures or other actions may be appropriate long before the above limits are reached. The point in specifying alarm criteria is that at some stage it must be acknowledged that the time for debate is over, the situation is out of control and evacuation must proceed directly. The limits proposed above are intended to be sufficiently conservative to provide several days forewarning in the case of residual strength slides, or at least 24 hours warning in the case of first-time slides with long monitoring records. However, these criteria may be too optimistic in some instances, particularly where a displacement-dependent accelerating mechanism is operating, or an additional displacement-independent accelerating mechanism is imposed (eg rainfall).

The situation may arise where a slide velocity exceeds its critical velocity but its acceleration is less than the threshold and decreasing. In this case there may be arguments in favour of accepting velocities up to, but not exceeding 10 times the critical velocity where site specific investigations confirm that accelerating mechanisms are clearly absent. Applying this factor to the above limits, indicates that it is quite unlikely that movement rates exceeding 500 mm/day could be considered acceptable for any hazardous landslide.

Although the criteria already discussed have been derived primarily from examination of case histories, they also have geotechnical bases, these being residual strength testing and frictional heating concepts, which require consideration.

(a) Residual shear testing (Fig. 9-2a) has clearly demonstrated that the strength of soils is dependent on rate of shearing (Skempton & Hutchinson, 1969). Rates and times of testing are appropriate to allow complete pore pressure dissipation, so the findings do relate to effective stresses. For ease of presentation, all shear strengths have been normalised with respect to the shear stress developed at an arbitrary standard shearing rate of 10 mm/day. Residual strength testing in the laboratory is usually a rate controlled test, that is, stress is measured as the dependent variable and plotted as ordinate. In the field, gravity imposes a stress controlled 'test', therefore Fig. 9-2b shows the same data re-plotted with the usual convention ie, dependent variable plotted as ordinate. In small scale laboratory tests, there are a number of factors that limit stress controlled testing, such as the difficulty in achieving steady state conditions (Chapter 7). Nevertheless for a large slide at residual strength, it is suggested that stress controlled behaviour can be estimated from rate controlled laboratory tests.

Note that on Fig. 9-2b, the conventional limit equilibrium factor of safety is given by the reciprocal of the normalised shear stress ratio. This diagram adopts (quite arbitrarily), a safety factor of 1.00 as the condition for a slide moving at 10 mm/day. Such accuracy has no application when considering an absolute safety factor for a stationary slide. However, small changes from the defined safety factor become highly significant when assessing changes in velocity of an actively moving slide.

Fig. 9-3a shows a limited number of residual strength tests on clays and silts. One feature of note is the trend for soils with low clay contents to have somewhat steeper curves, ie the change in velocity of slides in these materials is more sensitive to small changes in

RATE DEPENDENCE OF RESIDUAL STRENGTH

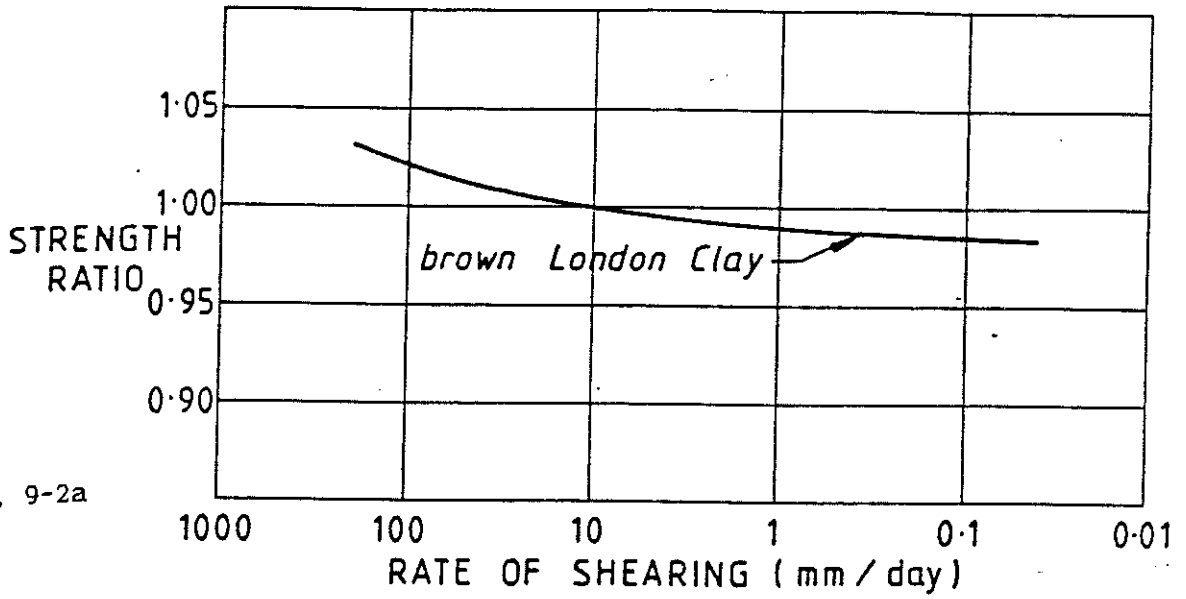


Fig. 9-2a

After Skempton and Hutchinson (1969)

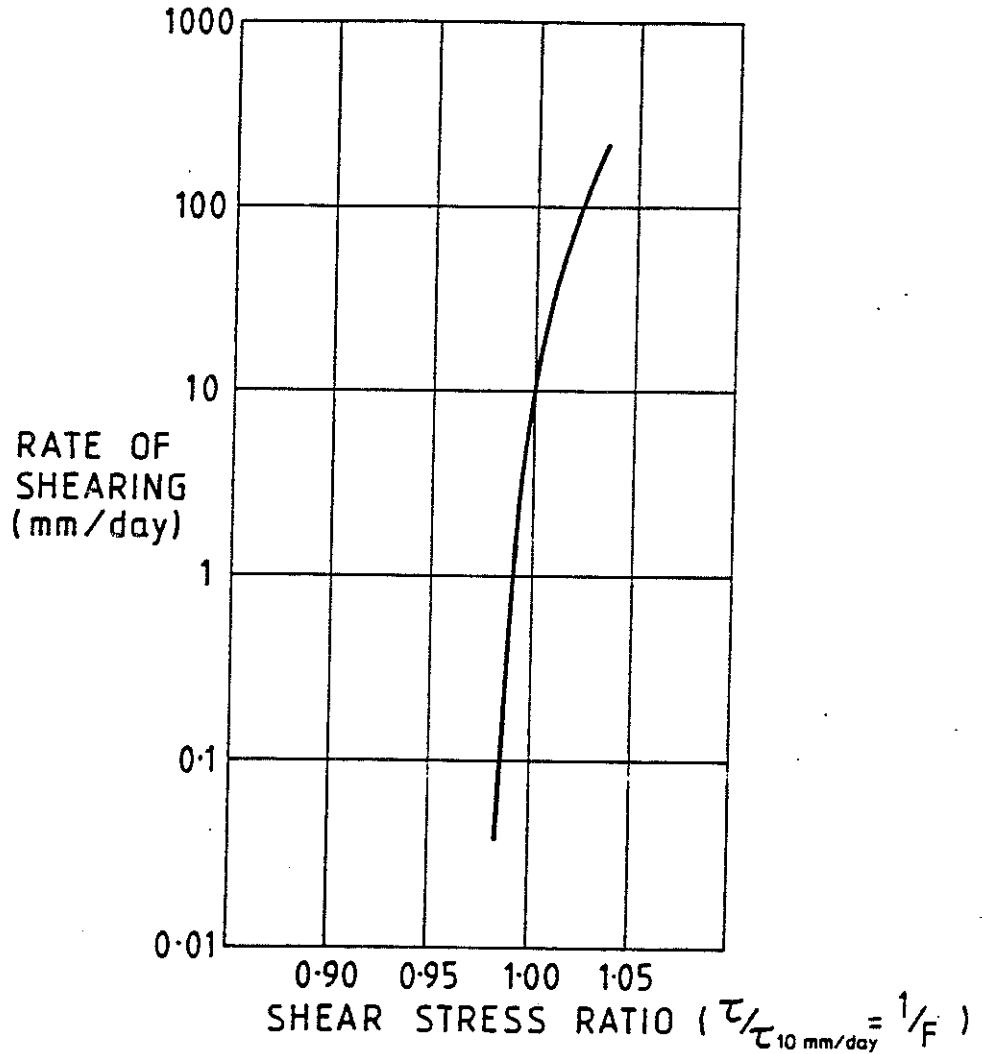
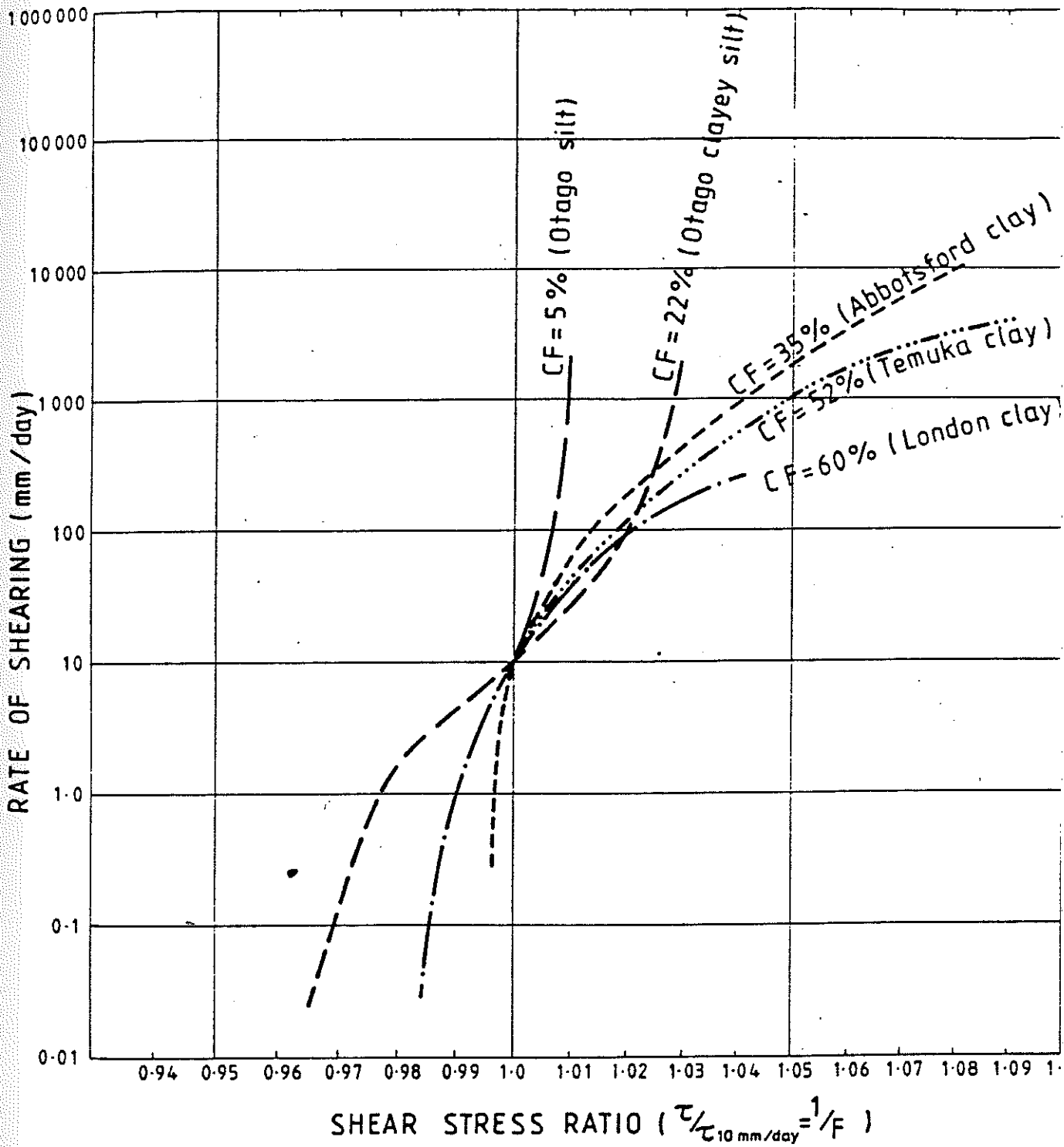


Fig. 9-2b

RESIDUAL STRENGTH DEPENDENCE ON SHEARING RATE



CF = Clay Fraction (% < 0.002 mm)

Fig. 9-3a

safety factor. Soils with high clay contents tend to be more tolerant. Regardless, determination of the rate dependence of strength allows the maximum velocity of steady yielding to be estimated. As shown on Fig. 9-3a, some of these curves appear to steepen, becoming asymptotic to an upper strength limit. The significance of a steep gradient is that a very small decrease in safety factor will induce a disproportionately large increase in slide velocity. A slide in this state will yield in an unsteady manner with rapid acceleration imminent. Note that for the examples shown, unsteady yielding may be expected in at least some soils at shearing rates in the region of about 50 - 500 mm/day.

Most soils show increasing effective strength with increasing rates of displacement, although anomalous strength properties have occasionally been reported, eg Cowden till (Lemos, Skempton & Vaughan, 1985), see Fig. 9-3b. If this type of characteristic can be confirmed with a stress controlled test, it indicates a soil that will shear more rapidly if the driving forces are reduced! A landslide in this material would surely fail with extreme rapidity, in apparent contradiction to Terzaghi's (1950) claim that "if a landslide comes as a surprise to eye witnesses, it would be more accurate to say that the observers failed to detect the phenomena which preceded the slide".

(b) Pore fluid expansion from frictional heating has also been shown to be relevant to slide acceleration in specific soil types, (Appendix 6). Numerical methods are now available to demonstrate the conditions which will induce significant pore pressure rises, that is, geotechnical characteristics can be used to set critical velocity and acceleration for a given situation. From the writer's calculations using the computer program developed by Smith (in prep.) it appears that pore pressures are likely to be affected by frictional heating, only in highly overconsolidated saturated soils of low permeability, subject to moderate or high normal stresses where velocities exceed about 50 to 500 millimetres per day, and accelerations are positive. Some other mechanism is usually required to initiate substantial velocity and acceleration before the effect becomes significant.

From both (a) and (b) above, therefore, it is apparent that the geotechnical characteristics of the failure surface soils are very relevant to the selection of threshold movement rates for alarm criteria.

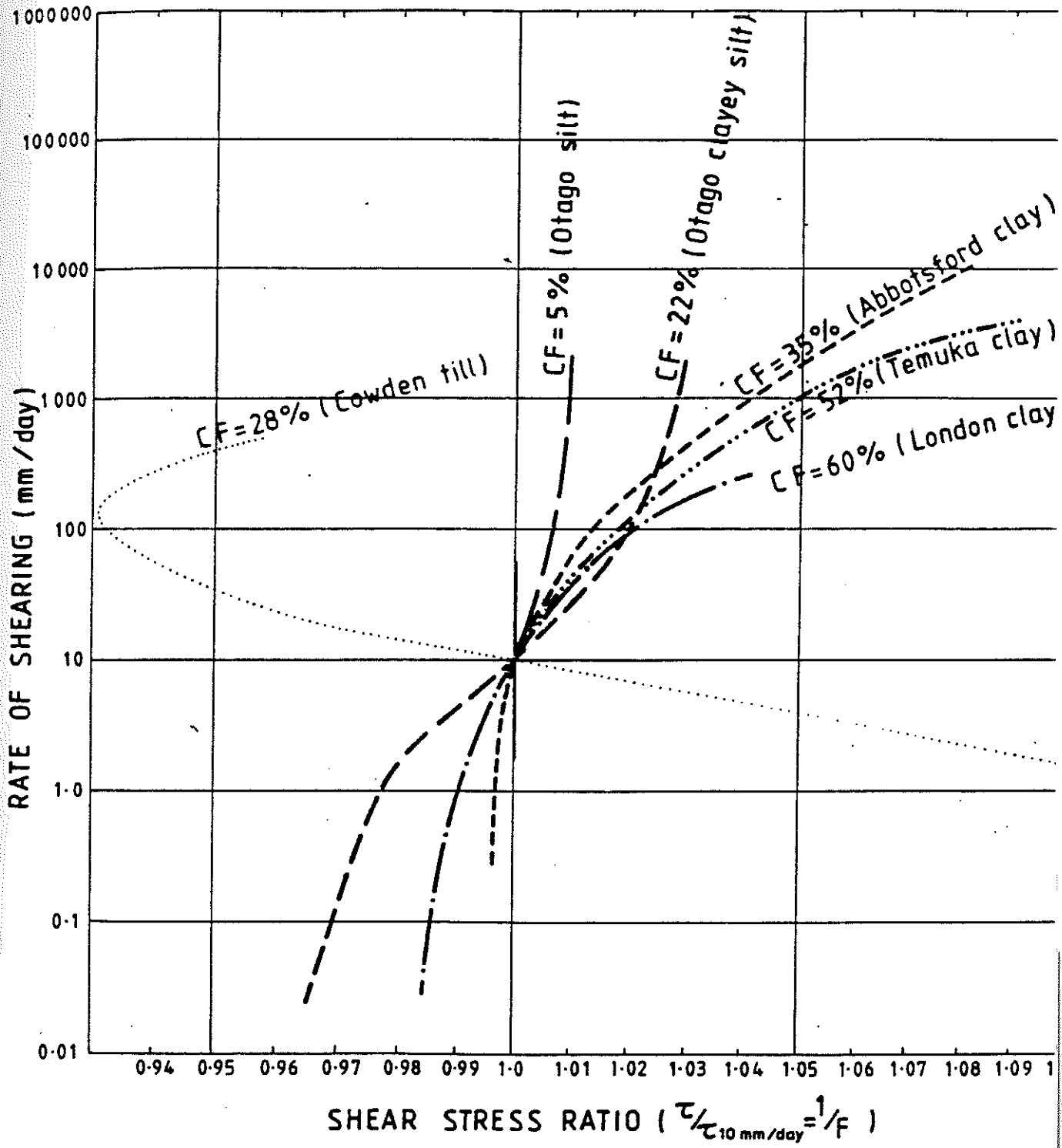
9.2.2 Monitoring Frequency.

9.2.2.1 Background

Case histories have demonstrated that in spite of monitoring, catastrophic failures have occurred without prior recognition simply because no procedures have been followed to determine whether a formerly adopted survey interval should be continued. Often, conditions will change so that more frequent surveys are required.

In a slide which has been monitored for a long period, there is a danger of over-familiarity. Ruahihi is a prime example: initial surveys were carried out daily, but intervals were gradually increased in spite of obvious acceleration. By the time of failure, readings had been extended to weekly intervals!

RESIDUAL STRENGTH DEPENDENCE ON SHEARING RATE



CF = Clay Fraction (% < 0.002 mm)

Fig. 9-3b

Procedures are suggested herein, in order to lessen the likelihood of rapid movements developing between monitoring surveys. Modifications will obviously be required for specific cases, by the application of engineering judgement, and giving due regard to the geotechnical characteristics of the slide materials. The proposals relate primarily to slides at residual strength, ie where displacements at the toe are sufficiently large to discount a major strength reduction from peak to residual. To satisfy this criterion downslope displacements at the slide toe should exceed 100 mm in non plastic soils, grading to about 2 m in highly plastic clays. First-time slides may be treated similarly but a much higher level of caution is clearly required.

9.2.2.2 Specific recommendations for determining landslide survey intervals.

(a) Plot displacement versus time. If velocity exceeds 0.5 mm/day then plot velocity and acceleration curves. If the acceleration is increasing, use the method described in Section 9.2.2.3 to extrapolate all plots.

(b) Determine the time rate of change in safety factor expected from any displacement-independent accelerating mechanisms (eg removal or addition of material to the slide head or toe, rising reservoir, other changes in piezometric levels etc). Methods are described in Appendix 2.

(c) Determine the distance rate of change of safety factor for any displacement-dependent accelerating mechanism (eg decline from peak to residual strength, slope deflation or self buttressing, pore pressure changes resulting from mass relocation, pore pressure changes from frictional heating etc). Methods are described in Appendices 4 and 6.

(d) Compute the expected change in downslope velocity caused by the predicted changes in safety factor from both types of accelerating mechanisms. This is done from laboratory tests (Chapter 7) to determine the strength-displacement rate relationship for the failure surface soil (or correlations from test on soils with similar index properties).

(e) From the extrapolation of the displacement curve (together with the velocity and acceleration curves if appropriate) determine the time interval which will satisfy the following criteria:

(1) Displacement. For first time slides, the change in downslope displacement should be no more than 5 mm (less if practicable). Slightly greater displacements are acceptable for slides where residual conditions clearly apply. However, the change should always be less than 50 mm and a value of 10 mm is often appropriate.

(2) Velocity. If any precedent velocity exceeds 0.5 mm/day, the extrapolated change in downslope velocity should be small compared with its latest value, say a change of no more than 10%. Where velocity is very low, this criteria may be extended to allow for survey accuracy, (usually 0.5 mm for inclinometers or 5 mm for surface deformation marks). If the velocity is approaching the specified critical limit, the time interval should be decreased to ensure the limit is not exceeded.

(3) Acceleration. Where movement rates are sufficient to enable meaningful determination of accelerations, the extrapolated change in acceleration should be no more than 10%. If the acceleration is approaching the critical limit, time intervals should be decreased accordingly.

(4) Time. If the acceleration is positive, the time interval should be a small percentage (say 10%) of the estimated time remaining to rapid failure, ie the time interval should not exceed 10% of $t(n) \cdot t(n) / (t(n-1) - t(n))$. (Symbols as defined above.)

The smallest of the time intervals determined above should be adopted unless precedent plus geotechnical reasoning clearly justify a longer interval. Additional surveys should be carried out after any rare event particularly seismic loading or sustained rainfall (giving due regard to infiltration delays in the latter case).

9.2.2.3 Prediction of accelerating slide movement.

(After Azimi et al, 1988).

The following procedure will tend to linearise the movement record of an accelerating slide and hence is useful for extrapolation. It may also be used to estimate time of rapid failure provided no displacement independent accelerating mechanism (eg reservoir filling) is operating. Note that the 'window' of accuracy of the prediction may be very large, and unconservative. (An overestimate of up to 400% for the time remaining to failure was found in the first example for which the method was proposed.) Accordingly it is suggested that any estimate of the remaining time to failure, should be divided by a factor of ignorance of at least 5.

(1) Plot (a) the raw data for the displacement versus time curve and (b) the same curve smoothed with regard to survey accuracy. Carry out the following steps with each curve.

(2) Divide all of the accelerating section into equal distance intervals which give due regard to the accuracy of the survey (about 3-10 times larger than the standard error), and read off the corresponding series of times; $T(0)$, $T(1)$, ... $T(i)$... $T(n)$, using the beginning of the accelerating portion as origin ($T_0 = 0$).

(3) Plot $T(i-1)$ versus $T(i)$ on natural graph paper. Draw on the line $T(i) = T(i-1)$. The projected intersection of the two lines gives the predicted time of failure. The raw data curve gives some indication of likely error limits. The smoothed curve may provide a more accurate prediction, but grossly unconservative estimates must still be anticipated. Extrapolated movement patterns may best be estimated from the smoothed curve.

(4) The graphical method is preferred because error limits may be crudely estimated. However, direct solutions are available from any selected data points:

$$\text{Time of failure} = (T(i).T(i)-T(i+1).T(i-1))/(2T(i)-T(i+1)-T(i-1))$$

or,

$$\text{Remaining time interval to failure} = t(n).t(n)/(t(n-1)-t(n))$$

$$\text{where, } t(i) = T(i) - T(i-1)$$

(5) Repeat steps 2, 3 and 4 to determine sensitivity with respect to selected distance interval.

(6) Use the most conservative extrapolation to estimate (a) the future displacement, velocity and acceleration for determination of the appropriate time interval to the next survey, and (b) the remaining time to failure assuming a factor of ignorance of at least 5.

9.3 PRACTICAL APPLICATION OF ALARM CRITERIA

9.3.1 Steady Creep.

Table 9-1a lists velocities (and accelerations where appropriate) for a number of active slides where creep has not been the forerunner to rapid movements. Many of these slides have suffered considerable displacement and most are located in reservoirs. All show consistency with the proposed limits (50 - 500 mm/day) for residual strength conditions. It is possible in some instances for faster movements to occur without catastrophic acceleration (particularly where normally consolidated clays are moving on relatively shallow failure surfaces, or movement causes significant self-buttressing). Nevertheless, it is suggested that for potentially hazardous slides, threshold limits which exceed the above, should not be set without detailed laboratory and field studies.

9.3.2 Catastrophic failure records.

At least 5 days forewarning would have been available if the proposed limits were adopted for Vaiont, Abbotsford or Ruahihi slides. Since producing these recommendations, additional raw data has been sought, but little obtained. One example received is the monitoring for the Jizukiyama Slide, where a disaster occurred, because neither the acceleration nor the sustained movements were predicted (Sassa, 1988). The monitoring data reported for this slide, are such that adoption of the above policy for threshold velocity and acceleration would have led to evacuation about 7 days before the final rapid advance.

Table 9-1. Landslides with historic records of steady creep failure. (Mostly in reservoirs).

Slide	Downslope speed (mm/day)
Downie (active toe)	< 0.03
Mica Reservoir	0.1
Needle Rock Slide	0.3
Morrow Point (Slide A)	1
Dirillo Reservoir	3
Futase Reservoir	3
Ankhangaran Reservoir	6
Fort Peck Dam	8
Waiomao	20
Vaiont (1960 filling only)	36
Wind Mountain	40
Jeffrey Mine	60
America Mine	110
Minnow	450
Hochmaiss	50 (a = 0.5)
Hochmaiss	190 (a = 2)

Note: Acceleration (a) in mm/day/day.

9.4 CONCLUDING REMARKS

This review has been prepared after a brief literature review, to provide a discussion document on alarm criteria. Undoubtedly, a more comprehensive search for field data and appropriate laboratory testing will lead to recommendations for more reliable alarm criteria than those identified so far. However, the reasons for suggesting limits at this stage is that failures continue to inflict unmitigated damage because appropriate limits (and procedures for assessing them) have seldom been considered. Further research will improve the state of the art for the prediction of rapid movements. Meanwhile it is suggested that two aspects which are generally overlooked (pre-setting of alarm criteria and selection of appropriate monitoring intervals) should be addressed through examination of geotechnical characteristics. Adequate appreciation of the nature of the governing materials will substantially diminish the risk of unexpected acceleration of creeping landslides.

CHAPTER 10

CONCLUSIONS

1. On the basis of laboratory studies, a number of papers published in the last decade report that pre-existing slides in fine grained soils can be accelerated rapidly as a result of a newly postulated mechanism. This mechanism is a loss in effective strength without an accompanying increase in pore pressure, ie it has been claimed that Terzaghi's effective stress principle does not apply. The originators have presented no case history to support their findings. An alternative explanation for the interpretation of rate effects in soils subjected to rapid shear in the laboratory, leads to the conclusion that an apparatus effect, of no relevance to field conditions, may have been observed.
2. Residual strength testing of partially saturated soils has been carried out for the first time. The effect of saturation on soils containing pre-sheared surfaces (at residual strength) is markedly different from the effect on peak strength. Where a pre-sheared but unsaturated soil has ever been subjected to effective wetting, and has experienced concurrent movement (ie in an active landslide), the effect of any future saturation will be small. However, if pre-shearing has occurred under only low moisture conditions, saturation can induce a dramatic decrease in strength.
3. An extension to the Casagrande resistance envelope procedure allows the field strength of partially saturated soils to be determined from existing slope profiles. Peak strength parameters derived from unsaturated soils may be used to determine effective strength parameters for the same material after reservoir submergence.
4. The integration of limit equilibrium methods with groundwater modelling allows insight to the way in which the safety factor of a reservoir slope will change with time as a reservoir is filled, maintained or drawn down. The lag of groundwater levels with respect to the reservoir level can produce critical values of safety factor at times which cannot be readily judged otherwise. Quantitative assessments of the magnitude of changes in safety factor and the times at which stability is critical, assist the safe management of a reservoir, particularly on first filling and drawdown.

5. Testing of landslide gouge has established a clear relationship between residual strength, shearing rate, and effective normal stress. A family of characteristic curves which show the mobile range of a soil may be determined in the laboratory. Rate dependence of shear strength provides an explanation for the observation that landslides in which residual strength conditions pertain, usually move in a steady manner. Determination of the mobile range of gouge from an existing landslide allows straightforward quantitative assessments (using standard limit equilibrium analysis) of the nature of future landslide movements for given changes in safety factor, including the likelihood of rapid acceleration. Therefore if a landslide (previously recognised or otherwise) is reactivated as result of works which involve de-stabilising factors such as toe submergence (or removal of material from the toe, head loading etc), a decision can be made on whether works should be continued, reversed, or deferred until the displacement rate of the slide reduces to an acceptable value. If landslide stabilisation is proposed, the appropriate minimum increase in factor of safety may be determined, depending on whether movements must be entirely arrested or if a specific creep rate is acceptable.

6. Examination of geological evidence from field experience and the case histories reviewed, indicates that there are 5 specific mechanisms which can cause a large pre-existing landslide (which has moved some tens of metres under gravitational forces) to be accelerated rapidly by seismic shaking. If the conditions required for these mechanisms can be shown to be absent, some degree of assurance of the seismic resistance of an active slide may be established. When assessing the stabilisation criterion for a hazardous slide submerged by reservoir filling, earthquake stability should be based on yield acceleration rather than the factor of safety, because reliance on precedent geological conditions will be otherwise invalid.

7. There are no recognised procedures for assessing the risk of rapid movement of an active landslide. Further research will improve the state of the art for the prediction of rapid movements, but meanwhile it is suggested that two aspects which are generally overlooked (pre-setting of alarm criteria and selection of appropriate monitoring intervals) should be addressed through examination of geotechnical characteristics. These allow the development of guidelines for specific cases. In the absence of such information, general procedures have been proposed, which will substantially diminish the risk of unexpected acceleration of creeping landslides.

APPENDICES

APPENDIX 1

COMPUTER PROGRAMS FOR DETERMINING FIELD STRENGTH PARAMETERS USING THE CASAGRANDE RESISTANCE ENVELOPE PROCEDURE WITH APPLICATION TO CUT SLOPE DESIGN

A1.1 INTRODUCTION

No program generally available, outputs the parameters required for analysis using the Casagrande Resistance Envelope Procedure. UTEXAS2 is a well proven limit equilibrium program for slope analysis, which comes with a clear well documented user manual, and is in common use by geotechnical consultants. This appendix provides a simple addition to the source code of UTEXAS2 to allow generation of a resistance envelope.

These and the subsequent file handling programs are intended to allow the user to apply the procedure very rapidly, check the computer interpretations visually and output the final graph of the resistance envelope.

From that stage, design proceeds in the usual manner. For simple slopes, with linear Mohr Envelopes and no groundwater present, chart solutions are available. More generally, an iterative process is required to provide the optimum batter angle to comply with a specified factor of safety. To eliminate the time consuming aspects, an additional program is supplied below. This rapidly generates design charts for cut or fill batters under a variety of slope conditions (namely geometry, material properties, groundwater conditions and required safety factor). The safe batter angle for minimum earthworks is generated iteratively by the program without any further call on the designer's time, until the output and checking stage.

Each process uses a main program which executes UTEXAS2 as a shell (sub-program). The main program then interprets the output, prepares another input file and then re-executes UTEXAS2. This has the advantage of eliminating the time required for keyboard entry. Slightly faster execution could be achieved by providing additional algorithms for iteration within UTEXAS2, but this has been purposely avoided in order to retain the proven program assurance. (No changes have been made to UTEXAS2 algorithms - only additional values are written to its output file, and input for each iteration is generated automatically.)

A1.2 PROGRAM MODIFICATION TO UTEXAS2

Program UTEXAS2, written by Wright (1985) has a FORTRAN source code containing 10 files namely UTEXAS.FOR, TEX2.FOR, TEX3.FOR TEX10.FOR.

The following modifications have been made:

(i) In UTEXAS.FOR which is the main program the following array sizes for the maximum number of points on an individual profile line has been increase from 15 to 31, ie:

```
MAXPLP (20 15) to MACPLP (20 31)
XPROFL (20 15) to XPROFL (20 31)
XPROFL (20 15) to XPROFL (20 31)
```

This is to allow input of the multiple benches typically found on local highway cuts. (Mainly because their coordinates are generated automatically by the site survey program used, but otherwise this degree of detail is of no added value to slope analyses.)

(ii) The last listing, (UTEX10.FOR) contains 3 similar subroutines for printing information pertaining to the solution of unknowns for individual slices. These are:

```
SUBROUTINE FOBISH
SUBROUTINE FOCORP
SUBROUTINE FOSPEN
```

which apply to Bishop's, Corps of Engineers', and Spencer's limit equilibrium methods respectively. Each subroutine has similar layout and line numbers, and each has a DO loop down to statement 350. The addition required is to insert the following code immediately prior to statement 350, in each of the 3 subroutines:

```
C ..... FROM HERE TO STATEMENT 350 ARE MODIFICATIONS TO THE STANDARD
C VERSION OF UTEXAS2.FOR, TO PROVIDE PARAMETERS FOR THE CASAGRANDE RESISTANCE ENVELOPE
C PROCEDURE
C     GSL IS SUMMATION OF BASE SLOPE LENGTHS OF SLICES: GSTSIG,
C     GSESIG C AND GSTAU ARE SUMMATIONS OF TOTAL, EFFECTIVE NORMAL AND SHEAR FORCES
C     IF(I .EQ. 1) THEN
C         GSL = 0
C         GSTSIG=0
C         GSESIG=0
C         GSTAU=0
C     ENDIF
C     GSL=GSL+DELTAL
C     GSTSIG=GSTSIG+TSIGMA*DELTAL
C     GSESIG=GSESIG+ESIGMA*DELTAL
C     GSTAU=GSTAU+TAU*DELTAL
C     IF (I .EQ. NCM1) THEN
C         AVTSIG=GSTSIG/GSL
C         AVESIG=GSESIG/GSL
C         AVTAU=GSTAU/GSL
C     IF (PRINTO) WRITE (OUNIT,1999) AVTSIG, AVESIG, AVTAU
C     ENDIF
1999 FORMAT (//10X,'PARAMETERS FOR CASAGRANDE RESISTANCE ENVELOPE'
1 /10X,'AVERAGE TOTAL NORMAL STRESS   =' ,F12.2,
2 /10X,'AVERAGE EFFECTIVE NORMAL STRESS =' ,F12.2,
3 /10X,'AVERAGE SHEAR STRESS           =' ,F12.2,
4 /10X,'LE METHOD   ')
```

The next line is statement 350 of the existing code which reads:
350 CONTINUE

In the line 4 of the FORMAT continuation statement above, the words LE METHOD may be replaced by BISHOP METHOD, CORP METHOD or SPENCER METHOD corresponding to the specific subroutine. (Note however that a single quote cannot be used in the FORMAT statement, ie BISHOP'S METHOD is invalid syntax).

The modified TEX10.FOR file has been named STEX10.FOR. No other modifications or additions were made to the original source code UTEXAS2.

A1.3 TECHNIQUE FOR GENERATING CRITICAL POINTS ON A RESISTANCE ENVELOPE

The basic principles of the Casagrande Resistance Envelope Procedure (REP) are described by Casagrande (1950) and Janbu (1973 and 1977).

The procedure usually assumes that average values for shear strength parameters are applicable in each individual slope analysed, and this is the situation commonly of interest in practice. A slope with multiple soil types can be addressed in some cases, but this is outside of the scope of this appendix. Variation of soil density can readily be accommodated in the usual manner, as can multiple piezometric lines.

Soil bulk densities can either be measured, or in less critical cases may often be assessed visually with sufficient accuracy because any errors in the slope analysis will be largely self cancelling when the same density is used in the design process. The key parameter to vary is the soil attraction (the normal effective stress at which the shear strength of the soil extrapolates to zero). This parameter is discussed by Janbu (197*). In practice this is done by using a sequence of decreasing friction angles to generate the mobilised stresses (see A1.4 for explanation) while at the same time increasing the cohesion. This combination will allow the maximum mobilised shear stress to be identified for a range of values of normal stress. The actual values of safety factor generated by UTEXAS are quite irrelevant to the process, and are not used in the REP.

A range of input values that should produce adequately well defined resistance envelopes for most slopes of interest in highway design or reservoir engineering is:

Analysis set number	1	2	3	4	5	6	7
Effective cohesion (kPa)	1	2	5	10	20	50	100
Effective friction angle (degrees)	80	65	50	35	20	10	5

For each analysis set, an automatic search for the location of the critical surface is specified in the UTEXAS2 input data set.

If the resulting envelope generated needs more points, to describe a continuous curve, other values may be interpolated from the above set. For additional points to be generated at very low (or very high normal) stresses, higher (or lower) friction angles should be input respectively. If there are problems with convergence in UTEXAS2 (unlikely if Bishop's method is used), then higher values of cohesion should be tried.

For the usual range of slopes of interest in a uniform soil type, the method of limit equilibrium used is not important. It is good practice to use the same method for both analysis and design, thus allowing automatic cancelling of any bias. Bishop's method is recommended for both speed and general reliability, with alternative methods used for checking. In any case where the toe of a critical circle dips into the slope, Bishop's method must be checked with a more rigorous solution.

Usage:

1. Prepare a standard input data file for UTEXAS2, as specified in the UTEXAS2 user manual, using only one slope per file, but change the soil strengths 6 to 7 times, each time repeating the command to search for the critical circle.
2. Run UTEXAS2 (compiled with modifications above). Disregard absolute values of safety factors as only the mobilised stresses are relevant.
3. View locations of critical surfaces (see Section A1.5) and then produce resistance envelope plots (see A1.6).

A1.4 THE CONCEPT OF MOBILISED SHEAR STRESS USED IN THE REP

The concept of mobilised shear stress (Janbu, 1973) offers a rational method for comparing and evaluating slopes (composed of similar material) which have unknown safety factors.

Using the limit equilibrium assumptions, the average mobilised shear stress on any active or potential failure surface within a slope is defined as the average shear stress acting on the full area of the failure surface, required to just maintain static equilibrium. It is a function of slide mass and geometry, and for practical purposes it is independent of the Mohr envelope for the failure surface soil.

On the other hand, the average available shear stress for the same surface being considered is a property of the both the slope geometry and the failure surface soil.

The limit equilibrium safety factor (F) of any (potential) failure surface is defined by:

$$F = \tau_a / \tau_m \quad \dots\dots\dots(1)$$

where,

τ_a is the average available shear stress

τ_m is the average mobilised shear stress.

The strength of a soil is usually defined in terms of effective stress parameters although total stress parameters may be required where partially saturated soils are involved or (rarely) if crude estimates are required for short term stability of saturated soils.

There are cases where (i) soil suction effects can be neglected, (ii) the failure envelope for the soil exhibits no significant curvature and is essentially frictional (ie with no significant cohesion). In these conditions the effective friction angle (ϕ') for the soil, (ie the available effective friction angle at failure) is found from the standard relationship:

$$\tau_a = \sigma' \tan \phi' \quad \dots\dots\dots (2)$$

ie.

$$\phi' = \arctan(\tau_a / \sigma') \quad \dots\dots\dots(3)$$

where σ' is the average effective normal stress.

The mobilised friction angle (ϕ'_m) can then be defined similarly in terms of effective stresses as:

$$\phi'_m = \arctan(\tau_m / \sigma') \quad \dots\dots\dots(4)$$

Dividing both numerator and denominator in (1) by σ' , taking tangents and substituting, then gives simply:

$$F = \tan \phi' / \tan \phi'_m \quad \dots\dots\dots (5)$$

The benefit in working in terms of mobilised effective friction angle (or simply, mobilised strength for cases where cohesion is zero) is that a factual parameter can be considered throughout the analysis process, and only at the final stage does the actual value of safety factor need to be assessed. This allows a percentage change in safety factor to be determined for a given potential failure surface (under some change in conditions caused by slope cutting, buttressing, drainage, river or reservoir effects, external loading etc). This allows preliminary design to proceed before the available strength parameters are determined. Also, for many cases where the net result is no net decrease in safety factor then there is no need to determine the frictional strength or corresponding values of absolute safety factor.

The absolute value of the safety factor can readily determined at any later stage (when a specific friction angle can be assigned) using equation (5).

A1.5 SUPPLEMENTARY PROGRAM TO UTEXAS2, FOR SLOPE AND SLIP CIRCLE GRAPHICS

UTEXAS2 has no graphics capability. The following program, TXGRAPH (written in TB) reads the output file from UTEXAS2 and converts the slope profile and critical circles to a separate file in a format suitable for importing directly into the program GRAPHER, (Golden Software Inc. 1988). The code assumes:

1. The ground profile is fully described by Profile 1 in the input for UTEXAS2.
2. UTEXAS2 is compiled with the additional code given in Section A1.

Usage:

1. Run UTEXAS2 (with or without resistance envelope addition).
2. Rename the output file from UTEXAS2 to a file with extension ".TXR", ie. filename.TXR. Files prepared for GRAPHER will automatically be written out with the following names:

G1.DAT (ground profile)
G2.DAT (first critical circle generated)
G3.DAT (second critical circle generated)
G4.DAT (third ...etc

2. Run GRAPHER using the above .DAT files at the import option. Note that only 10 graphs can be handled by GRAPHER at any one time. However, this is not normally a limitation because an adequate resistance envelope can usually be generated using 6 or 7 critical circles, if the selection of the input range of nominal shear strengths is appropriate.

A1.6 SUPPLEMENTARY PROGRAM TO UTEXAS2, FOR RESISTANCE ENVELOPE GRAPHICS

The following program, TXSUM, reads the output file(s) from UTEXAS2 (compiled using the additional code in Section A1.2) and prepares a summary file containing the average normal effective stress and average shear stress for each critical circle found. As many UTEXAS2 output files as desired, can be combined for presentation on a common resistance envelope. The resulting file is in a suitable format for input to the program HARVARD GRAPHICS. This displays all critical circles with data point symbols differentiating between individual slopes.

Usage:

1. Run UTEXAS2 as in Section A1.3
2. Run TXSUM. Prompts request the file names for input.

The output filename is displayed on completion. The output file is formatted for HARVARD GRAPHICS. Import, view and plot.

A1.7 SUPPLEMENTARY PROGRAM TO UTEXAS2, FOR GENERAL DESIGN OF CUT OR FILL SLOPES

Where a single soil type with low watertable, linear Mohr Envelope and simple geometry is involved, chart solutions may be used for slope design. In more general situations, the determination of the optimum slope angle to comply with a specified safety factor is a time consuming process, particularly where a parametric study is required.

The following program TXDESIGN carries out the iterative calculations and generates a file for viewing and producing a hard copy plot of the slope design with HARVARD GRAPHICS. The same program may be used either for generation of general charts for preliminary design or for optimisation of final slope design for a specified section, ie once subsurface conditions are known for a specific site and the location of the toe of batter fixed, the design slope with geometry for minimum earthworks at any specified safety factor may be generated automatically.

Usage:

- (i) For general design: Prepare the slope analysis data to meet all requirements of the UTEXAS2 user manual, but the topography must be defined by PROFILE LINE No. 1. This must be described by at least 3 pairs of coordinates (Points A, B and C). These three points must be the last 3 in the input list. The toe of the batter will be placed at Point A, taken to be fixed. Point B (moveable) is taken at the top of batter, and the vertical height between A and B is taken as the highest batter to be considered. Points B and C will be used as starting values, but thereafter both will be lowered progressively during the general design process. It is therefore necessary to check the design to see that definitions of other profiles lines and piezometric lines always remain valid (eg piezometric levels for unconfined aquifers should never rise above the ground). The coordinates of Point C are used to calculate the grade of the natural ground above the batter (from the slope of line BC) and C is also used to define the maximum x coordinate to be used. A check is required to confirm that critical circles are contained within the defined geometry rather than coincident with either limit, as such profiles may exclude base failures. For specific design: As for general design except that point C is regarded as fixed (a point on the existing cross section beyond which cutting is unlikely to be economic). The existing slope angle is defined by the inclination of BC and point B is optimised to find the minimum cut volume for the specified safety factor.

(ii) Execute TXDESIGN. Values will be prompted for -

1. input filename
2. design safety factor (1.4 by default)
3. convergence criteria for safety factor (2% by default)
4. lowest vertical height of batter required (2 m default)
5. watertable option (input file values by default)
6. general or specific design (general by default)

Recommended safety factors are those from GCO (Tables 5.1 - 5.4) unless higher values are nominated by the client.

The watertable options are -

- (a) that defined in the UTEXAS2 input (no check is made)
- (b) a nominated watertable gradient from the toe of the batter (in which case a check is made to see that the watertable remains below the ground profile as the height is reduced)

(iii) View the TXDESIGN output file using HARVARD GRAPHICS and plot. This shows the maximum allowable slope of batter as a function of vertical height, for the specified safety factor and slope conditions.

(iv) Check before adopting:

- (a) validity of input and output files generated, including -
- (b) location of critical circles and number of slices analysed
- (c) possibility of more than 1 local minimum factor of safety
- (d) reasonableness of design against precedents (field observations)
- (e) groundwater assumptions during and after construction.
- (f) effects of near surface saturation during rainfall
- (g) whether superficial erosion protection needs will govern design
- (h) potential for, and implications of, progressive failure
- (i) damage or blockage potential (using residual strength parameters)
- (j) any other criteria (external loading, seismic acceleration etc)

A1.8 EXAMPLE OUTPUTS

Trial circles plotted from Grapher:

Resistance Envelopes

General Slope Design Charts

CRITICAL FAILURE SURFACES

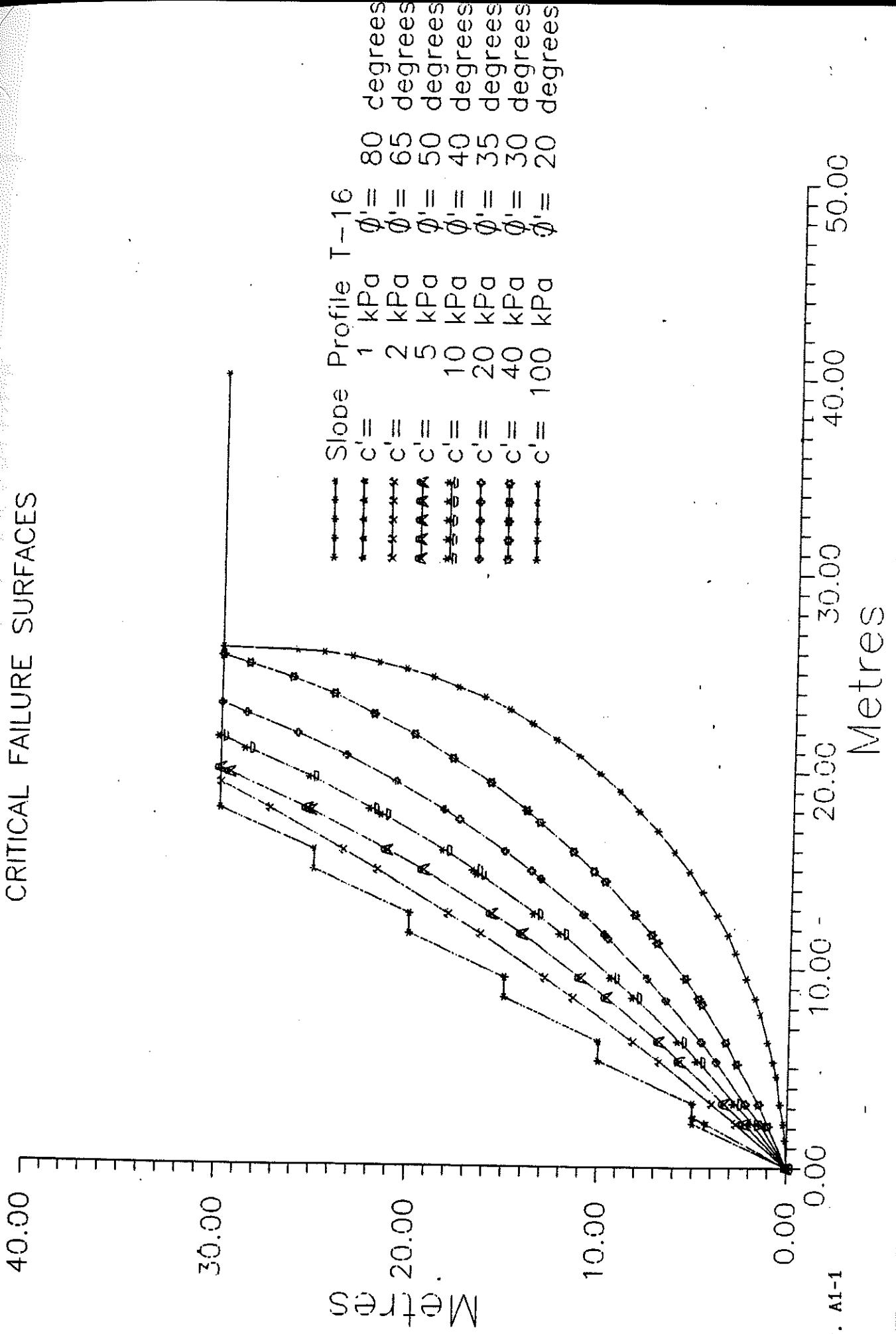
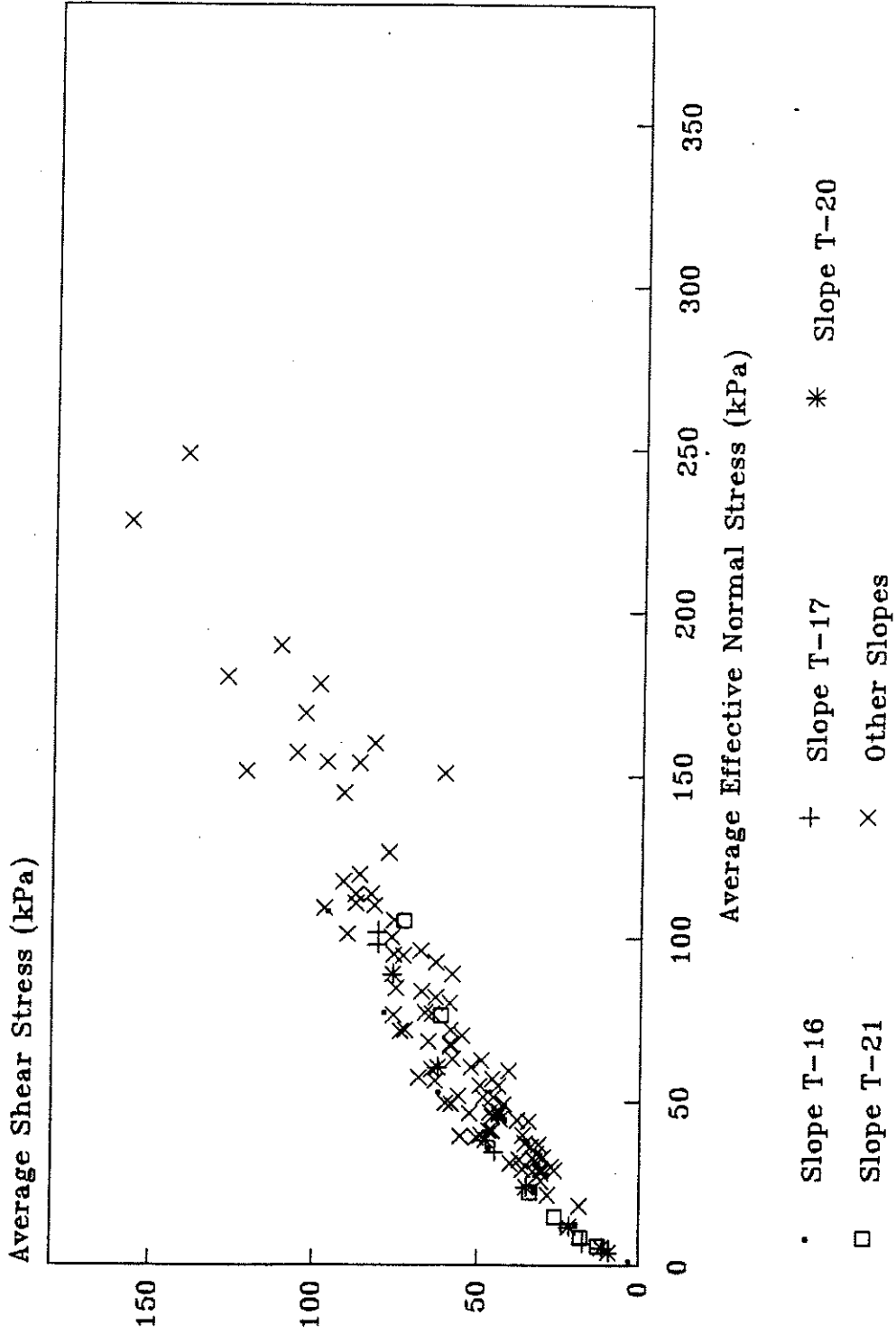


Fig. A1-1

CASAGRANDE RESISTANCE ENVELOPE

Weathered granite, Geotechnical Unit A



Cht CR1

Fig. A1-2

CASAGRANDE RESISTANCE ENVELOPE

Weathered granite, Geotechnical Unit A

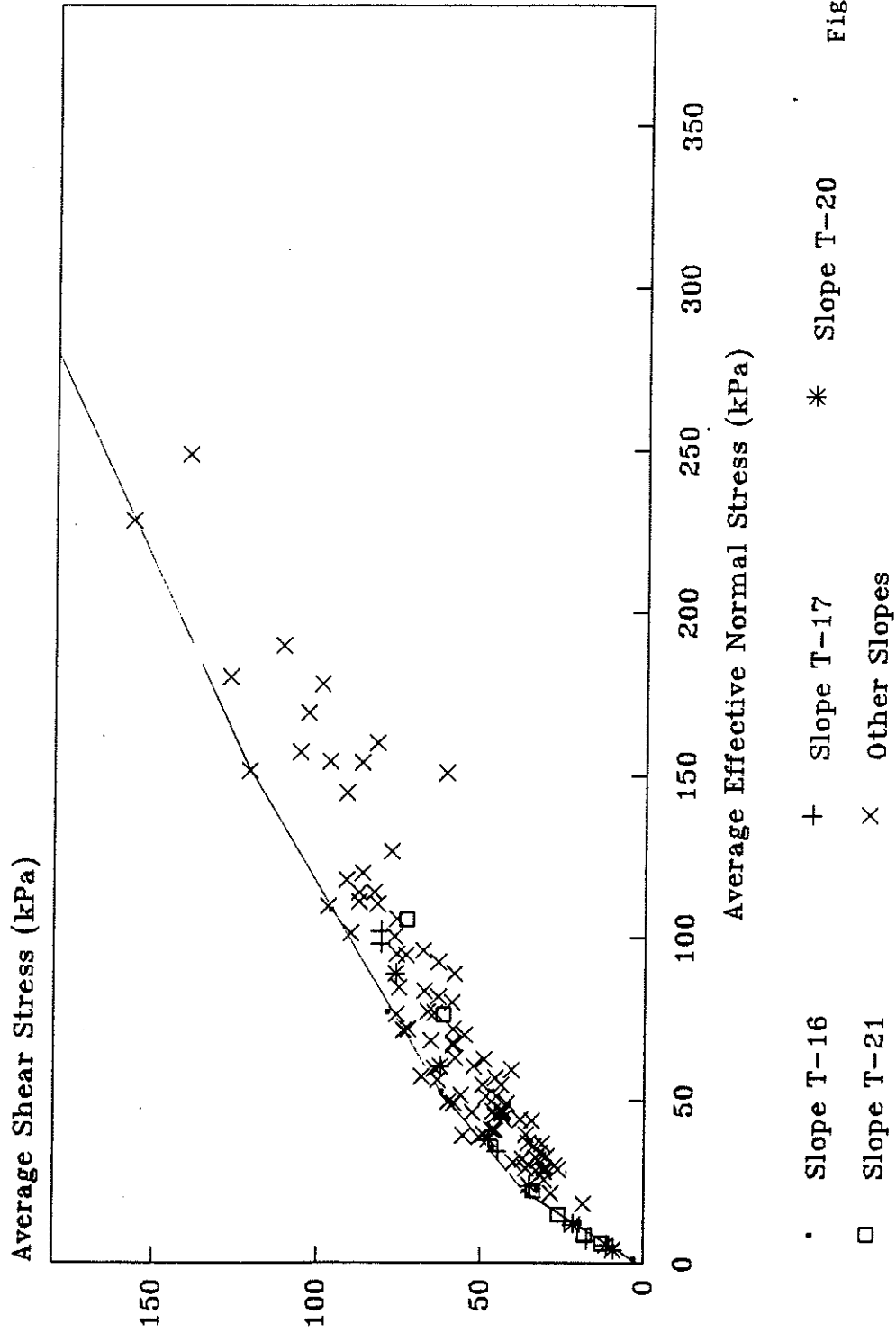


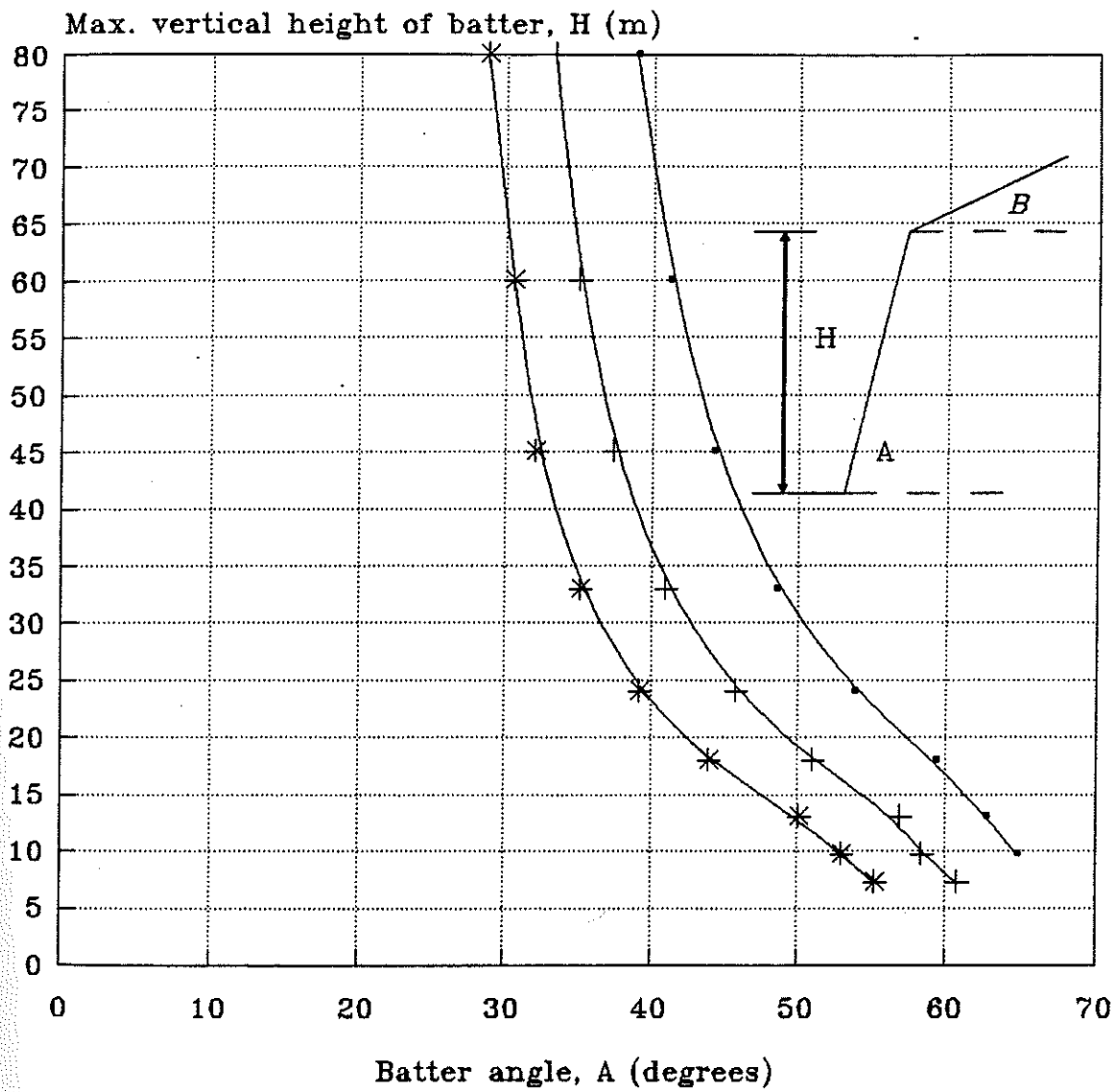
Fig. A1-3

Cht CR1

SLOPE DESIGN FOR CUTS

Geotechnical Unit A

Well drained in situ cut slopes



—●— Factor of safety=1.1 —+— Factor of safety=1.3
 —*— Factor of safety=1.5

Fig. A1-4

Cht DS1F0S

A1.9 RECOMMENDED FACTORS OF SAFETY FOR SLOPE DESIGN

**SOURCE: GEOTECHNICAL MANUAL FOR SLOPES
GEOTECHNICAL CONTROL OFFICE
HONG KONG (G.C.O. 1984)**

Table 5.1 - Recommended Factors of Safety for New Slopes for a Ten-year Return Period Rainfall

RISK TO LIFE		Recommended Factor of Safety against Loss of Life for a Ten-year Return Period Rainfall		
		Negligible	Low	High
Recommended Factor of Safety against Economic Loss for a Ten-year Return Period Rainfall	ECONOMIC RISK			
	Negligible	>1.0	1.2	1.4
	Low	1.2	1.2	1.4
High	1.4	1.4	1.4	

- Note : (1) In addition to a factor of safety of 1.4 for a ten-year return period rainfall, a slope in the high risk-to-life category should have a factor of safety of 1.1 for the predicted worst groundwater conditions.
- (2) The factors of safety given in this Table are recommended values. Higher or lower factors of safety might be warranted in particular situations in respect of economic loss.

Table 5.2 - Typical Examples of Slope Failures in Each Risk-to-Life Category

Example	Risk to Life		
	Negligible	Low	High
(1) Failure affecting country parks and lightly used open-air recreation areas.	✓		
(2) Failures affecting roads with low traffic density.	✓		
(3) Failures affecting storage compounds (non-dangerous goods).	✓		
(4) Failures affecting densely used open spaces and recreational facilities (e.g. sitting-out areas, playgrounds, car parks).		✓	
(5) Failures affecting roads with high vehicular or pedestrian traffic density.		✓	
(6) Failures affecting public waiting areas (e.g. railway platforms, bus stops, petrol stations).		✓	
(7) Failures affecting occupied buildings (e.g. residential, educational, commercial, industrial).			✓
(8) Failures affecting buildings storing dangerous goods.			✓

Table 5.3 - Typical Examples of Slope Failures in Each Economic Risk Category

Example	Economic Risk		
	Negligible	Low	High
(1) Failures affecting country parks.	✓		
(2) Failures affecting rural (B), feeder, district distributor and local distributor roads which are not sole accesses.	✓		
(3) Failures affecting open-air car parks.	✓		
(4) Failures affecting rural (A) or primary distributor roads which are not sole accesses.		✓	
(5) Failures affecting essential services which could cause loss of that service for a temporary period (e.g. power, water and gas mains).		✓	
(6) Failures affecting rural or urban trunk roads or roads of strategic importance.			✓
(7) Failures affecting essential services, which could cause loss of that service for an extended period.			✓
(8) Failures affecting buildings, which could cause excessive structural damage.			✓

Note : These examples are for guidance only. The designer must decide for himself the degree of economic risk and must balance the potential economic risk in event of a failure against the increased construction costs required to achieve a higher factor of safety.

Table 5.4 - Recommended Factors of Safety for the Analysis of Existing Slopes and for Remedial and Preventive Works to Slopes for a Ten-year Return Period Rainfall

Risk to Life	Recommended Factor of Safety Against Loss of Life for a Ten-year Return Period Rainfall		
	Negligible	Low	High
	> 1.0	1.1	1.2

Note : (1) These factors of safety are minimum values to be used only where rigorous geological and geotechnical studies have been carried out, where the slope has been standing for a considerable time, and where the loading conditions, the groundwater regime and the basic form of the modified slope remain substantially the same as those of the existing slope.

(2) Should the back-analysis approach be adopted for the design of remedial or preventive works, it may be assumed that the existing slope had a minimum factor of safety of 1.0 for the worst known loading and groundwater conditions.

(3) For a failed or distressed slope, the causes of the failure or distress must be specifically identified and taken into account in the design of the remedial works.

A1.10 PROGRAM SOURCE CODES

PROGRAM UTEXAS

```
cls:print:print"TB Program UTEXAS, to run UTEXASR as a child process
print"UTEXASR includes data for Resistance Envelopes in the .TXR output file
print"    and a summary of stresses in the output file .SUM
print"
print"Any files named 'INPUT' or 'OUTPUT' in this directory will be deleted
input"Type input filename (.TEX extension assumed);fin$
f1out$ = fin$ + ".TXR":f2out$ = fin$ + ".SUM":fin$ = fin$ + ".TEX"
open fin$ for input as #1
ftemp$ = "INPUT":open ftemp$ for output as #2
while not eof(1)
  line input #1, t$:print #2, t$
wend
close
SHELL "UTEXASR.EXE"
gosub cursor
fin$ = "OUTPUT":open fin$ for input as #1
open f1out$ for output as #2:rem open f2out$ for output as #3
while not eof(1)
  line input #1, t$:print #2, t$
wend
end

cursor:
cursorx = pos:cursory = csrlin
locate (cursory+2),1,1,0,13
return
```

PROGRAM TXSUM

```
cls:Print"TB Program TXSUM to extract resistance envelope data generated
print" from TEXASR
dim avsigma(300), avtau(300)
input"Type first filename to process (.TXR extension assumed) ";fin$
slope = 1
fout$ = fin$ + ".TXS":fin$ = fin$ + ".TXR"
open fin$ for input as #1:open fout$ for output as #2
print #2,"File ", fout$:rem , " from UTEXASUM: AVESIGMA AVTAU AVTSIGMA ";
rem print #2," X Y R FOS COHESION PHI DENSITY & METHOD
gosub process
gosub extrafiles
gosub hgfile
print
print "Completed summary for Resistance Envelope with output on file ";fout$
end

process:
while not eof(1)
  gosub storelast
  line input #1, t$
  if left$(t$,40) = "          Unit weight of material =" then gosub unit
  if left$(t$,40) = "***** FINAL CRITICAL CIRCLE IN" then gosub xyx
  if left$(t$,40) = "PARAMETERS FOR CASAGRANDE RESI" then gosub stress
wend
return

extrafiles:
print"For output filing purposes, enter the number of slope files wanted
input" (1 will put all data on one file, so only one symbol can be used) ";symbols
print
nextfin$ = "a"
while nextfin$ > < ""
  print"Type next filename to process (.TXR extension assumed) "
  if slope=symbols then gosub warning
  input" or enter nul to end ";nextfin$
  close #1:if nextfin$ = "" then exit loop
  fin$ = nextfin$ + ".TXR":open fin$ for input as #1
  slope = slope + 1: gosub process
wend
return

warning:
Print"***** WARNING*****";symbols; "was limit imposed."
print" All subsequent entries will use the same symbol in Harvard Graphics "
return
```

```

storelast:
tt$(0)=t$:for i=3 to 1 step -1:tt$(i)=tt$(i-1):next i
return

```

```

unit:
print"Executing subroutine unit"
density=val(mid$(t$,41))
for i=1 to 3:line input #1, t$:next i
cohesion=val(mid$(t$,41))
line input #1,t$:phi=val(mid$(t$,41,6))
print"Density, cohesion and phi are: ";density,cohesion,phi
return

```

```

xyr:
print "Executing subroutine xyr"
line input #1, t$:x=val(mid$(t$,47))
line input #1, t$:y=val(mid$(t$,47))
line input #1, t$:r=val(mid$(t$,47))
line input #1, t$:fos=val(mid$(t$,47))
line input #1, t$:sideforceincl=val(mid$(t$,47))
print"x y r and FOS are ";print using "#####.###";x,y,r,fos
return

```

```

stress:
numvals=numvals+1
Print "Executing subroutine stresses
numslices=val(left$(t$,15))
line input #1,t$:avtsigma=val(mid$(t$,51))
line input #1,t$:avesigma(numvals)=val(mid$(t$,51))
line input #1,t$:avtau(numvals)=val(mid$(t$,51))
line input #1,t$:method$=mid$(t$,10)
print method$
hglimit=slope:if hglimit>symbols then hglimit=symbols
avesigma(numvals)=.01*int(100*avesigma(numvals))+ (hglimit)/10000
avtau(numvals)=.01*int(100*avtau(numvals))+ hglimit/10000
if numvals>1 then gosub sortstress
gosub xprint
return

```

```

xprint:
print:print "SUMMARY"
p r i n t u s i n g
"#####.###";avesigma(numvals),avtau(numvals),avtsigma,x,y,r,fos,cohesion,phi,density,
print " ", method$
rem print #2, " ",method$
return

```

```

sortstress:
print "Sorting ",numvals," ....."
for i=int(numvals) to 2 step -1
  if avesigma(i) < avesigma(i-1) then
    swap avesigma(i), avesigma(i-1)
    swap avtau(i), avtau(i-1)
  print
end if
next i
return

hgfile:
for i=1 to numvals
  nspace=int(100*(100*avesigma(i)-int(100*(avesigma(i))))+.1)
  if nspace > 40 then nspace=0
  print #2, using "#####.###";avesigma(i);
  print #2," ";
  for j=2 to nspace: print #2, "      ",":next j
  print #2, using "#####.###";avtau(i)
next i
return

```

PROGRAM TXGRAPH

```

cls:Print"TB Program TXGRAPH to view profile and critical arcs found
print" after using UTEXASR for resistance envelopes.
dim g$(1000)
input"Type filename to process (.TXR extension assumed) ";fin$
fout$=fin$+".HGD":fin$=fin$+".TXR"
open fin$ for input as #1:open fout$ for output as #2
print #2,"File "; fout$;" from UTEXASR
print #2,"Slope profile and arcs
xlast=-999:ycirclelast=-999:x1=-999:y1=-999
while not eof(1)
  line input #1, t$
  if t$= "      * NEW PROFILE LINE DATA *" then gosub profile1
  if t$= "      TABLE NO. 19" then gosub table19
wend
close
gosub sorter
print"Completed and ready for HG with file ";fout$
end

profile1:
for i=1 to 7:line input #1,t$:next i
print"Ground profile found: "

```



```

while not eof(1)
input #1,t,x,y
if t>0 then
print #2, using "#####.##";x,y
print using "#####.##";x,y
else
exit loop
end if
wend
return

```

```

table19:
flag1=0:circles=circles+1
for i=1 to 8: line input #1,t$:next i
input #1,x,ycircle:gosub circleprint
for i=1 to 1000
line input #1,t$
if val(left$(t$,5))=1 then exit for
input #1, x,ycircle
gosub circleprint
next i
return

```

```

circleprint:
if x=xlast and ycircle=ycirclelast then
circles=circles-1
RETURN
end if
if circount+1=circles then
if circles>1 then
if xmissed>xlast and ymissed<ycirclelast then gosub xcprint
end if
print "Circle found is number ";circles
circount=circount+1
end if
rem if x=x1 and ycircle=y1 then print x1,y1:circles=circles-1:RETURN
smoother=int(3+circles/2)
if flag1=0 then counter=0: rem checking if first point on circle
if flag1>0 then counter=counter+1
if int(counter/smoother)<>counter/smoother then
xmissed=x:ymissed=ycircle:flag1=1:RETURN
end if
gosub xcprint:
return
xcprint:
print #2, using "#####.##";x,

```

```

for j=1 to circles:print #2,"      ",:next j
print #2, using "#####.#";ycircle
print using "#####.#";x,ycircle
xlast=x:ycirclelast=ycircle
return

```

```

sorter:
print "Sorting....."
open fout$ for input as #1
input #1,t1$,t2$
input #1,g$(1):i=1
while not eof(1)
  i=i+1
input #1, g$(i):t=val(left$(g$(i),10))
for j=i to 2 step -1
  if t<val(left$(g$(j-1),10)) then swap g$(j),g$(j-1) else exit for
next j
wend
close #1
open fout$ for output as #1
print #1,t1$,t2$
for jj=1 to i:print #1,g$(jj):next jj
close #1
return

```

PROGRAM TXDESIGN

```

cls:print:print"TB Program TXDESIGN, to produce height versus slope inclination
Print" design chart, using UTEXASR.
Print" type 111 at break if change in increment is required.
print"
print"Any files named 'INPUT' or 'OUTPUT' in this directory will be deleted
dim fstart$(100), fstore(100),astore(100)
input"Type input filename for UTEXAS data (.TEX extension assumed)":f1in$
f2out$=f1in$+".TXD":f1in$=f1in$+".TEX"
open f1in$ for input as #1:open f2out$ for output as #2
input"Enter number of points in the PROFILE LINE (default is 3) ";npoints
if npoints>0 and npoints<3 then print "Error, must have at least 3 points:end
if npoint=0 then npoints =3
input"Enter watertable gradient (eg 0.5) or nul to use PZ line in dataset ";wtg
if wtg=0 then
  print "***** Warning ***** Check output data sets: "
  print "Watertable may rise above ground during design, with no error message

```

```

else
  print"Data set must have only one PIEZ LINE, with points on separate lines
end if
input"Enter target factor of safety (default is 1.4) ";targetfos
if targetfos < .01 then targetfos = 1.4
input "Enter convergence criteria (%) for safety factor (default is 2%) ";errp
if errp < .01 then errp = 2
errc = targetfos * errp / 100
input "Enter minimum height of batter to design (default 2 m) ";hmin
if hmin < .1 then hmin = 2
ratioh = 0.07
gosub readindata:close #1
gosub abccoords
call freeinputana(fstart$(analineno + 2),xcircle,ycircle,increment,ylimit)
h = by - ay:arad = atn((by - ay)/(bx - ax)):brad = atn((cy - by)/(cx - bx))
gosub iterations
close #2
end

```

```

abccoords:
for i = 1 to 3
j = (prolineno + npoints + 1 - 2) + i - 1
call freeinput(fstart$(j),tx,ty)
select case i
  case 1
    ax = tx:ay = ty
  case 2
    bx = tx:by = ty
  case 3
    cx = tx:cy = ty:xmax = cx
end select
next i
return

```

```

sub freeinput(tq$,tx,ty)
if tq$ = "" then print "Free input error ":end
k = 1:tq$ = tq$ + " "
while k < 1000 and (mid$(tq$, k, 1)) = " ": k = k + 1:wend:start1 = k
while k < 1000 and mid$(tq$, k, 1) > < " ": k = k + 1:wend:end1 = k
tx = val(left$(tq$, end1)):ty = val(mid$(tq$, end1))
end sub

```

```

sub freeinputana(t$,xcircle,ycircle,increment,ylimit)
if t$ = "" then print "Free input error ":end
k = 1:t$ = t$ + " "
while (mid$(t$, k, 1)) = " ": k = k + 1:wend:start1 = k
while mid$(t$, k, 1) > < " ": k = k + 1:wend:xcircle = val(left$(t$, k))

```

```

while mid$(t$,k,1) = " ":k = k + 1:wend:start = k
while mid$(t$,k,1) > < " ":k = k + 1:wend:ycircle = val(mid$(t$,start,(k-start + 1)))
while mid$(t$,k,1) = " ":k = k + 1:wend:start = k
while mid$(t$,k,1) > < " ":k = k + 1:wend:increment% = val(mid$(t$,start,(k-start + 1)))
while mid$(t$,k,1) = " ":k = k + 1:wend:start = k
while mid$(t$,k,1) > < " ":k = k + 1:wend:ylimit = val(mid$(t$,start,(k-start + 1)))
end sub

```

readindata:

```
inlines = 0:readingprofile = 0
```

```
while not eof(1)
```

```
  inlines = inlines + 1
```

```
  line input #1, fstart$(inlines)
```

```
  if left$(fstart$(inlines),4) = "PROF" or fstart$(inlines) = "PROFILE LINES" then
```

```
    prolineno = inlines
```

```
    readingprofile = 1
```

```
  end if
```

```
  if left$(fstart$(inlines),3) = "ANA" or fstart$(inlines) = "ANALYSIS" then
```

```
    analineno = inlines
```

```
  end if
```

```
  rem find first piez. 1
```

```
  if left$(fstart$(inlines),3) = "PIE" and lastpzline = 0 then
```

```
    if wtg > 0 then
```

```
      pzlineno = inlines:lastpzline = 999
```

```
    end if
```

```
  end if
```

```
  if lastpzline = 999 and len(fstart$(inlines)) < 3 then
```

```
    lastpzline = inlines - 1:rem now find x value at point A
```

```
    for i = pzlineno + 2 to lastpzline
```

```
      call freeinput(fstart$(i),tx,ty)
```

```
      if tx >= ax then lastvalidpz = i - 1:exit for
```

```
    next i
```

```
  end if
```

```
wend
```

```
return
```

iterations:

```
while tan(arad) < 100
```

```
  its = its + 1:rem print "Number of different batter heights = ";its
```

```
  if hitkey > 0 then print "Hit any key to interrupt":hitkey = 1
```

```
  if inkey$ > < "" then input "Hit enter to continue or 999 to quit ";t$
```

```
  if val(t$) = 999 then end
```

```
  if val(t$) = 111 then
```

```
    input "Enter increment as a percentage (of batter height) ";percenth
```

```
    ratioh = percenth / 100
```

```
  end if
```

```
  foserr = 100:heightstatus = 0
```

```

while abs(foserr) > errc
  if foserr = 100 then aits = 1 else aits = aits + 1
  if inkey$ > < "" then input "Hit enter to continue or 999 to quit "; t$
  if val(t$) = 999 then end
  gosub writeinputdata
  print "Executing UTEXASR ....."
  SHELL "UTEXASR.EXE"
  gosub cursor
  rem utexasr is fortran program producing file OUTPUT
  gosub readoutput
  print "  H    A    xc    yc    r    FOS slices increment H its A its"
  print using "#####.###"; h; 180*arad/3.14; xc; yc; r; fos; ncm1; increment; its; aits
  if FOS = 0 then print "FOS is zero in OUTPUT - aborted. ": end
  if ncm1 < 8 then
    print "Warning number of slices is only "; ncm1
    input "Hit <Enter> to continue or 999 to end"; t$
    if val(t$) = 999 then end
  end if
  foserr = fos - targetfos
  if tan(arad) > 100 then
    print "Fos greater than target for height of "; int(h)
    heightstatus = 1
    EXIT LOOP
  end if
  if abs(foserr) > = errc then
    aradmax = 1E10; aradmin = 0; storedarad = storedarad + 1
    fstore(storedarad) = fos; astore(storedarad) = arad
    if storedarad = 1 then
      arad = atn(tan(arad)*fos/targetfos)
    else
      i = storedarad
      if fstore(i) - fstore(i-1) = 0 then
        print "No change in value of f.o.s. enter new trial angle ";
        input " or type 999 to end"; a
        if a = 999 then end
        arad = a*3.1417/180
      else
        mgradient = (tan(astore(i)) - tan(astore(i-1))) / (fstore(i) - fstore(i-1))
        arad = atn(tan(astore(i)) + mgradient*(targetfos - fstore(i)))
      end if
    end if
  end if
end if
wend
if heightstatus = 1 then EXIT LOOP
print #2, using "#####.###"; (180/3.1416)*arad, h, fos, xc, yc, r, ncm1, increment, its, aits
for i = 1 to 100: fstore(i) = 0; astore(i) = 0; next i: storedarad = 0
hlast = h

```

```

h=.75*h
if h > 10 then h=int(h)
if h < 10 then h=0.1*int(h*10)
if h < hmin then END
wend
return

writeinputdata:
chec=0
fitemp$="INPUT":open fitemp$ for output as #3
for i=1 to prolineno+1+npoints-2:print #3, fstart$(i):next i
if arad=0 then print"Error arad 0":end
by=ay+h:bx=ax+h/tan(arad)
if bx>cx-h/200 then bx=cx-h/200:print"Warning - cannot meet FOS extend x"
print #3, using "#####.###"; bx; by
cx=xmax:cy=by+tan(brad)*(cx-bx):rem define these
print #3, using "#####.###"; cx; cy
if wtg=0 then
  for i=prolineno+npoints-3+5 to analineno+1:print #3, fstart$(i) : next i
else
  for i=prolineno+npoints-3+5 to lastvalidpz:print #3, fstart$(i):next i
  gosub printwater
  for i= lastpzline+1 to analineno+1:print #3,fstart$(i): next i
end if
increment=h*ratioh+.1
print #3, using "#####.###";xcircle ,ycircle,increment,ylimit
for i=analineno+3 to inlines:print #3, fstart$(i): chec=1
next i
close #3
if chec=0 then print "error writeinputdata":end
return

printwater:
print #3, ax,ay
if wtg >= tan(arad) then print #3, bx,by: print #3, cx,cy:return
rem find where water rises above ground
for xground=ax+h/200 to cx step h/200
  yintercept=cy-cx*tan(brad):yground=yintercept+tan(brad)*xground
  ywater=ay+xground*wtg
  if ywater>yground then exit for
next xground
if cx-xground>h/50 then print #3,xground,ywater
print #3, cx,ywater
return

```

newdata:

arad = atn(hlast*tan(arad)/h)

return

cursor:

cursorx = pos: cursory = csrlin

if cursory > 22 then cls: cursory = 0

locate (cursory+2), 1, 1, 0, 13

return

readoutput:

flin\$ = "OUTPUT": open flin\$ for input as #1

gosub process

close #1

return

process:

while not eof(1)

 gosub storelast

 line input #1, t\$

 if left\$(t\$, 40) = "

***** FINAL CRITICAL CIRCLE IN" then gosub xyr

 if left\$(t\$, 40) = "

PARAMETERS FOR CASAGRANDE REST" then gosub stress

wend

return

xyr:

line input #1, t\$: xc = val(mid\$(t\$, 47))

line input #1, t\$: yc = val(mid\$(t\$, 47))

line input #1, t\$: r = val(mid\$(t\$, 47))

line input #1, t\$: fos = val(mid\$(t\$, 47))

line input #1, t\$: sideforceincl = val(mid\$(t\$, 47))

return

storelast:

tt\$(0) = t\$: for i = 3 to 1 step -1: tt\$(i) = tt\$(i-1): next i

return

stress:

numvals = numvals + 1

numslices = val(left\$(t\$, 15))

for ii = 1 to 4: line input #1, t\$: next ii

method\$ = mid\$(t\$, 10): ncm1 = val(right\$(t\$, 4))

return

APPENDIX 2

COMPUTER PROGRAM FOR THE PREDICTION OF GROUNDWATER RESPONSE TO RESERVOIR FILLING, INCLUDING SAFETY FACTOR CHANGES

A2.1 INTRODUCTION

This appendix provides the source code listing of the regional groundwater and slope stability analysis program LSFLOW. Also included is an outline of field requirements for obtaining input parameters, data preparation, and output presentation. A working knowledge of geohydrological modelling principles and programming familiarity is assumed as this has been found to be the only way to accommodate the large variety of situations encountered in practice, where each new case seems to present some non-standard aspect. All programs are in modular form to allow modifications to be made readily.

A2.2 INPUT DATA PREPARATION

A2.2.1 Field Procedures and Interpretation.

Drill core and penetration characteristics.

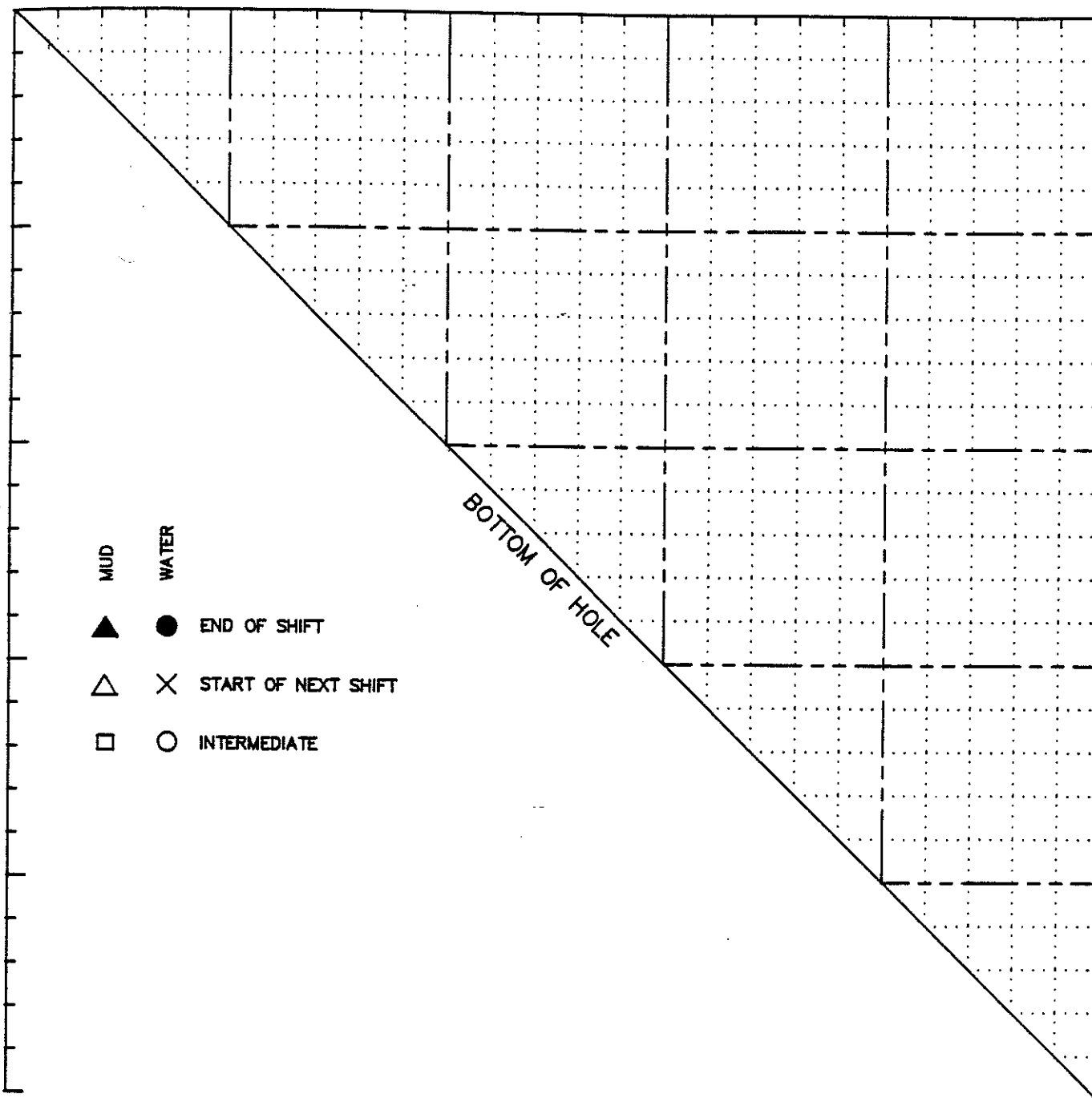
Where core is recovered, the location of aquicludes (eg gouge zones) can be readily inferred. However gouges are often washed away. The driller's comments are therefore of particular significance for each section of lost core. Rate of bit penetration and changes in colour or nature of fluid return are the main indicators. Other reasons for lost core (eg inner tube mis-latch) require the driller's inference regarding the nature of unrecovered material.

Drilling fluid level record.

The drilling fluid level record is the prime means of locating both confined and unconfined aquifers. All holes are initially drilled with water only, until conditions dictate otherwise. Readings are taken before and after each substantial break in drilling activity, ie lunch break and overnight in particular but also at any other opportunities. Before drilling commences at the start of any shift, the readings are evaluated to determine whether aquifer testing is appropriate at that stage. The standard procedure for recording is on both the driller's record and on the drillhole depth versus fluid level depth plot (Fig. A2-1). These record: depth of drillhole, depth of drill bit, depth of casing shoe bit, fluid type, grouted intervals, fluid level at end of last shift, fluid level at beginning of new shift and % fluid return.

DEPTH OF HOLE
(metres)

DEPTH TO FLUID
(metres)



- | | | |
|-----|-------|---------------------|
| MUD | WATER | |
| ▲ | ● | END OF SHIFT |
| △ | × | START OF NEXT SHIFT |
| □ | ○ | INTERMEDIATE |

EXPLANATION

- CASING
- ▼ UNCONFINED WATER TABLE
- ▲ CONFINED WATER TABLE
- ▣ PIEZOMETER SAND POCKET

PROJECT:

DRILLHOLE:

ORIGINAL
SCALE:

LOCATION:

DRILLING FLUID LEVEL RECORD

Fig. A2-1

Aquifer testing.

Where any indications of perched or confined aquifers are noted, response testing is carried out before drilling proceeds, to confirm that water pressure equalisation has been achieved. The alternatives are bailing or rod withdrawal, (accompanied by regular fluid level readings) followed by pump in or rod replacement. The rising and falling limits then establish the bounds of the aquifer head over that interval.

Piezometer installation and positioning

Appropriate positioning of piezometer tips can be rationally decided only from inspection of the fluid level record plot and results of aquifer testing. In general, at least 3 piezometers are installed to confirm expectations in a simple inclined perched aquifer situation: one on either side of the aquiclude and the third close to the phreatic surface. This will (i) confirm the location of a horizon where the shear to normal effective stress ratio is at a minimum, and (ii) allow determination of the aquifer gradient. If 19 mm steel conduit is used, 5 or more Casagrande piezometers can be inserted fairly readily where HW casing has been installed. If an inclinometer is required, (53 mm) all joints are effectively sealed and the tip is used to double as a Casagrande piezometer and usually 2 other 19 mm piezometer tubes can be accommodated also, at higher levels. The permeable filter pockets (containing the piezometer ports) should be located as close as practical to, but not within, any aquiclude on which critical pore pressures are expected to act, and the aquiclude itself must be effectively re-sealed to prevent local aberration of measured pressures from representative values on either side.

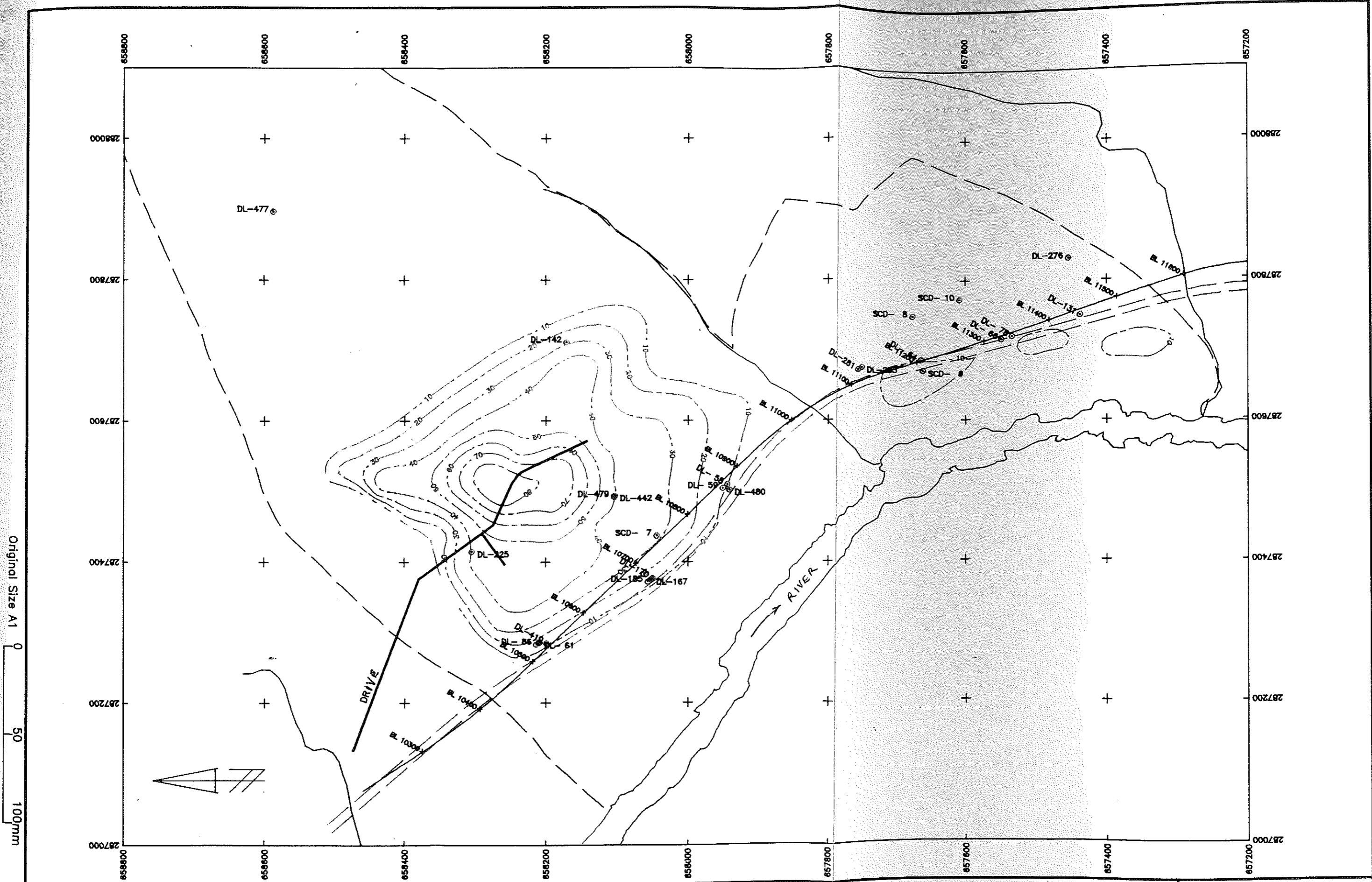
Piezometer as-built.

There are always difficulties in achieving the desired positions of filter pockets and seals. An as-built with relevant comments on effectiveness of seals is essential for assurance.

Piezometer response testing and interpretation.

Pump-in and preferably bail-out tests are required to determine permeability and check the reliability and response times of all piezometers. These plus longer term readings confirm when equalisation has taken place, at which time meaningful readings can be adopted. Interpretation of aquifers relies heavily on the drillhole depth/fluid level depth plot for initial positioning of piezometers at relevant locations. Usually the pattern on the depth/depth plot will show repeated (start-shift) fluid levels at a specific level, followed by a step decrease or rise in fluid levels as an aquiclude is penetrated. In substantially thick sloping aquifers on hillsides, the piezometric levels in each aquifer will tend to decrease as the drillhole is deepened, as equipotentials will be inclined downslope rather than vertical. Assuming all flow lines are practically parallel (homogeneous isotropic permeability), then because equipotentials will be orthogonal to the flow lines, the piezometric gradient ($\tan\alpha$) in a tabular aquifer is given directly from geometry by:

$$\cos^2\alpha = dy/dl$$



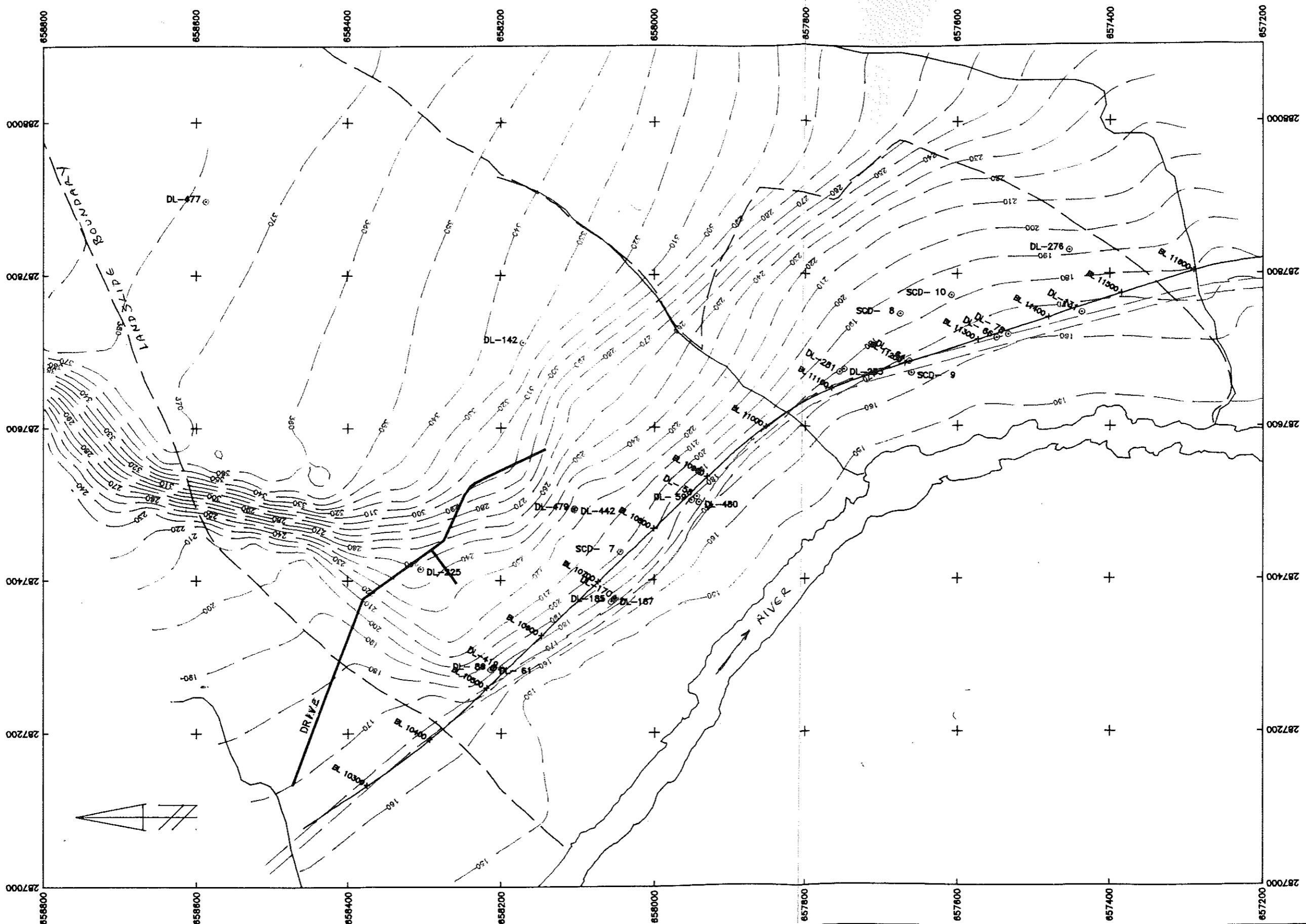
GRAPHIC SCALE
EXPLANATION
Initial net drainable head acting below the basal failure surface.

ORIGINAL SCALE 1:2500
Tr.
Ck.

Fig. A2-2b Regional Model
Initial drainable head

DRWG.NO.	
FILE	Sheet of
REPORT	Date

Original Size A1
 0 50 100mm



GRAPHIC SCALE

ORIGINAL SCALE
 1:2500

EXPLANATION

MODEL DL2AR1 - Sub-basal aquifer, piezometric surface, calibrated to initial conditions.

Tr.
 Ck.

Fig. A2-2a Regional Model
 Initial piezometric surface

DRWG.NO.	
FILE	Sheet of
REPORT	Date

where dy/dl is the inclination of the depth/depth plot (decrease in piezometric level with depth). For an unconfined aquifer, the phreatic surface is found directly from the depth/depth plot by extrapolating readings for that aquifer back to the point where the drillhole depth and fluid level depth are equal. (A correction is needed to account for the effective column of water if the drilling fluid is significantly more dense than water.) The method is particularly good when drilling with air or foam. Drilling with water will usually charge the aquifer to some degree and levels may not stabilise for several weeks. In that case, the same calculation may be applied to any 2 piezometers (installed in the same aquifer), after equalisation.

Slip indicator monitoring.

All Casagrande piezometers provide useful slip indicators. Mandrel sizes of 500, 400, 300, 200 and 100 mm may be lowered successively to determine if deformation from sliding deformation is progressively affecting the tubing.

A2.2.2 Digital Models

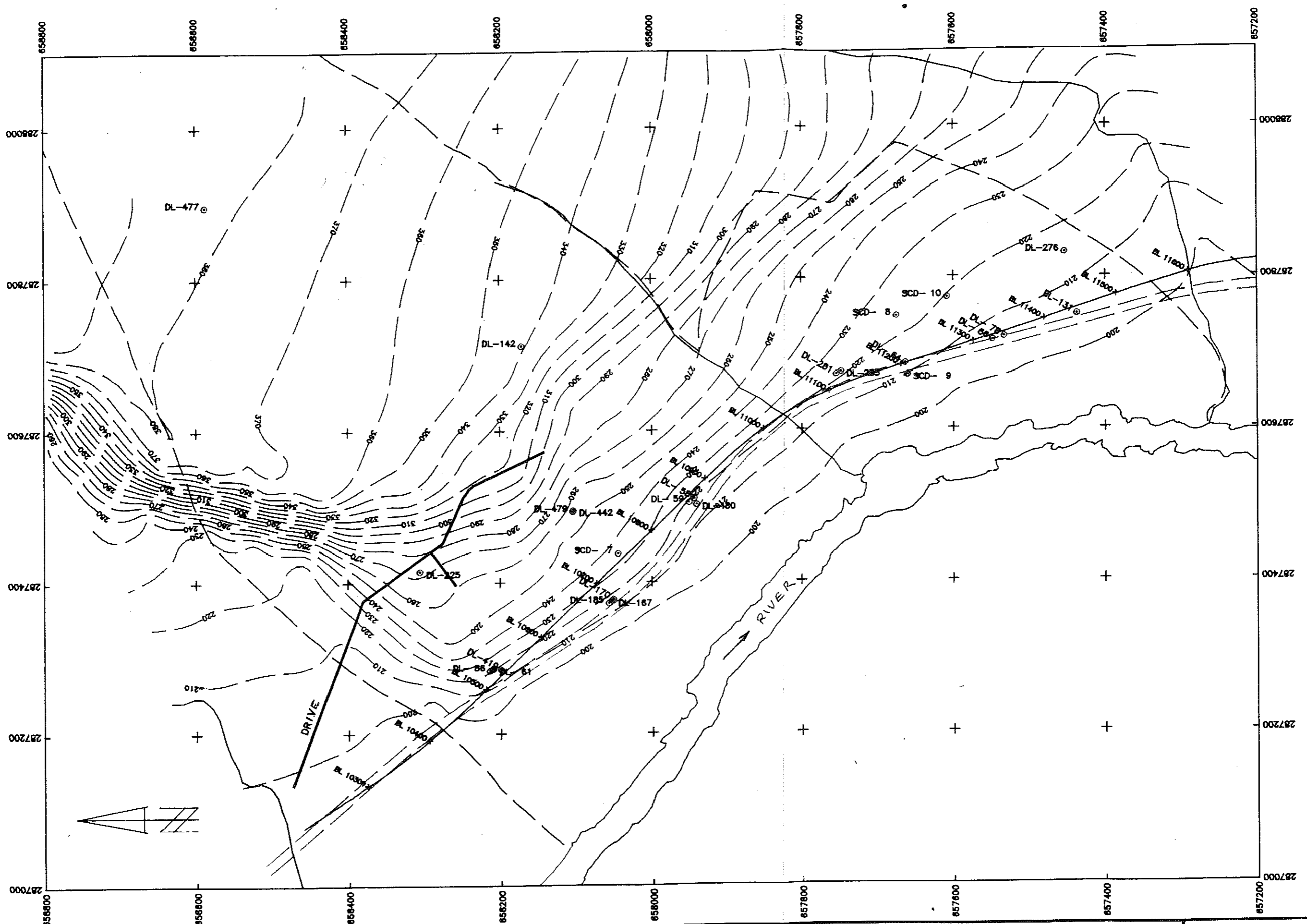
The topography and failure surfaces of specific slides are digitised into standard digital terrain modelling packages, eg TECHBASE (Minesoft Corporation), or SURFER (Golden Software Inc). Input data for topography usually come from 3 alternative sources;

- (i) directly from commercially available files created after aerial photogrammetry,
- (ii) by digitising along contours of a topographic plan or
- (iii) from files of survey coordinates and levels.

Most aquicludes or aquitards used in groundwater modelling, correspond to existing or potential failure surfaces. Input data for failure surfaces are derived by digitising scarps in plan, as well as the geological interpretations on sections. Where failure is not controlled by defects, the expected arcuate rather than planar nature of the surface is modelled through the use of additional (dummy) points at locations where the interpolated contours depart from expectation.

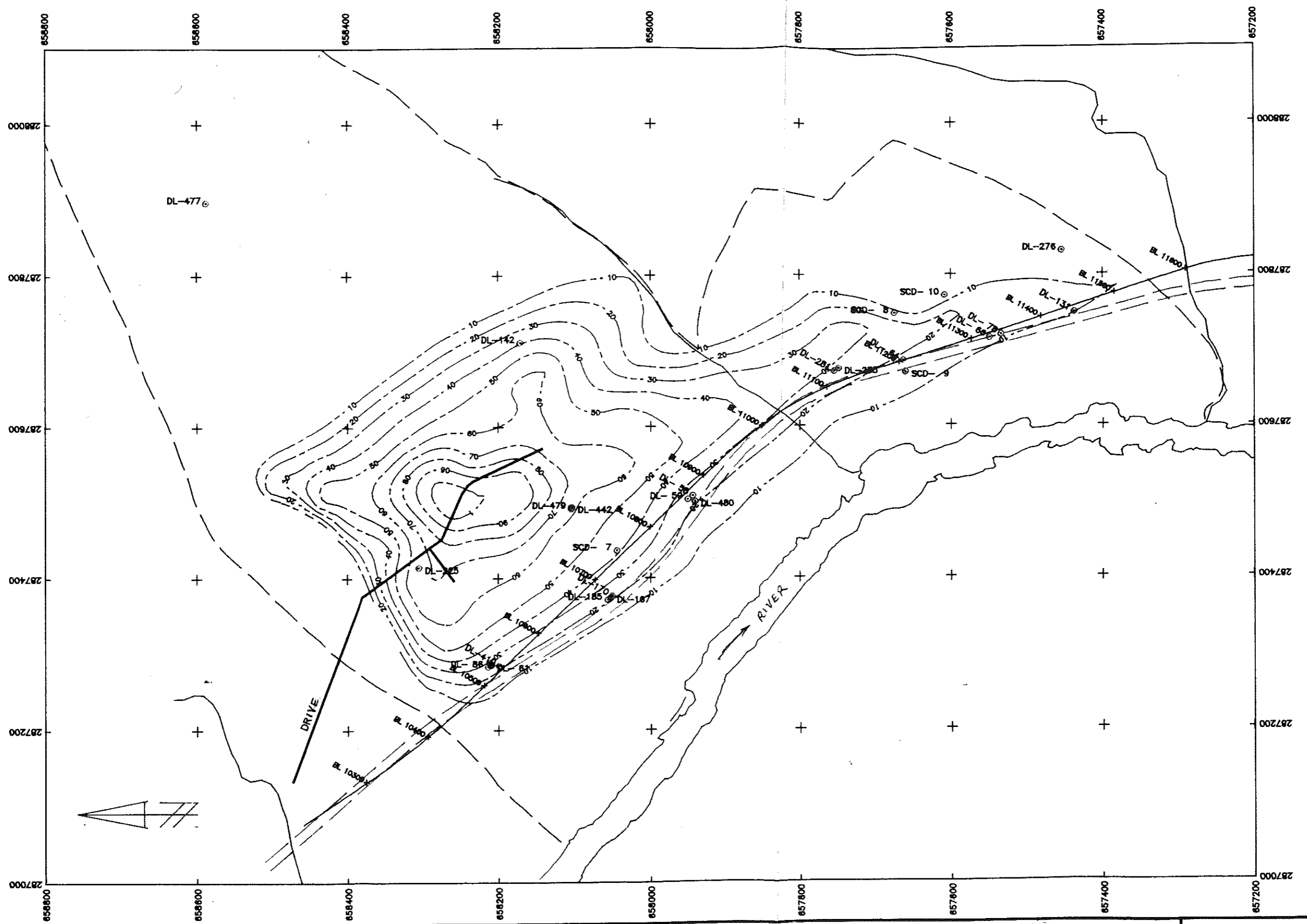
Standard interpolation routines are then used to generate a 10 (or rarely 20 m) grid over each surface, a cell size which adequately defines tracks, roads and other features and is more than adequate for modelling of slides which extend over areas of many hectares. Sampling is then carried out at an appropriate interval (usually 25 to 100 m) for the groundwater model. A model size of about 400 to 800 nodes has been found to offer adequate definition of groundwater surfaces, while still allowing rapid execution and calibration.

Original Size A1 0 50 100mm



GRAPHIC SCALE	ORIGINAL SCALE	Fig. A2-3a Regional Model		DRWG.NO.	
	1:2500			FILE	Sheet of
EXPLANATION	Tr.	Predicted piezometric surface, full pool		REPORT	Date
	Ck.				
<p>MODEL DN_2AR2 - Sub-basal aquifer, predicted full pool piezometric surface assuming no remedial drainage.</p>					

Original Size A1 0 50 100mm



GRAPHIC SCALE

ORIGINAL SCALE
1:2500
Tr.
Ck.

EXPLANATION

--- Predicted full pool net drainable head acting below the basal failure surface assuming no drainage measures.

Fig. A2-3b Regional Model
Predicted net drainable head, full pool

DRWG.NO.	
FILE	Sheet of
REPORT	Date

TECHBASE can output ASCII files with the local model row number, column number and elevation of the specific surface. The file sequence is standardised and readily manipulated to conform with the input sequence for LSFLOW. Miscellaneous programs have been written for file handling, but these could be managed in a number of other ways, (or by hand), so long as the standard input format is generated for the groundwater program.

Program PREFLOW

This preprocessing routine generates the two required input data files for LSFLOW. These are named MESH.DAT and K.DAT.

File MESH.DAT contains the standard input format, namely the standard global node numbering system and gives the relationships for the local node numbering. It also contains default initialising values for some of the expected variables (to maintain consistency with the format of Hunt, 1986). Defaults are overwritten by real values when the main program is executed.

File K.DAT contains the elevations of the upper and lower boundaries of the aquifer at each node and also a section for the subsequent input of aquifer permeabilities (refined during calibration). Subroutines read in the TECHBASE generated files, strip unwanted data and write the elevations of the surfaces to file K.DAT in the form: node number, upper boundary of aquifer, lower boundary of aquifer and a confinement condition. The files commence and end with a sequence of the number $(N+1)$ where N is the number of nodes in the problem. This sequence is used as a flag to separate batches of input data and signal the end of input.

A2.3 OUTPUT PRESENTATION

Sections may be used for presentation, and these have the advantage of showing the local situation very simply. However, contour plans have been utilised to a considerable extent, because once familiarity with them is obtained, the opposing effects of reservoir filling and drainage measures can be readily assimilated, giving an overall appreciation of the entire slope response.

A2.3.1 Terminology

A terminology for explanation of drawings has evolved to facilitate presentation of the effects of piezometric changes in one or more aquifers on a specific failure surface. An example is:

Initial net drainable head above/below/at the failure surface.

Usage:

- "Initial" - the condition pertaining prior to any remedial measures, ie the initial average river level acts as the fixed head control and no drainage drilling, drives or other effect is considered to effect the initial watertable.
- "Full Pool" - the condition pertaining at full reservoir level (usually either Initial or Full Pool will begin the description).
- "Piezometric Surface" - the actual level of the piezometric surface expressed as metres above mean sea level (cf. "Head").
- "Head" - the piezometric head expressed in metres above the failure surface, ie as required for stability analysis. Negative values are meaningless and are recorded as zero, as are values in regions where the failure surface does not exist.
- "Above/Below/At" - these are used to distinguish between pressures acting on a failure surface which arise from an overlying aquifer (Above), an underlying aquifer (Below), or the greater of the pressures acting on either side of a failure surface (At). The latter is the key requirement for inputting to a stability analysis as it is the higher of the two pressures which governs the available shear strength of the failure surface. The term "Governing" is sometimes included to reinforce the meaning of "At".
- "Aquifer Demarkation Line" - The line on a contour plan which shows where the piezometric surfaces from the aquifers above and below a failure surface are coincident. (That is, the areas where the respective aquifers are governing can be delineated on the plan.)

"Drainable head"

- The head acting on the failure surface, that can be removed by gravity drainage with the river present. (Not often used).

"Net drainable head"

- The head acting on the failure surface that can be removed by a gravity drainage system located at proposed full pool level. This is calculated as the head acting on the failure surface, but deducting the depth of the failure surface below full pool level. A plan of predicted net drainable head at full pool, is particularly useful in that it illustrates at a glance, where drainage targets exist.

"Change in Head"

- The difference in head acting on the failure surface in the specified condition, from that acting initially. Rises in head (adverse) are generally shown in red, while decreases (favourable) are shown in green. Piezometric levels are neglected once they fall below the failure surface. This illustrates at a glance the combined impact of drainage and reservoir filling and allows immediate qualitative appreciation of whether gains have offset losses.

A2.3.2 Plans

TECHBASE provides an ideal means to present interpretation of groundwater modelling, through its facilities for posting of drillholes, drawing of boundary lines and interpolation routines for contouring of piezometric surfaces, net drainable head etc. Standard input requirements for contouring are 4 parameters: northing, easting, level and surface identifier. The output tables of LSFLOW are readily transformed for input to TECHBASE, using the simple file handling program PC_TBASE.

The program PC_TBASE prompts for the TECHBASE coordinates which correspond to Node 1 (lower left corner) of the LSFLOW output table, the node spacing, the bearing of the first column of the table (in the sense that is away from Node 1), and the file identifier (defaulting to drive a:).

Two options are prompted for:

(i) Addition of a small number. This has turned out not to be relevant to TECHBASE, but was included for other plotting programs (eg CONTOUR) which produce superfluous lines when a large number of cells have zero values to be contoured (as for instance will often occur in a surface showing net drainable head). This could always be overcome for tidy presentation purposes by inserting a small negative number when contouring positive numbers (and vice versa).

(ii) Elimination of 1 (or more) rows, starting from upslope. LSFLOW uses the most upslope row, solely to define its boundary condition and the heads in this row are meaningless for the way in which the program is normally operated. The value of 1 is usually entered at this prompt.

Example presentations are given in Figs. A2-2 (before reservoir filling) and A2-3 (predicted steady state conditions after filling) which illustrate the manner in which the locations of drainage targets (both before and, more importantly, after reservoir filling) can be simply appraised, to optimise remedial drainage works both for location and extent. A drainage drive (shown) was planned here and the predicted full pool drainable head drawing indicates that areas that were unsaturated initially, could be targeted with an extension of the drive shown (comparing Fig. A2-2b with A2-3b).

One multiple aquifer situation not shown here, but found relevant in several cases, was where the governing piezometric surface changes from one side of a failure surface aquiclude to the other, on reservoir filling. In this situation, modelling has a two-fold benefit:

(i) it allows remedial drainage to focus primarily on drainage locations that are of principal benefit at the most critical period (long term, unless drawdown is planned)

(i) it highlights need for drainage of the aquifer on the critical side of the failure surface, as there is no benefit in reducing piezometric levels below the governing level otherwise.

Plan presentations for this case use an "aquifer demarkation line" using TECHBASE drawings to show whether the higher piezometric levels on the failure surface come from the aquifer above or below (using different pen styles for the respective piezometric contours).

A2.3.3 Sections for Stability Analysis

The initial and predicted groundwater conditions are best appreciated using contour drawings and sections. However, stability analysis will generally need to be considered using a conventional 2D limit equilibrium method of slices. A simple program, PZPOINTS has been written for transfer of piezometric lines as sets of coordinates to a slope stability program such as UTEXAS (Appendix 1). A number of steps are involved, but these can all be executed using a single keystroke for all sections on a slide, by setting up an appropriate macro:

- (i) Isolate the desired table from the standard LSFLOW output.
- (ii) Run program CONTOUR (written by R Friday, Golder Associates).
- (iii) View the contoured piezometric surface on screen
- (iv) Type in the beginning and end points of the section in terms of the LSFLOW local coordinates, view sections on screen, print if required, then write section coordinates to disk.
- (v) Repeat the last step for as many sections as required.
- (vi) Exit from CONTOUR and execute PZPOINTS

The prompts for PZPOINTS are the filenames, sign and distance of the baseline station from the edge of the LSFLOW mesh. The sign value allows the section to be viewed from the appropriate side (usually looking downstream) and the baseline distance provides for the origin of section co-ordinates to be located at standard nominated location.

Program listings are contained in Section A5.4.

A2.4 ASSURANCE

A2.4.1 Alternative Groundwater Modelling Packages

The LSFLOW model has been developed to integrate groundwater modelling with slope stability determination in a time dependent manner. The validity of results has been tested on a number of problems. Other modelling packages have been used to verify the groundwater predictions, both for steady and unsteady conditions, and for confined and unconfined aquifers.

Verification of the limit equilibrium results has been carried out to some degree by checking the change in safety factor computed over the defined surface with the results on individual sections.

A2.4.2 Comparison with Standard Analytical Solution

The analytical solution for the piezometric response of a laterally infinite aquifer adjacent to a fluctuating river is described by Hunt (1983). A worked example is given for a piezometer located a given distance (x) from a straight reach of river. A rapid change in head (h_0) in the river (to a new constant value) will cause a sympathetic change in head (h) at the piezometer after a given delay time (t), which is a function of the ratio of the aquifer storage coefficient to transmissivity (S/T).

Analytical results for $x = 50$ m, $t = 9$ hours, are given by Hunt as:

S/T	0.411	0.015	0.004
h/h_0	0.90	0.95	0.99

A numerical model was set up, approximating the semi-infinite aquifer with a 5 km long aquifer (100 nodes at 50 m spacing). A timestep of 0.1 hours was used, giving 90 timesteps to 9 hours. A comparison of the numerical results with the analytical solution follows:

	S/T	0.411	0.015	0.004
(Analytical)	h/h_0	0.9000	0.9500	0.9900
(Numerical)	h/h_0	0.8993	0.9493	0.9803

For practical purposes, this indicates full agreement of LSFLOW with the general (non-steady state) analytical solution. As expected, the error increases with decreasing S/T ratio, but this would be minimised by using a smaller timestep.

A2.4.3 Example Problems

A2.4.3.1 Section Modelling

A preliminary analysis was carried out for a large dormant landslide about to be submerged by a proposed reservoir. Very little information was available at the stage this work was done, so sensitivity was examined for a credible range of aquifer parameters. Failure surfaces were conjectured from limited subsurface investigations and the location of mapped scarps. Coarse alluvium was present at the toe of the slide, (assumed as free

draining) but elsewhere ranges of permeability were used for calibration in relation to credible ranges of recharge. Aquifers were identified both above and below the basal failure surface. The initial steady state piezometric line (prior to any reservoir filling) is shown on Fig. A2-4. The general nature of the way in which the water from the reservoir infiltrates the slide is shown at various stages in Figs. A2-5 to A2-8. (The piezometric gradients are relatively flat in this particular case.) For the steady state condition, the ratio of permeability to recharge is necessarily fixed (Chapter 5), ie in the initial calibration process, a value of recharge (infiltration) may be adopted and permeability deduced, or vice versa. A slow response model was chosen using the lowest credible average permeability for the aquifer concerned. The fast response model was determined from an average annual recharge value at the uppermost credible limit for the climate. Storage coefficient values can be determined only by pumping tests, as they are unrelated to steady state conditions, so values were adopted from work in a nearby area. These 3 parameters were varied over relevant ranges in the sensitivity analysis shown in Fig. A2-9. (Both values of storage coefficient were used for the slow response assumption.) The range of geologically inferred failure surface locations has also been included. A 90 day reservoir filling period was assumed but time is shown normalised to make an obvious distinction between of times that are shorter or longer than the filling period. The analyses illustrate various generalisations (usually but not always true) discussed in other chapters:

- (i) small slides are proportionately more affected by a given rise in water level,
- (ii) the ultimate steady state factor of safety is independent of storage coefficient,
- (iii) slow response (infiltration of reservoir water to the slide) results from low permeability and high storage (effective porosity),
- (iv) where slow response applies, safety factors will actually increase during the filling stage, before decreasing,
- (v) where fast response applies, safety factors will decrease rapidly to their ultimate values,
- (vi) the credible ranges of aquifer parameters indicate that in this instance the proposed reservoir filling time of 90 days may be too fast, to ensure that 'piezometric lag' (and consequent hazards, Chapter 5) will not present a problem.

A2.4.3.2 Regional Modelling

The following example relates to the case of a large active landslide for which drainage works were being planned before submergence by a proposed reservoir. The basal failure surface was defined by a diamond drilling program, and multiple piezometers were installed both above and below the basal failure surface, and many permeability tests were carried out.

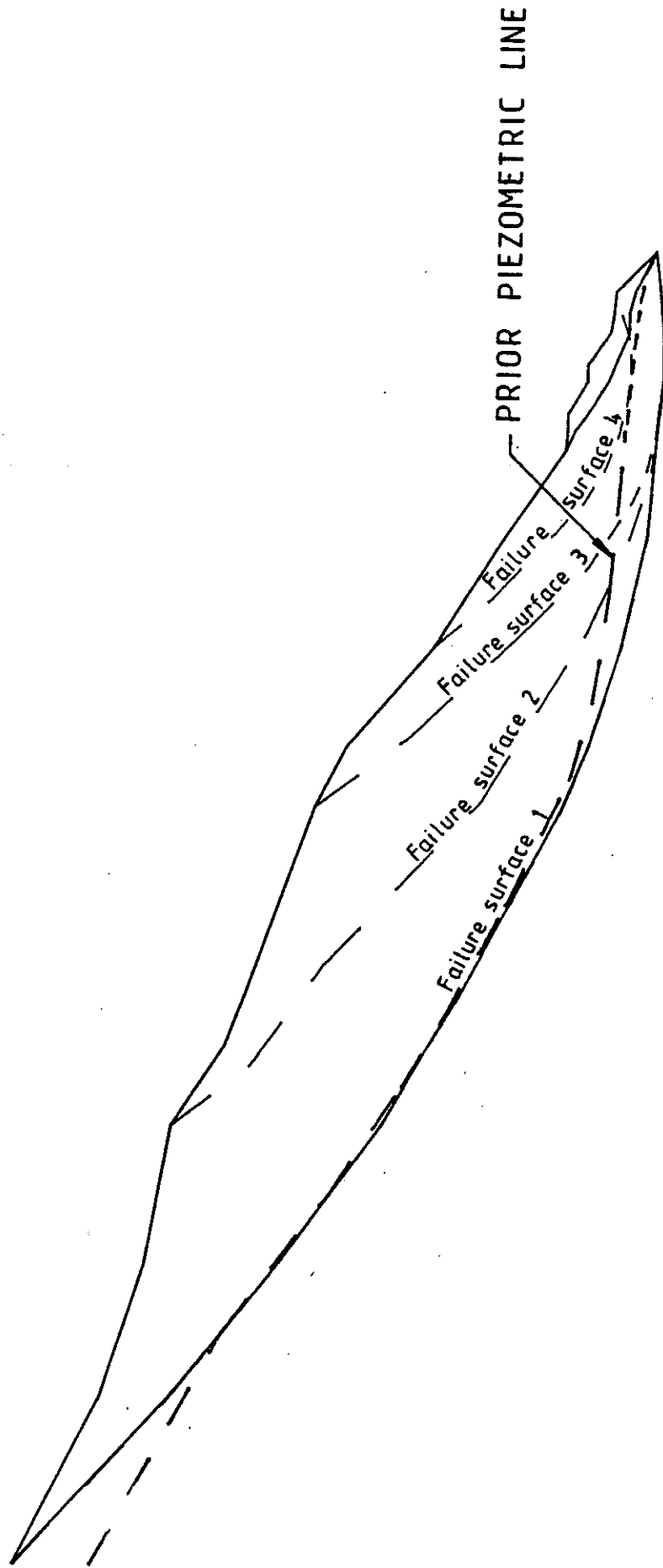


Fig. A2-4 Section Model
Initial condition (1)

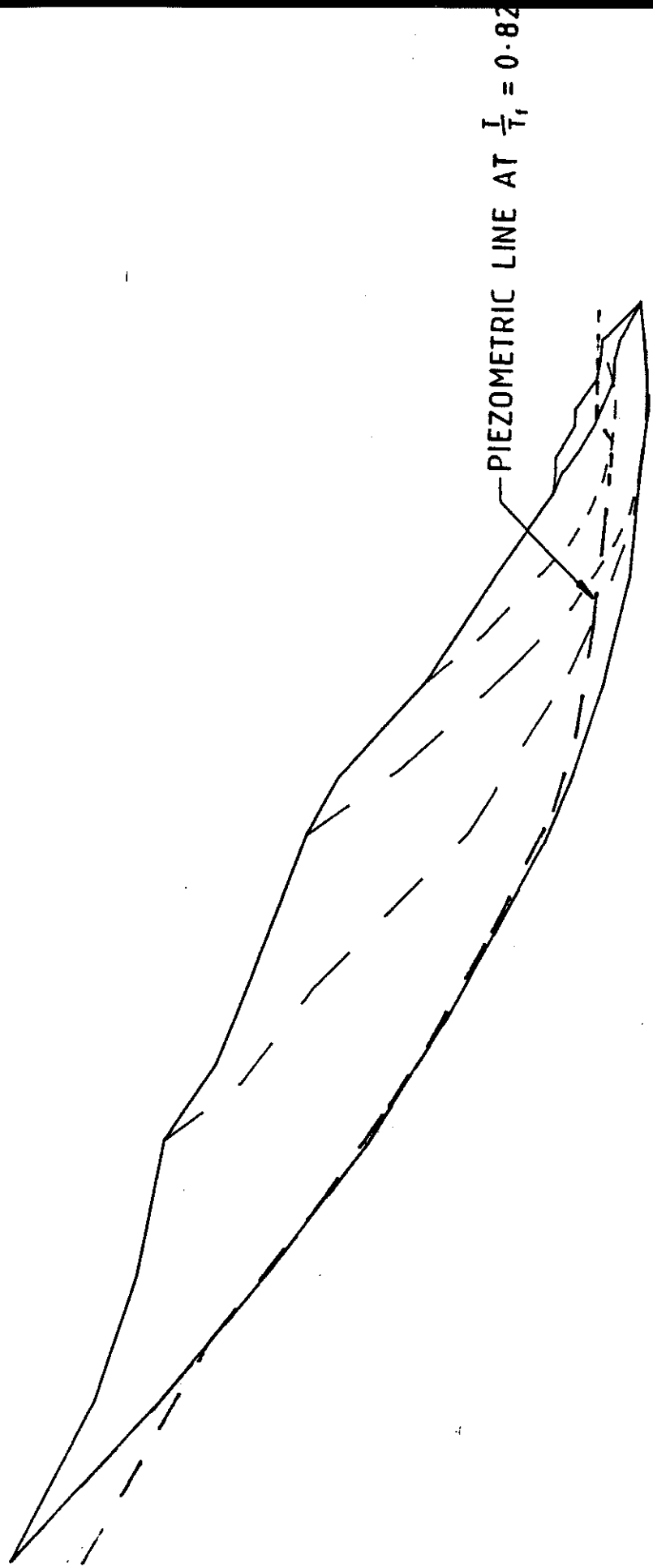


Fig. A2-5 Section Model
Rising piezometric line (2)



PIEZOMETRIC LINE AT $\frac{T}{T_1} = 1.6$

Fig. A2-6 Section Model

Rising piezometric line (3)



Fig. A2-7 Section Model
Rising piezometric line (4)

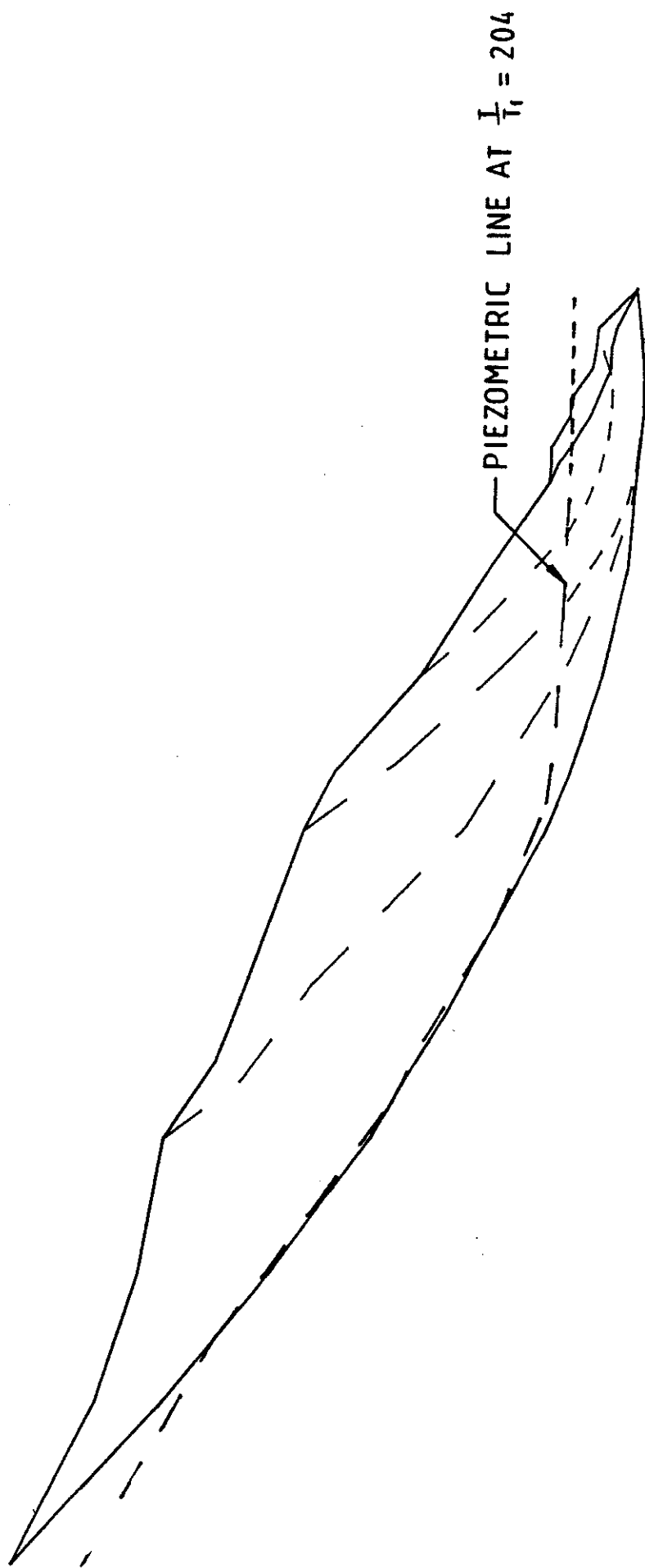
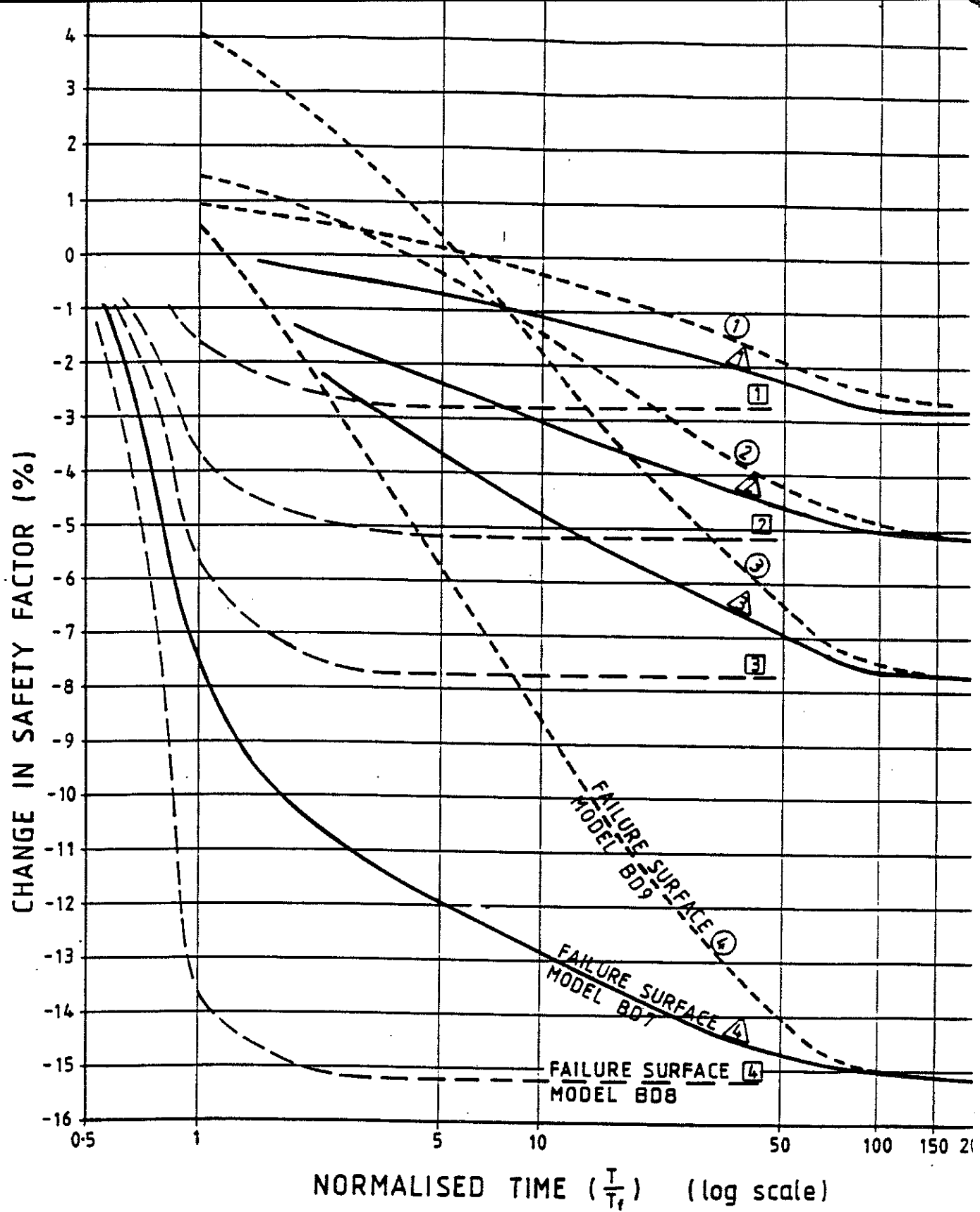


Fig. A2-8 Section Model
Steady state piezometric line (5)



NOTES

- ==== Slow response assumption
- — Fast response assumption

PERMEABILITY	INFILTRATION	STORAGE COEFFICIENT
1×10^{-7} m/s	7.5 mm/yr	0.05
1.4×10^{-6} m/s	100 mm/yr	0.005

Time of reservoir filling (T_f) = 90 days.

Fig. A2-9 Section Model
Sensitivity analysis

In this case 35 piezometers were available for calibration of the LSFLOW model. Nine different permeability zones were required to obtain reasonable calibration. For assurance, a check of the steady state case was carried out using MODFLOW (McDonald et al, 1988), producing results that were practically indistinguishable.

The time dependent (transient) piezometric responses and the changes in safety factor of the basal failure surface, determined from LSFLOW have been shown in Chapter 5. (Fig. A2-10 shows one of the set described earlier.) Attention is drawn again to these figures and the accompanying discussion on safety factor implications because these are one of the main end products of LSFLOW. The physical reasoning for the safety factor changes can be seen from the similar problem shown in the time sequence of Figs. A2-4 to A2-9.

Another case history is shown on Fig. A2-11. Initial stages of drainage and buttressing had been carried out. Modelling indicates that the net improvement in long term safety factor would be barely adequate. A drawdown is modelled, immediately after maximum pool level is reached. This shows that the drawdown would cause a temporary decrease in stability, but long term safety factors would still become even lower. The implication is that a slower, more marked drawdown or more drainage would be required to maintain a net increase in safety factor.

Figs. A2-12 and A2-13 show the way in which the model can be used to consider the viability of remedial drainage measures. In this case, proposed observation well locations were studied, to assist in deciding on appropriate sites. Fig. A2-12 studies the drainage response, assuming that 2 years of drainage will be achieved before reservoir filling commences, then examines the rising response. Fig. A2-13 studies the same situation in the longer term to determine the effects of a delay to reservoir filling on the amount of drainage achieved.

In all cases a sensitivity analysis is required, but as soon as any remedial drainage is instigated, all parameters can be determined much more reliably by calibration of the model to the time dependent piezometer responses recorded in the field.

LSFLOW EXAMPLE PROBLEM DRAINAGE AND FILLING CASE

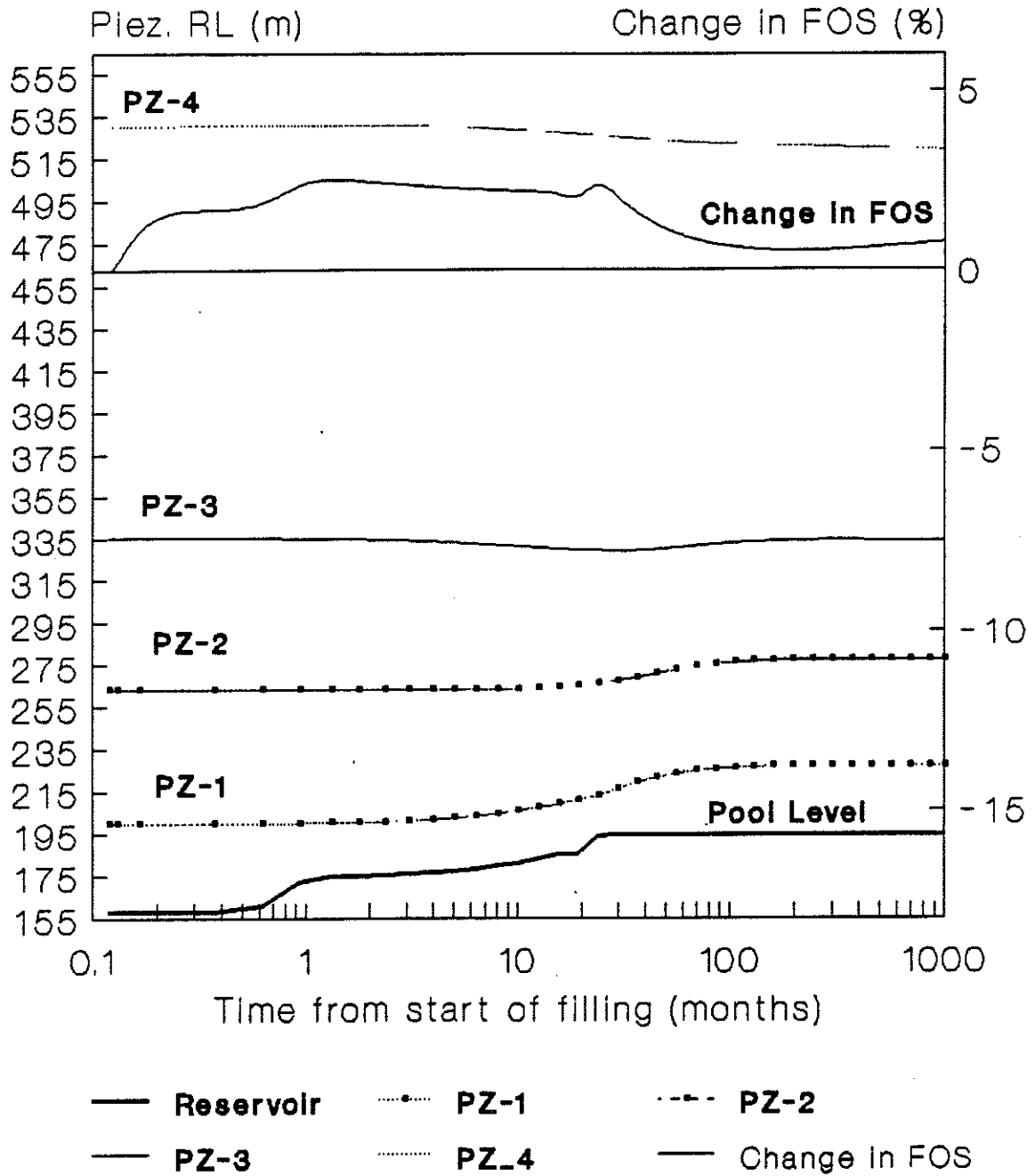


Fig. A2-10 Piezometer Responses

SLIDE DRAWDOWN EFFECTS

Drive and drainage holes

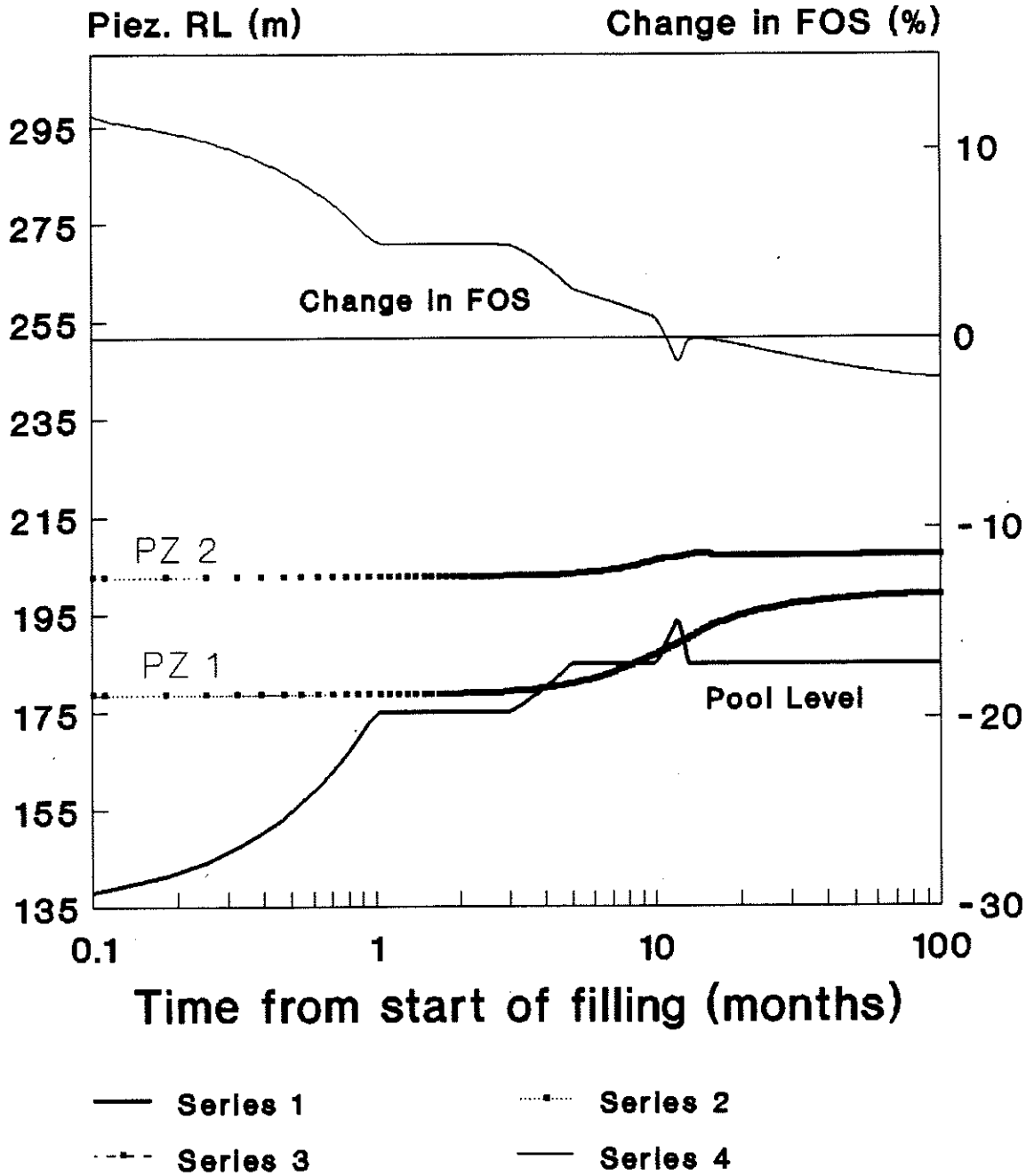


Fig. A2-11

SLIDE PIEZOMETRIC RESPONSES

Proposed drainage drive and drains

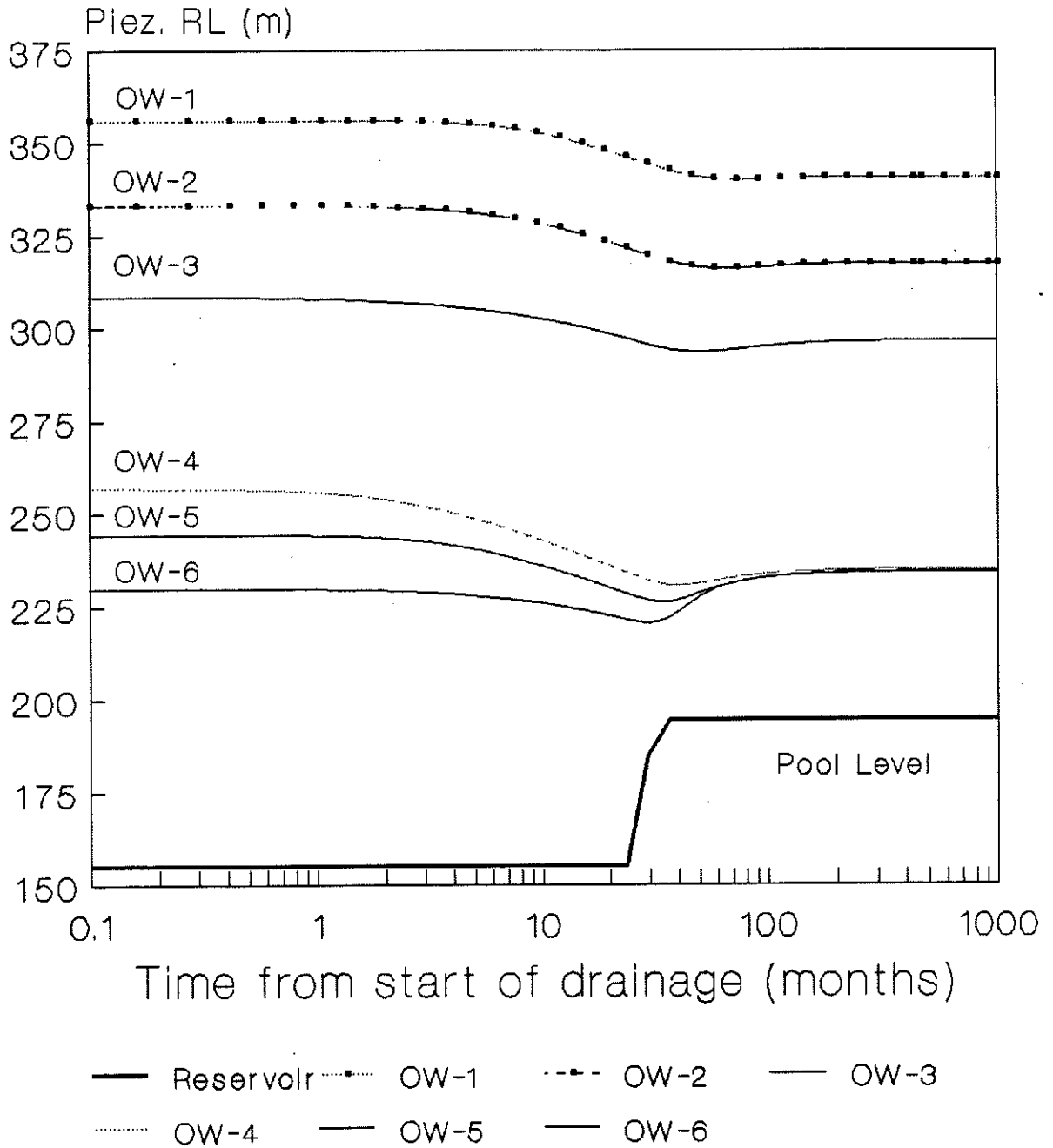


Fig A2 - 12

SLIDE PIEZOMETRIC RESPONSES

Proposed drainage, delayed filling

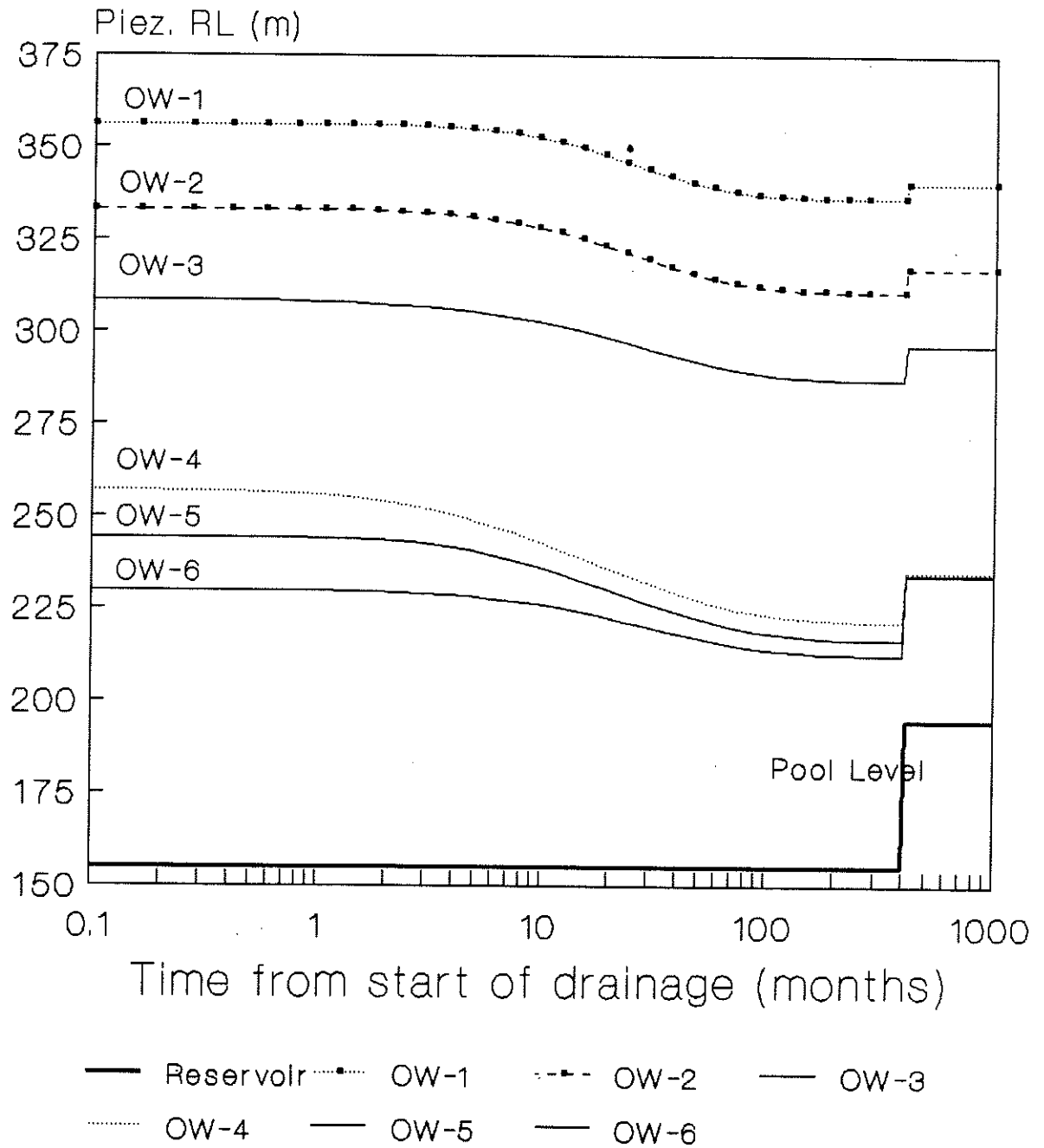


Fig. A2-13

A2.5 PROGRAM DETAILS

A2.5.1 Subroutine Sequence

The sequence of primary subroutines and the secondary and tertiary subroutines which they call in turn, are listed below. Their labels are largely self explanatory, with further detail in the next section.

- parameters
 - slidename
- standardinput
- permfile
- boundaryconditions
- stresses
- solution
 - driveflows
 - flownode
 - fixedheads
 - verticalflows
 - transmissivities
 - reservoirrise
 - safetyfactor
 - calibration
 - calculatea
 - anomalies
 - internala
 - screenprint
 - calibration
 - overrelax
 - risingheads
- screenprint
 - calibration
- fileoutput
 - diskfile
 - arrayprint
 - presentstate

A2.5.2 Subroutine Functions

Subroutine parameters:	Selects case for specific slide given by prompt for "slidename" and defines non-specific constants used.
Subroutine slidename:	Defines specific data for the aquifer in the nominated slide and allocates input files.
Subroutine standardinput:	Dimensions arrays and inputs the basic data file.
Subroutine permfile:	Inputs the file containing nodal permeabilities and vertical limits of the aquifer.
Subroutine boundaryconditions:	Specifies default parameters, fixed head boundaries, inflows, infiltration and initial values.
Subroutine stresses:	Calculates initial average shear and normal effective stresses on the failure surface and selects the option for calculation of change in safety factor, using the limit equilibrium method of either Sarma, Janbu, Bishop or the Ordinary method.
Subroutine solution:	Main subroutine for calculating nodal piezometric heads and flows, establishes timesteps and determines acceptability of solution convergence.
Subroutine driveflows:	Specifies which nodes are located at drives and horizontal or vertical drainage holes. (Case specific.)
Subroutine flownodes:	Specifies the confinement condition parameter and head condition for nodes affected by drainage measures. Calculates total flow from drives and drains. (Case specific.)
Subroutine fixedheads:	Selects which fixed heads will be affected by reservoir filling. (Case specific.)

Subroutine verticalflows:	Main adjustment procedure to improve the Dupuit approximation limitation in accounting for vertical flows, accommodating leaky aquifers, flows at springs and drives and the effect of the reservoir flooding over previously unsubmerged nodes.
Subroutine transmissivities:	Calculates nodal transmissivities, including an option to model permeability variation with depth.
Subroutine reservoirrise:	Determines the level of the reservoir at the beginning of each timestep from the pre-specified programme for filling, controlled drawdown or rapid drawdown, and writes to disk the transient heads in each piezometer within the aquifer.
Subroutine safetyfactor:	Integrates the change in piezometric head acting over the full failure surface and computes the corresponding change in safety factor from the initial conditions.
Subroutine calibration:	Calculates the difference between the piezometric head observed in the field at each piezometer installation and the current head in the model.
Subroutine calculatea:	Calculates the piezometric heads at each boundary node, and determines whether the confined or unconfined storage coefficient applies at internal nodes at that timestep.
Subroutine anomalies:	Tests for anomalous piezometric values and prints appropriate warnings.
Subroutine internala:	Calculates the piezometric heads at each internal node, and checks for transition between unconfined and confined states to determine the appropriate storage coefficient.
Subroutine screenprint:	Prints to screen, the model piezometric levels at known piezometers, reservoir level, error criteria and change in safety factor.
Subroutine overrelax:	Calculates the optimum successive over-relaxation factor for rapid convergence.

Subroutine risingheads:	Checks whether termination or a rising reservoir case is sought and stores the piezometric levels existing prior to reservoir filling.
Subroutine fileoutput:	Prompts for file names when writing outputs to disk.
Subroutine diskfile:	Outputs both the input data and calculated data to disk file.
Subroutine arrayprint:	Transforms the internal sequential organisation of nodal values to a table which corresponds to the same spatial order as viewed in plan.
Subroutine presentstate:	Writes the present model parameters and calculated heads to a disk file which is ordered correctly for subsequent input if a restart is required.

A2.5.3 Definitions of Variables

Variables (and common constants) used in the program LSFLOW are defined below. Those with asterisk (*) are from the base code from which this program has been developed, and background details are therefore given by Hunt (1983).

a *	Temporary assignment for piezometric head before calculating errc.
a0(i) *	Where $i > nb$, coefficient for finite difference equations for internal nodes.
a1(i), a2(i) *	Where $i \leq nb$, coefficients for finite difference equations for boundary nodes.
a1(i) ... a4(i) *	Where $i > nb$, these are resultant transmissivities for inter-nodal flows.
a1, a2, a3, a4 *	Resultant transmissivity between nodes, (sq. m/s).
alpha0	Average inclination of the entire failure surface.

alpha	Average angle of failure surface in the region where changes to the water table level are expected.
alpha(i) *	Boundary condition identifier for node i
analysismethod\$	Method of limit equilibrium analysis for computing changes in safety factor with piezometric rises. Options are "Janbu", "Sarma", "Bishop" and "Ordinary". The latter two give the same result and are used as the default.
b0(i) *	Where $i > n_b$, coefficient for finite difference equations for internal nodes.
beta(i) *	Boundary condition identifier for node i
bk(i) *	Leakance term for node i, if needed for variable leakance. (Usually put equal to leakance, q.v.).
c(i)	Condition identifier for aquifer type at node i. - unconfined, $c(i) = 0$, - confined, $c(i) > 0$ and equal to the proportion of node i area that is occupied by the confining aquiclude. - gravity drainage, $c(i) < 0$
ce(i)	Control node number. This is the nearest node downslope from control point i.
ceer(i)	Control point i, calibration error in metres, $(ch(i) - ct(i))$
ch(i)	Modelled piezometric head interpolated for control point i.
cp(i)	Control point identifier (Drillhole number) Control points cannot be defined adjacent to any boundary. (Each must be surrounded by internal nodes.)
cc(i)	Control point coefficient. This is a ratio defined as upslope component of the distance from cp(i) to the next node upslope, divided by the node spacing. It is used for interpolating the head at cp(i) from the heads at the nearest internal nodes.
ct(i)	Control point target piezometric level in metres.

dummycontour	Used as a substitute where zero values are found in the output file for net drainable head, when these are to be contoured. Usually a value which is small compared with the contour interval is input, eg -1 will allow realistic contour drawings to be produced if the contour interval is 5 or 10 m.
d(i) *	Node spacing at node i, if needed for variable mesh. (Usually put equal to nspace.)
damw	The level of water at the dam in metres, at anytime after the start of the filling program.
dw	Depth of saturated aquifer used in transmissivity calculation.
dF	Total change in safety factor (%) of the entire slide from the original condition to the current piezometric condition. ($dF = dFi + dFp + dFh$) The program currently assumes that a sub-basal aquifer is being modelled. If an aquifer overlying the failure surface is modelled, the piezometric surface solution will be valid, but safety factor calculations will require respecifying in subroutine "Safetyfactor".
dFi	Change in safety factor for the slide (%) from the original condition to that at ideal drainage with the river present. (Piezometric level everywhere at the same level as the river.)
dFf	Change in safety factor for the slide (%) from the ideal drainage condition with the river present, to the ideal drainage condition at full pool.
dFp	Change in safety factor for the slide (%) from the ideal drainage condition with the river present, to the ideal drainage condition at the current pool level. (Normally interpolated from dFf.)
dFh	Change in safety factor for the slide (%) from the ideal drainage condition at the current pool level, to the current piezometric condition at the current pool level.
dp(i) *	Shortest distance to boundary from boundary node i

drelax	The depth (m) of relaxed, more permeable material below the upper boundary of the primary aquifer. Used for adjusting the base permeability where required by permult (q.v.).
drflow	Flag for operation of subroutine "Driveflows" which recognises the presence of drives or drains. A value of 1 turns drives on, 0 is off. Note that drflow is turned on automatically at the time given by the variable startdrive if subroutine "Reservoirrise" is invoked.
drlevel	Level (metres) of drainage control assumed in any drives. Usually RL 197 m.
dt	Timestep in seconds.
el(i)	Elevation (metres) of the lower boundary of the primary aquifer at node i.
errc *	Error in convergence for current iteration.
errclast *	Error in convergence for last iteration.
errt *	Target error criterion acceptable for convergence.
eta	The asymptotic residual depth of flow in the principal aquifer (metres). (Usually 0.1). This is used to avoid mathematical oscillation in trivial cases when the saturated thickness of the aquifer becomes very small.
extremehead	The highest artesian head expected, in metres. A warning message is displayed each time any node exceeds this value. Usually set at 500.
f0	Janbu's safety factor correction (usually 1.05).
f(i) *	Fixed head condition identifier for node i, in metres.
Fsens	Sensitivity of the safety factor of the whole slide to a change in head of 1kPa acting over 1 square metre.
fullpool	The final level of the reservoir at full pool, in metres.
h(i) *	Current piezometric level (metres) within the primary aquifer at node i.

hlast(i) *	Piezometric level (metres) within the primary aquifer at node i, at the last iteration for constant t(i).
hmax(i)	Level (metres) of the upper boundary of the primary aquifer
hp(i) *	Piezometric level (metres) operating external to the primary aquifer, (across the leakance barrier at node i).
id(i,j) *	Local node identification number for node i
infil	Infiltration (mm/year) applied to each unconfined node (where c(i)=0).
iterations	The number of iterations allowed before the problem is terminated. Usually 1000.
k	Timestep number
leakance	The vertical leakance from the centre of the principal aquifer to the external control head, hp. Leakance at any node can only be through either the upper or lower boundary but minor changes to the program would be required to address both at once. The direction of vertical flow (into or out of nodes) is determined. The leakance is defined as the resultant permeability/vertical thickness ratio. (Units (m/s)/m, ie /s).
maxperm	This the largest value input from the permeability file which is to be interpreted as a value in m/s. (Usually 9E-4.) Any greater number will be multiplied by the predominant permeability defined by p. This allows either relative or absolute values to be entered from the permeability file.
mintransmissivity	The value of transmissivity, below which an error can be inferred, and a corresponding message is output. Units are sq. m/s. Usually 1e-9.
n *	The total number of nodes.
nb *	The number of external (boundary) nodes. These are numbered is a specified sequence from 1 to nb. All other nodes are termed internal nodes and are numbered in a specified sequence from n1 to n.

n1 *	The first internal node (= nb+1)
nc	Number of control nodes (known levels from piezometers.)
ns	Number of pairs of data points needed to define the reservoir filling programme. (Usually 6.)
nspac	The spacing in metres between nodes, taken as constant in both directions. Usually chosen to give a total number of nodes between 400 and 800.
nu	Aquifer flow depth below which the linear transmissivity relation is replaced by non-linear relation for smooth transition (very small compared to the aquifer thickness eg 3 m for a 100 m thick aquifer).
ofreq	Frequency of output of transient heads predicted for each piezometer to file named PZRISE.OUT. Usually 2, or such other number to give less than 240 data points for handling in Harvard Graphics.
p	Predominant base permeability for the principal aquifer in m/s. All coefficients entered from the permeability file will be multiplied by p, unless they are less than the value of maxperm.
perm(i)	Base permeability at node (i) in m/s, as input in subroutine permfile, if the filed value is less than maxperm. If the filed value is greater than maxperm then the filed value is multiplied by p. The latter system of input allows a uniform change to the permeabilities throughout the mesh to be applied readily during calibration.
permmult	Permeability multiplier. Used if the permeability of the principal layer is not constant. The base permeability at node i is increased linearly from the value of perm(i) to permmult*perm(i) at the upper boundary of the aquifer. The transition begins at depth drelax below hmax(i).
pg	Product of density and gravitational constant for slide material. Units are kN/cu. m. Usually 23.
phi	Effective friction angle of the failure surface in degrees.

phim	Average effective mobilised friction angle of failure surface in degrees.
program	Internal flag to indicate reservoir rise program is operating (= 1)
q(i)	Outflow (cu. m/s) from well pumping at node i.
qt	The default applied concentrated discharge calculated from qtop. Normally negative (for inflow it is applied along the line of internal nodes at the upslope end of the model. The value of qt is calculated as $-(qtop/1000)*y*n\space*n\space/siy$. If only the lower half of the total recharge area has been defined in the model then usually qtop is taken equal to infil. If more than half of the recharge area has been disregarded, then qtop should be increased proportionately.
qtop	The infiltration value used to calculate the concentrated inflow (qt) applied at the upslope side of the model. Units of qtop are mm/year, and calculations assume that the model extends only over the lower half of the total recharge area. Higher values of qtop are required if the upslope catchment is more extensive (see qt). If non-uniform inflow is to be modelled this can be modified in Subroutine "Boundaryconditions".
rad	Constant: number of degrees in one radian.
r(i) *	Recharge (inflow) in m/s from infiltration on internal node i. Note that no infiltration can enter at any boundary node.
river	The initial level of the fixed head boundary. For a slide of considerable lateral extent where there is a significant fall in river levels over the length of the problem, a varying initial level can be defined in Subroutine "Boundaryconditions".
rmax	Current level in metres of the fixed head control at the toe of the slope.
rstage(i)	The level of the reservoir at time tstage(i), in metres.
s	Storage coefficient (effective porosity) for unconfined conditions (Usually .05 to .005, but immaterial for steady state.)

sc	Storage coefficient (dimensionless) for confined conditions. (Usually .005 to .0005, but immaterial for steady state.)
screenfreq	Frequency to output results to screen. Usually set for 5 iterations.
sigma	Average effective mobilised shear stress on failure surface, (kPa).
siy	Constant. The number of seconds in a year.
slidebeta	Average slope angle of slide in degrees.
slidedepth	Average depth of slide in metres.
slidelength	Length of slide in metres.
slidename\$	Slide name. This is used for those parts of the program which are slide specific. Any new slide used must be defined in the select-case portion of subroutine "Parameters", and for valid execution, the subroutine slidename\$ must be positioned above that for any other slide. (This is to ensure the correct data statements are read for the screen display.)
slidewidth	Width of slide in metres.
slopefactor	The square of the cosine of the average inclination of the central streamline in the aquifer. This is a correction factor to account for the slope of an aquifer and hence improve the Dupuit approximation. A value of 1.0 is usually assumed because the effect is accommodated implicitly during calibration. However, to give similar solutions to finite element programs which use the true aquifer thickness and flow path length, a value should be calculated, (usually 0.9 to 1.0).
startdrive	Time in months from the start of the reservoir filling program, that the program recognises the presence of drives or drains. The variable drflow is set to 1 at this time.
t(i)	Transmissivity at node i, in sq. m/s.
tadd	Timestep in years to add to last value when calculating increments. Usually 2/365. (See tmult also.)

tau	Average shear stress on failure surface, (kPa).
theta	Ratio of error criteria used for determining the optimum over-relaxation factor.
times(k)	Time at the end of the step k. Units are in seconds internally, but interactive data taken in years.
tmult	Multiplier to apply to the last timestep when calculating increments. Usually 1.01 to 1.15. (See tadd also.)
toelevel	The external water level in metres at the toe of the slide, once reservoir filling has begun (set as zero before filling commences).
tstage(i)	The time in months when the reservoir level is at rstage(i).
x	Number of nodes in the x direction. The finite difference mesh is an array of x columns and y rows. The last row of x nodes is taken as a fixed head boundary.
xn(i) *	Boundary condition components in x direction for node i.
y	Number of nodes in the y direction.
yn(i) *	Boundary condition component in y direction for node i.
w	Successive over-relaxation factor
wt	Weight of the entire slide in kN

A2.5.4 Source Code Listings

LSFLOW

```
cls
print "LSFLOW: Unsteady regional flow with Dupuit approximation, for a
print "  landslide aquifer affected by reservoir filling."
print "  N.B. Check algorithms for each specific application.":print
gosub parameters :rem specific problem parameters
gosub standardinput :rem standard input data
gosub permfile :rem read in permeabilities and aquifer geometry
gosub boundaryconditions:rem specific values for fixed heads,recharge etc
gosub stresses :rem initial shear and normal effective stresses
gosub solution :rem solve finite difference equations
gosub screenprint :rem output to screen
gosub fileoutput :rem output to disk
end

fileoutput:
input "Type filename to file general output, (null otherwise) ";fileout$
if fileout$ > < "" then gosub diskfile
input "Type filename for present state (null otherwise)";file3out$
if file3out$ > < "" then gosub presentstate:rem file present state
headfile$="PZLEVEL.OUT":open headfile$ for output as #2
for i=1 to n:v(i)=h(i):next i:gosub arrayprint:close #2
print "Final Pz levels filed on PZLEVEL.OUT"
if program=1 then print "Transient Pz levels for each piezo filed on PZRISE.OUT"
print"Execution completed."
return

standardinput:
dim id(n,4),d(n),f(n),t(n),a0(n),a1(n),a2(n),a3(n),a4(n),b0(n),v(n)
dim bk(n),hp(n),r(n),q(n),hlast(n),times(1001),el(n),hprior(n),hdelta(n),perm(n+1),hmax(n+1),c(n+1)
dim alpha(n),beta(n),xn(n),yn(n),dp(n)
for i=1 to nb
input #1, id(i,1),id(i,2),alpha(i),beta(i),xn(i),yn(i),dp(i),d(i),f(i),el(i),h(i)
d(i) = nspace:perm(i) = p:hlast(i) = h(i)
a = (alpha(i) + beta(i) * dp(i)) / d(i):a1(i) = a * yn(i):a2(i) = a * xn(i):a0(i) = a1(i) + a2(i) + beta(i)
next i
n1 = nb + 1
for j = n1 to n
input #1, id(j,1),id(j,2),id(j,3),id(j,4),el(j),h(j),d(j),bk(j),hp(j),r(j),q(j)
d(j) = nspace:perm(j) = p:bk(j) = leakance:hlast(j) = h(j)
next j
times(1) = 0:count = 0:close #1:rate$ = "pzrise.out":open rate$ for output as #1:rem rate of rise
return

solution: rem the equations are solved by iteration after each time step
for k = 2 to iterations
if drflow > 0 then gosub driveflows:rem subroutine for drive flows *****
if tolevel > 0 then gosub fixedheads:rem rising reservoir affects fixed heads
gosub verticalflows :rem leakance and vertical flow components
gosub transmissivities:rem compute transmissivities
count = 0
```

```

for i=n1 to n
i1=id(i,1):i2=id(i,2):i3=id(i,3):i4=id(i,4)
a1(i)=2*t(i)*t(i1)/(t(i)+t(i1)):a2(i)=2*t(i)*t(i2)/(t(i)+t(i2)):a3(i)=2*t(i)*t(i3)/(t(i)+t(i3)):a4(i)=2*t(i)*t(i4)/(t(i)+t(i4))
a0(i)=a1(i)+a2(i)+a3(i)+a4(i)+bk(i)*d(i)*d(i):b0(i)=-q(i)+(bk(i)*hp(i)+r(i))*d(i)*d(i)
next i

```

```

if k=2 or finish=1 then times(k)=10 else times(k)=times(k-1)/siy+10
if times(k)>1e20 then input" warning large time, hit enter to continue ";ttt
if toelevel>0 then times(k)=tmult*times(k-1)/siy+tadd:rem time now in years
if program=1 or toelevel=1 then gosub reservoirrise:rem new reservoir level
gosub calibration:rem print target nodes
print"Time, toelevel, errt, errc, dF:";
print using "####.####";times(k-1)/siy;toelevel;print using "####.####";errt;errc;dF
qqq$=inkey$:if qqq$="q" or qqq$="Q" or finish=1 then
  finish=0:input " time step? (years):";times(k)
end if
accept=0:if times(k)=0 then times(k)=times(k-1):finish=1:accept=1
if accept=0 then
  times(k)=times(k)*siy
  if times(k)<=times(k-1)then print "Timestep too small!":times(k)=times(k-1)+.00001
  dt=times(k)-times(k-1)
end if

```

```

while accept=0
  errclast=errc:errc=0:errt=10:if k>2 then errt=.005+10*10^(1-k/3)
  if program=1 then errt=n/1000000
  count=count+1
  gosub calculatea
  errc=sqr(errc)
  if int(count/screenfreq)=count/screenfreq then gosub screenprint
  qqq$=inkey$:if qqq$="q" or qqq$="Q" then accept=1
  if errc > errt and count<10 then gosub overrelax else accept=1
wend

```

```

rem solution has converged or been accepted (accept=1)
for i=1 to n:hlast(i)=h(i):next i
if finish>=1 then
  input"Enter new reservoir level, 0 to end, 1 for rise program, 9 to abort ";toelevel
  if toelevel>0 then
    k=1:gosub risingheads:rem reservoir rise
    else
    k=iterations
    end if
end if
next k
close #1
return

```

```

stresses:
tau=pg*slidedepth*cos(alpha0/rad)*sin(alpha0/rad)
sigma=tau/tan(phi/rad):rem average shear and normal eff. stresses calculated
wt=pg*slidedepth*slidewidth*slidelength
select case analysismethod$
  case "janbu"
Fsens = -(f0*tan(phi/rad))/(cos(alpha0/rad)*cos(alpha0/rad)*wt*tan(alpha0/rad))

```

```

case "sarma"
Fsens = -(3.33*sin(phi/rad))/(wt*cos(alphai/rad))
case else
Fsens = -(tan(phi/rad))/(cos(alphai/rad)*wt*sin(alpha0/rad))
end select
return

transmissivities: rem compute transmissivities
for j=1 to n
if h(j)>hmax(j) then dw = hmax(j)-el(j) else dw=h(j)-el(j)
if dw < nu then dw=eta+(nu-eta)*exp((dw-nu)/(nu-eta)):if dw<eta or dw>nu then print"error 237
t(j)=perm(j)*dw
if permult > <1 then
tw = dw + el(j)-(hmax(j)-drelax)
if tw>0 then t(j)=t(j)+perm(j)*(permult-1)*tw*tw/(2*drelax)
end if :rem **** if relaxed zone put permult>1
if t(j)<mintransmissivity then t(j)=mintransmissivity:print "Transmissivity error at node ";j;
t(j)=t(j)*slopefactor
next j
return

```

```

calculatea: rem calculate a
for i=1 to nb
i1=id(i,1):i2=id(i,2):a=h(i)+w*(f(i)+a1(i)*h(i1)+a2(i)*h(i2)-a0(i)*h(i))/a0(i)
gosub anomalies:rem test for anomalies
errc=errc+(a-h(i))^2: h(i)=a
next i
for i=n1 to n
i1=id(i,1):i2=id(i,2):i3=id(i,3):i4=id(i,4):s1=s*d(i)*d(i)/dt
if c(i)>0 and hlast(i)>hmax(i) then s1=sc*d(i)*d(i)/dt
gosub internala: rem calculate a
if hp(i)><0 then v(i)=bk(i)*(hp(i)-h(i))*d(i)*d(i):rem calculate flow v
if flag=1 then s1=s1*ratio+(1-ratio)*sc*d(i)*d(i)/dt:gosub internala
if flag=-1 then s1=s1*ratio+(1-ratio)*s*d(i)*d(i)/dt:gosub internala
gosub anomalies :rem test for anomalies
errc=errc+(a-h(i))^2: h(i)=a
next i
return

```

```

anomalies: rem subroutine to test for anomalies
if a < el(i) then a = el(i): print "Negative water depth ";i;
if a > hmax(i) + extremehead and c(i) > 0 then print i;"?";
return

```

```

verticalflows: rem subroutine for leaky aquifer or flow at springs or drives
rmax = river:if tolevel > river then rmax = tolevel
for i=n1 to n
if h(i) >= hmax(i) then
hp(i) = hmax(i):if rmax > hmax(i) then hp(i) = rmax
rem ***** above line must be modified for pumped drainage
if c(i) <= 0 then
bk(i) = perm(i)/(0.5*(hmax(i)-el(i) + .1))
if slidename$ = "example" and c(i) = 0 then bk(i) = 1e-4
else
bk(i) = leakance

```



```

end if
else
if c(i) = < 0 then
if rmax > hmax(i) then
hp(i) = rmax:bk(i) = perm(i)/(0.5*(hmax(i)-el(i) + .1))
else
bk(i) = 0
end if
else
if rmax > hmax(i) then
hp(i) = rmax -(hmax(i)-hlast(i)):bk(i) = leakance
else
bk(i) = 0
end if
end if
end if
next i
return

```

```

calibration: rem subroutine for piezo match print
for jk = 1 to nc:ch(jk) = cc(jk)*h(ce(jk)) + (1-cc(jk))*h(ce(jk)-1)
ceer(jk) = ch(jk)-ct(jk):next jk
print:print "Pz RL ";:for i = 1 to nc:print using "#####";ch(i);:next i:print
print "Pz No."::for i = 1 to nc:print using "#####";cp(i);:next i:print
print "Match ";:for i = 1 to nc:print using "#####.#";ceer(i);:next i:print
return

```

```

internala: rem subroutine to calculate internal node a
if hlast(i) < -1 or hlast(i) > 4000 then print "error internala",i, hlast(i)
a = h(i) + w*(a1(i)*h(i1) + a2(i)*h(i2) + a3(i)*h(i3) + a4(i)*h(i4) + b0(i) + s1*hlast(i) - (a0(i) + s1)*h(i))/(a0(i) + s1)
flag = 0:if c(i) > 0 and a > hmax(i) and hlast(i) < hmax(i) then flag = 1:ratio = (hmax(i)-hlast(i))/(a-hlast(i))
if c(i) > 0 and a < hmax(i) and hlast(i) > hmax(i) then flag = -1:ratio = (hmax(i)-hlast(i))/(a-hlast(i))
return

```

```

screenprint: rem subroutine for print to screen
print:gosub calibration
print"TIME, toelevel, errt, errc, dF.";
print using "#####.#";times(k-1)/siy;toelevel;:print using "#####.#";errt;errc;dF
return

```

```

overrelax: rem subroutine for calculation of sor w
if errclast = 0 then w = 1.6 else theta = errc/errclast:w = 2/(1 + sqrt(abs(1-theta)))
return

```

```

permfile: rem subroutine for varying perm and confined nodes
for i = 1 to n+1:input #3, j, perm(j):if j = n+1 then i = n+1
if perm(j) < 0 then input #3, lastj, stp:for ii = j to lastj step stp:perm(ii) = abs(perm(j)):next ii:rem put in intermediate perms
next i
for i = 1 to n:if perm(i) > maxperm then perm(i) = perm(i)*p:rem caution if high perms input
next i
for i = 1 to n+1
input #3, j, hmaxt, elt, c(j):rem unconfined c = 0, confined c = 1
if hmax(j) > 0 then print"Aborted: duplicate hmax at node "; j:end
hmax(j) = hmaxt: el(j) = elt
if j = n+1 then print"Nodes read in = ";i-1:i = n+1

```

```

next i :close #3
for j=1 to n:if hmax(j)=0 then print "++++ No hmax for node + + + + ";j
next j
return

```

```

boundaryconditions: rem sub to put in default values for input*****
for i=1 to n:d(i)=nspace:next i:rem node spacing
for i=1 to x:h(i)=river:next i:rem fixed heads
for i=1 to x:f(i)=h(i):next i
for i=1 to n:if h(i)=0 then h(i)=el(i)+1
if h(i)<river and q(i)=0 then h(i)=river
next i: print "Minimum initial heads set at river or 1 m above base of aquifer"
for i=n1 to n:if c(i)=0 then r(i)=infil/(1000*siy)
next i
print "Infiltration (mm/yr) is ";:print using "#####.##";infil
qt=-(qtop/1000)*y*nospace*nospace/(siy)
print "Upslope inflow m2/yr is ";:print using "#####.##";-qt*siy/nospace
for i=nb+1 to nb+1+(x-3)*(y-2) step (y-2):q(i)=qt:next i
return

```

```

risingheads:
rem subroutine for reservoir above river level
if tolevel=9 then print"Aborted":end
for ii=1 to n:hprior(ii)=h(ii): next ii: times(k)=.0000001
return

```

```

fixedheads: rem subroutine for rising reservoir, caution if Dupuit *****
select case slidenamess
case "" :rem startnode =?:finishnode=?
case else :startnode=1:finishnode=x
end select
for ii=startnode to finishnode: if tolevel>river then h(ii)=tolevel:f(ii)=tolevel
next ii
return

```

```

diskfile: rem subroutine to file input and output data to disk
open fileout$ for output as #2:print #2, time$, date$
print #2, "Spring outflows in l/min neglecting recharge"
for i=1 to n:v(i)=-v(i)*60000.0:next i:gosub arrayprint
print #2, "Net drainable head over failure surface":for i=1 to n
if hmax(i)>fullpool then v(i)=h(i)-hmax(i) else v(i)=h(i)-fullpool
if v(i)<0 or c(i)=0 then v(i)=dummycontour
next i:gosub arrayprint
print #2,"h(i)":for i=1 to n: v(i)=h(i):next i:gosub arrayprint
print #2, " times(";k;) = ";:print #2, using"#####.###";times(k)/siy
print #2, "h-el":for i=1 to n:v(i)=h(i)-el(i):next i:gosub arrayprint
print #2,"hmax":for i=1 to n:v(i)=hmax(i):next i:gosub arrayprint
print #2, "Change in piezometric head (increase on failure surface only)":neutral=0
for i=1 to n
cc=c(i):if cc<0 then cc=1:hmax(i)=-10000.0*c(i):rem *****
initialh=(hprior(i)-hmax(i))*cc:if initialh<0 then initialh=0
finalh=(h(i)-hmax(i))*cc:if finalh<0 then finalh=0
v(i)=finalh-initialh:add1=v(i)*d(i)*d(i):neutral=neutral+add1
addi=addi+initialh*d(i)*d(i):addf=addf+finalh*d(i)*d(i)
next i:gosub arrayprint

```

```

print #2,"Thrusts from pore pressures (kN) Initial, Final and Change are ";
print #2,addi*9.81,addf*9.81,neutral*9.81
print #2,"hprior":for i=1 to n:v(i)=hprior(i):next i:gosub arrayprint
print #2,:for j=1 to x:print #2, using "#####":j;:next j
print #2,:print #2,"h-hprior":for i=1 to n:v(i)=h(i)-hprior(i):next i:gosub arrayprint
print #2,:print #2,"q(i)*1e5 m3/s":for i=1 to n:v(i)=1e5*q(i):next i:gosub arrayprint
print #2,:print #2,"log10(perm(i)) m/s":for i=1 to n:v(i)=log10(perm(i)):next i:gosub arrayprint
print #2,:print #2,"r(i)*e-10 m/s":for i=1 to n:v(i)=r(i)*1e10:next i:gosub arrayprint
print #2,:print #2,"i":for i=1 to n:v(i)=i:next i:gosub arrayprint
print #2,:print #2,"c(i)":for i=1 to n:v(i)=c(i):next i:gosub arrayprint
print #2,time$,date$,slidename$
print #2,"Upslope inflow, infil, nodespace = ";
print #2, using "#####.#";qtop;infil;nspace
print #2,"Output time (years),drflow, totflow = ";times(k);drflow;totflow
close #2
print:print "Steady state Pz levels and parameters filed on ";fileout$
return

```

```

presentstate: rem file present state
open file3out$ for output as #3
print #3, nb,n,.00001
for i=1 to nb
print #3, id(i,1),id(i,2),alpha(i),beta(i),xn(i),yn(i),dp(i),d(i),f(i),el(i),h(i)
next i
for j=n1 to n
print #3, id(j,1),id(j,2),id(j,3),id(j,4),el(j),h(j),d(j),bk(j),hp(j),r(j),q(j)
next j
close #3 :print "Filed data on "file3out$
return

```

```

arrayprint: rem print the array to disk
for i=2*x+y-2 to x+y-1 step -1:print #2, using "#####.#"; v(i);:next i: print #2, " "
for i=2*x+y-1 to nb:ii=i
for ii=i to i+(x-2)*(y-2) step y-2:print #2, using "#####.#"; v(ii);:next ii
print #2, using "#####.# ";v(3*x+2*y-3-i):next i
for i=1 to x:print #2, using "#####.#";v(i);:next i: print #2, " "
return

```

```

driveflows: rem subroutine for drive flows *****
totflow=0
rem for i= 281 TO 282 :gosub flownodes:next i
return

```

```

flownodes: rem sub for nodes in drive
if c(i) >= 0 then c(i)=-hmax(i)/10000.0:if hmax(i) < drlevel then print "Error";i
hmax(i)=drlevel + 5
totflow=totflow+v(i)
return

```

```

reservoirrise: rem reservoir rise programme
gosub safetyfactor:rem calculate safety factor relative to ideal drainage *****
if int((k-2)/ofreq)=(k-2)/ofreq then
print #1,using "#####.#";times(k-1)/(siy/12);h(1);
for jk=1 to nc:print #1,using "#####.#";ch(jk);:next jk
print #1,using "#####.#";dF

```

```

end if
tm = times(k)*12:rem time in months
if tm > tstage(ns) then
    damw = rstage(ns)
else
    for i = ns-1 to 1 step -1
    if tm > tstage(i) then damw = rstage(i) + (rstage(i+1)-rstage(i))*(tm-tstage(i))/(tstage(i+1)-tstage(i)):exit for
    next i
end if
if damw > fullpool then toelevel = fullpool:print "Error damw";damw
if damw < river then toelevel = river else toelevel = damw
program = 1:if tm > startdrive then drflow = 1
return

safetyfactor:
rem Calculate the integral of the piezometric head over the confining aquiclude, relative to the ideal drainage case.
integralh = 0: for i = 1 to n
    upper = h(i):if h(i) < hmax(i) then upper = hmax(i)
    lower = toelevel:if toelevel < hmax(i) then lower = hmax(i)
    head = upper-lower:integralh = integralh + c(i)*d(i)*d(i)*head
next i
dFh = Fsens*integralh*9.81*100:rem dFh is percent change in F from ideal
if toelevel > river then dFp = dF*(toelevel-river)/(fullpool-river) else dFp = 0
dF = dFi + dFp + dFh
return

parameters: rem select slidename for parameters to input
input "Enter slidename in lower case ";slidename$
select case slidename$
    rem case "example":gosub example
    case else:print "No parameters defined for this slidename ":end
end select
siy = 86400.0*365.0:rad = 180/(atn(1)*4)
return

example: rem (slide NIC) sub-basal aquifer only
x = 31:y = 20:river = 158:fullpool = 194.5:iterations = 1000:extremehead = 500
dummycontour = -3:qtop = 66.2:infil = 0 :nspace = 100: leakance = 0 :w = 1.6
f$ = "th.dat":open f$ for input as #1: rem node file is mesh.dat
p$ = "k.dat": open p$ for input as #3
permmult = 1:drelax = 50:rem perm multiplier for depth of relaxed rock in m
rem below fai sur. (perm reduces linearly to perm at drelax)
p = 1e-7 :s = .015 :sc = .005 :nu = 3 :eta = .1 :rem predominant perm, storativity
rem storage coeff and depth of subslide aquifer,
rem nu and eta smoothing for minimum water thickness
input #1, nb, n, errt :mintransmissivity = 1e-9:maxperm = 1e-2:slopefactor = 1
drflow = 0 :drlevel = 197:dim dn(1):tmult = 1.2315 :tadd = 5/365:ofreq = 1:screenfreq = 5
rem drflow 0 for no drives,drlevel is drive level
rem tmult & tadd specify output timestep, ofreq is output frequency
analysismethod$ = "ordinary":f0 = 1.05:alpha0 = 28:alpha1 = 15:phi = 25:phim = 25
pg = 23:slidedepth = 150:slidelength = 1000:slidewidth = 2000
dfi = 49.66:dff = -2:rem change in F from original to ideal (river and full pool)
nc = 5:dim h(n+1),cp(nc),ct(nc),ch(nc),ce(nc),ceer(nc),cc(nc)

```

```

rem no of controls,identifiers,targets, calc h, calc error & coeffs
rem define target heads at controls ***** put in coeff and lower node only
for i=1 to nc:read cp(i),ct(i),cc(i),ce(i):next i
data 240,0,1,240
data 237,0,1,237
data 234,0,1,234
data 231,0,1,231
data 228,0,1,228
rem define reservoir filling program
ns=8:dim rstage(ns),tstage(ns):for i=1 to ns:read rstage(i),tstage(i):next i
data 138,0, 175,1, 175,2, 185,15, 185,20, 194.5,24,194.5, 26,194.5,28
return

```

PREFLOW

```

cls:print"Pre-processing program for regional groundwater flow,
print"to generate mesh of x nodes along river and y nodes up the slope "
print"then read in data files for aquifer boundaries.":print
Input "Number of nodes along the river side of the mesh "x
Input "Number of nodes along the side running upslope "y
Input "Average river level ";h
nb=2*(x+y)-4:n=x*y:c3=x+y-1:c4=2*x+y-2:r=y-2:s=x-2:t=c4+1
t$="MESH.DAT":open t$ for output as #1
print #1, using "#####";nb;n;;print #1, .00001
rem print boundary nodes
for i=1 to x-1
print #1, using "#####"; nb+r*(i-1);i+1;;gosub boundary:next i
i=x:print #1, using "#####";x+1;x-1;;gosub boundary
k=0
for i=x+1 to c3-1
print #1, using "#####";i+1;n-k;;gosub boundary:k=k+1:next i
i=c3:print #1, using "#####";c3-1;c3+1;;gosub boundary
k=t+s*r
for i=c3+1 to c4-1:print #1, using "#####";k;i+1;;gosub boundary:k=k-r:next i
i=c4:print #1, using "#####";c4+1;c4-1;;gosub boundary
for i=c4+1 to t+r-2:print #1, using "#####";i+1;i+r;;gosub boundary:next i
print #1, using "#####";1;t+2*r-1;;gosub boundary
rem interior nodes
k=1
for i=t+r to n
i1=i+r:i2=i-1:i3=i-r:i4=i+1
if i1>n then gosub calci1
gosub calci2:rem check i2
gosub calci4:rem check i4
print #1, using "#####";i1;i2;i3;i4;i5;i5;i5;i5;i5
next i
print "Mesh generated on file ";t$:print
close #1
gosub techbaseinput
end

```

boundary:

```
dim a(9):rem subroutine to put in boundary parameters
for j=1 to 9:a(j)=0:next j
a(1)=1:if i <= x then a(1)=0:a(2)=1
if i <= x then a(3)=0 else a(3)=1
if i > x+y-1 and i < 2*x+y-2 then a(3)=0
if i=1 then a(3)=.7
if i=x then a(3)=.7
if i=x+y-1 then a(3)=.7
if i=2*x+y-2 then a(3)=.7
a(4)=(abs(1-a(3)*a(3)))^0.5
a(5)=0
if i <= x then a(7)=h:a(9)=h
for j=1 to 9:print #1, using "#####.#";a(j);:next j
print #1,
return
```

```
calci1: rem subroutine for i1
k=n+1-i:i1=x+k
return
```

```
calci2: rem subroutine for i2
for jj=1 to s
if i=t+jj*r then
k=(i-t)/r:i2=c4-k
end if
next jj
return
```

```
calci4: rem subroutine for i4
for jj=t+2*r-1 to n step r
if i=jj then k=(i+1-t)/r:i4=k
next jj
return
```

techbaseinput:

```
rem strip techbase files for regional flow model
xy=x*y:c3=x+y-1:c4=2*x+y-2:t=c4+1:r=y-2:s=x-2
dim f(xy), b(xy),hmax(xy),c(xy),v(xy),bb(xy)
input"Enter filename for upper surface (or null to terminate)";f$
if f$="" then end
Print"Enter number of lines of description at the front of each file "
Input"Note, add one line for any comma present.";nline
print"Enter 0 if upper surface is unconfined (free draining boundary),
rem only 2 surfaces to input or create if sur=0 or 2
input" 2 if fully confined or 3 if part confined (No. of surfaces)";sur
if sur>1 then ci=1
open f$ for input as #1:gosub finput:close #1
for i= 1 to xy:f(i)=v(i):next i
if sur=0 or sur=2 then
for i=1 to xy:hmax(i)=f(i):c(i)=ci:next i
end if
if sur=3 then
rem need 2 more surfaces
print"Enter filename for upper aquiclude, (note 0 data values in this file
```

```

input" imply local unconfined conditions");upaq$
rem if lower and upper values equal, implies confined
open upaq$ for input as #1:gosub finput:close #1
for i=1 to xy: hmax(i)=v(i):c(i)=1:if v(i)=0 then hmax(i)=f(i):c(i)=0
next i
gosub basesurface
end if
gosub wdata:rem write data file
return

```

```

finput: rem subroutine for techbase file input
for i=1 to nline:input #1, tt$:next i:print"River node RLs:"
j=1
500 input #1,tt,tt,v(j):print v(j)
for iii=t+r*j-1 to t+r*(j-1) step -1
input #1,tt,tt,v(iii):next iii:
input #1,tt,tt,v(c4+1-j)
if j<x-1 then j=j+1:goto 500
for i=x to c3
input #1,tt,tt,v(i)
next i
return

```

```

wdata: rem subroutine to write data
t$="K.DAT":open t$ for output as #1
print #1, using "#####";n+1;n+1
for i=1 to xy:print #1, using "#####";i:hmax(i);b(i);c(i):next i
print #1,using "#####";n+1;n+1;n+1;n+1
close #1
print "Aquifer bounding surface levels written to file "; t$
print"No. of error points and total error are: "count;total
return

```

```

basesurface:
input"Enter filename for base of flow region (nul for constant depth)";b$
if b$>" " then
open b$ for input as #1:gosub finput:close #1
for i=1 to xy:b(i)=v(i):next i
else
input"Enter constant depth to be created below overlying surface ";cd
for i=1 to xy:b(i)=hmax(i)-cd:next i
end if
return

```

PC_TBASE

```

cls:print "PC_TBASE.BAS Converts matrix of local mesh co-ordinates to
print"Survey Grid for techbase contour, PUT DISK INTO A."
input" Filename to be prepared for techbase contour (USE lower case) ";t$
input" Number of lines to remove from top (normally 1)";blank
open t$ for input as #1
dim n(44,44),e(44,44),rl(44,44)
input"slide name, or enter 0 for new slide";sn$
select case sn$
rem case
rem case
case "example" : gosub example
case else : gosub manual
end select
y=y-blank
while blank > 0 :input #1, t$ :blank=blank-1 :wend :rem remove lines at top
a=theta*3.1415927/180.
print"radian bearing is "; a
rem input matrix rls
for j=y to 1 step -1
for i=1 to x
input #1, rl(i,j)
total=total+rl(i,j)
next i
next j
if not eof(1) then input #1, tt$
print "read check (should be nothing) = ";tt$
rem see if additional number needed to avoid zeros
print"average of all numbers is ";total/(x*y)
input"hit enter or small number to avoid zeros ";add
rem calculate eastings and northings for Survey Grid
for i=1 to x
for j=1 to y
e(i,j)=e(1,1)+(i-1)*nspace*cos(a)+(j-1)*nspace*sin(a)
n(i,j)=n(1,1)-(i-1)*nspace*sin(a)+(j-1)*nspace*cos(a)
next j
next i
input"name of output file (a: assumed, use lower case, no extension *****);o$
if o$="" then o$="techb.out"
xout$="a."+o$:open xout$ for output as #2
gosub xprint :rem print out
print"output file created on ";xout$
close #1:close #2
end

manual:
print"Slide unknown, proceeding with manual input: "
input"x ";x
input"y ";y
input"node spacing";nspace
input"origin at bottom left point of matrix, northing ";n(1,1)
input"origin at bottom left point of matrix, easting ";e(1,1)
input"bearing from matrix origin along first column (y dirn) ";theta
return

```



```

xprint:
rem sub to print data
  for i=1 to x
    for j=1 to y
      print #2,using "#####.### ";n(i,j);e(i,j);rl(i,j) + add;
      print #2," ";o$
    next j:next i
  return

```

```

example:
x = 29;y = 19:n.space = 100:n(1,1) = 661194.9:e(1,1) = 282958.3:theta = 30
return

```

PZPOINTS

```

cls:print"Convert regional sections to POINT data for stability analysis
print"Put blank disk in a: drive"
on error goto erhandler:count=0:rem sign depends on way input file is viewed
input"Slidename (NB use lowercase) ";slidename$
input"Model number for title ";modnumber$
xout$="a:\"+ modnumber$+".tex"
print xout$
input"number series for points (default is 400)" ;istart
if istart=0 then istart=400
print xout$
open xout$ for output as #2:print #2,"$ piez lines for ";slidename$;" model ";modnumber$
select case slidename$
  rem case
  case "example":gosub example
  case else:print "Unknown slide. Add to program code ":end
end select

```

```

close #2:print "No. of files written = ";count
print "Finished with output ready on file ";xout$
end

```

```

erhandler:
print "Aborted with error ";err, " at line "; erl
end

```

```

example:
sign = 1
xin$="t.con" :bsdistance = 630 :gosub xinput
xin$="u.con" :bsdistance = 670 :gosub xinput
xin$="v.con" :bsdistance = 688 :gosub xinput
xin$="w.con" :bsdistance = 726 :gosub xinput
xin$="y.con" :bsdistance = 725 :gosub xinput
return

```

```

xinput:
open xin$ for input as #1:start=istart :i=0
print #2," POINTS $ for piez. line on section ";xin$
while not eof(1)
  i=i+1: input #1, x,y

```

```
print #2, start + i; print #2, using "#####.#"; sign*(x-bsdistance); y
wend
print #2, "PIEZ 1";
for j = 1 to i: if j > 1 and int((j-1)/12) = (j-1)/12 then print #2, " - "
print #2, start + j; :next j
print #2, " "
count = count + 1; print xin$; " file written "
close #1
return
```

APPENDIX 3

SENSITIVITY ANALYSES FOR LANDSLIDE SUBMERGENCE

The sensitivity of slope stability analyses to material strengths, failure surface geometry and groundwater conditions.

A3.1 INTRODUCTION

When a dormant or active landslide is to be submerged by a proposed reservoir, an aspect of preliminary interest is the sensitivity of safety factor changes assuming changes of specific geotechnical or geohydrological characteristics. The features of interest are:

- Loss of frictional strength (with saturation or displacement)
- Loss of cohesive strength
- Differences in density from assumed values
- Changes in groundwater levels (within a slide)
- Changes in reservoir levels (external to a slide)
- Rate of change of reservoir levels (rise or rapid drawdown)
- Changes in aquifer boundary conditions

This chapter provides charts for examining sensitivity of any slide to changes in basic properties. These solutions are derived simply by resolving forces perpendicular and parallel to the failure surface of a translational slide - an approximation which is generally quite adequate for practical purposes, when determining **changes in**, rather than **absolute** values of safety factors for gently arcuate slides. Slides with depth to length ratios greater than about 1:10, would need more rigorous analyses. It is shown that in practice, the main sensitivity of concern arises from changes in assumed boundary conditions of aquifers, with the consequent changes in piezometric pressures on failure surfaces. Simple, yet accurate methods for calculating safety factor changes under any changes in piezometric pressures are described. A worked example is provided which demonstrates that only a few minutes of straightforward calculation is required with no need for computer methods.

The parameters of interest in slide modelling are:

- Slope length along the failure surface (L)
- Depth of reservoir above the slide toe (R)
- Average inclination of the failure surface (β)
- Average inclination of the failure surface in the region of piezometric rises (β_1)
- Average vertical depth of slide (Z)
- Average vertical depth from the groundwater surface to the failure surface (mZ)
- Soil unit weight(ρ)
- Effective friction angle of the failure surface soil (ϕ')
- Effective cohesion of the failure surface soil (c')
- Safety factor (F)

In some cases it is desirable to consider that F is 1.0 initially. In this case one or more of the above parameters may be a dependent variable, ie implicit or dictated by the equations for equilibrium.

A3.2 LOSS OF FRICTIONAL STRENGTH

Frictional strength may be affected by saturation (the wetting effect) or strength degradation through particle attrition. Figs. 1a to 1c show sensitivity of safety factor changes to decreases in friction angle for given values of cohesion and average slide depth.

Assumptions:

Soil unit weight	23.5 kN/cu m
Initial friction angle	25 degrees
Initial safety factor	1.0
No initial pore water pressure	
Slope inclination - dependent variable.	

Note that these figures assume the entire failure surface will suffer a uniform decrease in friction angle, therefore if (as will usually occur with submergence) only part of the failure surface becomes saturated, the safety factor changes shown should be diminished in proportion.

In summary, these show that approximately similar decreases in safety factor will occur regardless of failure surface depth. The actual value of cohesion has little effect except in shallow slides.

Typical worked examples for this and the following parameters will be given below.

A3.3 LOSS OF COHESIVE STRENGTH

Cohesive strength may be affected by saturation. Figs. 2a to 2c show sensitivity of safety factor changes to decreases in cohesion for given values of friction angle and average slide depth.

Assumptions:

Soil unit weight	23.5 kN/cu m
Initial cohesion	50 kPa
Initial safety factor	1.0
No initial pore water pressure	
Slope inclination - dependent variable.	

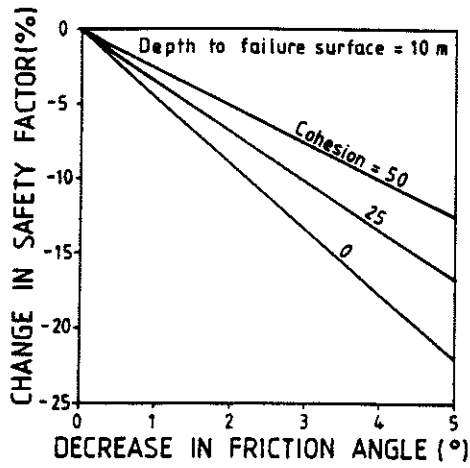


Fig 1a

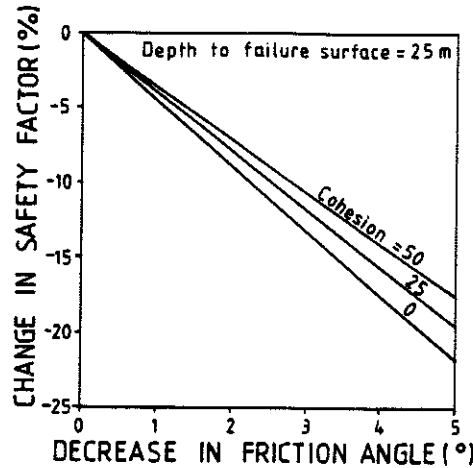


Fig 1b

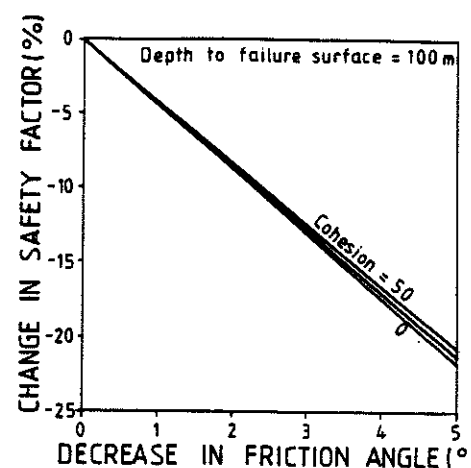


Fig 1c

SENSITIVITY TO DECREASE IN FRICTION ANGLE

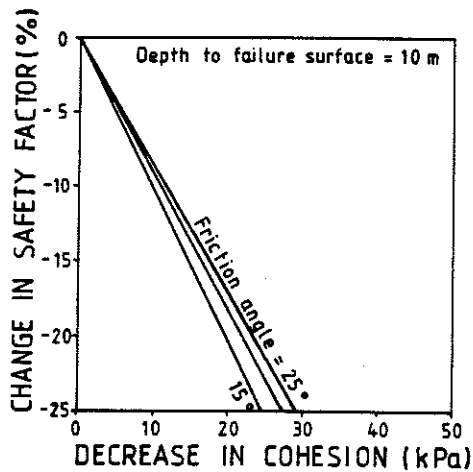


Fig 2a

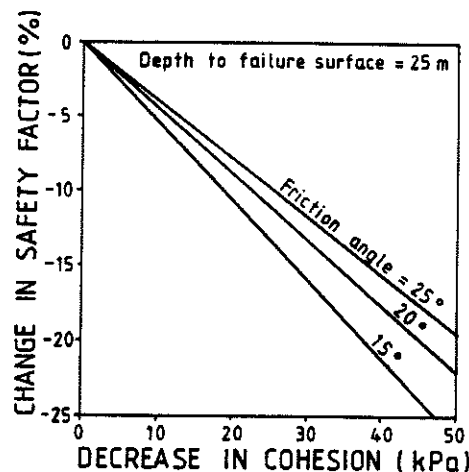


Fig 2b

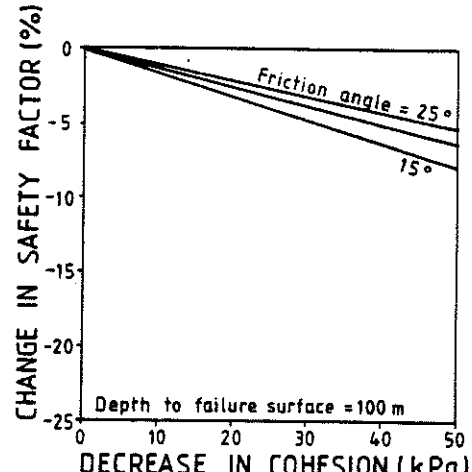


Fig 2c

SENSITIVITY TO DECREASE IN COHESION

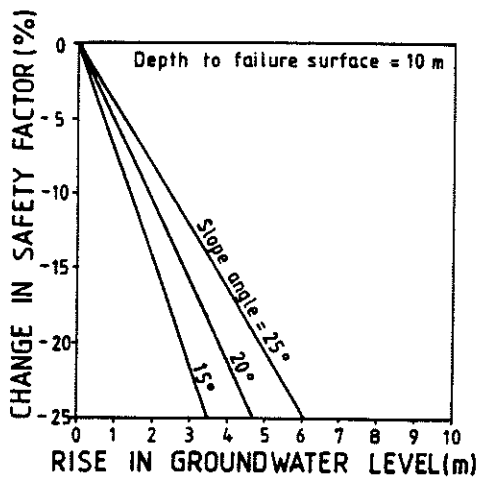


Fig 3a

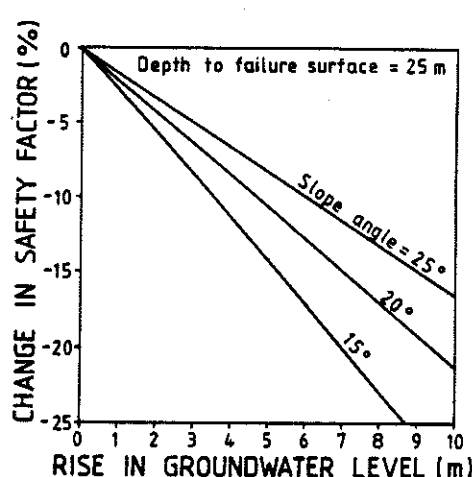


Fig 3b

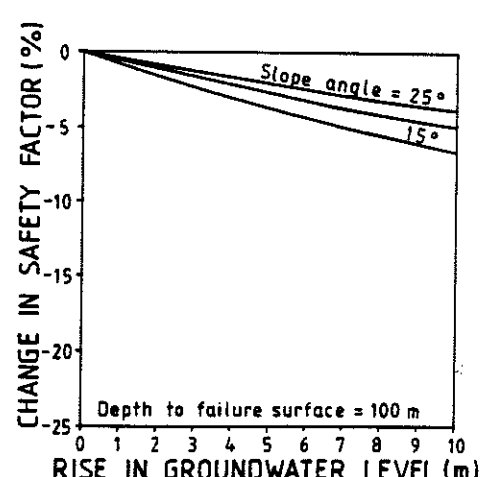


Fig 3c

SENSITIVITY TO INCREASE IN PIEZOMETRIC LEVEL

Note that these figures assume the entire failure surface will suffer a uniform decrease in cohesion, therefore if (as will usually occur with submergence) only a proportion of the failure surface becomes saturated, the safety factor changes shown should be diminished in proportion.

In summary, these show that for variable cohesion, shallow slides would be affected much more than deep seated slides and there is little sensitivity to the initial cohesion value.

A3.4 RISE IN GROUNDWATER LEVEL

The usual effect of reservoir filling will be to raise groundwater levels within the slide. Figs. 3a to 3c show sensitivity of safety factor changes to increases in groundwater levels for given values of slope inclination and average slide depth.

Assumptions:

Soil unit weight	23.5 kN/cu m
Friction angle	25 degrees
Cohesion	0 kPa
Initial safety factor	1.0
Initial pore water pressure - dependent variable	

Notes:

(i) These figures assume the entire failure surface will suffer a uniform rise in groundwater levels, therefore if (as will usually occur with submergence) only a proportion of the failure surface is affected, the safety factor changes shown should be diminished in proportion.

(ii) These are changes in groundwater (phreatic surface) levels. Changes in piezometric levels will produce similar effects, which can be calculated with slightly greater accuracy by dividing the safety factor change shown by the square of the cosine of the slope inclination, $(\cos\beta)^2$. This factor is often close to 1.0, and will not change results greatly.

In summary, these show that shallow slides are more affected by rises in groundwater level than deep slides.

A3.5 DIFFERENCES IN DENSITY OF THE SLIDING MASS

The effect of density changes is best considered in terms of the neutral point. Most slides with gently arcuate concave upward failure surfaces will experience an increase in safety factor for an increase in gravity loading towards the toe, with the converse applying toward the head of the slide. Somewhere about one third to one half the way up the slide, a point can be located where an increase in vertical loading has no effect on stability. This point is defined as the neutral point for the section. Submergence usually affects only the lower part of the slides of interest, and the density of the slide mass can only increase as water infiltrates. Therefore submergence below the neutral point will generally provide a slight increase in density, with consequent very slight increases in safety factors. The effect has generally been neglected (conservatively) as of little significance to safety factor changes on submergence. However, it may be readily quantified using simple stress vectors, as shown below.

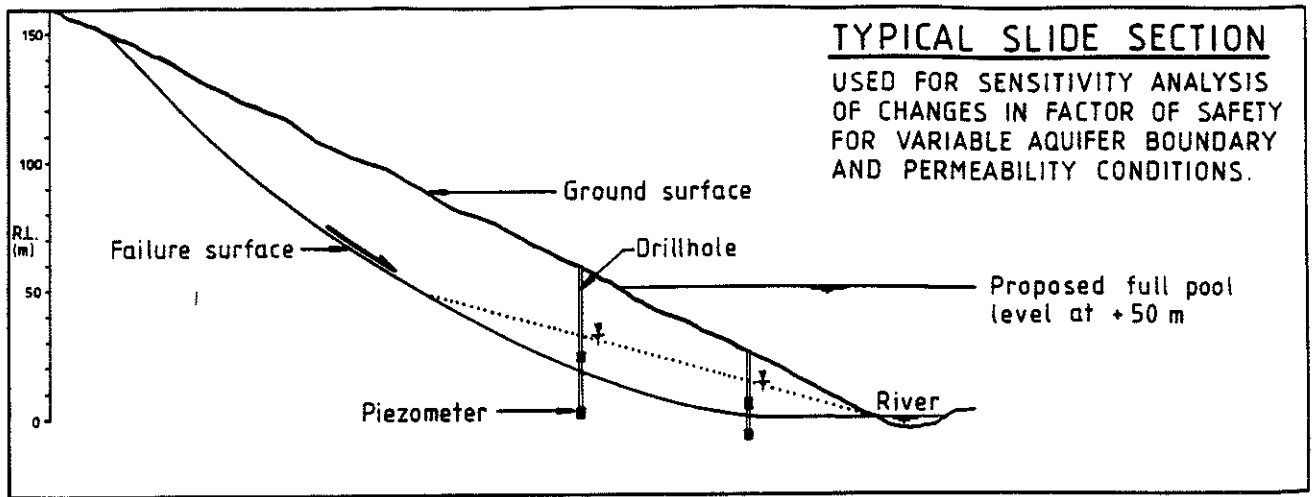
A3.6 CHANGES IN AQUIFER BOUNDARY CONDITIONS

The distribution of permeability and the sources of recharge dominate the effects of piezometric changes within a slope subjected to reservoir level changes. Varying permeability within aquifers and the presence of aquitards or aquicludes between aquifers, all effect the results of predictive modelling. Without realistic prediction of changes in piezometric conditions likely to occur with reservoir filling it is not practical to estimate changes in safety factors and hence predict whether displacement can be expected, or how far slides will travel before movements result in sufficient slope deflation to restore safety factors to prior values.

To illustrate some of the main difficulties in reliable modelling, the extremes of piezometric response of a model (typical) slope are shown below. Fig. 4.0 illustrates a slide, 350 m long with a maximum depth of about 50 m. A typical slope inclination of 2:1 (27 degrees) has been adopted and it is assumed that 2 drillholes have been installed on the section to determine piezometric conditions above and below the inferred failure surface. The dotted line shown, indicates only the governing piezometric pressure on the failure surface. (Using the effective stress principle, the piezometric pressure governing stability will be the higher of the pressures above or below the failure surface.) The slope is to be subjected to a 50 m rise in reservoir level.

Figures 4.2 to 4.8 show the full ranges of ultimate steady state piezometric rises that might occur together with an indication of the type of soil characteristics and boundary conditions that would lead to each response. Two extremes of rapid reservoir change were included for appreciation of rapid rise (Fig. 4.9) and rapid drawdown (Fig. 4.10). (Note that much more adverse rapid drawdown models could be generated by using full pool conditions such as those shown in Figs 4.7 or 4.8).





The piezometric lines drawn were then analysed to determine mobilised friction angles (assuming zero cohesion) and changes in safety factor from the initial condition.


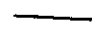

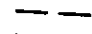





TYPICAL SLIDE SECTION
 USED FOR SENSITIVITY ANALYSIS
 OF CHANGES IN FACTOR OF SAFETY
 FOR VARIABLE AQUIFER BOUNDARY
 AND PERMEABILITY CONDITIONS.

KEY TO SECTIONS

SOIL TYPES

-  Insensitive to permeability
-  High permeability
-  Moderate permeability
-  Low permeability

-  Ground surface.
-  Soil boundary.
-  Impermeable failure surface.
-  Permeable failure surface.
-  Prior, higher piezometric line.
-  Ultimate piezometric line.
-  Base of flow region.

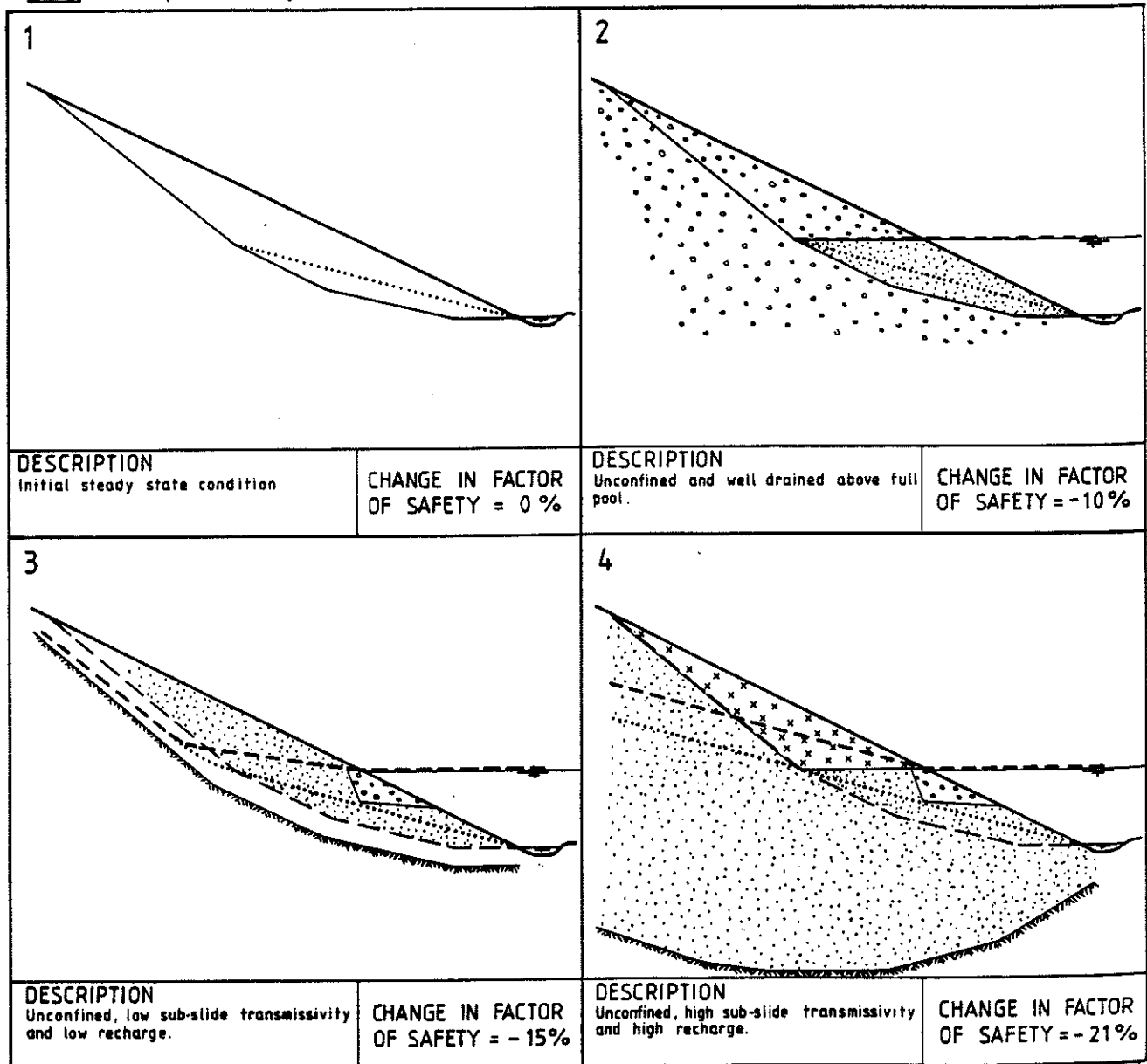


Fig 4

SENSITIVITY TO RESERVOIR RISE

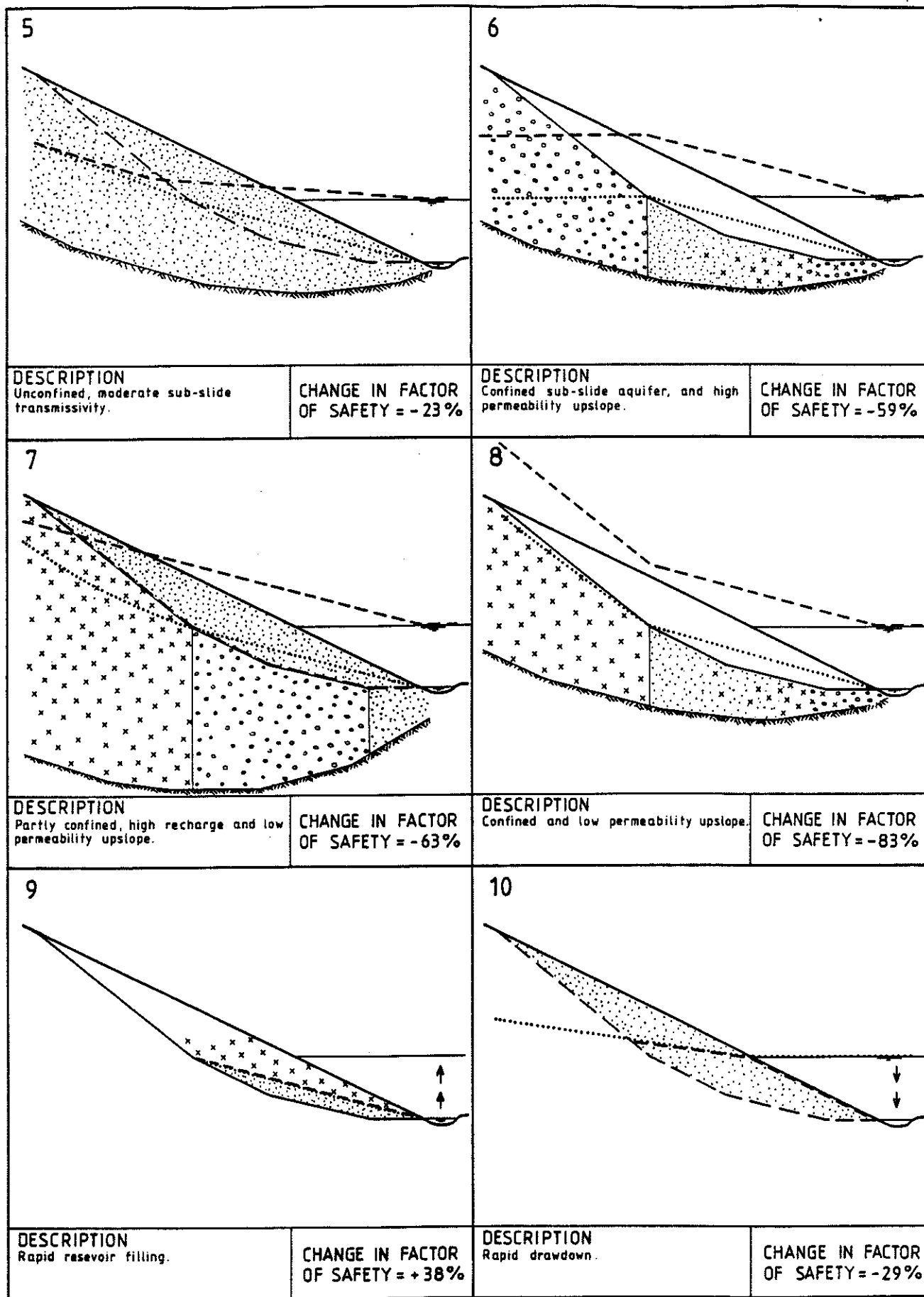


Fig 4

SENSITIVITY TO RESERVOIR RISE

Results:

Model Figure	Mobilised Friction (degrees)	Change in Safety Factor (%)	Comments
4.1	24.2	0	Initial conditions
4.2	26.6	-10	Unconfined, well drained above full pool
4.3	27.8	-15	Unconfined, low sub-slide transmissivity
4.4	29.6	-21	Unconfined, high sub-slide transmissivity
4.5	30.2	-23	Unconfined
4.6	47.5	-59	Confined, high permeability upslope
4.7	50.2	-62	Unconfined, high recharge
4.8	69.7	-83	Confined, low permeability upslope
4.9	18.0	+38	Rapid reservoir filling
4.10	32.3	-29	Rapid drawdown

In summary, it is apparent that the most adverse effects come from high recharge conditions and/or where confined aquifers are present.

A3.7 COMBINED SENSITIVITY

To obtain a realistic perspective of decreases in safety factor caused by wetting effects (loss of frictional strength and loss of cohesion) or alternative aquifer boundary conditions, it is appropriate to look at an example. For the slide shown in Fig. 4.5, with maximum depth 50 m, the average failure surface depth is about 25 m. The figure indicates that about 5% of the failure surface will change from the unsaturated to saturated state.

(i) Loss in frictional strength:

If testing demonstrated a decrease of 1 degree in frictional residual strength as a result of wetting, then from Fig. 1b, the decrease in safety factor for a 25 m deep surface is about 4%. Taking into account the proportion of failure surface affected would produce a safety factor change -

$$- 4\% \times 5\% \quad \text{ie about } - 0.2\%.$$

(ii) Loss of cohesive strength:

For a loss in cohesion of 5kPa on wetting, Fig. 2b for a 25 m deep slide indicates a decrease in safety factor of about 2%. Taking into account the proportion of failure surface effected suggests a safety factor decrease of -

$$- 2\% \times 5\%, \quad \text{ie about } - 0.1\%$$

(iii) Change in safety factor from changes in pore pressures:

Groundwater rise and reservoir rise affect pore pressures within the slope and water pressures acting externally on the slope.

The two components act in opposition and their net effect may be determined from the stress vector concepts discussed below, in conjunction with Fig. 3 (reduced for the proportion of the failure surface affected). However, for this case the resultant effect has already been determined in Fig. 4.5 (no additional reduction for failure surface proportion is required). This indicates a reduction of -

$$\text{about } - 3\%$$

(iv) Combined change in safety factor:

Combining the above gives a net change in safety factor of -

$$\text{about } (- 0.2 - 0.1 - 23) \%, \quad \text{ie about } - 23.3\%$$

The point which this example is intended to convey is that the **aquifer boundary conditions strongly dominate any sensitivity analysis, for submergence of moderate or large slides**. Shallow slides which are initially unsaturated and are to be submerged for large proportions of their failure surfaces may be significantly affected by strength losses on saturation as well as decreases in stability caused by positive pore pressures.

A3.7 SIMPLIFIED METHOD OF SLOPE ANALYSIS

A straightforward method of slope analysis, which transparently demonstrates what is happening within a slope subjected to stress changes is to plot the average shear and normal effective stress acting on the (potential) failure surface of interest, as described in the resistance envelope procedure (Appendix 1).

The basis of the method is that any potential failure surface passing through a soil (with either known or unknown strength parameters) may be analysed using any of the conventional methods of limit equilibrium, to calculate the average shear and normal effective stresses on that surface.

The appropriate points for several of the examples shown in Fig. 4 have been plotted on Fig. 5a. Note that no soil strength parameters need be assumed. Points P1 (initial condition), P2 etc apply to the respective conditions shown on Figs 4.1, 4.2 etc.

Fig. 5b shows the stress vectors for the failure surface as it is subjected first to rapid reservoir filling (P9), then to a steady state full pool condition (P3) then to rapid drawdown (P10). The following observations can be made, which when related to the physical situation, become self evident.

(i) For practical purposes the same average shear stress is mobilised for the initial condition and rapid drawdown on the failure surface - points P1 and P10. (Very slight differences do occur because of assumptions used by the computer program regarding the way in which stresses within the slide are distributed.)

(ii) The same average shear stress is mobilised at full pool level for all various cases of differing piezometric conditions. (P2 to P8.)

The above 2 observations are physically logical because the only external force acting on this slide to cause shear stress (besides gravity), is the reservoir thrust.

(iii) Increasing piezometric levels within the slide correspond simply to reduced normal effective stresses, at constant shear stress, as expected from statics.

(iv) Changes in safety factors may be determined directly from this diagram if the ratio $c'/\tan\phi'$ is known. (Neither c' nor ϕ' need be known explicitly.) A construction line required is to connect the point ($\sigma = -c'/\tan\phi'$, $\tau = 0$) to the initial stress state (P1).

For simplicity of illustration two examples are shown on Fig. 5c. If $\phi' = 0$, the horizontal thick dashed line applies. If $c' = 0$, the solid inclined line applies. The change in safety factor from the condition at stress state P1 is then given simply by subtracting 1.0 from the ratio of ordinates of the constructed line to the point in question.

As example, the change in safety factor for point P3 assuming cohesionless soil (solid line) is $(157/185)-1.0 = -0.151$ or -15.1% .

Similarly for cohesive and frictionless soil (dashed line), the change in safety factor for Point P3 is $(212/185)-1.0 = 0.146$ or $+14.6\%$.

These examples demonstrate the opposing findings which result from considering either cohesionless or frictionless soils.

(v) Absolute values for safety factors may be determined directly by constructing the Mohr envelope and determining simply the ratio of ordinates of the constructed line to the stress condition in question. Slight corrections are required if the strength envelope is markedly curved but for most practical cases this may be neglected. The stress vectors

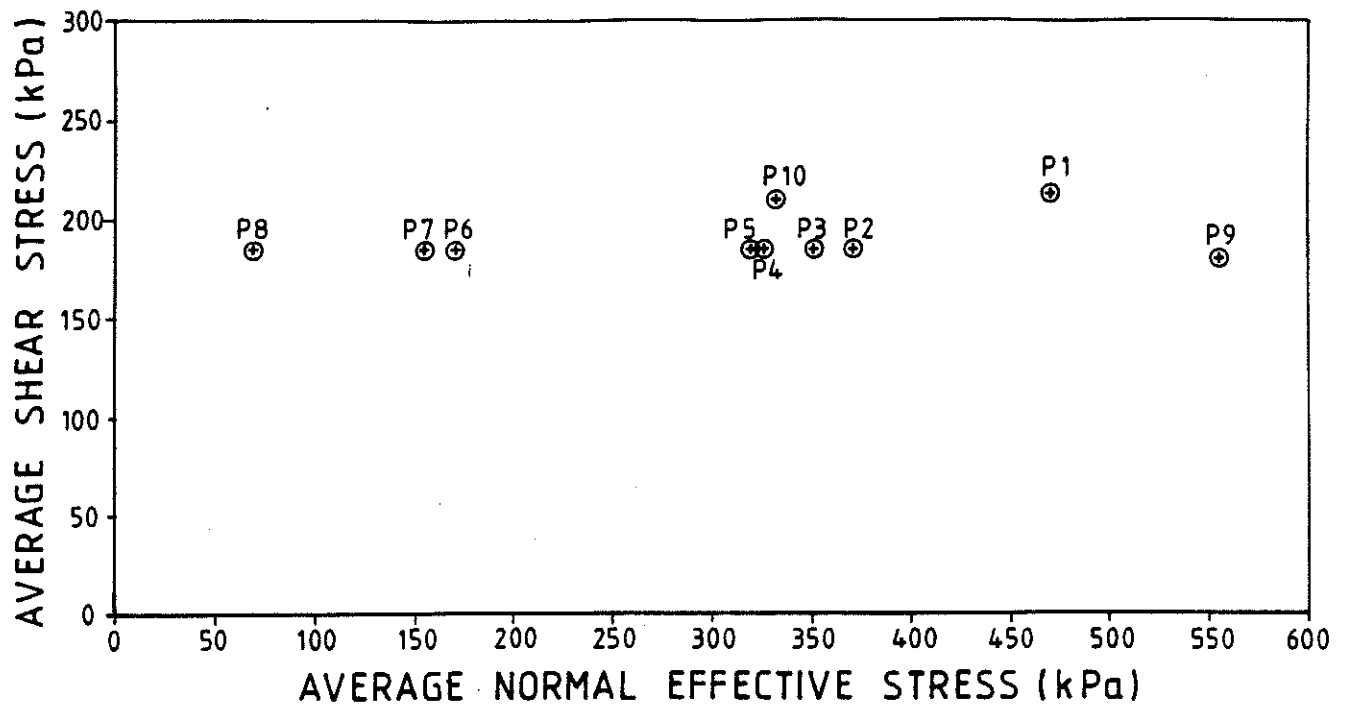


Fig 5a AVERAGE STRESS CONDITIONS ON FAILURE SURFACE

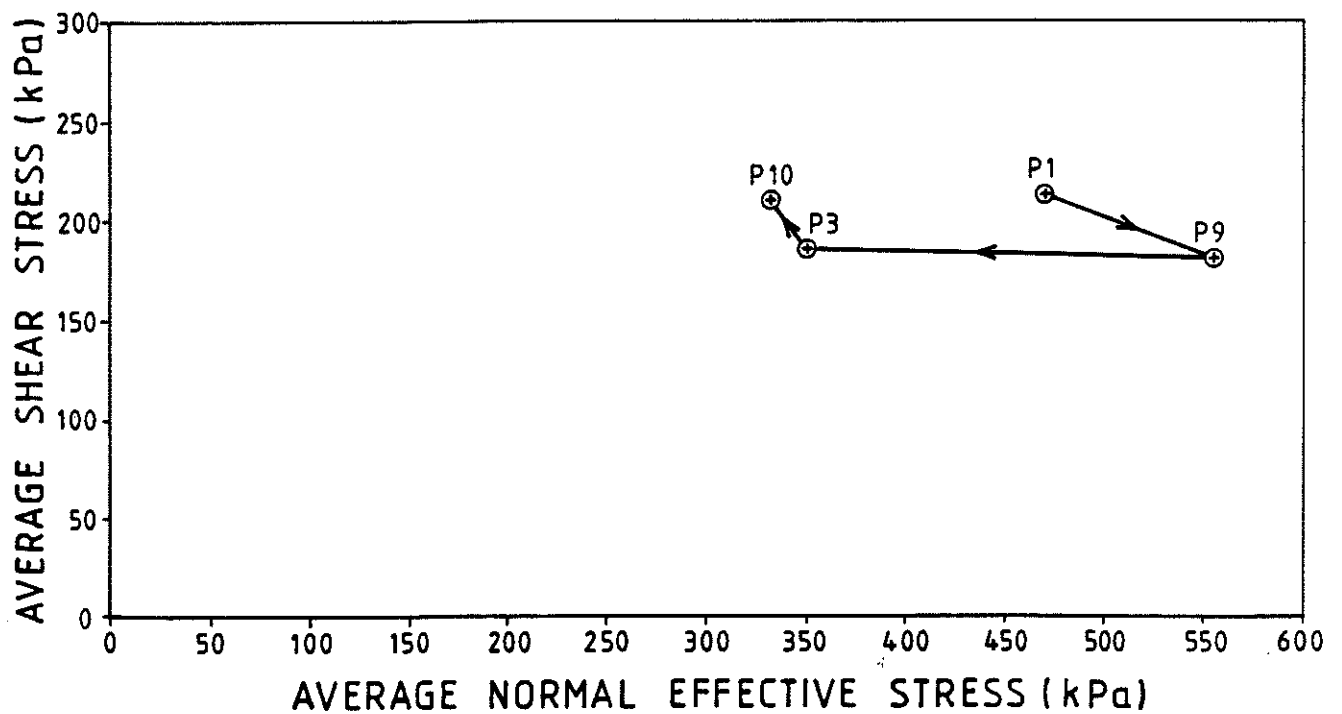


Fig 5b STRESS VECTORS FOR CHANGED PIEZOMETRIC CONDITIONS

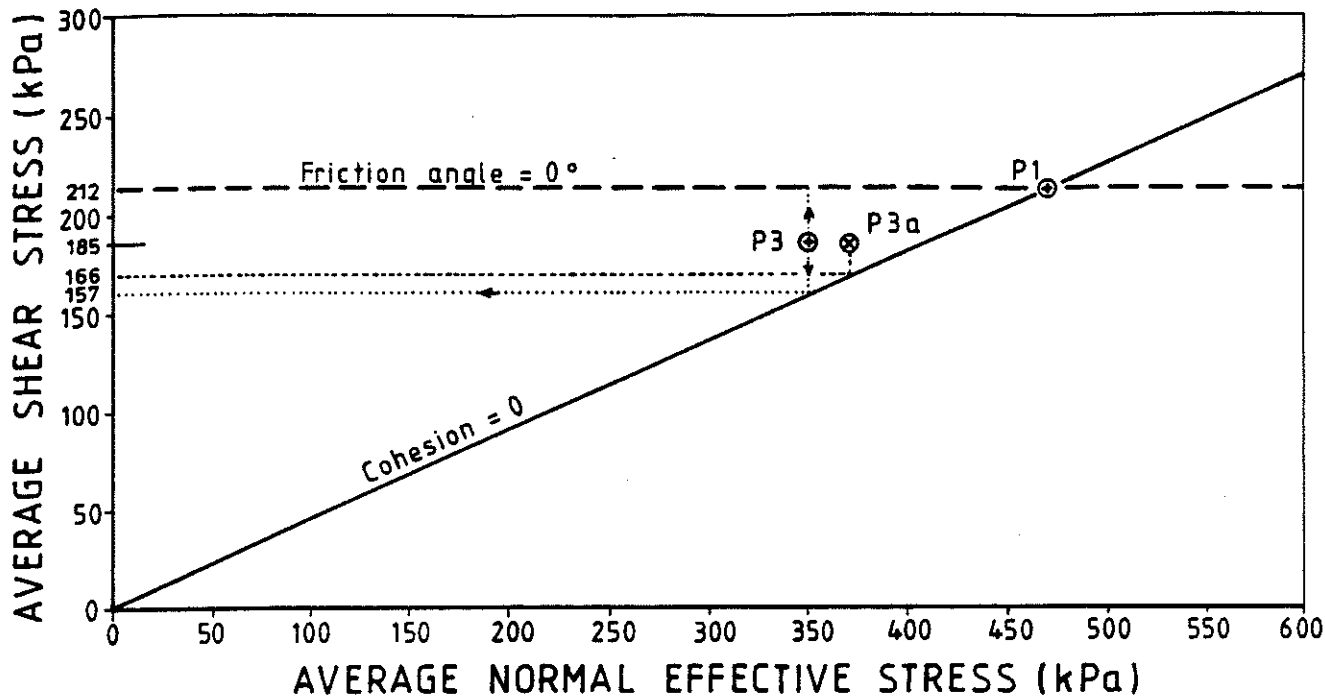


Fig 5c EXAMPLES FOR DETERMINING SAFETY FACTOR CHANGES

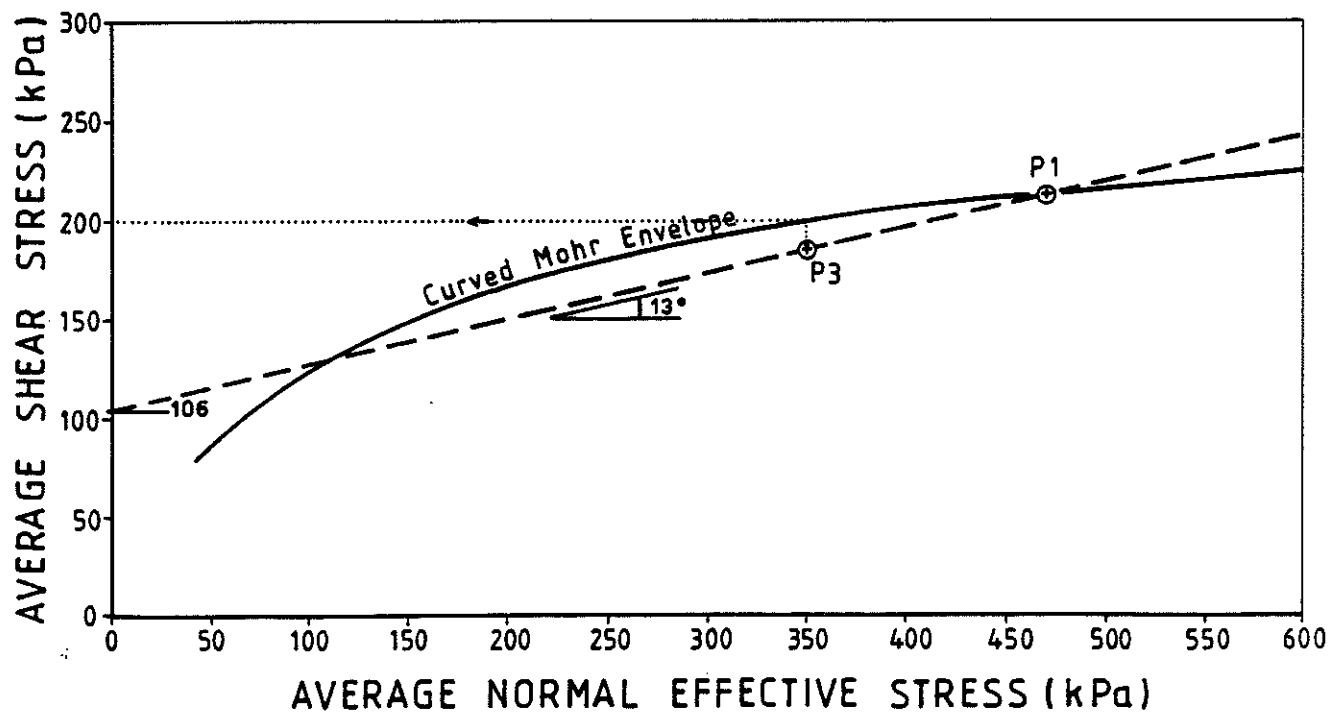


Fig 5d EXAMPLES FOR DETERMINING THE ABSOLUTE SAFETY FACTORS

drawn in relation to Mohr envelopes readily demonstrate that under conditions of decreasing effective stress (eg slow reservoir filling or head unloading) minimising of the cohesion value produces a conservative analytical result, while under increasing effective stress (eg toe loading), the greatest likely value of cohesion must be adopted for conservative analysis. It is immediately apparent that all points beneath the Mohr envelope will have safety factors greater than 1.0 while points which lie outside the envelope will be unstable (safety factors less than 1.0). Two examples are shown in Fig. 5d. The solid curved Mohr envelope indicates that point P3 has an absolute safety factor of $200/185 = 1.08$. The dashed line (deliberately drawn through points P1 and P3) shows that for strength parameters of $c' = 106$ kPa, $\phi' = 13$ degrees, the safety factor of point P3 is $(185/185)$ ie 1.0, and there is no change in safety factor from point P1.

(vi) Sensitivity of changes in safety factor to any combination of c' and ϕ' may be determined simply and immediately. From the dashed line on Fig. 5d it is clearly evident that if point P1 has an initial safety factor of 1.0, then if the cohesion is greater than 106 kPa, submergence to the P3 state would increase the safety factor of the slope. More usually of course, for slides at residual strength, the cohesion is very small and the converse applies. (Note that approximately the same argument applies if this line is the tangent to a curved Mohr envelope, with a pseudo-cohesion of 104 kPa at 250 kPa normal effective stress.)

(vii) Once the initial stress state for a slope has been analysed (using any rigorous method) for a given condition of raised reservoir, all subsequent analyses for different piezometric conditions within the slope can be carried out immediately and accurately (with no need for additional stability analysis by computer). Only the difference in the position of the new piezometric line from its former position need be found (an area calculation) and the appropriate additional reduction in average normal effective stress drawn on the stress plot, and the change in safety factor found directly, as described above.

Example: Point P3 on Fig. 5d shows some former prediction for steady state stress conditions for full pool. If after filling, piezometric pressures were found to be 7 m lower over a 100 m length of the 350 m long failure surface, than predicted by the model, determine the new stress conditions (at P3a) from the P3 condition with stress conditions (350, 185) and the change in safety factor from the initial condition at Point P1 with stress coordinates (σ, τ) of (470, 212). The failure surface soil is assumed to be cohesionless. First the diminished piezometric head from condition P3 is calculated as $7 \text{ m} \times 100 \text{ m}/350 \text{ m} = 2 \text{ m}$ (average on the failure surface). Next, the average increase in effective stress is calculated from the unit weight of water as $2 \text{ m} \times 9.81 \text{ kN/cu. m} = 20 \text{ kPa}$. Point P3a therefore has coordinates (350+20, 185) ie (370, 185). The change in safety factor is found simply by subtracting 1.0 from the ratio of the P3a ordinate from ordinate of the line constructed from the origin to P1: ie $(166/185-1.0)$ or -10%.

(viii) Where lateral flows (eg with drainage drives) or narrow slides, necessitate that 3 dimensional effects are considered, the same approach may be taken to assess overall slope stability. This is carried out by drawing as many sections (parallel to the inferred direction of potential movement) as necessary to define the slide geometry. The mean stresses for the three dimensional analysis are then found by summing the products of the individual section areas and stresses and then dividing by the area of the whole slide, ie if Section i has length L_i and width B_i and there are n sections then:

$$\tau_3 = \sum_{i=1}^n \tau_i \times L_i \times B_i / A$$

$$\sigma_3' = \sum_{i=1}^n \sigma_i' \times L_i \times B_i / A$$

Where A is simply the area of the failure surface, ie

$$A = \sum_{i=1}^n L_i \times B_i$$

The aquifer modelling program in Appendix 2 can provide direct output of the parameter U^* , defined as the increase in piezometric pressure acting on a failure surface, integrated over the area upon which the pressure acts. The failure surface may be of irregular shape, concave or convex, leaky, subjected to drainage drives or wells, affected by lateral flows at the slide boundaries and subjected to either transient or steady state flows. If the piezometric pressure increase modelled is the change resulting from reservoir filling then the average increase in pore pressure can be simply found by dividing U^* by the failure surface area, ie:

$$u_3 = U^* / A$$

Provided a check is made that the governing piezometric pressure has been affected (ie the higher of the pressures on either side of the failure surface at all points), then the change in safety factor of the 3D slide may be determined accurately by using the values of τ_3 , σ_3' and u_3 in the same manner described for the above example (Fig. 5d).

(ix) For approximate analyses of gently arcuate slides in cohesionless soils, changes in safety factors can be determined with sufficient accuracy for practical purposes by determining the initial stress conditions from translational slide approximations. (Skempton and Hutchinson, 1969). This allows rapid assessment of the effects of known piezometric changes, using a hand calculator.

A3.8 THE IMPLICATIONS OF DECREASES IN SAFETY FACTORS

The primary implication of a reduction in safety factor of an existing active slide (where residual strength conditions pertain) is that accelerated movement rates can be expected. In some situations, it is relevant to estimate the expected displacement of a slide required for the geometric change from slope deflation to restore the safety factor prior to reservoir filling. If movement rates never exceed slow to moderate rates (say less than about 1 metre/day) reasonable displacement estimates should be possible using standard equilibrium methods which incorporate the relevant geometric and piezometric changes. (Note that at faster displacement rates, particularly above about 1 metre/minute, vibrational effects will probably invalidate the static normal effective stress relationship and indeterminately large displacements can be expected.)

Simplistic methods have been suggested to estimate a rough order of magnitude for displacement of smoothly arcuate failure surfaces (Appendix 4). Typical values are shown on Fig. 6a to 6c, to show the displacement expected per 1% decrease in safety factor as a function of slide length, for given values of initial slope angle and frictional strength

Assumptions:

Soil unit weight	23.5 kN/cu m
Initial safety factor	1.0
Cohesion	0
Headscarp angle	45 degrees
Failure surface at toe - horizontal	
Pore water pressure - dependent variable	
Failure surface waviness - none	

These show the displacement per percent decrease in safety factor is largely dependent on the slope length, L (and implicitly, the angle θ between the inclination of the headscarp and the inclination of the failure surface at the toe).

For an approximate relationship, it appears from inspection of these figures that:

$$\text{Displacement (m/\%)} = 0.007 \times L \times \phi' / \theta$$

A3.9 DISPLACEMENT OF WAVY SURFACES

The commonly accepted means of considering field waviness is to model the failure surface as an equivalent surface with strength $(\phi' + i)$ where i represents the increase in strength attributable to waviness. In practice, some difficulties arise, which can be self cancelling if a consistent approach is taken. Nevertheless it appears appropriate that the implications are well understood. The difficulties which arise are firstly in the plotting of stress vectors in relation to Mohr envelopes, and also in displacement estimates.

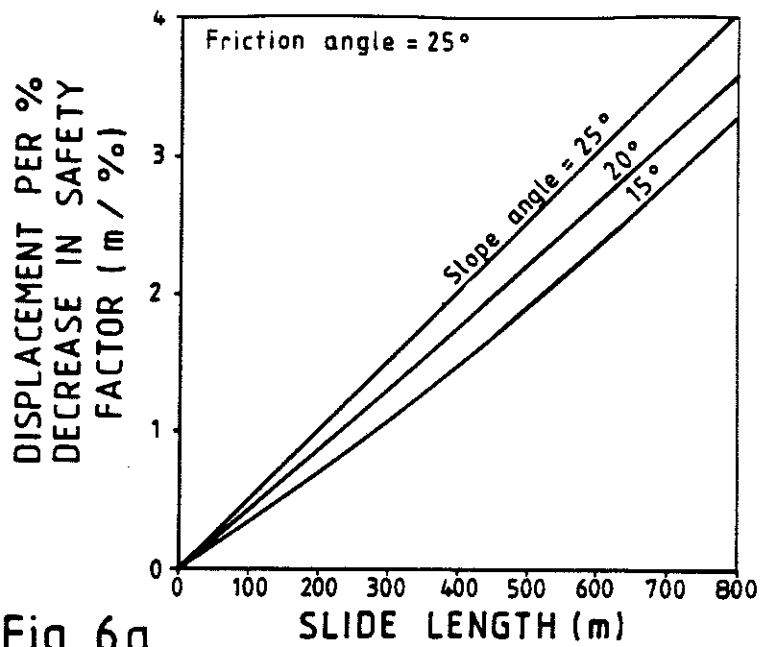


Fig 6a

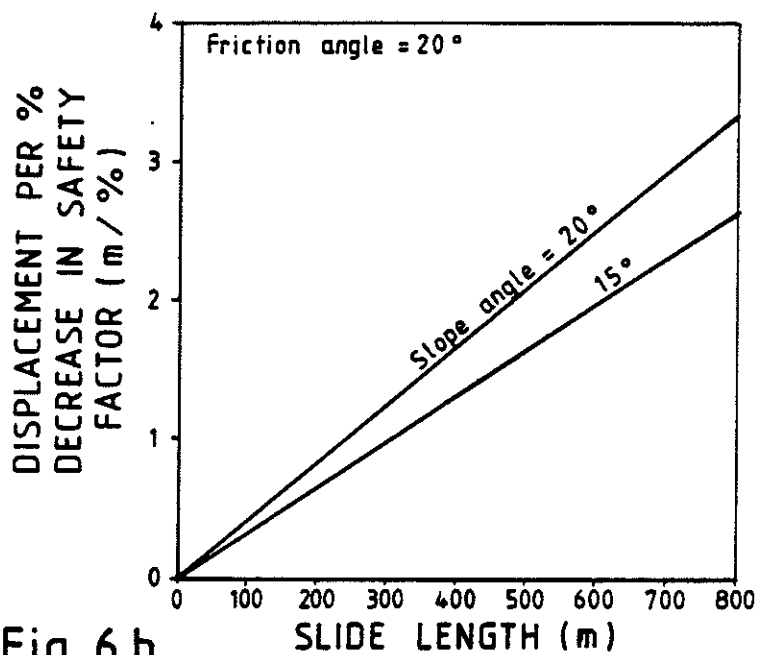


Fig 6b

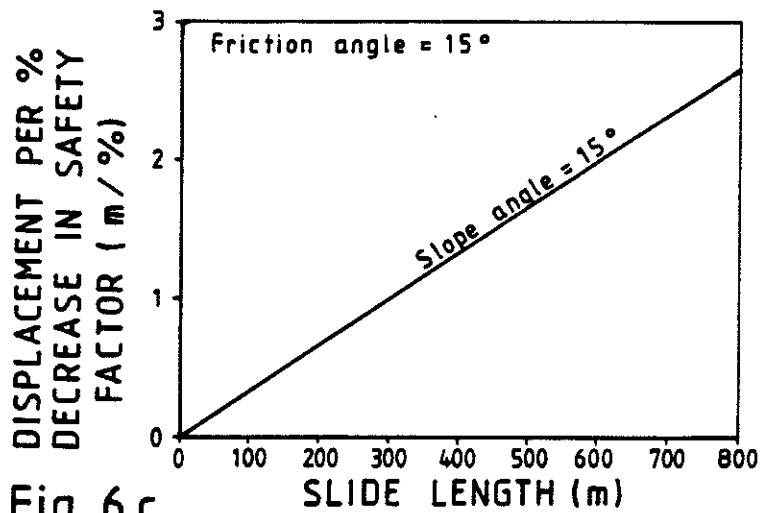


Fig 6c

SENSIVITY OF DISPLACEMENT TO CHANGES IN SAFETY FACTOR

The safety factor of a cohesionless planar failure surface of inclination β , is given by:

$$F = \tan\phi' / \tan\beta \dots\dots (1)$$

Traditionally for waviness (Barton, 1976) of i , the above becomes:

$$F = \tan(\phi' + i) / \tan\beta \dots\dots (2)$$

This expression is obtained by resolving in the direction of β (a surface which is hypothetical rather than real). Now in practice β is usually positive while it is quite possible to have both ϕ' and i equal to or greater than 45 degrees, ie the numerator in Equation 1 may be the tangent of a number greater than 90 degrees (a negative value). A large negative safety factor is therefore implied. There is apparently some lack of accord with reality here since negative safety factors imply movement in the opposite direction to that assumed.

By resolving in the direction of $(\beta-i)$, a surface containing the real failure surface soil is considered. This produces the expression:

$$F = \tan\phi' / \tan(\beta-i)$$

This expression has the advantage that it becomes negative only when $i > \beta$, ie the surface on which the load is carried begins to slope in the opposite direction to the assumed movement direction. This is entirely logical, and furthermore,

- (i) the stress vectors may be plotted sensibly,
- (ii) changes in safety factors can be rationally considered and
- (iii) displacements can be estimated systematically.

Stresses on the actual failure surfaces of modelled wavy features rather than hypothetical surfaces have been considered in the following sensitivity analyses.

A3.10 SENSITIVITY TO FAILURE SURFACE WAVINESS

- (i) Change in safety factor with watertable rise

Fig 7a shows sensitivity of safety factor changes to increases in groundwater levels for a given combined friction angle (ie $\phi' + i$ constant at 25 degrees), but i varying from 0 to 20 degrees. (ϕ' varies correspondingly from 25 to 5 degrees.)

Assumptions:

Soil unit weight	23.5 kN/cu m
Failure surface depth	50 m
Friction angle	25 degrees
Cohesion	0 kPa
Initial safety factor	1.0
Initial pore water pressure - dependent variable	

Notes:

(a) These figures assume the entire failure surface will suffer a uniform rise in groundwater levels, therefore if (as will usually occur with submergence) only a proportion of the failure surface is affected, the safety factor changes shown should be diminished in proportion.

(b) These are changes in groundwater (phreatic surface) levels. Changes in piezometric levels will produce similar effects, which can be calculated with slightly greater accuracy by dividing the safety factor change shown, by the square of the cosine of the piezometric gradient. Often, this factor is close to 1.0, and will not change results greatly.

In summary, these show that wavy failure surfaces will experience considerably greater decreases in safety factors than smoothly arcuate surfaces with the same overall strength.

(ii) Displacement per percent change in safety factor

Simplistic methods have been used to provide an approximate comparison of displacement of wavy surfaces compared with smoothly arcuate failure surfaces. Typical values are shown on Fig. 7b, to show the displacement expected per 1% decrease in safety factor as a function of failure surface waviness, for given values of initial slope angle and constant overall frictional strength ($\phi' + i$ of 25 degrees).

Assumptions:

Soil unit weight	23.5 kN/cu m
Slope length	300 m
Initial safety factor	1.0
Cohesion	0
Headscarp angle	45 degrees
Failure surface at toe - horizontal	
Pore water pressure - dependent variable	

These show the displacement per percent decrease in safety factor decreases markedly as failure surface waviness increases. There is thus some cancellation of the effect on safety factors shown on Fig 7a.

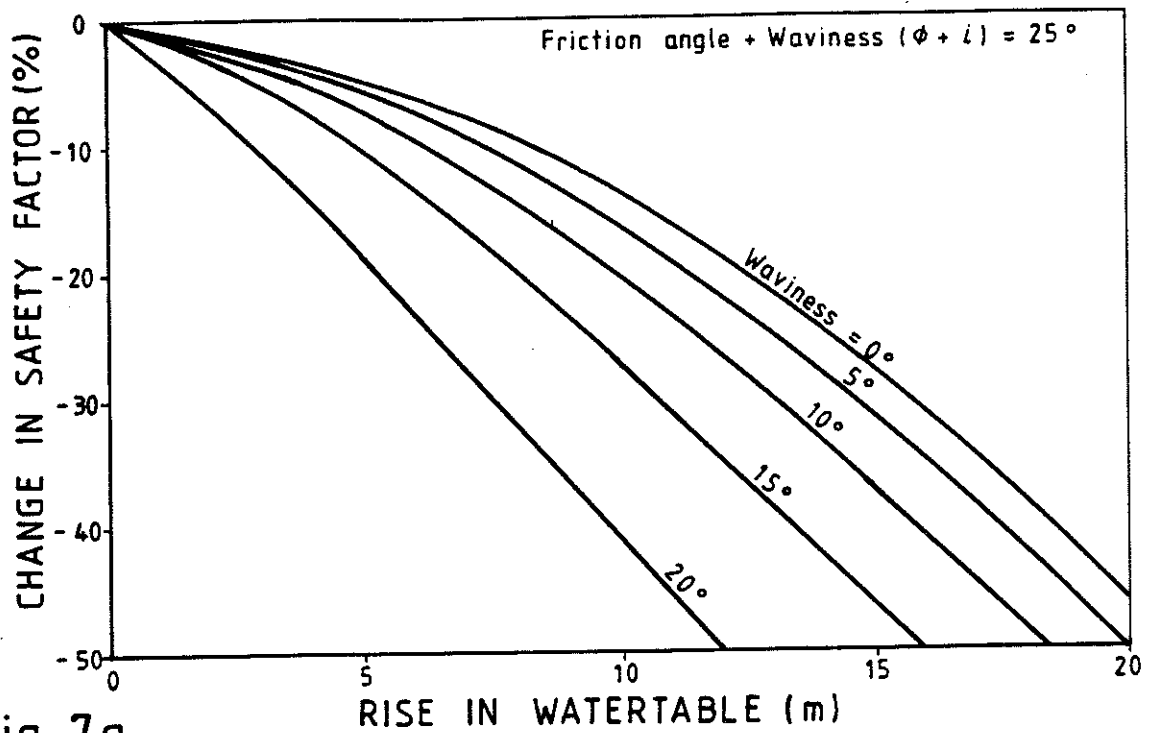


Fig 7a

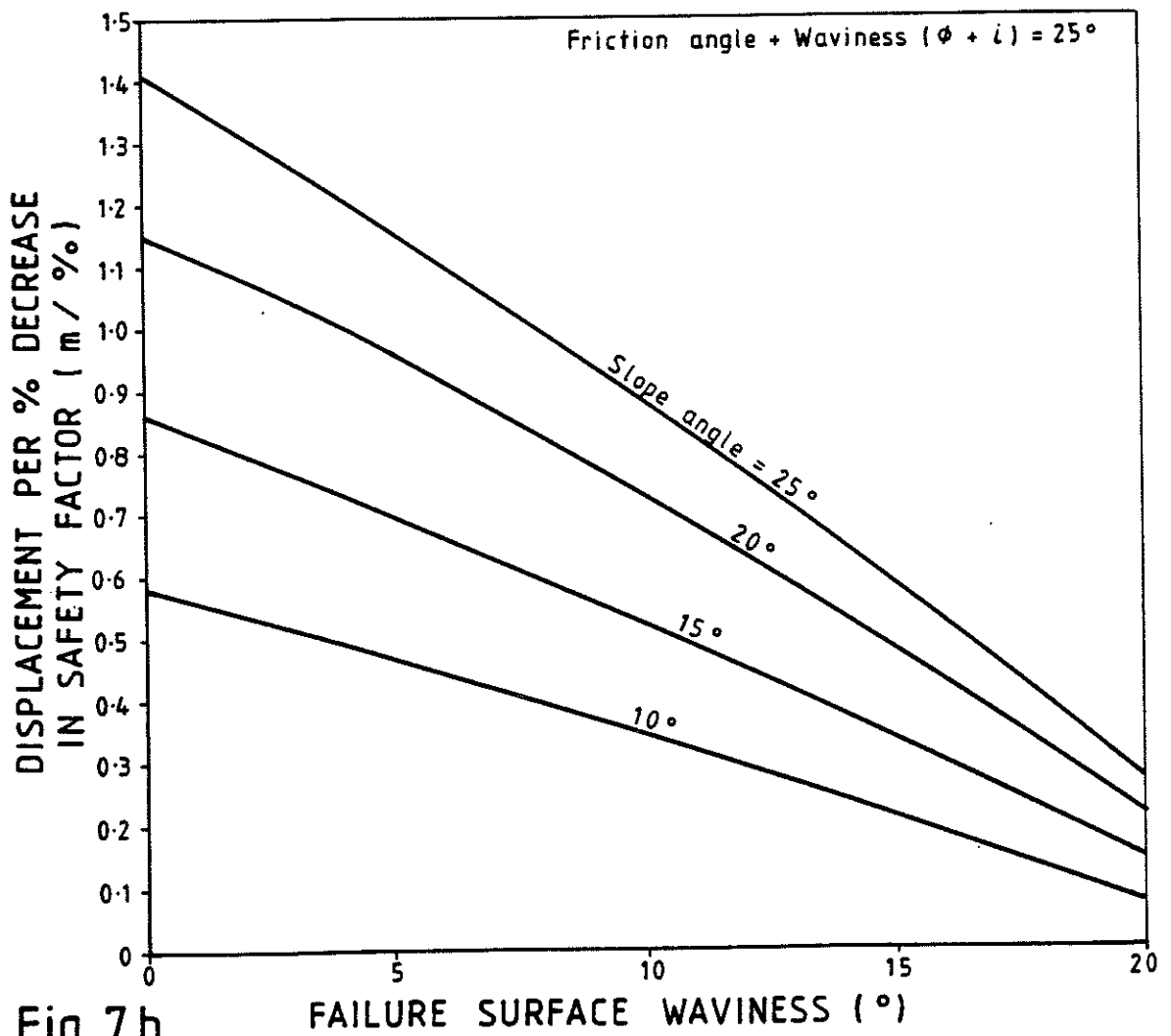


Fig 7b

SENSITIVITY TO FAILURE SURFACE WAVINESS

APPENDIX 4

CASE HISTORIES OF LANDSLIDE MOVEMENTS

A4.1 GENERAL

An extensive literature search has encountered only two cases where sufficient documentation has been provided to allow some interpretation of the effect of reservoir impoundment on the increase in creep rate of a large landslide where residual strength conditions pertained.

However in each case, the decrease in safety factor by submergence was countered to some degree by geometric changes resulting from displacement so an approach was developed to quantify the effect with reasonable accuracy.

A4.2 ESTIMATION OF THE RECOVERY IN SAFETY FACTOR FROM SLIDE DISPLACEMENT

The method was developed for application to any actively creeping landslide which experiences a small, gradually applied decrease or increase in safety factor (from mass redistribution, toe submergence etc). To calculate the distance the slide will move so that slope deflation will just compensate for the safety factor change, a valid slide model is required (giving a safety factor close to 1.0). The slope of the ground beyond the toe of the slide and appropriate strength must also be determined. A nominal displacement is then considered and about 5% of the total slide length has been found to be an appropriate compromise between accuracy considerations and excessive changes from initial geometry. The difference in safety factor between the initial and final position is then used to calculate (by proportion) the displacement required for a 1% increase in safety factor. Note that for the case of reservoir submergence, it is conservative to assume "slow movement" ie the piezometric levels within the slide are maintained relative to the reservoir level. "Fast" displacement changes can be computed simply by making appropriate piezometric assumptions, ie the piezometric line would be reduced in accordance with the slide movement vector, but less conservative estimates for displacement will result.

A standard slope stability program using the method of slices, SARMA (Hoek, 1986) has been modified to carry out the procedure. The program source codes and compiled versions (both original and modified) are contained on the accompanying diskette. The application is as follows:

- (i) Prepare input data by dividing the slide model into about 20 - 30 slices, ensuring the base lengths (measured along the failure surface) are all equal, and define an additional weightless slice at the slide toe. The base of the extra slice is given the same slope angle as the topography beyond the slide toe, and the slice is given a small (but not zero) height. Use a constant density for each slice,

(adjusting slice heights to compensate if changes in density are large).

(ii) Run the standard program, SARMA, inputting model geometry and parameters at the appropriate prompts. Calculate FOS, adjusting soil strengths and piezometric conditions to give a valid model for the creeping slope ($F = 1.0$), and file the data set.

(iii) Insert the following line into the standard code (filed as SARMADX on the accompanying diskette)

```
742 FOR K=1 TO N-1:A(10,K)=A(10,K)*A(21,K+1)/A(21,K):NEXT K:A(10,N)=0
```

(iv) Run the modified program, reading in the filed dataset. Calculate the new safety factor and exit the program without reading or writing to any other files.

(v) Calculate the displacement sensitivity from the increase in safety factor as described below.

In the modified program, as the file is read in, the weight of soil within each slice is replaced with the weight of the next slice upslope, (by changing the density of each slice in the ratio of the slice weights) to determine the safety factor after nominal displacement.

A more approximate method is to use an 'equivalent rotating segment'. This is the simplest approach yet accuracy appears sufficient for practical purposes (from comparisons on slides which are long in relation to their greatest depths). An equivalent slide on a gently arcuate failure surface is considered. If the average inclination of the slide is defined as the angle (A) of a line joining the head of the slide to the toe, then the percentage increase in safety factor after displacement is given approximately by:

$$P = (\tan(A_i)/\tan(A_f) - 1) \times 100\% \quad \dots\dots\dots (2)$$

where A_i and A_f are the average slope angles before and after displacement. If the displacement applied is S metres, then the displacement sensitivity (D), is given by:

$$D = S/P \text{ m/\%} \quad \dots\dots\dots (3)$$

A simple empirical relationship that gave similar results to the above, was found to be:

$$D = 0.007 L \phi' / \theta$$

where L is the slide length, ϕ' is the effective friction angle and θ is the difference in angle between the inclination of the failure surface at the headscarp and that at the toe.

In practice (for the cases of landslides studied), displacement sensitivity for significantly large landslides was often found to be in the range of 1 to 6 m/%. (Corresponding to slide lengths of about 100 and 1000 m respectively). As many of the slides studied had lengths of 500 m, a value close to 3 m/% was common, ie the slide would be expected to move about 3 m for each 1% decrease in safety factor.

In many cases, only small proportions of the slide lengths were to be submerged by reservoir filling. Predicted decreases in safety factors were commonly 1 to 5%, therefore, at 3 m/%, expected displacements were in the range of 3 to 15 m.

In all the literature examined, only two examples have been found in which adequate information has been provided, to allow interpretation of the contribution of strength rate dependency on landslide movements reactivated by reservoir filling.

A4.2 CASE HISTORIES OF ACTIVE SLIDES AFFECTED BY RESERVOIR FILLING

Models used for the Gepatsch Reservoir Slide (Breth, 1967) and the Dirillo Reservoir Slide (Jappelli & Musso, 1981) are shown in Figs. A4-1 and A4-2 respectively. In neither case was piezometric information provided, so the assumption has been made that piezometric levels within each slide were at the same level as reservoir, at the beginning and end of each interval used in the calculations. The lack of confirmatory piezometric data is a significant limitation to both analyses. However, as no other more appropriate case of a monitored landslide affected by a reservoir could be found, this study was pursued.

The steps carried out were:

- (i) The standard limit equilibrium analysis program (SARMA) was carried out to confirm the appropriate soil strengths for a safety factor of 1.0, then the change in safety factor for alternative reservoir levels was found, assuming no displacement.
- (ii) The modified SARMA program was used to calculate displacement sensitivity.
- (iii) Time intervals were selected from the monitoring data supplied, using beginning and ending times at which the reservoir levels were not changing rapidly, as much as possible. (To minimise selection of times when a piezometric lag condition may have affected pressures within the slide.) Three time intervals were taken for each slide, and corresponding displacement rates were noted.
- (iv) The net change in safety factor from the beginning to the end of the time interval was calculated from the algebraic sum of the safety factor change due to changing reservoir levels, and that caused by slide displacement.

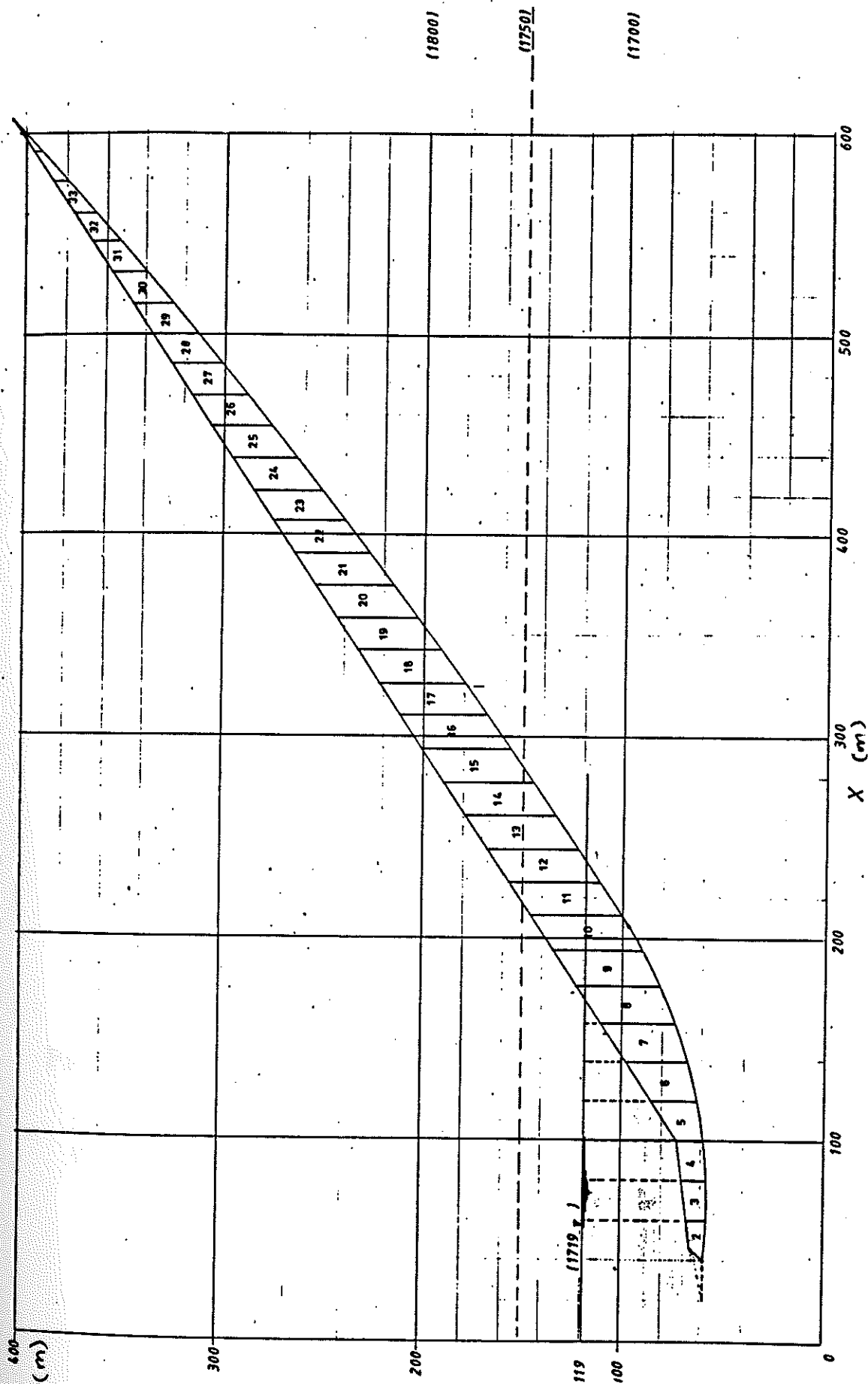
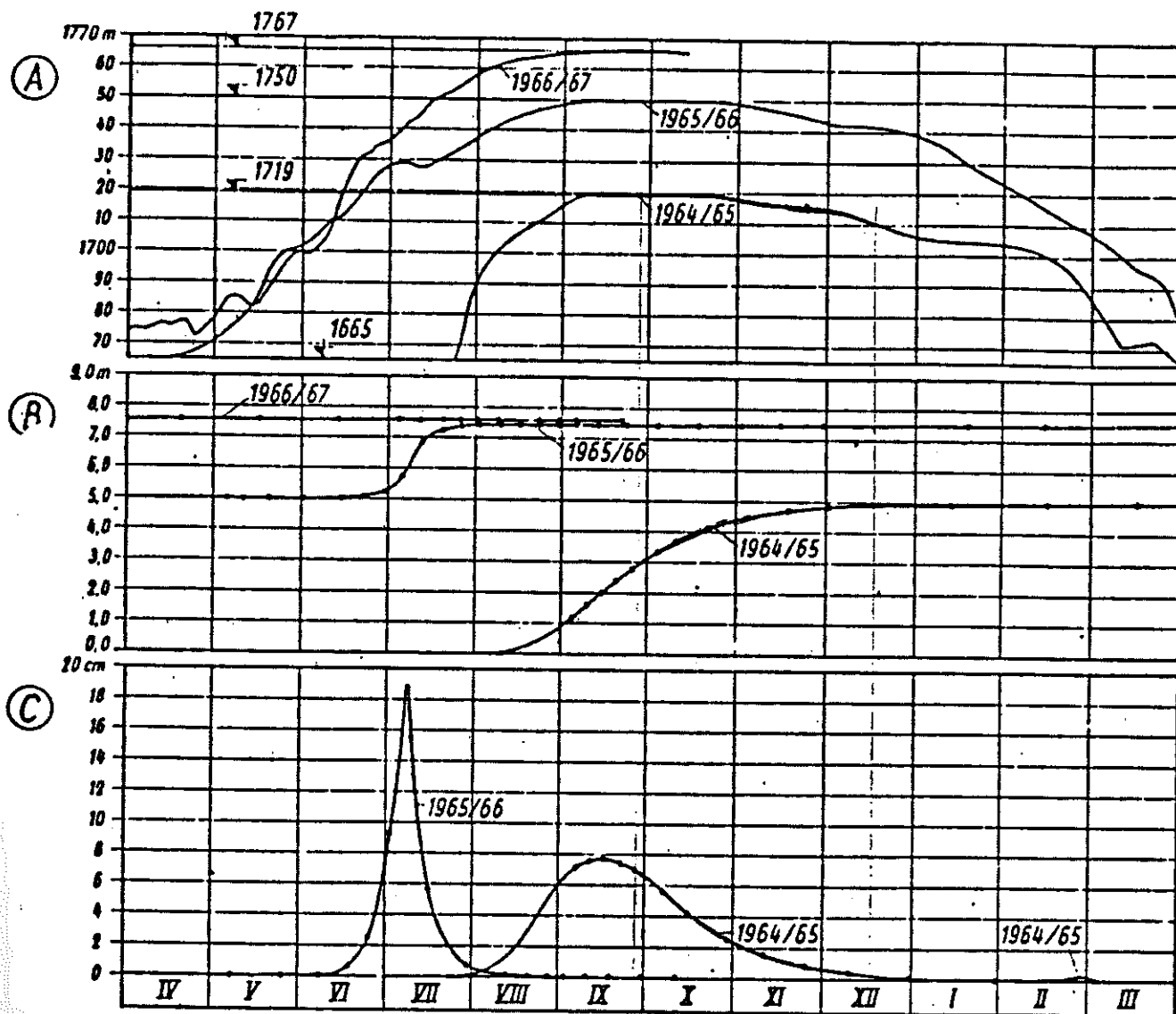


Fig. A4-1a

Gepatsch Slide Area
 Displacement analysis model



Filling curves and time curves for the settlement on medium slope elevation
 (A) Filling curves 1964/65, 1965/66 and 1966/67.
 (B) Average total settlement between 1964 and 1966.
 (C) Average daily settlement for 1964/65 and 1965/66 (almost zero 1966/67).

Courbes de remplissage et de tassement en fonction du temps à l'altitude moyenne de la pente.

Fig. A4-1b Getpatsch Slide Movements

(from Lauffer et al, 1967)

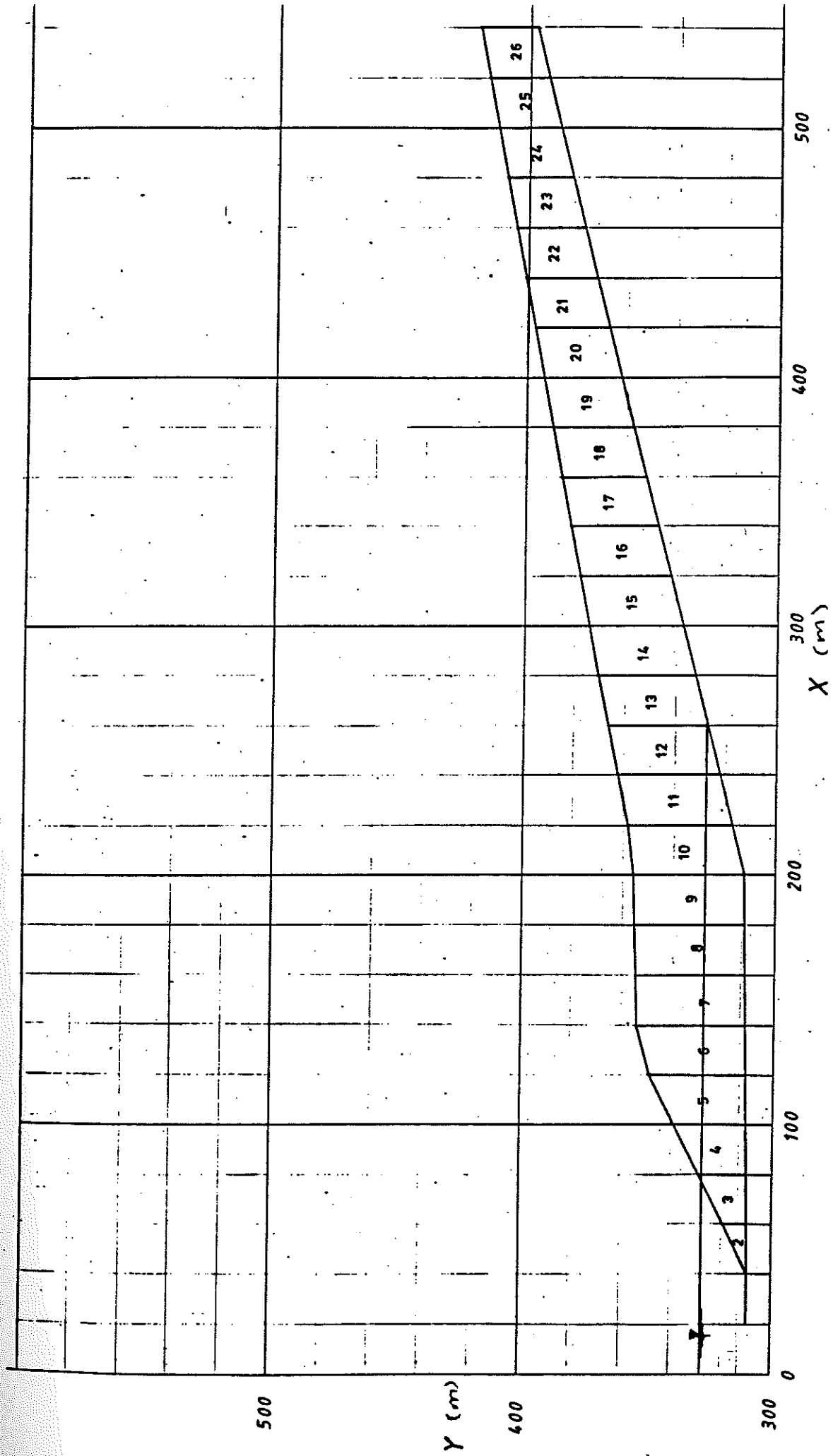


Fig. A4-2a

Dirillo Reservoir Slide
 Displacement analysis model

TABLE I - Basic response of slope to filling events

event	1 m/month	2 m m.s.l.	3 months	4 cm/month	5 months
E1	12	315÷327	6.0	10	0.5
E2	3.2	308÷324	4.0	2	1.5
E3	8	320÷328	7.0	5	2.5

- 1) rate of water level rise
- 2) from elevation to elevation
- 3) permanency of maximum water level
- 4) maximum rate of horizontal displacements
- 5) time lag

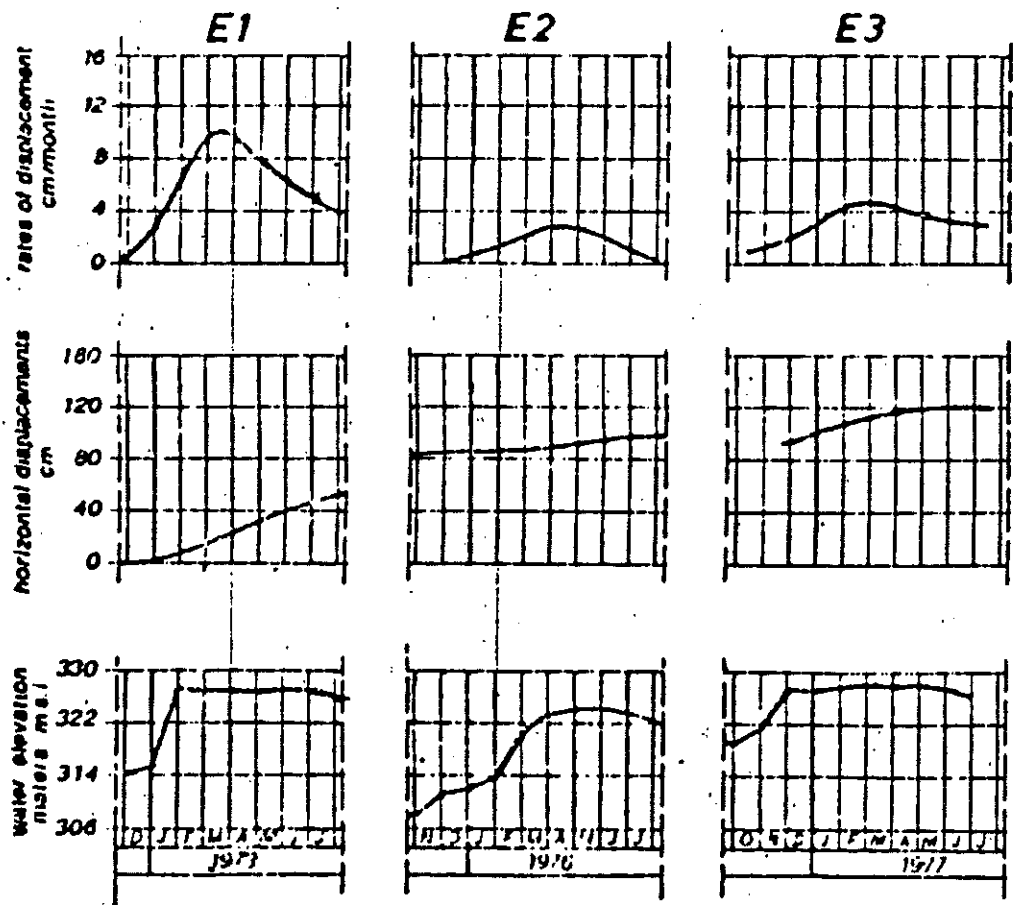


Fig. A4-2b

Dirillo Slide Movements
from Jappelli & Musso, 1981

(v) Using equation (1) from Chapter 7, the mobile range coefficient was calculated for the velocity interval considered.

Results:

(Times, displacements and velocities are taken directly from the referenced papers.)

Gepatsch Reservoir Slide

Displacement sensitivity 3.1 m/%

Back-analysed friction angle 33 degrees.

Selected Time Interval	Corresponding Displacement (metres)	Velocity Range (mm/day)	Net Change Safety Factor (%)	Mobile Range Coefficient (%)
28.9.64 - 15.12.64	2.0	3 - 70	1.3	11
15.4.65 - 7.07.65	1.1	5 - 190	0.7	129
7.7.65 - 25.07.65	1.1	16 - 190	0.6	51

Dirillo Reservoir Slide

Displacement sensitivity 2.8 m/%

Back-analysed friction angle 20 degrees.

Selected Time Interval	Corresponding Displacement (metres)	Velocity Range (mm/day)	Net Change in Safety Factor (%)	Mobile Range Coefficient (%)
1.4.73 - 1.02.74	0.62	0.4- 3.3	5.6	1.5
1.4.73 - 1.06.76	0.75	0.3- 3.3	1.7	3.9
1.2.76 - 1.03.77	0.27	0.4- 1.6	5.4	1.3

Conclusions

The conclusions drawn from these analyses can only be tentative in view of the piezometric assumptions. The accuracy in calculated values of the mobile range coefficient is proportional to the safety factor change considered, therefore when changes are less than 1 to 2%, the reliability is low. However, from the above results, the inferences drawn are:

(i) The Gepatsch Reservoir Slide material has a relatively limited mobile range (not much more than 3%) while that for Dirillo, is likely to be very large (well in excess of 6%). Consequently, the mobile range coefficient for the former is much larger than for the latter.

(iii) Using the back-calculated residual friction angles as a guide to clay content, the inferred strength rate dependence exhibited in the field appears consistent with the laboratory behaviour of similar soils (Chapter 9, Fig. 3a).

Comparative testing to determine the laboratory characteristics of the failure surface materials from these two slides would be enlightening.

An attempt was made by the writer, to sample materials from the Gepatsch area, but the failure surface was not accessible. A sample of silty sand was recovered at some distance from the failure surface, and on testing, yielded a residual friction angle of 34 degrees. The relative lack of fine plastic material made testing in the ring shear difficult, (sufficiently steady reading to determine rate effects were not possible without scalping) but it was clear that the mobile range was much smaller than those for the clayey silt gouges tested previously (at 7 to 8%), ie observations were consistent with the estimate of 3% above.

A4.3 CASE HISTORIES OF OTHER ACTIVE SLIDES (WITHOUT RESERVOIRS).

So far, the writer has used strength rate dependence to predict the movement of 2 active slides, **before** remedial works were instigated.

(A) Slide activated by head loading.

This slide of about 500,000 cubic metres was reactivated some time after construction of a highway embankment across the head region. Failure appeared to be controlled by highly plastic bedding planes dipping at 10 degrees downslope. No piezometric levels were available at the time the slide was first observed. Movement rate was measured at 100 mm/month, a rate which would soon have required major repair of the highway. An interim proposal was required to reduce the movement rate, while investigations and long term proposals were formulated. Assuming a mobile range coefficient of 4, the percentage increase in safety factor required to reduce movement rates to 1 mm/month was determined and used for the design of an immediate toe buttress. Fill of 12,000 cubic metres was applied in accordance with the design, resulting in movement rates of just under 2 mm/month. This largely fulfilled the objective, and was a very satisfactory outcome in view of the absence of any subsurface information, and a design based solely on outcrop geology and inferred strengths and piezometric conditions. (In hindsight, a smaller coefficient might have been used for a highly plastic clay.) The interim measures allowed investigations to proceed, following which, further buttressing was carried out efficiently, without the constraints of an emergency situation.

(B) Slide activated by toe removal.

Fig. A4-3, shows one of a number of slides within a proposed reservoir. The failure surface material (moderately plastic, clayey sandy silt) was formed under identical geological conditions to those applying to the material tested for Fig. 7-1.

The slide contained an unconfined perched aquifer above the failure surface, and was also subject to a confined aquifer acting beneath the failure surface. It was moving at 12 mm/year. Using the methods described in Chapter 5, the predicted decrease in stability on lakefilling was large (over 10%), with possibly 50 metres of expected displacement.

Drainage both above and below the failure surface, greatly diminished the predicted change in stability, but the net affect of drainage and reservoir filling was still a small decrease in safety factor. Hence buttressing was required as well. A difficulty arose, in that a loess mantle of silty sand had to be stripped before buttressing fill could be placed. From the known strength rate dependence of Fig. 7-1, the implications of removing the proposed volumes without concurrent backfilling, were pointed out to the contractor. Excavation without backfilling was carried out and the rate of slide movement soon increased from 12 mm/year to 8 mm/day. Backfilling then began and movements were reduced. Another cycle of excavation and backfilling took place, with a similar sequence of slide movement. At each stage, earthwork volumes were estimated to allow calculations of safety factor changes. (The SARMA program was used, and results were weighted to take into account the 3 dimensional geometry of the slide.)

Results are shown on Fig. A4-4, overlaid on the laboratory values from Fig. 7-1. The average effective normal stress applicable to the field case is about 500 kPa, hence the closest relevant laboratory curve for comparison is that shown for 580 kPa. As no field data corresponding exactly to the adopted origin for safety factor changes (10 mm/day) were available, the data cannot be matched exactly. However, the 8 mm/day field data is sufficiently close to plot this point on the laboratory curve. The other 3 field data points can then be used to examine the difference between field and laboratory behaviour.

The inferences drawn from this data are:

- (i) The field and laboratory data fit reasonably over the range of displacement rates for which comparative data are available.
- (ii) The field curve appears steeper at very slow rates, probably because only the fine fraction (passing 600 micron) was used in the laboratory test. Therefore predictions of expected rates of movement are likely to be unconservative under conditions of decreasing safety factor, but conservative with increasing safety factor.
- (iii) If (as the contractor originally intended) the volume excavated had been doubled, (safety factor decreased by another 3%), the shape of the laboratory characteristic curve suggests that very rapid failure would have been inevitable.

800 -

- 80

700 -

- 70

600 -

- 60

500 -

- 50

400 -

- 40

300 -

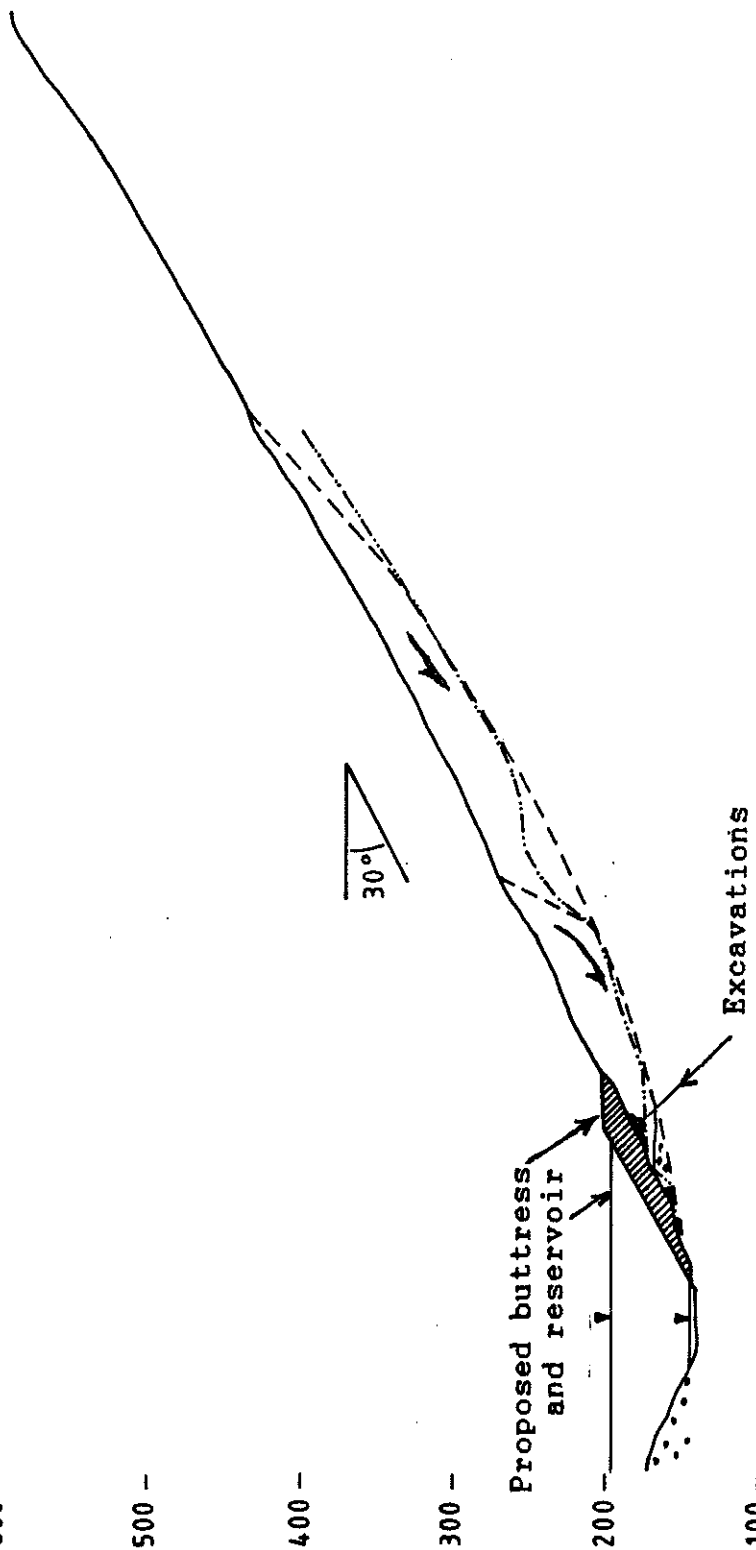
- 30

200 -

- 20

100 -

- 10



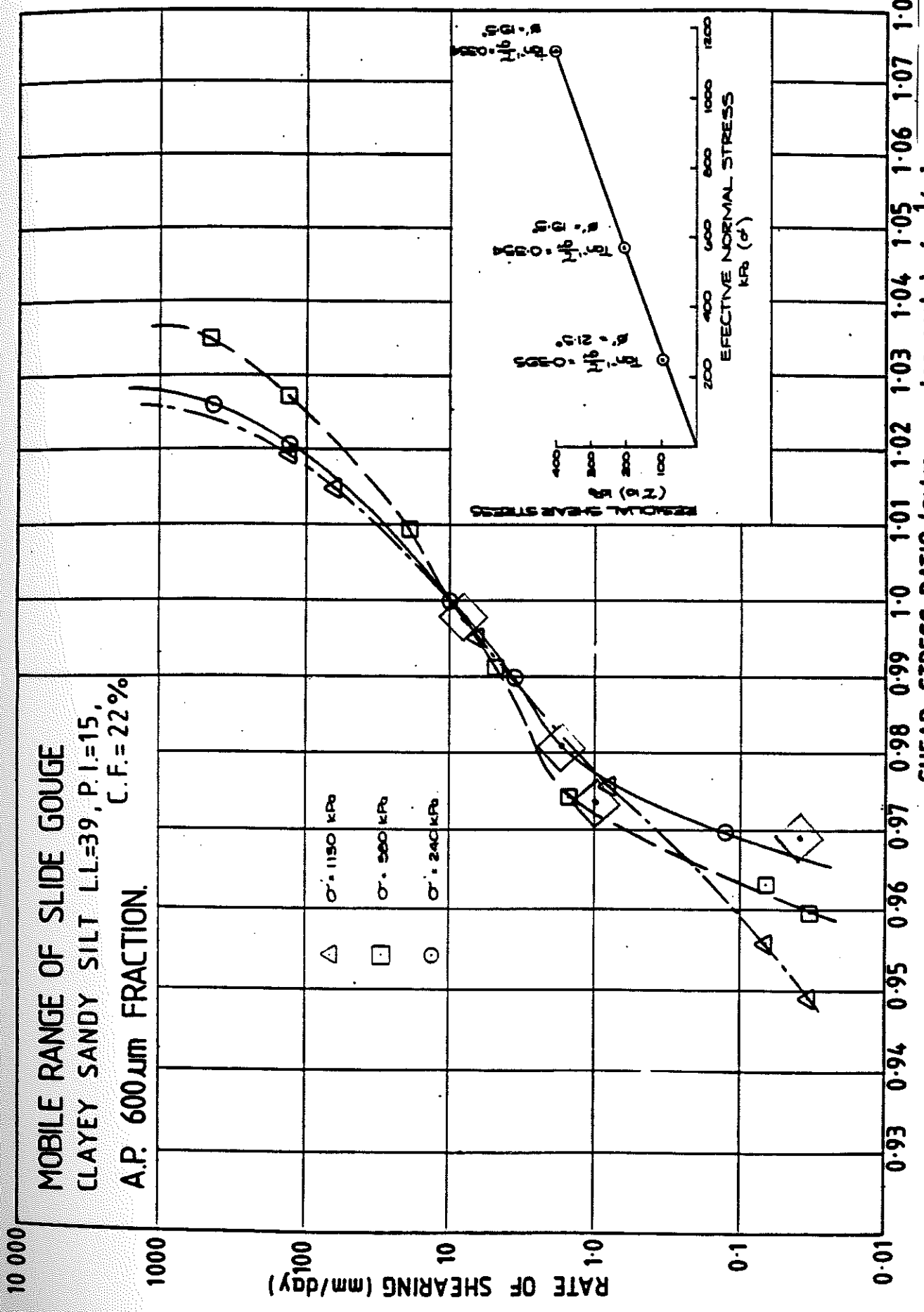
0 1 0 100 200 300 400 500 600 700 800 900

LEGEND

- Ground surface
- - - Failure surface
- · - · - Piezometric line
- ▨ Alluvium
- ▩ Fill material

Fig. A4-3 Slide activated by toe excavation

Scale 1:5000



◆ Field data points

Fig. A4-4 Comparison of field and laboratory rate effects

Conclusions

From the applications so far, the rate dependence of residual strength, appears to provide useful insight to the likely behaviour of active (slides where residual strength conditions pertain in silty or clayey materials) affected by remedial works.

Under conditions of increasing safety factor, changes in displacement rate should be able to be estimated with sufficient reliability for practical purposes.

Under conditions of decreasing safety factor, changes in displacement rates are more difficult to predict and predicted movement rates must be regarded as a lower bound, requiring close monitoring of response. Predicted movement rates can be readily applied to determining whether a proposed decrease in safety factor is clearly impractical.

The limited cases studied, require that these conclusions be applied with caution, but at the present time, there are no other guidelines for assessing the mobility of creeping landslides where residual strength conditions pertain.

APPENDIX 4

CASE HISTORIES OF SEISMICALLY REACTIVATED LANDSLIDES

CONTENTS

1906 San Francisco earthquake,	M 8.3
1929 Buller earthquake,	M 7.6
1931 Napier earthquake,	M 7.9
1941 Chai-yi earthquake,	M 7.1
1959 Hebgen Lake earthquake,	M 7.1
1960 Arauco earthquakes,	M 8.4
1964 Alaska earthquake,	M 8.5
1966 Matsushiro earthquake swarm.	
1968 Inangahua earthquake,	M 7.0
1968 Borrego Mountain earthquake,	M 6.4
1970 Adelbert Range earthquake,	M 7.0
1970 Peru earthquake,	M 7.7
1971 San Fernando earthquake,	M 6.6
1972 Managua earthquake,	M 5.6
1976 Friuli earthquake,	M 6.4
1976 Guatamala earthquake,	M 7.5
1978 Santa Barbara earthquake,	M 5.5
1978 Izu-Ohshima earthquake,	M 7.0
1979 Montenegro earthquake,	M 6.6
1980 Irpinia earthquake,	M 6.5
1983 Coalinga earthquake,	M 6.7
1983 Borah Peak earthquake,	M 7.3
1985 New Britain earthquake,	M 7.1
1985 North Nahanni earthquake,	M 6.6
1987 Edgecumbe earthquake,	M 6.3
1988 Ecuador earthquakes,	M 6.1 & M 6.9

1906 San Francisco earthquake, M 8.3

Youd & Hoose (1978) have collated reports on ground failures associated with the great San Francisco earthquake. Earlier reports had no appreciation of the phenomenon of liquefaction and terminology is often unclear. Even the more basic geotechnical distinctions are not made (eg sand versus clay etc).

By far the most common manifestation of the earthquake was the 'earth slump'. It is inferred that this refers to rotational failures, probably where saturation was not evident and displacements relatively small.

Earthflows were also reported as

'originating in valleys, in gullies or on hillsides, where the weight of the earth, combined with the weight of the added water, was sufficient and the substratum was rendered plastic, gravity caused it to creep like a lava stream, leaving a hollow in the place from which it came and a fan or tongue of debris down the slope below'.

These are referred to as both 'large' and 'small' but no clearer definition of absolute size given.

Anderson (1907) also refers to earthflows:

'they were formed on gentle as well as steep slopes and both in previously dry drainage depressions and on convex hillsides'.

This writer does give some indication of size:

'In the largest flows, thousands of tons of earth and rock detritus were removed and carried hundreds of yards leaving great cavities. In one case a hole ten feet deep was excavated over an area of nearly an acre and a five degree slope, and the material was spread over two acres.'

It appears that this is an example of liquefaction, but no geotechnical description of the soil was given.

Youd & Hoose note that hillside landslides (namely, those less likely to be liquefaction related) were mostly 'small or involved little displacement'.

Several instances were reported of the same type of failure occurring repeatedly at the same location in subsequent earthquakes. All examples quoted by Youd & Hoose were failures in steep cliffs or involved liquefaction. No examples were reported of large slides reactivated in soils not susceptible to liquefaction.

1929 Buller earthquake, M 7.6

Henderson (1973) discusses landslides occurring in the 1929 Buller earthquake. The terrain is geologically youthful. Failures were generally on

'steep slopes and especially sharp spurs and the ends of terraces, which suffered more than gentle declivities'.

One particularly relevant example is given with the reactivation of a large pre-existing slide in material not susceptible to liquefaction. A slide near Whitecliffs involving about 10 million cubic metres of predominantly overconsolidated sediments was interpreted by Henderson as being remobilised by detachment of a large block from behind the former headscarp, ie creating an enlargement to the original slide. This mechanism of retrogressive enlargement appears to provide a logical exception to the commonly observed resistance of large pre-existing slides to seismic reactivation.

Pearce and O'Loughlin (1985) studied the Murchison area many years after the event and concluded that landsliding was most common on well-bedded and jointed mudstones and sandstones. Also failures were concentrated on scarp slopes, particularly of escarpments. Large dip slope failures were found in the sedimentary rocks but smaller scale slides were more common in igneous formations.

1931 Napier earthquake, M 7.9

Henderson (1933) and Marshall (1933) discuss some of the failures during the 1931 Napier earthquake. In the Te Hoe River, the inferred first-time failure of a steep sided, 200 metre high gorge in Tertiary sandstone, caused a natural dam 30 metres high. This was ultimately breached many years later, during a flood, reportedly releasing a 20 metre high wave. Recent investigations in this area by the writer encountered two very large active earthflows, composed of highly plastic clays, and a large number of apparently dormant slides derived from siltstones and sandstones. No reactivation of these was reported during the earthquake. Stability may have been enhanced by favourable antecedent climatic conditions, but these are seen as additional examples of typical seismic resistance of pre-existing slides in non-liquefiable materials.

1941 Chai-yi earthquake, M 7.1

Ishihara (1985) discusses a number of landslides triggered by the Chia-yi earthquake in Taiwan. The largest was the Tsaoling Slide which was a pre-existing feature, reportedly initiated by an earthquake in 1862. The first event opened an 800 m long head scarp with unspecified (but evidently small) displacement. The 1941 earthquake, caused catastrophic movement of 100 million cubic metres of the pre-existing slide, which moved on a 12 degree bedding plane in a sequence of sandstone and shale. Some months later, after heavy rain, multiple retrogressive failures developed.

1959 Hebgen Lake earthquake, M 7.1

Hadley (1964) documents one of the rare instances of instability of a newly formed reservoir during significant seismic shaking. A concentration of slides close to the fault trace was noted.

'The slides occurred only in colluvial material on slopes steeper than 10 degrees which extended below reservoir level. Slopes as steep or steeper that were distant from the lake did not slide in spite of the fact that some of them were very close to the Hebgen Fault'.

Sounding also showed many entirely sub-lacustrine slides had taken place also.

'Rockfalls were the most common type of landslide resulting from the earthquake. In general these were falls of individual fragments, in small of large numbers from the upper parts of bedrock cliffs; only in a few places did the volume of falling material approach avalanching'.

A particularly interesting example was provided by the Kirkwood Earthflow. This was a large pre-existing slide with an average slope of 10 degrees and about 800 metres long, in 'clayey' materials, ie the type of slide most resistant to seismic reactivation. However movement rates averaging about 1000 mm/day were observed for about a month. Pertinent to the inferences drawn from this slide are that no movement was noted for five days after the earthquake, and that a segment of the active trace crossed the slide, creating a 1 metre high scarp, facing in the direction of downslope movement. Additionally, regional tilt took place, steepening the former gradient of the slide by 0.4 degrees.

Hadley (1978) documents the Madison Canyon Rockslide which was clearly triggered by the Hebgen Lake earthquake.

'It occurred almost immediately after the first and strongest earthquake shock, and in less than one minute it sent more than 20 million cubic metres of weathered schist, gneiss, and dolomite onto the canyon floor and part way up the opposite wall. The principal determining factors of the rockslide were a high, mechanically unstable slope of sheared and weathered rock maintained by a natural buttress of relatively strong dolomite, and a large input of kinetic energy contributed by the earthquake. ... Study of pre-slide aerial photographs suggests that movement along one edge of the slide had taken place more than three years earlier, and therefore the potential for massive sliding might have been predicted.'

Features of particular interest are:

- (i) the slide was predominantly in schistose materials on a scarp slope
- (ii) the average topographic slope was about 23 degrees
- (iii) large rapid displacements occurred
- (iv) the full width of the valley floor was blocked to about 60 m depth
- (v) rapid failure (up to 50 m/s) was attributed to brittle fracture of an intact portion of rock "buttressing" the toe.

This example demonstrates that rapid failure can be expected under earthquake (or presumably by reductions in static stability) where a brittle (first-time) failure mechanism operates even if the slope angle is relatively moderate. Some displacement had taken place prior to the earthquake, (probably several metres) but it appears that this was only on one side of the slide which was incipiently rotating in plan. It may be that this form of rotation in a slide should be regarded as an indicator of potential for rapid movement. No mention is made of whether other large pre-existing slides existed in the area affected by this earthquake.

1960 Arauco earthquakes, M 8.4

Davis and Karzulovic (1963) discuss the landslides triggered by the earthquakes at Lago Rinuhue, Chile. A liquefaction mechanism was identified for the first-time sliding. At least three ancient landslides, inferred to be related to previous earthquake activity, were mapped in the same area and no reactivation was reported.

1964 Alaska earthquake, M 8.5

Hansen (1966) and Coulter & Miglialaccio (1966) report on the effects of the 1965 Alaska earthquake at Anchorage and Valdez. Almost all major slides have been attributed to liquefaction in normally consolidated saturated sand/clay sequences. No failures are reported involving reactivation of large pre-existing slides in materials not susceptible to liquefaction.

1966 Matsushiro earthquake swarm.

Morimoto et al (1967) report on a number of landslides which developed after a series of tremors. However, in no cases were catastrophic movement rates precipitated directly. The Makiuchi Slide developed over a period of at least 2 days with the velocity increasing rapidly over the last day from about 10 mm/hr to 30 mm/hr, then within another hour a secondary accelerating mechanism developed, causing the maximum slide velocity of about 200 mm/s. Some properties of the constituent soils were reported, but these do not allow inferences to be drawn. The slides were probably first time features but this is not stated.

1968 Inangahua earthquake, M 7.0

Johnston (1974) documented a large slide which blocked the Buller River, after disturbance by the 1968 Inangahua earthquake. This was a rockslide dislodged from a precipitous slope.

Lensen & Suggate (1968, 1969) discuss the Oweka Slide, a block slide of about 3 million cubic metres of Tertiary siltstone which slid for many tens of metres on a thin bedding plane of highly overconsolidated plastic clay. The slide was considered notable in that the basal failure plane dipped at only 3.5 degrees. Subsequent examination of the slide and strength testing by the writer, revealed that the clay had moderate residual strength. ie not anomalously low and initial failure could reasonably be explained with moderate piezometric levels together with active earth pressure developed on the initially high rear boundary. After the initial seismic impulse which displaced the block along strike, slickensides showed that the slide movement was arcuate in plan with the displacement vector turning down dip and sliding continued under gravity for the remarkable total distance which exceeded 60 metres. No reactivations of existing slides were reported.

1968 Borrego Mountain earthquake, M 6.4

Landslides triggered by the 1968 Borrego Mountain earthquake have been discussed by Castle & Youd (1970, 1972) who noted various forms of new slides but 'older landslides within the zone of intensive slumping were non-existent or at least inconspicuous. The general configuration of the hills, however, suggests that slumping may have been locally operative for a long time. The boundary between the hills and the surrounding alluvial lowlands forms a convoluted pattern in plan view that, together with the prominently steepened ridge crests toward the ends of their respective spurs, suggest great viscous flows edging out upon the adjacent plain.' The above description is highly suggestive of cohesive, rather than liquefiable materials, however no soil descriptions are given.

Only one movement relates to a pre-existing slide:

'a reactivated slump or block glide within the generally silty quaternary lacustrine deposits, about 65 km southeast of the epicentre ...constituted the largest single slope failure identified during the post-earthquake investigation. This failure was expressed as a simple break ...vertical separations along this break of as much as 50 mm formed a subdued headwall scarp that extended for more than 0.4 km.'

The soil description is again inadequate to judge whether liquefaction contributed here, however, the amount of movement is obviously minimal.

1970 Adelbert Range earthquake, M 7.0

Pain (1972) in a study of the 1970 Adelbert Range earthquake in Papua, provides one of the few instances in which some relevant parameters are recorded (slide dimensions, slope angle, rock and soil type, weathering, vegetation etc). Although the study area was predominantly rainforest about 25% of the slopes of the 240 square kilometre area had failed. These were categorised as debris avalanches, earthflows, rockfalls etc but all were shallow failures (less than 1 metre thick) and the average slope of all failure surfaces was greater than 35 degrees. No reactivated slides were reported.

1970 Peru earthquake, M 7.7

The Huascarán debris avalanche was one of the most destructive earthquake triggered events in history (Plafker et al, 1971). It originated on a sheer face and incorporated a volume of about 100 million cubic metres of rock and ice, sliding over 14 km at a velocity of about 300 km/hr. Landslides involving slumps and rotational slumps of large masses were rare. These were reportedly in fluvio-glacial sediments, ie, liquefaction mechanisms probably operated. The overwhelming majority of landslides involved thousands of falls or slides of rock, and slides of loose debris, along steep valley walls, stream banks, and roadcuts. Extensive reactivations occurred during the following rainy season.

The Huascarán debris avalanche occurred in a region of severe landslide hazard under non-seismic conditions (Keefer et al 1979). In the 30 years before the 1970 event (which killed more than 18,000 persons), eight destructive rock fall-avalanches and debris flows had occurred in the region (one of which killed about 4,000 people. None of these was triggered by earthquake. However, Keefer et al (1979) point out that many landslides occur in areas with little or no historic record of slope instability under non-seismic conditions. This conclusion may not necessarily stand when longer time periods are considered from detailed mapping to assess the geologic record.

1971 San Fernando earthquake, M 6.6

The 1971 San Fernando earthquake (Morton 1971) triggered more than 1000 landslides over an area of 250 square kilometres, with slide lengths up to about 300 m. Many areas were also badly fractured rather than displaced, but these were considered likely to develop into slides after substantial rainfall.

'Superficial (0.2 to 1 m thick) debris slides and avalanches were probably the most widespread and common types of failure and were especially pronounced in areas underlain by sedimentary rocks. Rockfalls were common on steep-walled canyon faces cut in well-fractured basement rock, but also occurred in sedimentary rock where a particularly resistant bed cropped out in over-steepened slopes. Soil falls occurred mainly at the free face of recent stream terrace deposits along major drainages. Slumping was found largely on reactivated pre-existing slumps.'

However, the reactivated landslides exhibited

'fresh scarps from 0.25 to 1 metre high. Some small old scarps failed as debris slides. Parts of other large old slides failed as a number of small discrete new slides generally concentrated along the toe of the old slideLarge rotational or complex landslides, which are characteristic of the San Gabriel and Santa Susana Mountains, did not form during the San Fernando earthquake. Apparently, such slides form when the ground is saturated by prolonged or heavy rain, or by seismic shaking with longer period vibrations or of longer duration than the San Fernando earthquake.'

Morton also comments on fracturing:

'Widespread ground fracturing throughout much of the area around San Fernando is closely related to landsliding. This fracturing appears to be most pronounced along ridge tops, where, given sufficient rainfall, the highly fractured surficial materials may give rise to abundant debris slides and flows. These materials may now conceivably have the potential for generating as many (or even more) landslides as were triggered during the earthquake.'

Youd (1971) discussed the man made lakes formed behind the Upper and Lower San Fernando dams:

'Because of the reservoirs and a confined aquifer in the Little Tijunga syncline, the watertable in the general area is at a relatively high level and intersects the surface at several locations. At the time of the earthquake, the watertable was probably not more than a few metres below the surface at any point in the alluvial areas surrounding the lakes.... A large number of landslides formed in the vicinity of the lakes in response to the earthquake.'

The distribution of slides provides another example of the potential for earthquake

disruption of semi-submerged slopes influenced by newly formed reservoirs. However, in this instance most failures were attributed to liquefaction.

Yen & Trotter (1978) attempted analyses of a selected group of slides triggered by the San Fernando earthquake. However, almost all slopes were steeper than 40 degrees and less than 2 metres thick as this type of slide was noted to be by far the most common. They proposed a method of analysis for predicting the length of slide likely to develop on steep slopes.

1972 Managua earthquake, M 5.6

Valera (1973) and Plafker & Brown (1973) discussed landslides in the Managua earthquake. Most failures developed on steep slopes forming the walls of 2 calderas. No reactivations of pre-existing slides were reported.

1976 Friuli earthquake M 6.4

Landslides triggered by the 1976 Friuli earthquake were almost entirely rockfalls (Govi 1977), generally re-occurring in the same proximity during the series of significant shocks which took place over a period of several months. Talus was observed to be one material type that, as a rule, was unaffected. This was attributed to rainfall assisted deposition. An alternative explanation is that talus deposits are naturally at their maximum angle of repose, ie will not be strain softening and although small displacements could occur under high accelerations, major seismic deformations would be expected.

1976 Guatamala earthquake, M 7.5

The 1976 Guatamala earthquake generated more than 10 000 landslides over an area of 16,000 square kilometres. Rockfalls and shallow debris slides of less than 15,000 cubic metres were the predominant form of mass movement. Harp et al (1978, 1981) reported:

'Without exception, rockfalls and debris slides from the earthquake were located along the steep canyon slopes. Rockfalls occurred as spalling failures on canyon slopes of between 30 and 50 degrees (mainly in sandy soils developed on pumice) and were generally less than 1 m thick. Both rockfalls and debris slides were heavily concentrated along narrow ridges and spurs, which suggests that the existing topography markedly amplified the level of seismic ground motion. In all cases observed, most landslide debris appeared relatively dry because the earthquake occurred at the height of the dry season when groundwater levels were low.'

'Pre-earthquake landslides were found to have been reactivated little, if at all during the earthquake.'

The possible relationship of pre-earthquake landslide deposits to the distribution of earthquake-induced landslides, were investigated. Most such features were large landslides or landslide complexes whose morphologies suggest deep-seated rotational slumps, block glides or flows. Despite strong seismic shaking from the 1976 earthquake, pre-earthquake landslide material mostly appeared to remain stable. Only at one site was a large part of an old landslide or landslide complex reactivated: cracks bounding the incipient landslide along the Rio Cotzibal were approximately along the margins of the pre-existing landslide and extended throughout most of the pre-existing slide mass'. The report gives no comment as to soil type here, nor amount of earthquake induced displacement, although it may be inferred that the latter was quite minor.

'Earthquake induced rockfalls and debris slides were not uncommon within old landslide deposits, although these failures were typically restricted to steep toes and headwall scarps... Evidence from other earthquakes shows a similar behaviour of dormant landslides during strong shaking. Keefer et al. (1978) documented the fact that, in general, few dormant landslides were reactivated by earthquakes. Plafker et al (1971) observed that most landslides in the 1970 Peru earthquake were rockfalls and debris slides related to steep slopes rather than to pre-earthquake landslides. The behaviour of pre-existing landslides during the 1976 Guatemala earthquake implies that such deposits may be relatively stable even under conditions of strong shaking and indicates that the landslide margins near headwall scarps and eroded toes, where slopes are steepest, are the areas most susceptible to rockfalls and debris flows.'

1978 Santa Barbara earthquake, M 5.5

Harp et al (1980) and Miller & Felszeghy (1978) report that in the 1978 Santa Barbara earthquake, landslides were not widespread or of large size. Most rockfalls and rockslides occurred in steep road cuts. Natural slopes were generally not susceptible to rockfalls except along the ocean cliffs. No reactivated slides were reported.

1978 Izu-Ohshima earthquake, M 7.0

In the 1978 Izu-Ohshima earthquake (Okusa & Anma 1980), report

'most failures occurred on convex slopes close to the inflection points of the slope angles. The convex part of a slope, in plan and in vertical section is mechanically unstable due to weak constraint from the surrounding rock masses.'

Especially large scale landslides occurred along the sea coast cliffs (100 to 300 m high at 50 to 80 degrees) near the activated faults. These failures were on a scale of 20-30 m

in width, 50-100 m in length along the slope, 2-10 m in depth and 200-500 cubic metres in volume.

A pre-existing rotational failure previously stabilised with a retaining wall showed distress but apparently little displacement. Soil type involved was not reported.

Some slide damming of rivers occurred but with no serious consequences.

The effect of incipient failures - ground fractures etc, was significant. In the two years following the earthquake, about 160 slopes failed during rain. The total area devastated was about 1.4 times that which failed as a direct result of the earthquake.

No marked reactivation of pre-existing slides was noted. However, one such slide showed widely distributed tension cracks in the back slopes of the main scarps and on the tongues of the landslide mass. Another pre-existing slide failed incipiently in the upper part with scarps 50 to -150 mm in height.

1979 Montenegro earthquake, M 6.6

Isihara (1985) and Anicic et al (1979) report that most damage from the Montenegro earthquake resulted from liquefaction of recently deposited fine sands. As many as 1000 rockfalls, rockslides, and debris avalanches were triggered. These landslides occurred most frequently on slopes steeper than 50 degrees; had volumes less than 100 cubic metres, and were geometrically defined by joint and bedding plane discontinuities. Wet climatic conditions preceding the earthquake influenced the seismic behaviour of existing landslides. At least six pre-existing slumps and block slides were reactivated, although they moved less than a metre. Wet conditions also contributed to the seismic triggering of at least three earthflows. The event induced minor displacement (much less than 5 metres) of the Kaliman Slide. This was composed of colluvial slope debris (weathered to a 'soft clay') derived from limestone and claystone. The activated slide which covered a slope area about 300 m wide and 700 m long, was further activated by rainfall two days after the earthquake. A large volume of about 1.2 million cubic metres, developed into a large scale earthflow which moved 50-100 m. Movement rates were not reported but apparently amounted to a few tens of metres per day. Although not stated, the geology suggests that residual strength conditions may well have pertained here.

1980 Irpinia earthquake, M 6.5

The Irpinia earthquake produced anomalous activity of landslides in that

"most of the mobilised slides were old, dormant or active slides. In most cases, there was some delay (a few hours to a few days) between the main shock and the sliding ... some of these slides had been set in motion also by the 1930 earthquake"

(D'Elia et al 1985). Two slides are discussed in detail. The first (Torella), involved 20 million cubic metres of debris including moderately plastic (PI = 20) clays on a saturated 8.5 degree slope. The slope movements

"evolved very slowly in the days following the earthquake, through a succession of slides, falls and flows. During the 24 hours immediately after the main shock, slight fractures were noticed on the surface of a road across the upper part of the slide. Large displacements occurred in the following 48-72 hours ...".

The actual movement rates are not stated, but a rate of about 2-3 m/day can be inferred. The second slide (Andretta) involved clay of similar plasticity, and was inferred

"to have been affected (by sliding) also a few centuries ago after a strong earthquake... the middle and upper parts of the slope had in any case remained quite stable over the last 200 years. The movements induced by the 1980 earthquake were evident at 12 hours from the shock and they developed over the ensuing 20 days."

The inferred movement rates of this slide are about 2 m/day.

The explanations offered for the observed behaviour were inconclusive, and the writers commented that "the failure mechanisms causing the landslides are far from being understood".

1983 Coalinga earthquake, M 6.7

Landslides associated with the Coalinga earthquake were reported by Keefer et al (1984). The most numerous and widely distributed landslides were rockfalls, rockslides, and soilfalls, on steep high ridges. Many small rockfalls with volumes less than 2 cubic metres were visible along road cuts. First-time slumps and one reactivated slump were identified but failure surface materials were not described.

1983 Borah Peak earthquake, M 7.3

The Borah Peak, Idaho earthquake caused several hundred landslides, the most numerous of which were rockfalls and rock slides in slopes containing conspicuous, through-going, open fractures or composed of weakly cemented rocks. Most of the rockfalls were from slopes steeper than 35 degrees. A complex rotational slump-debris flow occurred in colluvium in an area where hummocky topography suggested prior landsliding. The landslide covered about 4 hectares and contained an estimated 100,000 cubic metres of broadly graded material from boulders to clay. Downslope speeds were guessed to have been at least several tens of metres per hour. Springs emanating from within and beside the landslide led to the suggestion that changes to the groundwater regime by the adjacent fault scarp (which passed beneath the debris flows) may have contributed to the reactivation. At another location close to the fault trace, a large mud

flow apparently developed about 2 days after the earthquake. New springs were found to be emerging in the source area of the flow.

It appears that hydrologic change caused by faulting of an aquifer presents an indirect mechanism for delayed seismic activation of first-time or pre-existing slides.

1985 New Britain earthquake, M 7.1

The New Britain earthquake in Papua New Guinea (King, Loveday & Schuster, 1988) caused extensive landsliding in weak, highly weathered rocks. The extensive area affected, was of high relief with steep slopes. A large bedding plane slide was reported, apparently a first-time event but this is not stated. A landslide dam formed, and its breaching was accompanied by a high (up to 100 m) wave involving over 100 million cu. metres of water and rock debris. No reactivations of pre-existing slides were reported.

1985 North Nahanni earthquake, M 6.6

The North Nahanni earthquake (Evans et al, 1987) triggered a major rock avalanche when detachment occurred against a steeply dipping (45 degree) fault in the head section of the slide. A second, significantly stronger event (M 6.9) occurred 2 months later but this caused no obvious displacement in the vicinity of the former slide, but did trigger numerous small rockfalls. No reactivations of pre-existing slides are reported.

1987 Edgumbe earthquake, M 6.3

This event was investigated in some detail by the writer to reconcile observed effects with those predicted from geotechnical analysis and laboratory testing.

The epicentre of the M 6.3 event was located on plains several km from hills. Very few slides were noted on undisturbed natural slopes: those that did occur were restricted almost entirely to deforested slopes and banks recently steepened by down cutting of streams. A large number of slides occurred in road cuttings: unsaturated slopes cut more steeply than the residual friction angle of the weakly cemented volcanic ash, failed rapidly to angles slightly flatter than residual.

Some incipient slides were apparent on deforested natural slopes (inclined only marginally flatter than their residual friction angle). About 0.5 to 1.0 m of cohesionless scoria overlies considerable thicknesses of ash. Drainage is excellent in the high permeability scoria and the relatively low ridges provide no significant catchment area. Failures appeared confined to the scoria or scoria/ash contact. Cracking was apparent particularly from about half way up the slope to the ridge crest where cracking was almost ubiquitous. Movements were therefore of a generally translational nature with low slide depth to length ratios. Displacements ranged from incipient cracking on 33 degree slopes to a metre or so on slopes of 40 degrees. No directional or aspect effects

were observed. A sample of scoria was recovered for shear testing, giving residual (ultimate) strength in the range of 42 to 46 degrees at low normal stress levels. It was concluded that the in situ material strength is likely to be towards or above the top end of the measured range.

The Matahina Dam recorded accelerations of over 0.3 g. Shoreline roading suffered severely. These were fill slopes of rockfill, close to their repose angle, extending well below reservoir level. Along several sections of the road, half of its width had disappeared from sight below reservoir level. Similar slopes closer to the epicentre but not submerged, showed deformations of only a few hundred millimetres.

No large pre-existing active slides were clearly identified in the affected area. One large slide (containing several million cubic metres) was inferred. This was probably subjected to accelerations of 0.2 to 0.25 g but the component soils could not be inspected and the pre-quake level of activity is unknown. However, no cracking was found in an inspection of the head area.

1988 Ecuador earthquakes, M 6.1 & M 6.9

The Ecuador earthquakes (Neito and Schuster 1988) caused widespread landsliding on steep slopes (commonly between 35 and 45 degrees). The slopes were densely forested, but abnormally high rainfall had been experienced in the month before the earthquakes. Most slips were superficial features, affecting the upper 5 m of weathered soils, derived from the underlying bedrock. Much damage was inferred to have been caused by river surges after breaching of landslide dams. No reactivations of pre-existing slides were reported.

APPENDIX 6

PORE PRESSURE EFFECTS IN RAPID LANDSLIDES

6.1 INTRODUCTION

A number of researchers have suggested that excess pore pressures may develop in a landslide as a result of pore fluid expansion from frictional heating eg: Anderson (1985), Davis et al (1989), Smith (in prep.), Voight & Faust (1982) on theoretical grounds, and by the writer on the basis of laboratory tests.

This appendix addresses the role of excess pore pressure development under firstly non-seismic and then seismic conditions. One highly mobile landslide case history of each type is suggested. In each case, there appears to be no more plausible explanation for the prime accelerating mechanism.

At first introduction, the concept appears somewhat exotic, and was initially considered implausible by the writer. However, after examining the theory and observing laboratory behaviour there appears to be no doubt that in certain soils, excess pore pressures developed by frictional heating are quite marked and this mechanism must be considered when assessing the potential for rapid acceleration of a landslide.

A6.2 LABORATORY TESTS OF PORE FLUID HEATING

The applicability of the phenomenon to a clayey silt gouge was investigated with a simple laboratory test. A sample was remoulded and reconsolidated in the ring shear apparatus, to its in situ normal stress level. Shearing was carried out for several metres until a stabilised residual strength value was obtained at 880 mm/day at 26 degrees room temperature. The water bath was then evacuated and replaced with water at 100 degrees. The result was an instantaneous reduction in shear strength of 4.8% followed by asymptotic recovery to the former value, which was effectively restored in about 1 minute. In view of the very short drainage path length in the ring shear apparatus, the short recovery time is not surprising. (Much longer times would be expected for thick failure surfaces with long in situ drainage paths.) Good repeatability (decreases consistently between 4 and 5%) was obtained after allowing cooling and the re-introduction of boiling water. The transient effect noted, could reasonably be attributed to a true reduction in effective normal stress as a result of increased pore pressure. The quick recovery (while the temperature would still be much closer to 100 degrees than the ambient level of 26 degrees) does not support the alternative hypothesis that residual strength might be significantly dependent on temperature.

In another test, the ring shear apparatus was modified to take a heating element (a single strand of high resistance wire) located in the lower third of the sample. In

practice, failure usually takes place near the top of the sample (close to the top platen). Therefore, efficiency of heating would have been low, but conservative inferences would result from the testing. A sample of highly plastic silty clay (CH classification) was sheared in a strain controlled mode at 880 mm/day until a stable residual strength (17 degrees friction angle) was recorded. At that stage, stress control was imposed. After about 1 minute of stable shearing, the heating element was turned on an energy of 0.6 W/cu.cm applied (comparable to the order of energy generated from moderately rapid creep rates in the slide from which the sample was taken). The results are shown in Fig. 6-0. The relatively steady initial creep rate soon accelerated to a rate too fast to record.

A6.3 BASIC THEORY

(After Smith & Salt, 1988)

To analyse the viability of pore fluid heating as a landslide accelerating mechanism it is assumed that all the gravitational potential energy lost with the downslope movement is transferred by friction into heat energy along a discrete failure surface. This heat is then assumed to dissipate equally in both directions away from the failure plane which, with the first assumption, forms a boundary condition for the general heat equation. Assuming an isothermal boundary exists at some distance from the failure surface, this enables the temperature profile to be determined as a function of time. Noting that the coefficient of thermal expansion of water is about 8 times that of common rock forming minerals and using the basic principles of mass conservation, a partial differential equation can be written which relates temperature change to pore pressure change. Consolidation theory can then be used to analyse the dissipation of these pore pressures which, with a finite difference numerical procedure, allows excess pore pressures to be calculated as a function of time. A computer program for analysis has been provided by Smith (pers comm), and is included in Section A6.7

Qualitatively the effect of pore fluid heating will become significant when the energy input from the sliding mass cannot be dissipated quickly enough, causing increased temperatures along with excess pore pressures if insufficient drainage can take place. This results in a decrease in the effective stress, a loss of strength and a decrease in the factor of safety. In these conditions, the slide will accelerate and the process will cascade, giving a sudden loss of stability.

Electrical Heating Effects

Stress controlled ring shear

Low permeability silty clay

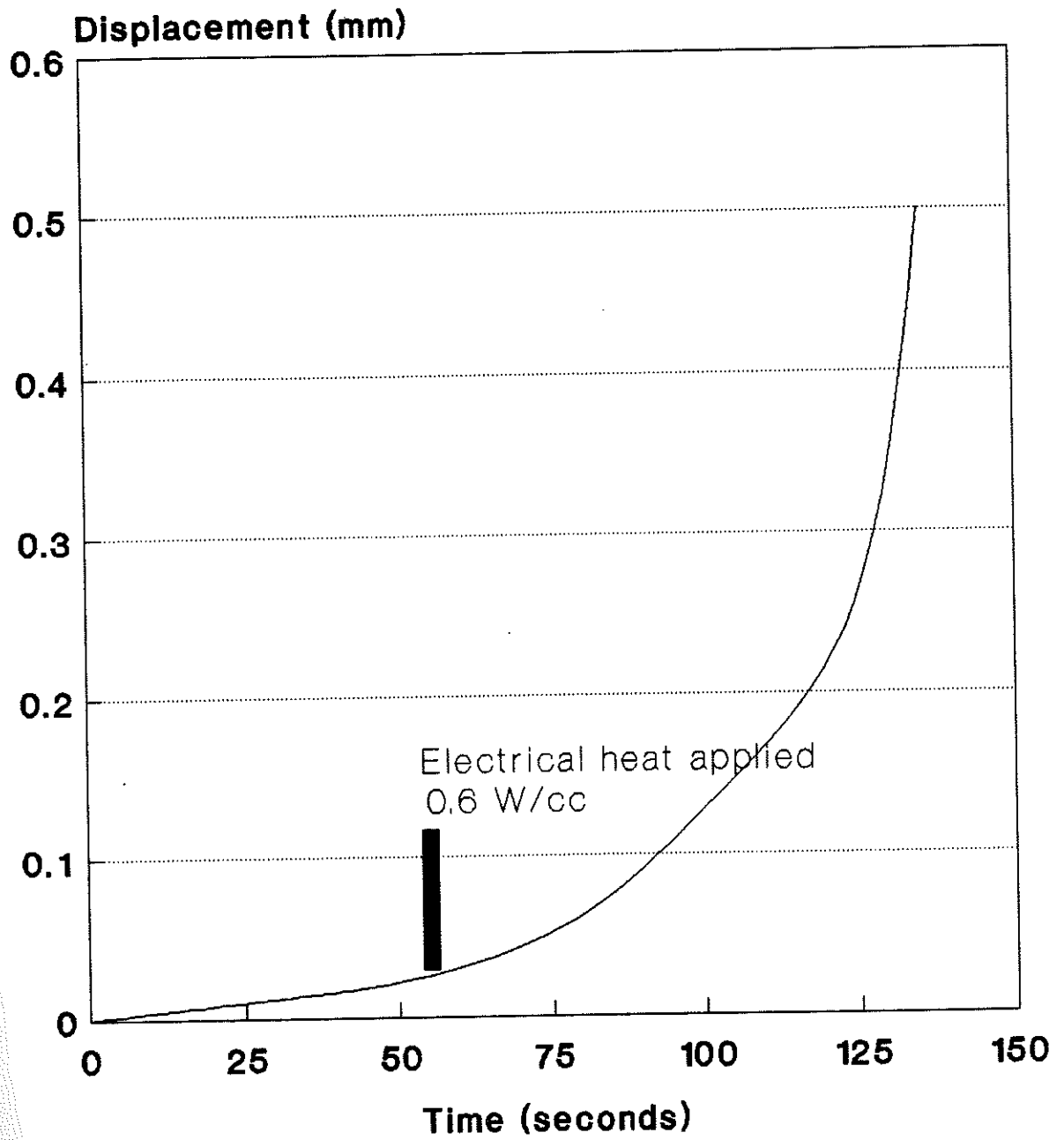


Fig. A6-0

(After Smith & Salt, 1988)

As possible example of frictional heating, the theory was applied to the East Abbotsford Slide. This slide accelerated unexpectedly after 10 years of incipient deformation. The sliding block, covering an area of about 20 hectares and involving more than 60 houses, moved in a predominantly translational manner down a thin plastic silty clay bedding plane, which dipped at 7 degrees. Classical active and passive Rankine zones developed in the head and toe areas respectively where the failure surface passed through very dense silty sand. Index properties of the bedding plane were LL:60, PI:38 and 35% clay fraction. It was highly overconsolidated and about 20-30 mm in total thickness although this contained multiple very thin lenses of silty fine sand. The depth of the failure plane averaged about 25 metres, while the watertable was located about 10 m above the slide plane and approximately parallel to it.

The slide was investigated and instrumented (partly during the creep phase but more extensively after the ultimate failure), allowing the relatively straightforward modelling by conventional limit equilibrium analysis. Input parameters were the measured piezometric levels and frictional strength of the silty sand forming the head and toe portions (effective friction angle of 33 degrees and zero cohesion). Back-analysis then indicated that an effective friction angle on the clayey bedding plane of about 8 degrees (assuming no cohesion) was mobilised at failure, this being fairly consistent with the residual shear strength measured in the laboratory at 7 to 7.1 degrees. The 1 degree difference may have been attributable to slight failure surface waviness, or greater average strength than measured in samples of sand from the head and toe areas. A plan and typical section are shown in Fig. A6-1. Incipient movements occurred over a period of 10 years. However about 3 metres of movement occurred in the 6 weeks preceding the sudden acceleration, when over 50 metres of displacement took place over a period of only 30 minutes. The maximum speed was estimated at 3 metres per minute.

To analyse the movement history of this slide, reasonable numerical values must be substituted into the model. Table A6-1 lists the required data, the ranges of values that would be expected for this case and the values used in the analysis to follow. Properties have been assessed from Hancox et al (1979), Clark (1962) and specific laboratory tests.

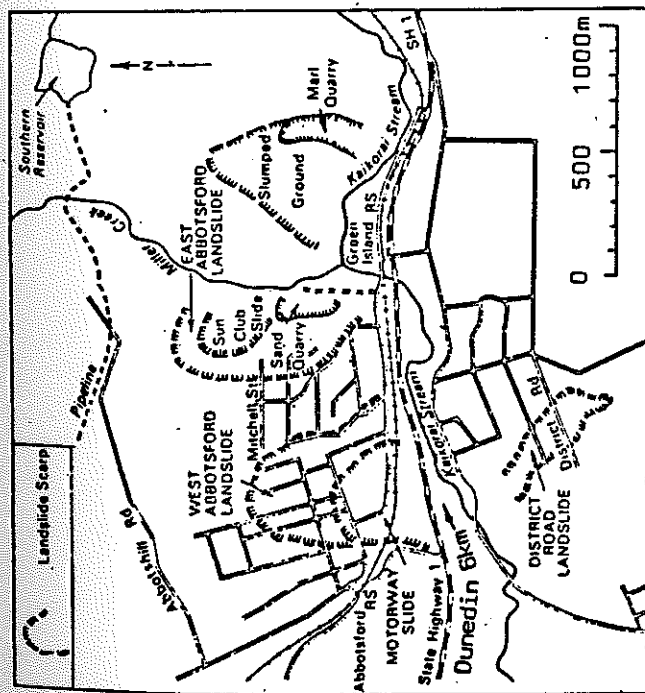


Figure 1a Locality map of the East Abbotsford Landslide

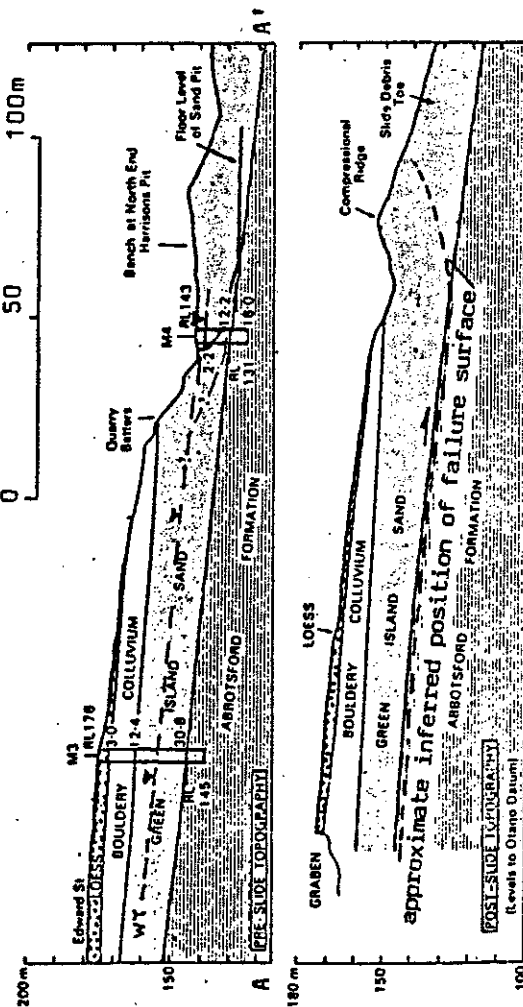


Figure 1c Generalised cross section of East Abbotsford Landslide (after Commission of Inquiry Report 1980)

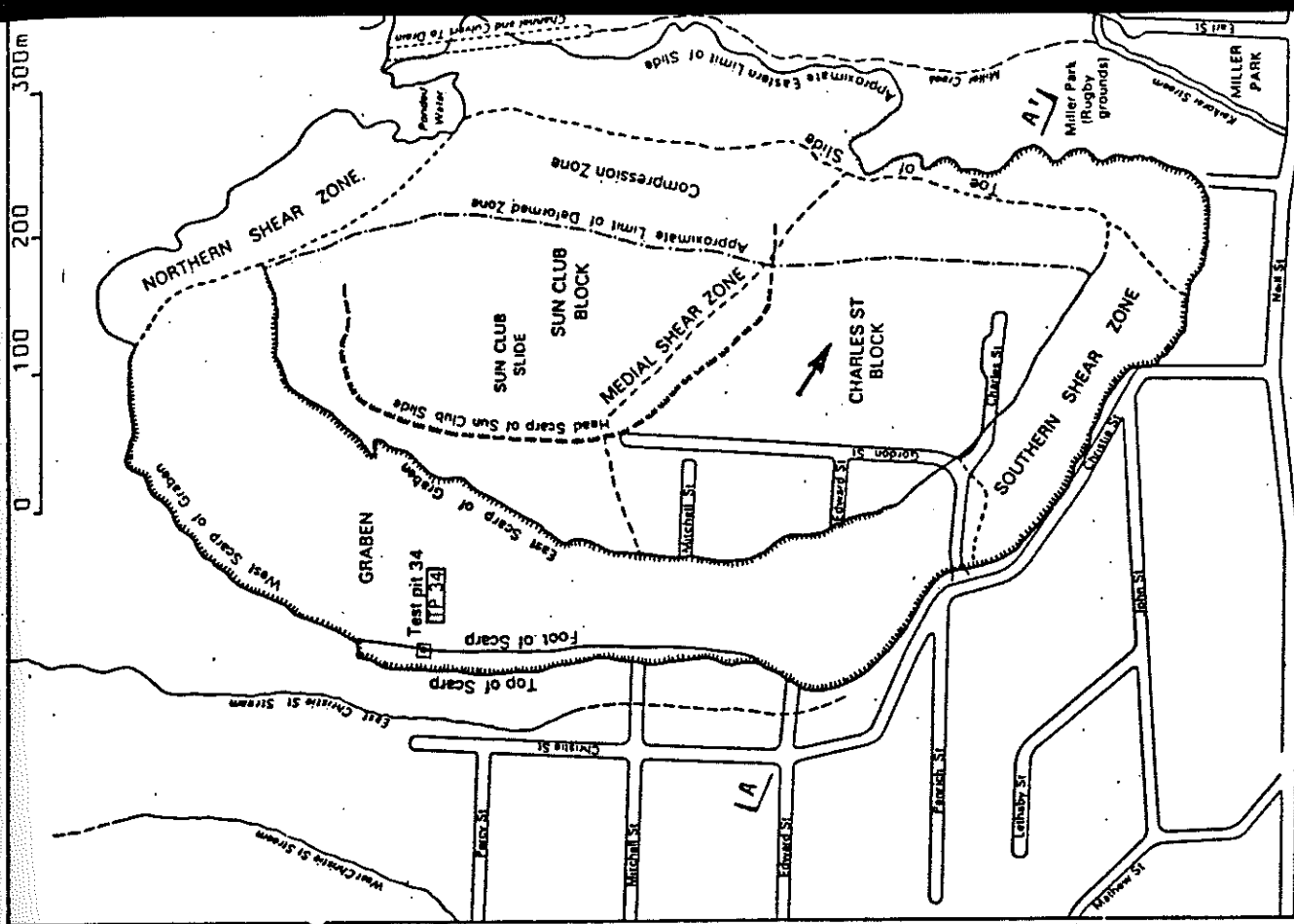


Figure 1b Map of East Abbotsford Landslide showing main features (after Commission of Inquiry Report 1980)

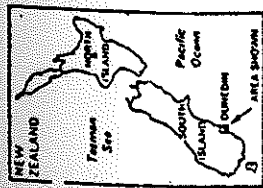


Table A6-1.

Data for Frictional Heating Analysis
of East Abbotsford Slide Plane

Variable	Probable range	Value adopted	Units
Thermal conductivity	2.5-3.7	3.3	J/s m degree C
Specific heat capacity	840-1000	940	J/kg degree C
Soil density	1800-2200	2000	t/cu m
Fluid density	1000	1000	t/cu m
Porosity	0.2-0.4	0.3	
Depth to drainage bdy	5-25	10	mm
Depth to isothermal bdy	10-30	20	m
Total vertical stress	200-600	400	kPa
Thermal expansion coef.	0.0002	0.0002	
Young's modulus (rebound)	50-200	100	MPa
Residual friction angle	7-8	8	degree
Permeability	1E-12 4E-11	1E-11	m/s

Using the above data the effects of frictional heating on pore pressures may be evaluated by inputting the velocity time function obtained from monitoring of this slide (Chapter 9, Fig. 9-1a) to the finite difference program below. The precursory movements of the first 30 days of movement were used for one model, and the movements in the last day only, on the second.

The results of the 30 day movement record (excluding the last day) are shown in Fig. A6-2.

Results of the analysis for the last few hours of movement, are shown on Fig. A6-3. These show the development of significant excess temperatures (up to 75 degrees) and accompanying excess pore pressures within the clayey band. Pore pressures dissipated relatively rapidly after movement ceased.

Frictional heating could also be modelled in the laboratory by imposing the observed velocities on a ring shear sample. However, there are two main sources of error: (i) the effect of loss of soil from the confining platen gap and (ii) the difficulties in achieving 100% saturation in conventional equipment. Small inclusions of air will diminish the pore pressure response greatly. Clearly, additional laboratory testing is required to refine the parameters listed in Table A6-1, and to measure directly the proposed strength loss. However, these preliminary calculations suggest that the pore fluid heating mechanism is worthy of further consideration to explain, at least in part, the sudden unpredicted acceleration of the East Abbotsford Slide.

East Abbotsford Landslide
Frictional Heating Model
Final month

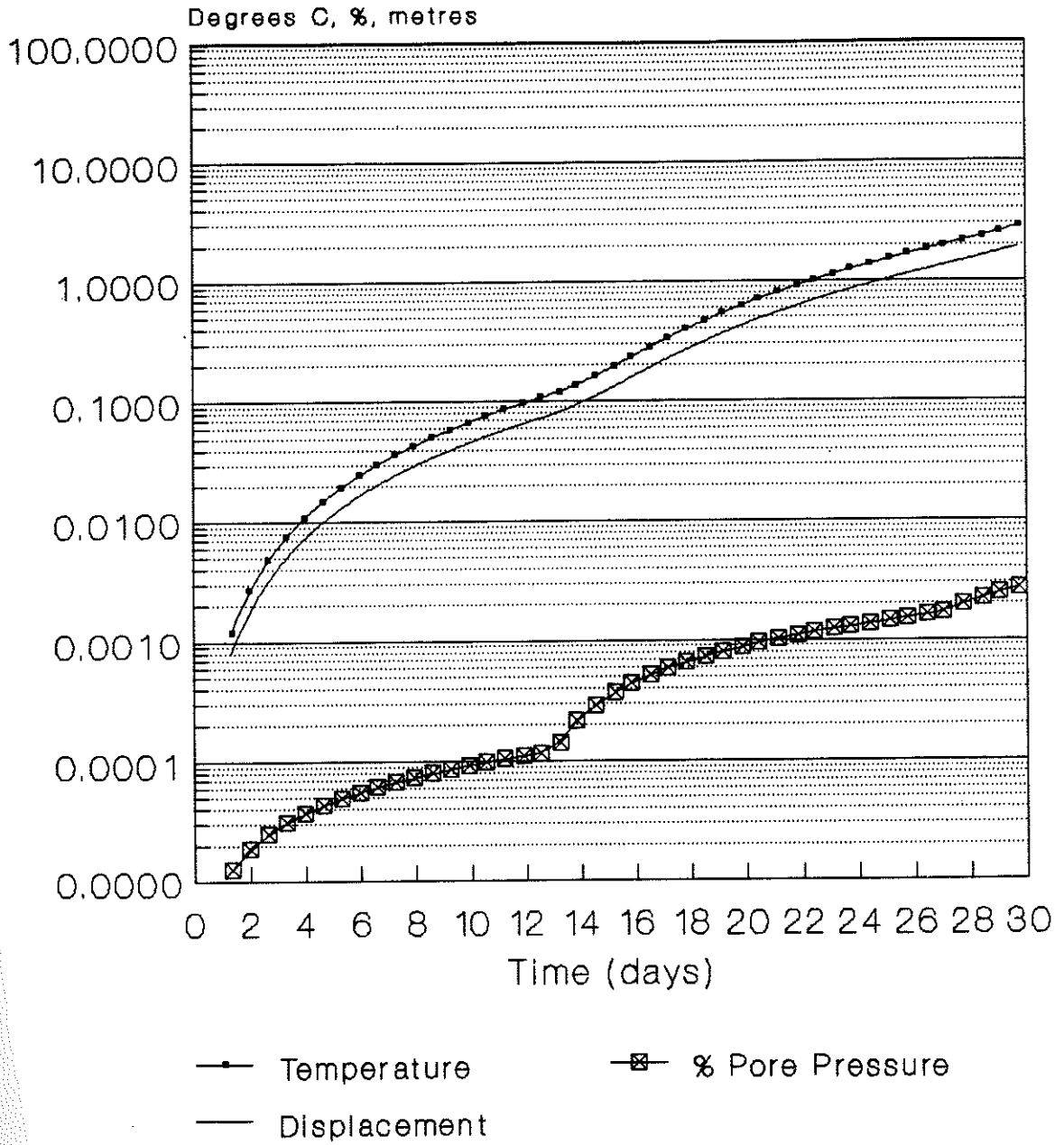


Fig. A6-2

East Abbotsford Landslide
Frictional Heating Model
Final day

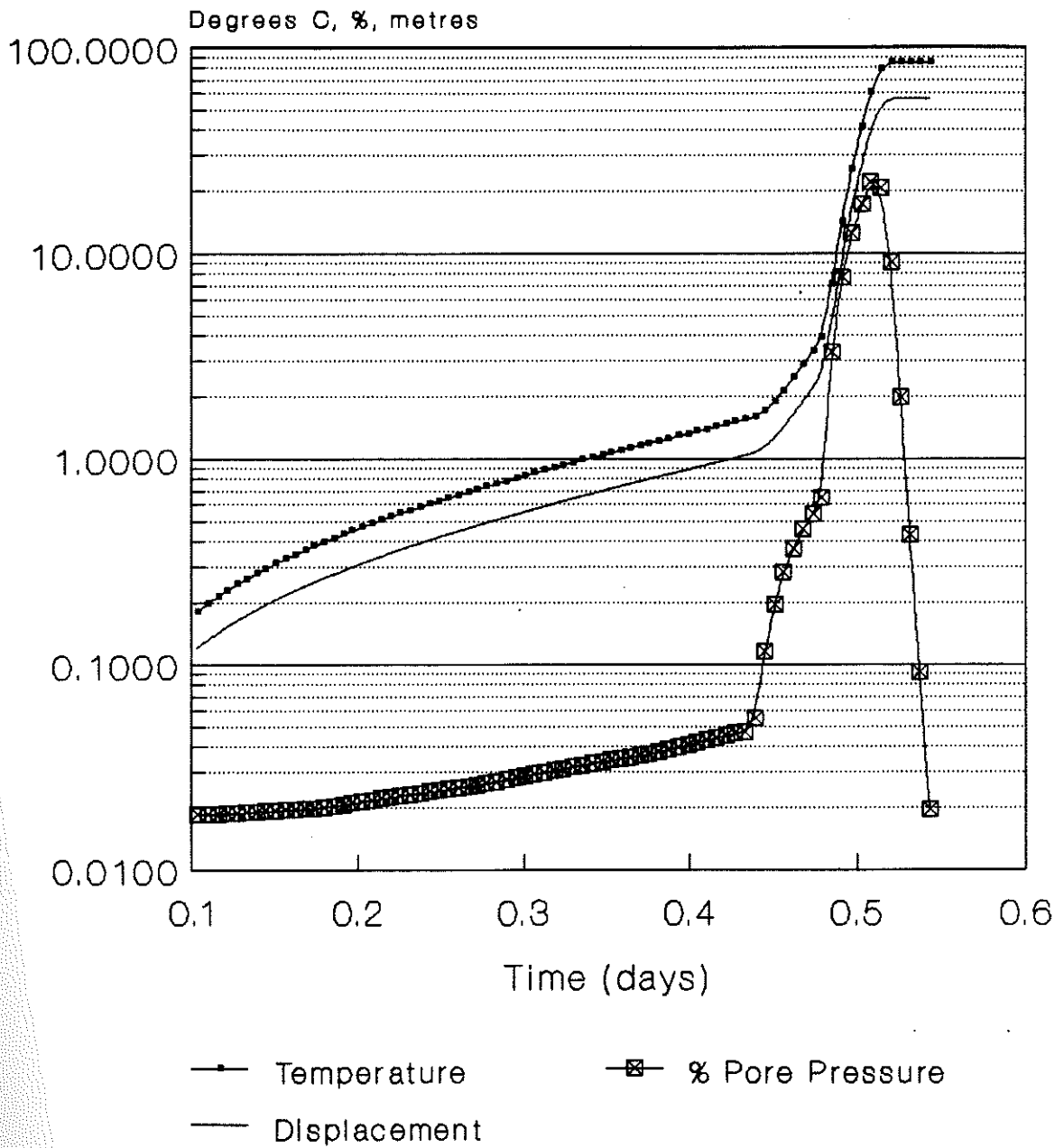


Fig. A6-3

A6.5 ANALYSIS OF marginally stable slopes under seismic conditions

Chapter 8 explains why conventional Newmark based methods for computing displacements of slopes under earthquake do not apply to slopes with safety factors close to 1.0. This section describes an improved procedure that appears to provide reasonable results (that are at least in accord with field observations) by taking into account the rate dependence of strength. Steps 1 to 6 alone apply if significant pore pressures will not be generated by frictional heating.

Steps 6 onwards include pore fluid heating effects. These can reach critical levels that will allow the slope to accelerate catastrophically either during or some time after the seismic loading ceases.

1. A section of the slide (with representative geometry and piezometric conditions) is adopted for the limit equilibrium model.
2. Failure surface materials are sampled and the mobile range curve (Chapter 7) is determined using the relevant range of normal stresses.
3. The slope is analysed to determine the creep mobilised strength (at safety factor of 1.00). The mobilised strength at rapid displacement rates is found by increasing the creep mobilised strength by the same percentage as the mobile range. (eg about 8% for clayey silt).
4. The limit equilibrium analysis (using the mobilised strength at rapid displacement rates) is output in a form suitable for Newmark type analysis. (The safety factor will then be found to be increased as a result of the increase in mobilised strength, to about 1.08 in the above example).
5. A design accelerogramme is selected (after modification for site response using programs such as SHAKE¹ if appropriate.)
6. A Newmark type analysis (eg DYNDISP¹) is then carried out, including pore pressure effects from cyclic shear densification and dynamic response as necessary. This produces a displacement time history for the slide during the earthquake loading.
7. The displacement-time history is applied to the slide model to determine excess pore pressures generated by frictional heating as potential energy is converted to kinetic and heat energy but calculations are terminated at the end of the earthquake record.
8. Step 6 is recomputed with the inclusion of excess pore pressures from Step 7 and the new displacement-time history used in Step 7 until compatibility of input and output pore pressures is achieved for the duration of the seismic record.

9. At the end of the earthquake loading the new safety factor of the model is calculated using the excess pore pressure. If the velocity of the slide is zero, the calculations stop. Otherwise further timesteps are taken as in Steps 7 and 8, until the velocity reduces to zero.

10. The final safety factor is computed after dissipation of all excess pore pressures, and the results of displacement, velocity and acceleration is output for each timestep.

(Note¹. Programs SHAKE, DYNDISP and accelerogrammes were obtained from US Bureau of Reclamation.)

In practice, once the procedure is set up, calculations are quite straightforward. (It is quicker to carry out than to describe here.) By interacting with files from a conventional slope stability program, DYNDISP and the frictional heating program, an operator can complete the above sequence in a few minutes and, more importantly, determine the sensitivity to input parameters. The results cannot be readily checked (until convenient earthquakes occur), hence the value in the procedure is considered to be in obtaining a general appreciation for displacement and the potential for rapid acceleration through sensitivity analyses of critically located landslides.

The output from DYNDISP may be used directly for the frictional heating model, taking each timestep (usually 10 to 20 milliseconds). However in view of other uncertainties, the average velocity over the relatively short period of loading is adequate for preliminary analysis. More simply, Steps 5 and 6 can be replaced using chart solutions (Ambrayseys & Menu 1988). In this case when iterating from Step 7, the design ground motion can be approximated by a convenient number of time steps.

The above assumes that the failure surface soil is at residual strength. Slides with any peak strength component would be much more difficult to quantify reliably. (Although the lower bound result assuming residual conditions may still be informative.) In principle, the procedure would follow all the above steps but the decrease in safety factor computed from the effective strength/displacement relationship of the failure surface soil would need to be included at each timestep.

Geometric changes (from slope deflation) also require consideration if displacements are large. The increase in safety factor with displacement (Appendix 4) should be included at each timestep.

CASE I

A case of a creeping landslide (Fig. A6-1) adjacent to an active fault was examined where the following properties were measured (#) and assumed:

Variable	Value adopted	Units
Thermal conductivity	3.3	J/s m degree C
Specific heat capacity	940	J/kg degree C
Soil density	2200 #	t/cu m
Fluid density	1000	t/cu m
Porosity	0.18 #	
Depth to drainage bdy	0.32 #	m
Depth to isothermal bdy	20	m
Total vertical stress	700 #	kPa
Thermal expansion coef.	0.0002	
Young's modulus (rebound)	73 #	MPa
Residual friction angle	28 #	degree
Permeability	1E-10 #	m/s

The peak ground accelerations for the Operating Basis Earthquake (OBE) and the Maximum Credible Earthquake (MCE) had been assessed at 0.2 and 0.5 g. These values were used to scale the Pacoima-Taft Mod. II accelerogramme¹ (PGA of 0.75 g) to use in the analysis.

The landslide displacements for the 2 earthquake events were:

- (a) OBE (0.2g): 0.15 m displacement in 22 seconds.
- (b) MCE (0.5g): 2.8 m displacement in 37 seconds.

The values may be used directly (without consideration of intermediate timesteps) for preliminary estimation of excess pore pressures from frictional heating. Simple uniform velocities of 0.15/22 and 2.8/37 m/s were applied for intervals of 22 and 37 seconds respectively in the finite difference model. Results in Figs. A6-4 and A6-5, indicate that pore pressures are negligible (0.5%) for the OBE, but are quite significant (7.8%) for the MCE.

Because the residual strength envelope for the failure surface soil was quite linear (no significant cohesion), the above percentages translate directly to the corresponding decreases in safety factors. The resulting significance in terms of continued movement can then be assessed in relation to the steady yielding mobile range of the soil (about 7 to 8%), ie excess pore pressures from the OBE are negligible whereas the MCE is predicted to give pore pressures approaching those with the potential to trigger rapid

Slide A
Earthquake Displacement Model
For OBE Frictional Heating

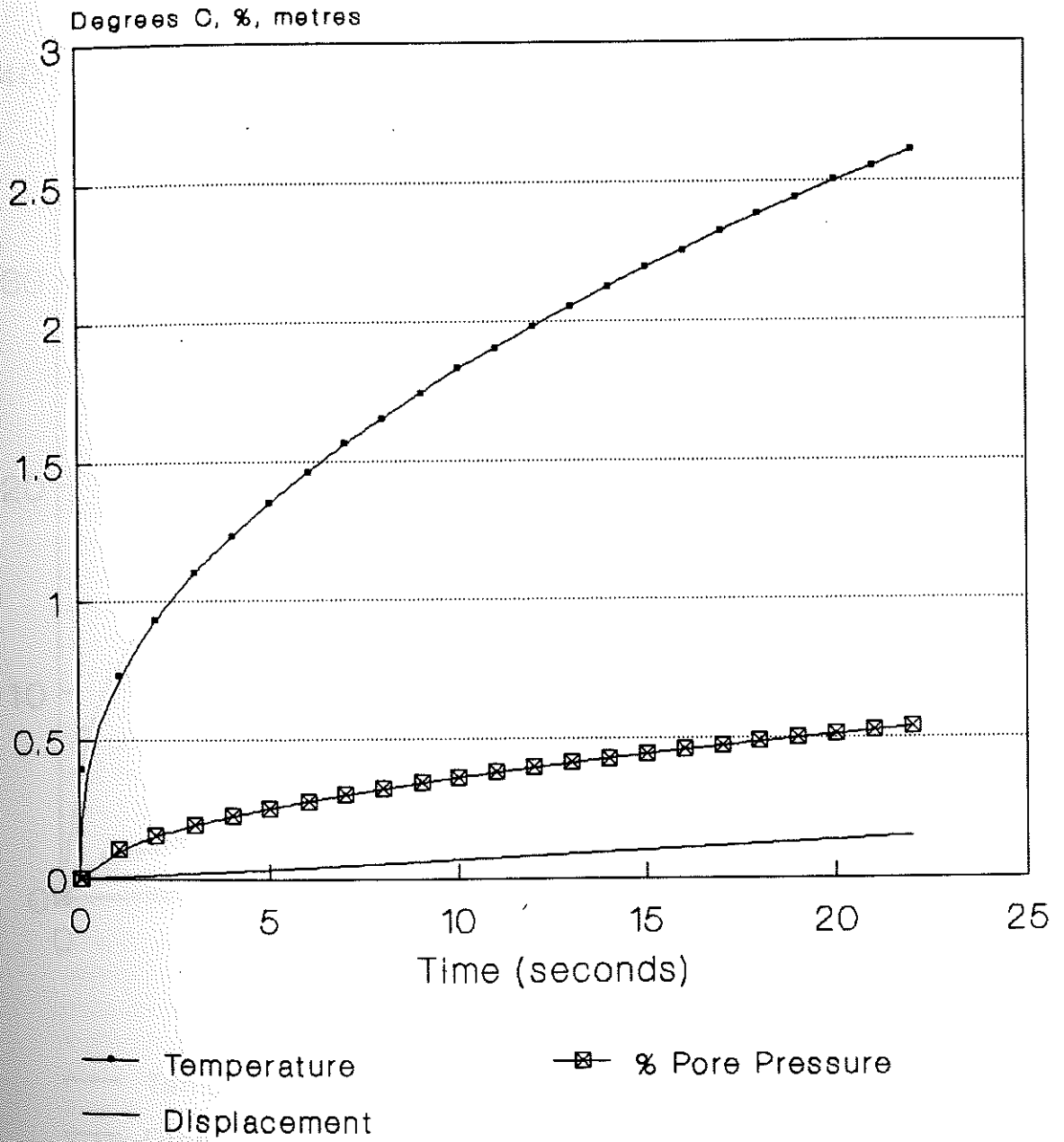
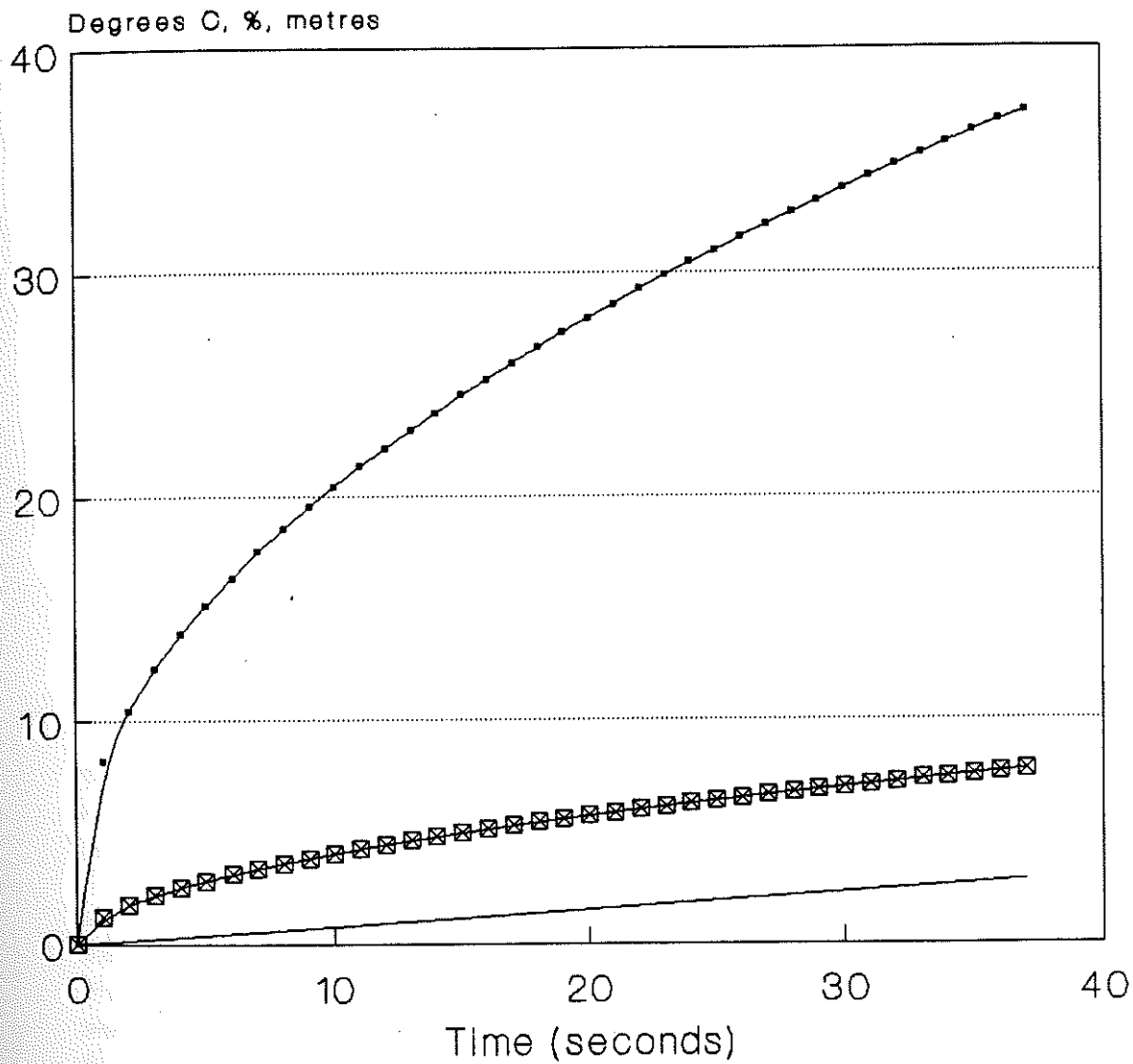


Fig. A6 - 4

Slide A
Earthquake Displacement Model
For MCE Frictional Heating



—●— Temperature —□— % Pore Pressure
— Displacement

Fig. A6 - 5

movement.

For the MCE, results from the numerical model are clearly borderline. As discussed above, the degree to which the model matches reality is unproven but the value in this instance was that more conservative remedial measures were recommended than might have been made otherwise.

CASE II

While the favoured explanation for the extreme rapidity of the Vaiont Slide, is now frictional heating, the multitude of alternative historic theories detract from the value of this example. Accordingly another case, will be proposed as probable evidence of the frictional heating mechanism. The case is the Oweka Slide (Appendix 5), triggered by the M 7.6 Inangahua earthquake.

The slide was not previously recognised as an existing feature. However, the presence of a very thin, relatively weak clay bedding plane within strata of heavily overconsolidated mudstone, suggests that residual strength conditions may have pertained in part, due to progressive failure (Bjerrum, 1967). The slide was a bi-wedge type, ie driving active wedge with the main mass being a block bounded by the bedding plane. The interesting feature was the large movement that was experienced. The failure surface was quite planar and a large expanse of the failure surface was left exposed by the translational slide. The bedding plane dip was close to horizontal (3.5 degrees) but the initial direction of sliding (evidenced by slickensiding) was almost along strike. The slickensides followed a gradual curve across the bedding plane showing that after several metres of movement along strike the plan movement vector then curved around so that the later movement of the block was down the 3.5 degree dip.

The writer was initially attracted to the site, by reports that the failure surface material was of exceptionally low strength (3.5 degrees residual strength was postulated by investigators). However, when tested, the failure plane produced a residual strength of 17 degrees. On reconstruction of the probable geometry at the time of incipient failure and analysing the slide with moderate groundwater assumptions, the measured strengths were found to compare quite closely with the mobilised strengths, ie the safety factor with respect to residual strength was close to 1.0 before displacement. The triggering of movement by earthquake was therefore not surprising. However, as movement progressed, the driving wedge collapsed onto the bedding plane, removing the large majority of the static driving force. A major strength loss must have occurred to allow the continuing extensive movement of the independent block as a purely translational slide on a 3.5 degree failure plane. (During that stage the slide had an apparent safety factor of about 5 with respect to residual strength). Excess pore pressures from frictional heating, would be expected in such a highly overconsolidated, low permeability failure plane. Pore pressures approaching overburden pressures would give a safety factor close to 1, thereby explaining the event.

Apart from the residual shear tests carried out, no other parameters have been

measured at the Oweka Slide. However, likely values of input parameters have been estimated. The field evidence indicates that the earthquake loading and active earth pressures propelled the slide at least 10 to 15 metres along the strike direction, after which failure apparently came predominantly under the influence of gravity as the movement vector turned down dip. As the duration of strong shaking would probably have been about 20 seconds, the assumption has been made that the slide moved 15 m in 20 seconds, under a combination of active earth pressure (driving wedge) and earthquake. Therefore modelling was carried out assuming a uniform velocity of $(15/20)$, ie 0.75 m/s for 20 seconds. The results are graphed in Fig. A6-6 which, while speculative shows that the guessed soil parameters are consistent with dramatic strength loss at the end of the 20 seconds modelled. Pore pressure increases are approaching the overburden pressure (equivalent to liquefaction in loose cohesionless soils). Because the shear testing confirmed negligible residual cohesion in the failure plane material, continuing movement on the low angle failure plane would not therefore be surprising.

(Programs and input/output data sets are filed on the accompanying diskette.)

Although few of the earthquake case histories reviewed provide adequate description of relevant geotechnical properties, other field examples of this mechanism do not appear to be common. The main reason (readily demonstrated in theory) probably being that particularly strong shaking is required in combination with a failure surface material of high modulus, low permeability and subject to relatively high normal effective stresses.

A6.6 ALARM CRITERIA FOR ACCELERATING LANDSLIDES

In the frictional heating program listed in A6.7, the subroutine beginning on line 5000 computes the time dependent velocity as a function of time from input parameters of velocity and acceleration. Alternative coding may be input to this section in either of following cases.

Setting Alarm Criteria for Steadily Moving Landslides

A sensitivity analysis can be carried out, using a series of different values for future acceleration, to determine alarm criteria for hazardous slides (Chapter 9). Comparative analyses will determine the value of future acceleration which will cause the excess pore pressure percentage (of the initial average effective normal stress on the failure surface) to approach the mobile range for the failing soil.

This approach was used to assess a hazardous landslide where several days would have been required to evacuate affected areas. Extensive precedent geological observations indicated that only slow creep movements of the large slide would be expected, ie the risk was regarded as very low. Therefore alarm criteria for velocity and acceleration were appraised in the following manner. The cases given in Chapter 9, Fig. 9-1 were examined to find the maximum rate of change of acceleration that occurred. These examples, (from landslides not subjected to external changes in driving forces) show that as a

Oweka Slide (M 7.6)
Earthquake Displacement Model
For Frictional Heating

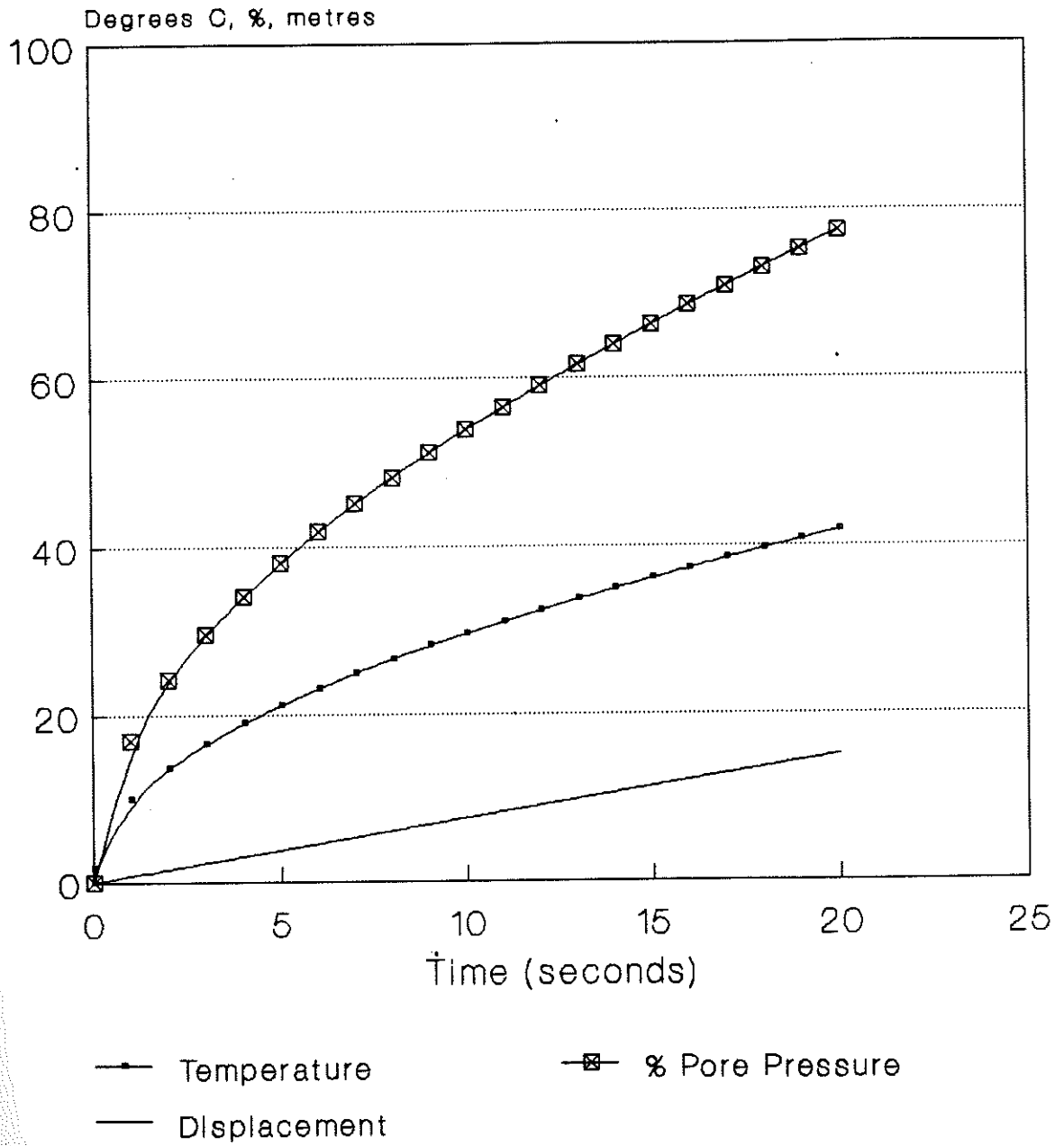


Fig. A6 - 6

reasonable upper bound, the acceleration could be considered to double every day. The limits of 50 mm/day and 5 mm/day/day for slide velocity and acceleration (suggested in Chapter 9) were adopted as a starting point. These values of velocity and acceleration and rate of change of acceleration were used in the frictional heating model. The results for the relatively permeable, normally consolidated soil type concerned indicated that pore pressures would be negligible until more than 5 days after the 50 mm/day, 5 mm/day/day criteria were exceeded. The criteria were therefore recommended as providing adequate forewarning.

Predicting Rapid Movements of an Accelerating Landslide.

Where monitoring is instigated for a hazardous accelerating slide, the data can be evaluated for insight to the risk. The program shown below requires that acceleration is constant but in cases of concern, the acceleration is likely to be non-linear. Accordingly a modified program (HEAT1) has been developed to accept either displacement/time or displacement/velocity data from a monitoring record. (The latter is preferable.) This allows an assessment to be made of whether pore fluid heating is significant at the current time (eg in the manner of Fig. A6-2). Subjective judgement of the risk of a sudden increase in acceleration can then be supplemented with a quantitative assessment. Example input and output data are contained on diskette.

A6.7 COMPUTER PROGRAM FOR PORE PRESSURES FROM FRICTIONAL HEATING

The following program by N. Smith, (pers comm) has been used to investigate the concept of frictional heating on pore pressures. Derivation of the constitutive relationships is given by Smith et al, (1989). The finite difference program has been found to be quite sensitive to timestep interval selected, and successively smaller timesteps and node spacings, need to be tried until consistent results are output.

All cases run, have yielded credible results but there has been no opportunity for independent verification. At this stage, the program has been used to provide insight to likely problems, rather than as a standard design method.

The present program is limited to a single soil type. Relatively minor modifications would be required to produce a multilayer analysis, in the event that the state of the art warranted more elaborate assessment.

Although the program has been written in BASIC, the accompanying program diskette includes an executable file compiled using Turbobasic which invokes a co-processor, as otherwise the run time is excessive.

The program seeks input from file "HEAT.IN". The first 2 lines are reserved for description and all data follows from the third line (1 value per line or comma delimited) in the sequence defined in lines 1040 to 1150.

```

10*****
20 ' ANALYSIS OF PORE PRESSURE RESPONSE TO FRICTIONAL HEATING
30 ' Velocity Input => Pore Pressure Output
40 ' Adapted from original program by Nick Smith Jan 1988
50*****
60 CLS
70 ' 1000 DATA INITIALIZATION
80 ' 2000 OPEN AND TITLE OUTPUT
90 ' 3000 CALCULATION CYCLE
100 ' 4000 PORE PRESSURE OUTPUT
110 ' 5000 VELOCITY FUNCTION
111 'Dimension Temperature(H) and Pore Pressure(U) Arrays
112 DIM H(1280),NH(1280),U(640),NU(640)
113 'OPEN & TITLE OUTPUT FILE
114 '
115 'Open Output File
116 OPEN "HEAT.OUT" FOR OUTPUT AS #1
118 PRINT " TIME TEMP %PORE VEL. DISP."
119 PRINT " SECONDS C PRESSURE M/S M
1010 DATA INITIALIZATION
1020 OPEN "HEAT.IN" FOR INPUT AS #2
1022 LINE INPUT #2, TITLE$:LINE INPUT #2,T$
1024 INPUT #2, K,C,DS,DW,N,A,B,S,CTE,E,TP,P,V,ACC,MINDT,MAXT,NA,NB
1030 'Physical Data (All in M.K.S Units)
1040 'K= Thermal Conductivity
1050 'C= Specific Heat Capacity
1060 'DS Soil Density
1070 'DW Fluid Density
1080 'N= Porosity
1090 'A= Distance to Free Draining Boundary
1095 'B= Distance to Isothermal Boundary
1100 'S= Total Vertical Stress
1110 'CTE= Coefficient of Thermal Expansion
1120 'E= Young's Moduli on Unloading
1130 'TP= Tangent of Residual Friction Angle
1140 'P= Permeability';P
1145 'V= Initial velocity
1146 'ACC= Acceleration
1147 'MINDT= Minimum timestep
1148 'MAXT= Maximum output time
1149 'NA= No. of Nodes in layer A
1150 'NB= No. of Nodes in Layer B
1170 'Computational Data
1180 DA=A/(NA-1) 'Distance between Nodes in layer A
1185 DB=B/(NB-1) 'Distance between Nodes in layer B
1190 '
1200 'Stable Time Step Calculation
1210 IF (DW*9.810001*K)/(DS*C*P*E) >= 1 THEN DT=(DS*C*DA^2)/(2*K) ELSE
DT=(DW*9.810001*DA^2)/(2*P*E)
1220 IF DT>MINDT THEN DT=MINDT
1340 'Determine Differential Equation Constants
1240 HC=(K*DT)/(DS*C*DA^2)
1250 HBC=(TP*DA)/(2*K)
1260 UC=CTE*N*E
1270 UDC=(P*DT*E)/(DW*9.810001*DA^2)

```

```

1280 '
2040 PRINT #1,"*****"
2050 PRINT #1,TITLE$
2060 PRINT #1," Analysis of Pore Pressure Response to Frictional Heating"
2070 PRINT #1,"      by Nick Smith Jan 1988  modified 10.3.88"
2075 PRINT #1," CAUTION CHECK SENSITIVITY TO SMALLER TIMESTEPS AND NODES
2080 PRINT #1,"*****"
2090 PRINT #1,"Data: Thermal Conductivity      ";K;"J / s m C"
2100 PRINT #1,"      Specific Heat Capacity      ";C;"J / kg C"
2110 PRINT #1,"      Soil Density      ";DS;"kg / m 3"
2120 PRINT #1,"      Fluid Density      ";DW;"kg / m 3"
2130 PRINT #1,"      Porosity      ";N
2140 PRINT #1,"      Distance to Free Draining Boundary ";A;" m"
2145 PRINT #1,"      Distance to Isothermal Boundary  ";B;" m"
2150 PRINT #1,"      Total Vertical Stress      ";S;" Pa"
2160 PRINT #1,"      Coefficient of Thermal Expansion ";CTE
2170 PRINT #1,"      Young's Modulus on Unloading    ";E;"Pa"
2180 PRINT #1,"      Tan of Residual Friction Angle  ";TP
2190 PRINT #1,"      Soil Permeability      ";P;"m / s"
2200 PRINT #1,"Computational Data:"
2210 PRINT #1,"      Number of Nodes in Layer A";NA
2215 PRINT #1,"      Number of Nodes in Layer B";NB
2220 PRINT #1,"      Numerical Timestep      ";DT;" s"
2230 PRINT #1," "
2240 PRINT #1," TIME  TEMP.  % PORE PRES.  VEL.  DISP."
2250 '
2260 'Output Control Data
2270 NS=0
3000 ' CALCULATION CYCLE
3010 FOR T=1 TO 1000000!
3015 TS=INKEY$:IF TS>< "" THEN INPUT"TYPE 999 TO END, ENTER TO CONTINUE ";TS
3017 IF VAL(TS)=999 THEN PRINT "FINISHED ":END
3020 RT=T*DT
3030 GOSUB 5000 'Determine Velocity
3040 ' Calculate Temperature Distribution
3050 H(1)=H(2)+S*HBC*V
3060 FOR J=2 TO NA-1
3070 NH(J)=H(J)+HC*(H(J-1)-2*H(J)+H(J+1))
3080 NEXT J
3081 IF A=B THEN 3090
3082 NH(NA)=H(NA)+HC*((H(NA-1)-H(NA))-((H(NA)-H(NA+1))*DA^2/DB^2))
3083 FOR J=NA+1 TO NA+NB-1
3084 NH(J)=H(J)+HC*(DA^2/DB^2)*(H(J-1)-2*H(J)+H(J+1))
3085 NEXT J
3090 ' Calculate Pore Pressure Distribution
3100 U(1)=U(2)
3110 FOR J=1 TO NA-1
3120 NU(J)=U(J)+UDC*(U(J-1)-2*U(J)+U(J+1))+UC*(NH(J)-H(J))
3130 NEXT J
3140 'Replace New H(J) U(J)
3150 FOR J=2 TO NA+NB-1
3160 H(J)=NH(J)
3163 NEXT J
3166 FOR J=2 TO NA-1
3170 U(J)=NU(J)

```

```

3180 NEXT J
3190 'Check if Output Time has passed
3200 IF RT>NS THEN GOSUB 4000
3210 NEXT T
3220 END
4000 'OUTPUT OF INTERVALS DATA
4002 DRT = RT/86400
4010 PRINT #1,USING "##.##^";RT;
4020 PRINT #1, TAB(10);
4030 PRINT #1,USING "#####.#" ;H(1);
4040 PRINT #1,TAB(20);
4050 PRINT #1,USING "###.###" ;U(1)*100/S;
4060 PRINT #1,TAB(30);
4070 PRINT #1,USING "##.##^";V;
4080 PRINT #1,TAB(40);
4090 PRINT #1,USING "###.###";DISP
4100 PRINT USING "##.##^";RT;
4110 PRINT TAB(10);
4120 PRINT USING "#####.#" ;H(1);
4130 PRINT TAB(20);
4140 PRINT USING "###.### %";U(1)*100/S;
4150 PRINT TAB(30);
4160 PRINT USING "##.##";V;
4170 PRINT TAB(40);
4180 PRINT USING "###.###";DISP
4190 NS=NS+1
4210 RETURN
5000 ' VELOCITY FUNCTION
5010 '
5020 V = V + ACC*DT
5030 DISP = DISP + V*DT + 0.5*ACC*DT^2
5035 IF RT>MAXT THEN PRINT "COMPLETED WITH OUPUT ON FILE'HEAT.OUT";END
5040 RETURN

```

REFERENCES

REFERENCES

- Adams, J. 1981. Earthquakes, landslides and large dams in New Zealand. Bull. N.Z. Nat. Soc. for Earthquake Engineering. 14 (2) 93-95.
- Allam, M. and Sridharan, A. 1981. Effect of wetting and drying on shear strength. J. Geotech. Eng. Div. ASCE Vol 107, No. GT4, 421-438
- Ambroseys, N.N. and Menu, J.M. 1988. Earthquake-induced ground displacements. J. Eq. Eng. Struct. Dynamics, Vol. 16, No. 7 985-1006. - pre-print from authors.
- Anderson, D.L. 1985. Heat generated pore pressure mechanisms. In: The Vaiont Slide, A geotechnical analysis based on new geologic observations of the failure surface. Geotechnical Lab. US Army Eng. Waterways Experiment Station, Vicksburg, Miss. Technical Report GL-85-5 by A.J. Hendron & F.D. Patton, Appendix F.
- Anicic D. et al. 1980. Reconnaissance Report: Montenegro, Yugoslavia Earthquake, April 15, 1979. Earthquake Eng. Res. Inst. Berkeley.
- Azimi, C., Biarez, J., Desvarreux, P. & Keime, F. 1988. Forecasting time of failure for a rockslide in gypsum. 5th Int. Symp. Landslides. Vol. 1, 531 -536 (in French. English translation by H. Moeung, (pers comm).
- B.C. Hydro. Vancouver. (pers comm.). Landslides affected by Mica Dam.
- Bishop, A.W. 1955. The use of the slip circle in the stability analysis of slopes. Geotechnique, Vol. 5, No. 1, 7-17.
- Bishop, A. W. et al. 1969 Geotechnical investigation at Aberfan. In: A selection of technical reports submitted to the Aberfan Tribunal. Welsh Office H.M.S.O. London
- Bishop, A.W., Green, G.E., Garga, V.K. Andressen, A. and Brown, J.D. 1971. A new ring shear apparatus and its application to the measurement of residual strength. Geotechnique, V 21, 4, 273-328.
- Bishop, A.W. and Blight, G.E. 1963. Some aspects of effective stress in saturated and partly saturated soils. Geotechnique, Vol. 13, No. 3, pp 177-197.
- Bjerrum, L. 1967. Progressive failure in slopes of overconsolidated plastic clay and clay shales. J Soil Mech. & Found. Div. ASCE Vol. 93, No. SM5 pp 3-49.
- Blanc, A., Durville, J.L., Follacci, J.P., Gaudin, B. & Pincent, B. 1987. Methods of supervision of a huge landslide: La Clapiere, Alpes Maritimes, France. Bull. IAEG, No. 35, 37-46.
- Breth, H. 1967. The dynamics of a landslide produced by filling a reservoir. 9th ICOLD Q 32
- Bromhead, E.N. 1979. A simple ring shear apparatus. Ground Engineering, Vol 12, No 5: 40-44.

- Carslaw, H.S. & Jaeger, J.C. 1959. *Conduction of Heat in Solids*. Clarendon Press, Oxford.
- Casagrande, A. 1950. Notes on the design of earth dams. *J Boston Soc. Civ. Engrs. ASCE* Vol. 37, pt 4, 405-429.
- Chandler, R.J. 1976. The history and stability of two Lias clay slopes in the upper Gwash valley, Rutland. *Trans. R. Soc. Lond. A.* 283, pp 463-491.
- Chandler, R.J. 1977. Back analysis techniques for stabilisation works: a case record. *Geotechnique*, Vol. 27, No. 4, pp 479-495.
- Clague J.J. and Souther, J.G. 1982. The Dusty Creek landslide on Mount Cayley, British Columbia. *Can. J. Earth Sci.*, 19, 524-539.
- Clark, J.B. 1962. *Physical and mathematical tables*. Oliver and Boyd. London.
- Corbyn, J.A. 1982. Failure of a partially submerged rock slope. *Int. J. Rock Mech. Min. Sc. & Geomech.* Vol. 19.
- Cornforth, D.H. Prediction of drained strength of sands from relative density measurements. *ASTM. STP 523* 281-303.
- Coulter, H.W. and Migliaccio, R.R. 1964. Effects of the earthquake of March 27, 1964 at Valdez, Alaska. *U.S.G.S. Prof. Paper* 542-C.
- Cruden, D.M. & Masoumzadeh, S. 1987. Accelerating creep of the slopes of a coal mine. *Rock Mechanics and Rock Engineering.* 20, 123-135.
- D'Elia, B. et al. 1985. Some effects on natural slope stability induced by the 1980 Italian earthquake. *11th Int. Conf. Soil Mech. Found. Eng.* V. 4, 1943-1949.
- Davis, R.O. Smith, N.R. & Salt, G. (in press) Pore fluid heating and stability of creeping landslides.
- del Prete, M. and Petley, D.J. 1982. Case history of the main landslide at Craco, Basilicata, South Italy. *Geologia applicata e idrogeologia*, V. 17, 291-304.
- Dieterich, J.H. 1978. Time-dependent friction and the mechanics of stick-slip. *Pageoph*, Vol. 116: 790-806.
- Erismann, T.H. 1979 Mechanism of large landslides. *Rock Mechanics*, Vol. 12, 15-46.
- Espinosa, A.F. 1976. The Guatemalan earthquake of February 4, 1976, A preliminary report. *U.S. Geological Survey Prof. Paper* 1002.
- Evans S.G. et al, 1987. A rock avalanche triggered by the October 1985 North Nahanni earthquake, District of Mackenzie, N.W.T. *Can. J. Earth Sci.*, 24, (1) 176-184.

- Fukuzono, T. 1985 A new method for predicting the failure time of a slope. Proc. 4th Int. Conf. & Field Workshop on Landslides, Tokyo, 145-150.
- G.C.O. 1984. Geotechnical Manual for Slopes. 2nd edition. Geotechnical Control Office, Government of Hong Kong.
- Golder Associates, 1979. Groundwater Computer Package. Unpublished.
- Govi, M. 1977. Photo-interpretation and mapping of the landslides triggered by the Friuli earthquake 1976. Bull. IAEG. No. 15 67-72.
- Habib, P. 1975 Production of gaseous pore pressure during rockslides. Rock Mechanics Vol. 7, 193-197.
- Hadley, J.B. 1964. Landslides and related phenomena accompanying the Hebgen Lake earthquake of August 17, 1959. In: The Hebgen Lake, Montana earthquake of August 17, 1959. USGS Prof. Paper 435, 107-127.
- Hadley, J.B. 1978. Madison Canyon Rockslide, Montana, U.S.A. Rockslides and Avalanches, B. Voight ed. Elsevier, Vol 1. 167-180.
- Hancox, G.T.; Bishop, D.G.; McKellar, I.C.; Suggate, R.P. & Northey, R.D. 1979. East Abbotsford Landslide. New Zealand Geological Survey Report EG 332.
- Hansen, W.R. 1964. Effects of the earthquake of March 27, 1964 at Anchorage, Alaska. USGS Prof. Paper 542-A.
- Harp, E.L. et al. 1981. Landslides from the February 4, 1976, Guatemala earthquake. USGS Prof. Paper 1204-A.
- Harp, E.L. et al. 1978. Landslides from the February 4, 1976 Guatemala earthquake: Implications for seismic hazard reduction in the Guatemala city area. 2nd Int. Conf. on Microzonation. V. 1, 353-366.
- Harp, E.L. et al. 1980. A comparison of artificial and natural slope failures. The Santa Barbara Earthquake of August 13, 1978. California Geology, V. 33 (5), 102-105.
- Hendersen, J. 1933. The geological aspects of the Hawke's Bay earthquakes. N.Z. J. Sci. and Tech. V. 15 (1), 38-51.
- Hendersen, J. 1937. The West Nelson earthquakes of 1929. N.Z. J. Sci. and Tech. V. XIX (2) 65-142.
- Hungr, O. 1981. Dynamics of rock avalanches and other types of slope movements. PhD thesis, Edmonton, University of Alberta.

- Hunt, B. 1983. *Mathematical Analysis of Groundwater Resources*. Butterworth & Co. Ltd.
- Hutchinson, J.N. et al. 1973. A landslide in periglacially disturbed Etruria Marl in Bury Hill, Staffordshire. *Quart. J. Eng. Geol.*, Vol. 6, pp 377-404.
- Hutchinson, J.N. 1977. Evaluation of the effectiveness of corrective measures in relation to geological conditions and types of slope movement. *Bull IAEG* 16: 131-155.
- Hutchinson, J.N. 1988. Morphological and geotechnical parameters in landslides in relation to geology and hydrogeology. General Report, 5th Int. Symposium on Landslides. (1) 3-35.
- Ishihara, K. 1985. Stability of natural deposits during earthquakes. 11th Int. Conf. Soil Mech. Found. Eng. Vol. 1, 321-376.
- Janbu, N. 1973. Slope stability computations. in: *Embankment-dam engineering*. Hirschfeld & Poulos, eds: Wiley & Sons: 47-86.
- Janbu, N. 1977. Slopes and excavations. State-of-the-art report. 9th Int. Conf. Soil Mech. Found. Eng., Tokyo, Vol. 2, 549-566.
- Jappelli, R. & Musso, A. 1981. Slope response to reservoir water level fluctuations. *Proc. 10th Int. Conf. Soil Mech. and Found. Eng.* Vol. 3, 437-441.
- Johnston, M.R. 1974. Major landslides in the upper Buller Gorge, South West Nelson. *N.Z. Inst. Engrs. Transactions* V. 1, 239-244.
- Johnson, R.S. 1982. Slope stability monitoring. *Proc. 4th Canadian Symp. on Mining Surveying and Deformation Measurements*. Can. Inst. of Surveying, Banff, 363-379.
- Karal, K. 1979. The energy method for soil stability analyses. *ASCE J Geotech. Eng. Div.*, Vol. 103, GT5, 431-445.
- Keefer, D.K. et al, 1978. Preliminary assessment of seismically induced landslide susceptibility. *Proc. Int. Conf. on Microzonation for Safer Construction - Research and Application*. 2nd: Vol. 1 279-290.
- Keefer, D.K. et al, 1979. Preliminary assessment of seismically induced landslide susceptibility. *USGS Circular* 807, 49-60.
- Keefer, D.K. 1984. Landslides caused by earthquakes. *Geol. Soc. Amer. Bull.* V. 95 406-421.
- Keefer, D.K. et al. 1984. Landslides and related ground failures. In: *Coalinga, California, Earthquake of May 2, 1983*. *Earthquake Eng. Res. Inst.* 99-105.
- Keefer, D.K. et al, 1985. The Borah Peak, Idaho earthquake of October 28, 1983-Landslides. *Earthquake Spectra*, Vol. 2 (1) 91-125.

- Kinzelbach, W. 1986. Groundwater Modelling. Developments in Water Science (25) Elsevier.
- Lane, K.S. 1967. Stability of reservoir slopes. In: Failure and Breakage of Rock, C. Fairhurst, Ed. Proc. 8th Symp. on Rock Mech.
- Lemos, L. 1986. The effect of rate of shear on residual strength. PhD Thesis, University of London.
- Lemos, L., Skempton, A. W. & Vaughan, P.R. 1985. Earthquake loading of shear surfaces in slopes. Proc. XI Int. Conf. Soil Mech. Found. Eng., 4, 1955-1958.
- Lensen, G.J. and Suggate, R.P. 1968. Inangahua earthquake - Preliminary account of the geology. In: Preliminary reports on the Inangahua earthquake, New Zealand. DSIR Bull. 193.
- Lensen, G.J. and Suggate, R.P. 1969. Geology (no ref.) In: Bull. NZ Soc. for Earthquake Eng. V.2, No. 1, 19-23.
- Lupini, J.F. Skinner, A.E. and Vaughan, P.R. 1981. The drained residual strength of cohesive soils. Geotechnique V. 31, (2), 181-213.
- Macrae, A.M.R. 1982. Case histories of deformation measurements in Canadian surface mines. Proc. 4th Canadian Symp. on Mining Surveying and Deformation Measurements. Can. Inst. of Surveying, Banff, 255-278.
- Marshall, P. 1933. Effects of the earthquake on coast line near Napier. N.Z. J. Sci. and Tech. V. 15 (1), 79-92.
- McDonald, M.G. and Harbaugh, A.W. 1988. A Modular Three-dimensional Finite Difference Ground-water Flow Model. Techniques of Water Resources Investigations of the United States Geological Survey.
- Miller, R.K. and Felszeghy, S.F. 1978. Engineering features of the Santa Barbara earthquake of August 13, 1978. University of California, Earthquake Eng. Res. Inst. UCSB-ME-78-2.
- Morimoto, R. et al. 1967. Landslides in the epicentral area of the Matsushiro earthquake swarm - their relation to the earthquake fault. Bul. Earthquake Research Institute. Vol. 45, 241-263.
- Morton, D.M. 1971. Seismically triggered landslides in the area above the San Fernando Valley. In: The San Fernando, California earthquake of February 9, 1971. USGS Prof. Paper 733, 99-109.
- Okusa, S. and Anma, S. 1980. Slope failures and tailings dam damage in the 1978 Izu-Ohshima-Kinkai earthquake. Eng. Geol. 16, (3/4), 195-224.
- Ongley, M. 1937. The Wairoa earthquake of 16th Sept. 1932. NZ J. Sci. & Tech. XVIII (12), 846-851.

- Pain, C.F. 1972. Characteristics and geomorphic effects of earthquake-initiated landslides in the Adelbert Range, Papua New Guinea. *Eng. Geol.* 6, (4), 261-273.
- Patton, F.D and Hendron, A.J. 1985. The Vaiont Slide, A geotechnical analysis based on new geologic observations of the failure surface. Geotechnical Lab. US Army Eng. Waterways Experiment Station, Vicksburg, Miss. Technical Report GL-85-5.
- Pearce A.J. and O'Loughlin, C.L. 1985. Landsliding during a M 7.7 earthquake: Influence of geology and topography. *Geology*, 13 855-858.
- Pearce, A.J. and Watson, A.J. 1986. Effects of earthquake-induced landslides on sediment budget and transport over a 50 yr period. *Geology*, V. 14, 52-55.
- Peck, R.B. 1967 Stability of natural slopes. *J. Soil Mech. Found. Div. ASCE*, SM4.
- Plafker, G. et al. 1971. Geological aspects of the May 31, 1970, Peru Earthquake. *Bul. Seis. Soc. Amer.* 61, (3) 543-578.
- Plafker, G. and Brown, R. D. 1973. Surface geologic effects of the Managua earthquake of December 23, 1972. In: Managua, Nicaragua Earthquake of December 23, 1972. Earthquake Engineering Research Institute Conf. Proc. V. 1 232-256.
- Rice, J.R. and Ruina, A.L. 1983. Stability of steady frictional slipping. *J. Applied Mechanics*. Vol. 50: 343-349.
- Romero, S. & Molina, R. 1974. Kinematic aspects of Vaiont Slide. *Proc. 3rd Congress ISRM, Denver*, Vol. 2-B, 865-870.
- Rouse, H. (ed) 1949. *Engineering Hydraulics*. Proc. 4th Hydraulics Conference. Iowa Inst. Hydraulic Research. Wiley & Sons.
- Rushton. K.R. & Redshaw S.C. 1979. *Seepage and Groundwater Flow*. Wiley & Sons.
- Saito, M. 1969. Forecasting time of slope failure by tertiary creep. *Proc. 7th Int. Conf. Soil Mech. Found. Eng.* 2, 677-683.
- Salt, G. Hancox, G. and Northey, R.D. 1980 Limit equilibrium analysis of the East Abbotsford Landslide and assessment of possible causes of the slide. *N.Z Geological Survey Report EG 341*.
- Sarma, S.K. 1973. Stability analysis of embankments and slopes. *Geotechnique*, Vol. XXIII No. 3, 423-433.
- Sarma. S.K. 1979. Stability analysis of embankments and slopes. *J. Geotech. Eng. Div. ASCE*. Vol. 105, No. GT12, 1511-1524.
- Sassa, K. 1988. Geotechnical model for the motion of landslides. *Proc. 5th Int. Symp. Landslides*. August 1988.

- Scott, R.F. 1978. Incremental movement of a rockslide. In, *Rockslides and Avalanches*, B. Voight (ed), Vol. 1: 659-668. Elsevier.
- Selli, R. & Trevisan, L. 1964. Caratteri e interpretazione della frana del Vaiont. *Giornale di Geologia*. Series 2, Vol. 32 (1): 8-65.
- Sharp, J.C. 1979. Drainage used to control movements of a large rock slide in Canada. 1st Int. Mine Drainage Symp. G.O. Argall, C.O. Brawner Eds. Freeman Publications. 423-436.
- Skempton, A.W. 1954. The pore pressure coefficients A and B. *Geotechnique* IV, No. 4: 143-147.
- Skempton, A.W. 1964 Long term stability of clay slopes. *Geotechnique*, Vol. 14, No. 2, 77-102.
- Skempton, A. W. 1977 Slope stability of cuttings in brown London Clay. 9th Int. Conf. Soil Mech. Found. Eng. Vol. 3, 261-270.
- Skempton, A. W. 1985. Residual strength of clays in landslides, folded strata and the laboratory. *Geotechnique*, 35, 1, 3-18.
- Skempton, A. W. and Hutchinson, J. 1969 Stability of natural slopes and embankment foundations. 7th Int. Conf. Soil Mech. Found. Eng. State of the Art Vol. 291-340.
- Smith, N. (in prep.) post-graduate thesis, University of Canterbury.
- Smith, N. & Salt, G. 1988. Predicting landslide mobility, an application to the East Abbotsford Slide. Proc. 5th ANZ Conf. on Geomechanics
- Stover B.K & Cannon, S.H. 1988. Reactivation of the Muddy Creek Landslide, West-Central Colorado, U.S.A. *Landslide News*, Japan Landslide Society. No 2. 8-10.
- Terzaghi, K. 1950. Mechanism of landslides. In: *Application of Geology to Engineering Practice*, Eng. Geol. (Berkey) Vol. Geol. Soc. Amer. N.Y: 83-123.
- Tika, T.M. 1989. The effect of rate of shear on the residual strength of soil. PhD Thesis. University of London
- Todd D.K. 1950. *Groundwater Hydrology*: Wiley & Sons.
- Trollope, D.H. 1980. The Vaiont slope failure. *Rock Mechanics* Vol. 13, 71-88.
- Valera, J.E. 1973. Soil conditions and local soil effects during the Managua earthquake of December 23, 1972. In: *Managua, Nicaragua Earthquake of December 23, 1972*. Earthquake Engineering Research Institute Conf. Proc. V. 1 232-256.
- Varnes, D. J. 1982. Time-deformation relations in creep to failure of earth materials. Proc. 7th SE Asian Geotech. Conf. 2, 107-130.

- Vibert, C. & Arnould M. 1987. An attempt at predicting the failure of a mountainous slope: the "La Clapiere" Slide at Saint-Etienne-de-Tinee (France). *Landslide News*. No. 1, 4-6.
- Vibert, C. 1988. Discussion of: An attempt at predicting the failure of a mountainous slope: the "La Clapiere" Slide at Saint-Etienne-de-Tinee (France). *Landslide News*. No. 2, 18.
- Voight, B. (in press). Law for failing materials applies to time forecasts of slope failure. Reference in *Landslide News*, No. 2, p 19.
- Voight, B. & Faust, C. 1982. Frictional heat and strength loss in some rapid landslides. *Geotechnique* 32 No. 1, 43-54.
- Voight, B. 1987. Phenomenological law enables accurate time forecasts of slope failure. Discussion, 6th Cong. Int. Soc. Rock Mech. Montreal.
- Voight, B. & Faust, C. 1982. Frictional heat and strength loss in some rapid landslides. *Geotechnique* XXXII No. 1, 43-54.
- Voight, B. & Kennedy, B.A. 1979. Slope failure of 1967-1969, Chuquicamata Mine, Chile. in: *Rockslides & Avalanches* Vol. 2, B. Voight (ed) Elsevier: 595-632.
- Ward, W.O. and Williams, J.W. 1987. Rainfall and accelerated landslide movement, America Mine Landslide, Santa Clara County, California. *Bull. Assoc. Eng. Geologists*, Vol. XXIV, No. 4, 557-561.
- Weischet, W. 1963. Further observations of geologic and geomorphic changes resulting from the catastrophic earthquake of May 1960 in Chile. *Bul. Seis. Soc. Amer.* Vol. 53, (6) 1237-1257.
- Yen, B.C. and Trotter, J.R. 1978. Proc. ASCE Geotech. Eng. Div. Specialty Conference on Earthquake Engineering and Soil Dynamics. 1076-1096.
- Youd, T.L. and House, S.N. 1978. Historic ground failures in Northern California triggered by earthquakes. USGS Prof. Paper 993.
- Youd, T.L. and Castle, R.O. 1972. The Borrego Mountain earthquake of April 9, 1968: Engineering Geology. U.S.G.S. Prof. Paper 787, 158-174.
- Zavodni, Z.M. & Broadbent, C.D. 1980. Slope failure kinematics. *Can. Inst. Mining Bulletin*, 73, No. 816, 69-74.